

JAERI - M  
91-133

JAPANESE CONTRIBUTIONS TO  
BLANKET DESIGN FOR ITER

August 1991

Toshimasa KURODA<sup>\*1</sup>, Hiroshi YOSHIDA  
Hideyuki TAKATSU, Yasushi SEKI, Kenji NODA  
Hitoshi WATANABE, Koichi KOIZUMI, Satoshi NISHIO  
Koichi MAKI<sup>\*2</sup>, Keisuke SATO<sup>\*3</sup>, Seiji MORI<sup>\*3</sup>  
Takeshi KOBAYASHI<sup>\*3</sup>, Tatsushi SUZUKI<sup>\*3</sup>  
Shingo HIRATA<sup>\*3</sup>, Seiichiro YAMAZAKI<sup>\*3</sup>  
Masayoshi UNO<sup>\*3</sup>, Yoshiyuki ISHIYAMA<sup>\*3</sup>  
and Hidenori MIURA<sup>\*3</sup>

JAERI-Mレポートは、日本原子力研究所が不定期に公刊している研究報告書です。

入手の問合わせは、日本原子力研究所技術情報部情報資料課（〒319-11茨城県那珂郡東海村）あて、お申しこしてください。なお、このほかに財団法人原子力弘済会資料センター（〒319-11茨城県那珂郡東海村日本原子力研究所内）で複写による実費頒布をおこなっております。

JAERI-M reports are issued irregularly.

Inquiries about availability of the reports should be addressed to Information Division, Department of Technical Information, Japan Atomic Energy Research Institute, Tokai-mura, Naka-gun, Ibaraki-ken 319-11, Japan.

© Japan Atomic Energy Research Institute, 1991

---

編集兼発行	日本原子力研究所
印刷	日立高速印刷株式会社

Japanese Contributions to  
Blanket Design for ITER

Toshimasa KURODA<sup>\*1</sup>, Hiroshi YOSHIDA<sup>+1</sup>, Hideyuki TAKATSU, Yasushi SEKI<sup>+1</sup>  
Kenji NODA<sup>+2</sup>, Hitoshi WATANABE<sup>+2</sup>, Koichi KOIZUMI, Satoshi NISHIO  
Koichi MAKI<sup>\*2</sup>, Keisuke SATO<sup>\*3</sup>, Seiji MORI<sup>\*3</sup>, Takeshi KOBAYASHI<sup>\*3</sup>  
Tatsushi Suzuki<sup>\*3</sup>, Singo HIRATA<sup>\*3</sup>, Seiichiro YAMAZAKI<sup>\*3</sup>, Masayoshi UNO<sup>\*3</sup>  
Yoshiyuki ISHIYAMA<sup>\*3</sup> and Hidenori MIURA<sup>\*3</sup>

Fusion Experimental Reactor Team  
Naka Fusion Research Establishment  
Japan Atomic Energy Research Institute  
Naka-machi, Naka-gun, Ibaraki-ken

(Received July 24, 1991)

ITER, the first integrated fusion nuclear experimental reactor, will be equipped with tritium breeding blanket to produce tritium required for the ITER operation, in which annual tritium consumption will reach 6 kg.

All participants (Japan, the EC, the USA and the USSR) in the ITER CDA (Conceptual Design Activity) have conducted conceptual design of ITER blanket (cooling water temperature  $\leq 100^{\circ}\text{C}$ ) utilizing their own technology bases. Because of superiority of currently available data base and technology, solid breeder blanket has been selected as the first option among many proposals including the solid breeder blankets, the liquid metal blankets and the aqueous lithium salt blankets.

This report describes the results of the following design and analytical studies on the Japanese proposal of  $\text{Li}_2\text{O}$  pebble type blanket: 1) blanket structural concepts, 2) neutronics, 3) thermal-hydraulics, 4) mechanical characteristics, 5) tritium recovery process and tritium inventory, and 7) fabrication and assembly technology.

Keywords : ITER, Blanket, Solid Breeder, Pebble Bed, Water Cooling, Tritium Producing, Neutronics, Thermal-hydraulics, Thermomechanics, Electromagnetic Force, Tritium Recovery, Tritium Inventory, Power Load Variation, Fabrication

---

+1 Department of Fusion Engineering Research

+2 Department of Fuels and Materials Research, Tokai Research Establishment

\*1 On leave from Kawasaki Heavy Industries Ltd.

\*2 Hitachi, Ltd.

\*3 Kawasaki Heavy Industries, Ltd.

## ITER用トリチウム増殖ブランケットの設計

日本原子力研究所那珂研究所核融合実験炉特別チーム

黒田 敏公<sup>\*1</sup>・吉田 浩<sup>+1</sup>・高津 英幸  
関 泰<sup>+1</sup>・野田 健治<sup>+2</sup>・渡辺 斉<sup>+2</sup>  
小泉 興一・西尾 敏・真木 紘一<sup>\*2</sup>  
佐藤 瓊介<sup>\*3</sup>・森 清治<sup>\*3</sup>・小林 武司<sup>\*3</sup>  
鈴木 達志<sup>\*3</sup>・平田 慎吾<sup>\*3</sup>・山崎 誠一郎<sup>\*3</sup>  
宇野 昌嘉<sup>\*3</sup>・石山 良之<sup>\*3</sup>・三浦 秀徳<sup>\*3</sup>

(1991年7月24日受理)

核融合原型炉(DEMO)開発を目指した国際熱核融合実験炉(ITER)においては、燃料として消費するトリチウム(約6kg/年)の大部分を自給するためのトリチウム増殖ブランケットが組み込まれる。この程(1990年12月)終了したITERの概念設計活動(Conceptual Design Activity; CDA)では、安全性の観点から信頼性の高い低温水冷却方式を用いるとして、日本および米国、欧州連合、ソ連の4極のそれぞれが自国技術に基づくブランケット設計を行った。可能性のある増殖ブランケットとして、固体増殖材系および液体金属増殖材系、リチウム塩水溶液増殖材系に誇る多くの構造概念が提案されたが、現時点で最もデータが多く技術的に見通しのつけやすい固体増殖材ブランケットが第一オプションとして選定された。

本報告書は、日本が提案しているLi<sub>2</sub>Oペブル充填型の増殖ブランケットについて実施した以下の設計および解析検討結果をまとめたものである。1) 構造概念、2) 核特性、3) 熱流動特性、4) 強度特性、5) トリチウム回収方式およびトリチウムインベントリー、6) ブランケット製作技術

---

那珂研究所: 311-01 茨城県那珂郡那珂町大字向山801-1

+ 1 核融合工学部

+ 2 東海研究所 燃料・材料工学部

\* 1 川崎重工業(株)より出向

\* 2 (株)日立製作所

\* 3 川崎重工業(株)

## Contents

1. Introduction .....	1
2. Executive Summary .....	3
2.1 Materials Selection .....	3
2.2 Layered Pebble Bed Blanket .....	3
2.3 Mixed Pebble Bed Blanket .....	10
3. Materials Selection .....	22
4. Mechanical Design of First Wall/Blanket/Shield .....	26
4.1 Blanket Segmentation .....	26
4.2 Integrated Design of First Wall/Blanket/Shield .....	26
4.3 Blanket Concepts .....	42
4.4 Conclusions .....	44
5. Fabrication and Assembly of First Wall/Blanket/Shield .....	60
5.1 Mixed Pebble Bed Blanket .....	60
5.2 Layered Pebble Bed Blanket .....	66
5.3 Pebble Production .....	69
5.4 Conclusions .....	72
6. Neutronics .....	73
6.1 Calculational Model and Method .....	73
6.2 Results of Calculations and Net TBR Estimates .....	81
6.3 Conclusions .....	100
7. Thermal Analysis .....	101
7.1 Mixed Pebble Bed Blanket .....	101
7.2 Layered Pebble Bed Blanket .....	118
7.3 Pebble and Block Blanket .....	143
7.4 Conclusions .....	151
8. Stress Analysis .....	152
8.1 Thermal Stress and Internal Pressure on the Blanket Box Structure .....	152
8.2 Disruption Analysis .....	161
8.3 Conclusions .....	165
9. Tritium Recovery/Inventory .....	166
9.1 Mixed Pebble Bed Blanket .....	166
9.2 Layered Pebble Bed Blanket .....	172
9.3 Conclusions .....	177

10. Accomodation to Power Load Variation .....	178
11. Separate First Wall Design for Test Article Containment .....	180
Acknowledgement .....	182
Appendix Material Properties of $\text{Li}_2\text{O}$ in Comparison with Other Ceramic Breeders and R&D Needs for $\text{Li}_2\text{O}$ .....	183

## 目 次

1. はじめに	1
2. 概 要	3
2.1 材料選定	3
2.2 多層型ブランケット	3
2.3 混合型ブランケット	10
3. 材料選定	22
4. 第一壁／ブランケット／遮蔽体の構造概念	26
4.1 ブランケット分割数	26
4.2 第一壁／ブランケット／遮蔽体の一体構造	26
4.3 ブランケット構造概念	42
4.4 まとめ	44
5. 第一壁／ブランケット／遮蔽体の製作性検討	60
5.1 混合型ブランケット	60
5.2 多層型ブランケット	66
5.3 ペブル製造	69
5.4 まとめ	72
6. ニュートロニクス解析	73
6.1 計算モデルおよび計算方法	73
6.2 計算結果および正味トリチウム増殖比評価	81
6.3 まとめ	100
7. 熱 解 析	101
7.1 混合型ブランケット	101
7.2 多層型ブランケット	118
7.3 多層（ベリリウムブロック）型ブランケット	143
7.4 まとめ	151
8. 応力解析	152
8.1 熱応力およびブランケット容器内圧	152
8.2 ディスラプション時の電磁力	161
8.3 まとめ	165
9. トリチウム回収とトリチウムインベントリ	166
9.1 混合型ブランケット	166
9.2 多層型ブランケット	172
9.3 まとめ	177

10. 出力変化への対応 .....	178
11. テストモジュール収納用別置第一壁概念 .....	180
謝 辞 .....	182
付録 候補増殖材の材料特性比較と $\text{Li}_2\text{O}$ に対する必要 R & D 項目 .....	183



## 1. Introduction

The following primary design goals in the ITER Conceptual Design Activity (CDA) can be achieved by incorporating a tritium breeding blanket:

- achieve a net tritium breeding ratio as close unity as practicable
- operate at an average neutron wall loading of about  $1 \text{ MW/m}^2$
- achieve an average fluence of at least  $1 \text{ MWa/m}^2$  and up to  $3 \text{ MWa/m}^2$
- be compatible with an overall machine availability of at least 10 % with a goal of reaching about 25 % in the Technology Phase
- tolerate accident condition with passive safety

Three major blanket concepts (solid breeder, liquid metal breeder and aqueous-salt breeder) proposed by four parties (Japan, the USA, the EC and the USSR) have been studied in the three-year CDA. The solid breeder blanket concept has finally selected as the first option for ITER with the LiPb breeder concept proposed as an alternate. As the solid breeder candidates,  $\text{Li}_2\text{O}$  or ternary ceramics such as  $\text{LiAlO}_2$ ,  $\text{Li}_2\text{ZrO}_3$  and  $\text{Li}_4\text{SiO}_4$  have been carefully evaluated. All blanket concepts employ an austenitic steel (Type 316) structure with low temperature ( $\leq 100^\circ\text{C}$ ) water coolant. The criteria for the design and selection of ITER blanket were performance capability, reliability, R&D requirements, reactor relevance and benefits, safety, and cost considerations.

This report summarizes Japanese contribution to the design and analytical works of ITER breeding blanket. The Japanese proposal has been devoted to the evaluation of pebble bed concepts of the solid breeder blanket, that are mixed pebble bed configuration of breeder/multiplier and separated pebble bed configuration (so-called layered type) of breeder/multiplier. As the reference materials for breeder and neutron multiplier,  $\text{Li}_2\text{O}$  and beryllium (Be) have been selected, respectively. Enrichments of  $^6\text{Li}$  are natural abundance for the mixed type and 50 % for the layered type. In respect to the layered type, another concept composed of  $\text{Li}_2\text{O}$  pebble and beryllium block was only preliminary studied. This concept has a compromised configuration between Japanese reference blanket ( $\text{Li}_2\text{O}$  pebble/Be pebble) and the US blanket concept ( $\text{Li}_2\text{O}$  block/Be block).

In all layered concepts, coolant channels are incorporated in the beryllium layers which also have a function to provide the desired temperature gradient between water coolant ( $60\text{--}100^\circ\text{C}$ ) and breeder layers.

Temperature control of the breeder in the layered concepts can be achieved by varying the thicknesses of breeder/multiplier layers. For the mixed pebble bed concept, coolant channels are incorporated in the tritium breeding zone, and the temperature control of the breeder is achieved by varying the thickness of helium gas gap between breeder/multiplier pebble bed and coolant tubes. Advantages of the layered concept are the separation of tritium breeding zone and coolant channel, reduction of possible compatibility problem between the breeder and multiplier, and the reduction of beryllium swelling due to its lower operating temperature (<500-600°C). Potential advantage of the mixed pebble bed concept is the possibility of utilization of natural  $\text{Li}_2\text{O}$  due to its expected high tritium breeding performance.

## 2. Executive Summary

Japanese design efforts of ceramic breeder blankets have been concentrated on the two types of the pebble bed blankets; (1) Layered breeder/multiplier pebble beds, and (2) Mixed breeder/multiplier pebble bed. Major design features of two blankets are summarized below.

### 2.1 Materials Selection

For both type of blankets, lithium oxide ( $\text{Li}_2\text{O}$ ) and beryllium (Be) were chosen as reference materials of breeder and neutron multiplier, respectively. They are both used in the form of small pebbles ( $\leq 1\text{mm}$  diameter). The advantages of using small pebbles are;

- (1) good toughness against thermal cracking
- (2) good predictability of thermal performance (e.g. thermal conductivity of pebble bed)
- (3) space preparation for volumetric expansion due to swelling
- (4) easy packing process of pebbles into blanket box

According to the ITER specification, Type 316 stainless steel and low temperature/pressure ( $\leq 100^\circ\text{C}/1.5\text{ MPa}$ ) light water were chosen as structural material and coolant, respectively.

### 2.2 Layered Pebble Bed Blanket

The concept of the layered pebble bed blanket is shown in Fig. 2.2.1. The major design parameters are summarized in Table 2.2.1. The first wall integrated with the blanket has rectangular coolant channels which are oriented toroidally and poloidally for the outboard and the inboard blankets, respectively.

In the blanket box, beryllium pebble packed layer and  $\text{Li}_2\text{O}$  pebble packed layer are alternately arranged. Packing ratio of 60 % is expected for both of  $\text{Li}_2\text{O}$  and beryllium layers. The enrichment of  $^6\text{Li}$  of 50 % is provided to obtain effective tritium breeding for this configuration.

Cooling panels with rectangular coolant channels are located in the beryllium pebble packed region and oriented in the poloidal direction. The  $\text{Li}_2\text{O}$  pebble layer is clad by 1 mm thick stainless steel to avoid direct contact with beryllium pebbles. The beryllium layer also works as a thermal

resistant layer between  $\text{Li}_2\text{O}$  and water coolant. The minimum temperature of  $\text{Li}_2\text{O}$  is maintained to be high enough for in-situ tritium recovery by adjusting the beryllium layer thickness. On the other hand, the maximum temperature of  $\text{Li}_2\text{O}$  is kept low enough to maintain its integrity by adjusting the thicknesses of  $\text{Li}_2\text{O}$  and beryllium layers increase in the radial direction to accommodate the attenuation of nuclear heating rate in the blanket. The thicknesses also vary in the poloidal direction to accommodate the poloidal variation of the neutron wall loading. Thus the total thickness of the blanket module varies in the poloidal direction. The minimum thickness of the blanket is 56.2 cm including the first wall and the back wall at the midplane, and the maximum thickness is 86.3 cm at the top/bottom ends of the blanket.

Calculated temperatures of  $\text{Li}_2\text{O}$  during the normal operation of the Technology Phase are within the range of 450 to 800 °C, which satisfy temperature limits for  $\text{Li}_2\text{O}$  (400 - 1000 °C) and leave a margin for accommodating ~20 % power increase. Beryllium temperatures calculated also for the normal operation of the Technology Phase are in the range of 100 to 700 °C. The optimization of layer thicknesses will be required to lower the maximum temperatures of  $\text{Li}_2\text{O}$  and beryllium because larger accommodation to power variation will possibly be needed, and high temperature of beryllium may cause compatibility and swelling problems.

Local tritium breeding ratios are calculated to be 1.35, 1.46 and 0.54 for the outboard midplane, the outboard top/bottom and the inboard midplane, respectively. Net tritium breeding ratio is estimated to be 0.8 based on these local values taking into account of the poloidal neutron wall load variation and the coverage loss due to ducts and blanket side walls.

Tritium generated in  $\text{Li}_2\text{O}$  breeder is recovered by low pressure (0.1 MPa) helium purge stream with protium swamping. Tritium inventory of the blanket in the Technology Phase was estimated to be around 120 g.

Table 2.2.1 Design parameters of the layered pebble bed blanket

	<u>INBOARD</u>	<u>OUTBOARD</u>
BREEDER		
MATERIAL:	Li <sub>2</sub> O	
FORM:	Pebble (60% PF)	
GEOMETRY:	≤ 1mm diameter	
MASS (MT):	~3	~90
TEMPERATURE (°C) WINDOW:	400 - 1000	
PHYSICS PHASE	} NA	
MIN./MAX. TEMPERATURE (°C) DURING		
NORMAL OPERATION:		
120% NORMAL OPERATION:		
150% NORMAL OPERATION:		
TRITIUM INVENTORY (g):		
TECHNOLOGY PHASE		
MIN./MAX. TEMPERATURE (°C) DURING		
NORMAL OPERATION:	450/700	450/800
120% THE NORMAL OPERATION:	~500/800	~500/900
150% THE NORMAL OPERATION:	NA	
TRITIUM INVENTORY (g):	9.2	117
MULTIPLIER		
MATERIAL:	Be	
FORM:	Pebble (60% PF)	
GEOMETRY:	≤ 1mm diameter	
MASS (MT):	~8	~185
TEMPERATURE (°C) WINDOW:		
PHYSICS PHASE	} NA	
MIN./MAX. TEMPERATURE (°C) DURING		
NORMAL OPERATION:		
120% NORMAL OPERATION:		
150% NORMAL OPERATION:		
TRITIUM INVENTORY (g):		

Table 2.2.1 (Cont'd)

	<u>INBOARD</u>	<u>OUTBOARD</u>
TECHNOLOGY PHASE		
MIN./MAX. TEMPERATURE (°C) DURING		
NORMAL OPERATION:	~100/500*	~100/700*
120% THE NORMAL OPERATION:	~100/600*	~100/800*
150% THE NORMAL OPERATION:	NA	
TRITIUM INVENTORY (g) FOR 51000 DT PULSES:	NA	
CLAD MATERIAL FOR BREEDER		316SS
MIN./MAX. THICKNESS (mm):		1
MASS (MT):	~4	~45
TEMPERATURE (°C) WINDOW:		<500****
PHYSICS PHASE		
MIN./MAX. TEMPERATURE (°C) DURING	} NA	
NORMAL OPERATION:		
120% NORMAL OPERATION:		
150% NORMAL OPERATION:		
TECHNOLOGY PHASE		
MIN./MAX. TEMPERATURE (°C) DURING		
NORMAL OPERATION:	400/600*	400/680*
120% NORMAL OPERATION:	450/700*	400/780*
150% NORMAL OPERATION:	NA	
STRUCTURE MATERIAL (COOLANT CHANNELS, SIDE WALLS, AND FIRST WALL)		316SS
TEMPERATURE (°C) WINDOW:		<400
MASS (MT):	~97	~500
PHYSICS PHASE		
MIN./MAX. TEMPERATURE (°C) DURING		
NORMAL OPERATION:	60/200**	60/300***
120% NORMAL OPERATION:	NA	
150% NORMAL OPERATION:	NA	

\* will be lowered by optimization of layer thickness

\*\* with radiative-cooled tile

\*\*\* at local high heat flux region of 0.6 MW/m<sup>2</sup> with radiative-cooled tile

\*\*\*\* Temperature limits for non-structural component should be reconsidered

Table 2.2.1 (Cont'd)

	<u>INBOARD</u>	<u>OUTBOARD</u>
TECHNOLOGY PHASE		
MIN./MAX. TEMPERATURE (°C) DURING		
NORMAL OPERATION:	60/170	60/170
120% THE NORMAL OPERATION:	NA	
150% THE NORMAL OPERATION:	NA	
BLANKET/SHIELD COOLANT		
MATERIAL:	H <sub>2</sub> O	
FLOW DIRECTION:	Poloidal	
IN/OUT TEMPERATURE (°C):	60/100	
IN/OUT PRESSURE (MPa):	1.5/1.3	1.5/1.2
MIN./MAX. VELOCITY (m/s):	<3.5	<3.5
TRITIUM PERMEATION RATE (Ci/D):	NA	
PUMPING POWER (MW):	NA	
BREEDER HELIUM PURGE GAS		
IN/OUT PRESSURE (MPa):	0.11/0.10	0.11/0.10
FLOW RATES (mol/s):	0.31	2.79
INLET H <sub>2</sub> (H <sub>2</sub> O),%:	0.817(1vpm),	0.817(1vpm)
MAX./AVE. OUTLET HT(HTO) PRESSURE (Pa):	15.5(0.82)/-	15.5(0.82)/-
H/T RATIO:	100	100
PUMPING POWER (kW):	NA	
GEOMETRICAL DETAILS		
FW/BLANKET RADIAL THICKNESS (mm)		
MIDPLANE:	15/150*	15/562*
TOP/BOTTOM:	15/TBD	15/863*
LAYER DIMENSION IN THE RADIAL DIRECTION		
MIDPLANE:	See Fig.2.2.1	See Fig.2.2.1

\* : including first wall and back wall

Table 2.2.1 (Cont'd)

	<u>INBOARD</u>	<u>OUTBOARD</u>
TRITIUM BREEDING PERFORMANCE		
NUCLEAR DATA BASE:	JENDL3	
TRANSPORT METHOD:	1-D SN	
MIDPLANE/TOP OR BOTTOM LOCAL POLOIDAL TBR:	0.54	1.35/1.46
NET ESTIMATED TBR:	0.8	
NET TBR BASED ON 3D CALCULATION:	NA	
NUCLEAR HEATING (MW)	}	NA
TOTAL NUCLEAR POWER		
PHYSICS PHASE:		
TECHNOLOGY PHASE:		
BREEDER POWER DENSITY (MW/m <sup>3</sup> )		
MIN./MAX. AT MIDPLANE:	1.5/18	1/24
MIN./MAX. AT TOP/BOTTOM:	0.7/8	0.06/19
MULTIPLIER POWER DENSITY (MW/m <sup>3</sup> )		
MIN./MAX. AT MIDPLANE:	1.4/3	0.17/4
MIN./MAX. AT TOP/BOTTOM:	0.62/1.3	0.02/1.8
DECAY HEAT AT SHUT DOWN (MW):	NA	



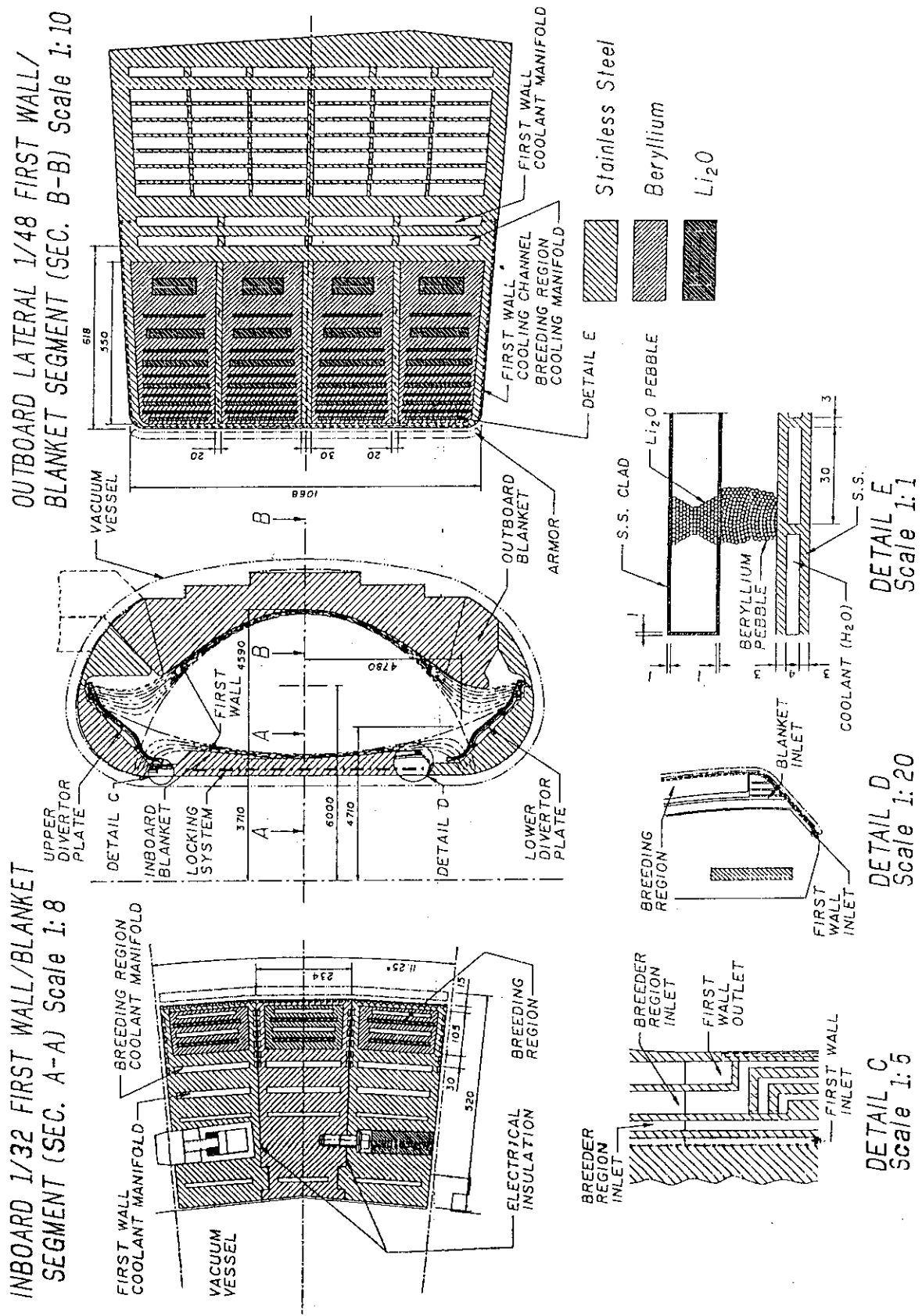


Fig. 2.2.1 Concept of the layered pebble bed blanket

### 2.3 Mixed Pebble Bed Blanket

The concept of the mixed pebble bed blanket is shown in Fig. 2.3.1. Major design parameters of the blanket are summarized in Table 2.3.1. The first wall integrated with the blanket has rectangular coolant channels which are oriented toroidally and poloidally for the outboard and the inboard blankets, respectively.

Homogeneously mixed  $\text{Li}_2\text{O}$  and beryllium pebbles are filled in the blanket box. The mixing ratio of  $\text{Li}_2\text{O}/\text{Be}$  is optimized to be 1/3 for tritium breeding performance. Packing ratio of pebbles is expected to be 60 %. With this configuration, sufficient tritium breeding performance is obtained without  $^6\text{Li}$  enrichment. Therefore  $\text{Li}_2\text{O}$  with natural lithium is used as the breeder.

For the outboard side module, breeding region in the blanket is poloidally separated into three zones by intermediate coolant plenums as shown in Figs 2.3.2 and 2.3.3 in order to accommodate the poloidal variation of the neutron wall loading. For the outboard center module, the blanket is originally divided into two parts; the top part and the bottom part as shown in Figs 2.3.4 and 2.3.5, and no blanket exists at the midplane.

To remove the heat generated in the breeder/multiplier pebble bed and keep  $\text{Li}_2\text{O}$  temperature below the allowable maximum temperature, circular cooling tubes oriented poloidally are arranged according to the attenuation of nuclear heating rates in the blanket. To keep  $\text{Li}_2\text{O}$  temperature above the allowable minimum temperature, thermal resistant layer (He gas gap) is provided around the cooling tubes and on the blanket box wall by liner tubes or liner wall. Thickness of the gas gap is varied poloidally and radially (1 to 3 mm) to accommodate the variation of nuclear heating rates.

The minimum and the maximum allowable temperatures for  $\text{Li}_2\text{O}$  are 400 °C to achieve in-situ tritium recovery and 1000 °C to maintain the material integrity, respectively. On the other hand, a nominal temperature range is considered to leave a margin for accommodating power variations of the reactor, i.e., 450 - 700°C as a design target. Temperatures of beryllium would be the same as those of  $\text{Li}_2\text{O}$ , which are within the range of 450 to 700 °C. Temperature of the liner (316SS) would be around 500°C during the normal operation.

Calculated temperatures of  $\text{Li}_2\text{O}/\text{Be}$  pebbles during the normal operation of the Technology Phase are in the range of 400 to 820 °C for the present configuration. The temperature spectrum in the blanket is shown in Fig. 2.3.6. Since the calculated temperatures (which satisfy the allowable temperature range) go beyond the nominal range, further optimization of placing cooling tubes and gap widths is required.

Local tritium breeding ratios are calculated to be 1.45, 1.49 and 0.57 for the outboard midplane, the outboard top/bottom and the inboard midplane, respectively. Net tritium breeding ratio is estimated to be 0.8 based on these local values taking into account of the poloidal neutron wall load variation and the coverage loss due to ducts and side walls.

Tritium generated in  $\text{Li}_2\text{O}$  breeder is recovered in the low pressure (0.1 MPa) helium purge gas with protium swamping. Tritium inventory in the blanket was estimated to be about 260 g.

Table 2.3.1 Design parameters of the mixed pebble bed blanket

	<u>INBOARD</u>	<u>OUTBOARD</u>
BREEDER		
MATERIAL:	Li <sub>2</sub> O	Li <sub>2</sub> O
FORM:	Pebble(60% PF)	Pebble(60% PF)
GEOMETRY:	≤ 1mm diameter (mixed with multiplier pebbles*)	
MASS (MT):	~3	~40**
TEMPERATURE (°C) WINDOW:	400-1000	
PHYSICS PHASE		
MIN./MAX. TEMPERATURE (°C) DURING	} NA	
NORMAL OPERATION:		
120% NORMAL OPERATION:		
150% NORMAL OPERATION:		
TRITIUM INVENTORY (g):		
TECHNOLOGY PHASE		
MIN./MAX. TEMPERATURE (°C) DURING		
NORMAL OPERATION:	450/820	450/820
120% THE NORMAL OPERATION:	450/950	450/950
150% THE NORMAL OPERATION:	NA	
TRITIUM INVENTORY (g):	18	240
MULTIPLIER		
MATERIAL:	Be	Be
FORM:	Pebble(60% PF)	Pebble(60% PF)
GEOMETRY:	≤ 1mm diameter (mixed with breeder pebbles*)	
MASS(MT):	~9	~130
TEMPERATURE (°C) WINDOW		
PHYSICS PHASE		
MIN./MAX. TEMPERATURE (°C) DURING	} NA	
NORMAL OPERATION:		
120% NORMAL OPERATION:		
150% NORMAL OPERATION:		
TRITIUM INVENTORY (g):		

\* Li<sub>2</sub>O/Be = 1/3 (volume fraction)

\*\* Mass estimation does not include loss due to ducts and test modules

Table 2.3.1 (Cont'd)

	<u>INBOARD</u>	<u>OUTBOARD</u>
TECHNOLOGY PHASE		
MIN./MAX. TEMPERATURE (°C) DURING		
NORMAL OPERATION:	450/800	450/800
120% THE NORMAL OPERATION:	450/950	450/950
150% THE NORMAL OPERATION:		NA
TRITIUM INVENTORY (g) FOR 51000 DT PULSES:		NA
LINER MATERIAL FOR HELIUM GAP		316SS
MIN./MAX. THICKNESS (mm):		0.5/1.0
MASS (MT)	~5	~32
TEMPERATURE (°C) WINDOW:		<500***
PHYSICS PHASE		
MIN./MAX. TEMPERATURE (°C) DURING	} NA	
NORMAL OPERATION:		
120% NORMAL OPERATION:		
150% NORMAL OPERATION:		
TECHNOLOGY PHASE		
MIN./MAX. TEMPERATURE (°C) DURING		
NORMAL OPERATION:	<500	<510
120% NORMAL OPERATION:	NA	<590
150% NORMAL OPERATION:	NA	
STRUCTURE MATERIAL (COOLANT CHANNELS, SIDE WALLS, AND FIRST WALL)		316SS
TEMPERATURE (°C) WINDOW:		<400
MASS (MT):	~94	~730
PHYSICS PHASE		
MIN./MAX. TEMPERATURE (°C) DURING		
NORMAL OPERATION:	60/200*	60/300**
120% NORMAL OPERATION:		NA
150% NORMAL OPERATION:		NA

\* with radiative-cooled tile

\*\* at local high heat flux region of 0.6 MW/m with radiative-cooled tile

\*\*\* Temperature limits for non-structural components should be reconsidered.

Table 2.3.1 (Cont'd)

	<u>INBOARD</u>	<u>OUTBOARD</u>
TECHNOLOGY PHASE		
MIN./MAX. TEMPERATURE (°C) DURING		
NORMAL OPERATION:	60/170	60/170
120% THE NORMAL OPERATION:	NA	
150% THE NORMAL OPERATION:	NA	
BLANKET/SHIELD COOLANT		
MATERIAL:	H <sub>2</sub> O	
FLOW DIRECTION:	Poloidal	
IN/OUT TEMPERATURE (°C):	60/100	
IN/OUT PRESSURE (MPa):	1.5/1.48	1.5/1.4
MIN./MAX. VELOCITY (m/s):	<1.5	<3
TRITIUM PERMEATION RATE (Ci/D):	NA	
PUMPING POWER (MW):	NA	
BREEDER HELIUM PURGE GAS		
IN/OUT PRESSURE (MPa):	0.101/0.10	0.101/0.10
FLOW RATES (mol/s):	0.31	2.79
INLET H <sub>2</sub> (H <sub>2</sub> O), %:	0.817(1vpm)	0.817(1vpm)
MAX./AVE. OUTLET HT(HTO) PRESSURE (Pa):	15.5(0.82)/-	15.5(0.82)/-
H/T RATIO:	100	100
PUMPING POWER (kW):		NA
GEOMETRICAL DETAILS		
FW/BLANKET RADIAL THICKNESS (mm)		
MIDPLANE:	15/150*	15/600**
TOP/BOTTOM:	15/150*	15/600**
TUBE DIMENSIONS AND ARRANGEMENT		
MIDPLANE:	See Fig.2.3.1	See Fig.2.3.1

\* Including first wall and 30 mm thick back wall

\*\* Including first wall and 50 mm thick back wall

Table 2.3.1 (Cont'd)

	<u>INBOARD</u>	<u>OUTBOARD</u>
TRITIUM BREEDING PERFORMANCE		
NUCLEAR DATA BASE:	JENDL3	
TRANSPORT METHOD:	1D SN	
MIDPLANE/TOP OR BOTTOM LOCAL POLOIDAL TBR:	0.57/-	1.45/1.49
NET ESTIMATED TBR:	0.81*	
NET TBR BASED ON 3D CALCULATION:	NA	
NUCLEAR HEATING (MW)	} NA	
TOTAL NUCLEAR POWER		
PHYSICS PHASE:		
TECHNOLOGY PHASE:		
BREEDER POWER DENSITY (MW/m <sup>3</sup> )**		
MIN./MAX. AT MIDPLANE:	2.5/6	0.4/8.5
MIN./MAX. AT TOP/BOTTOM:	1.1/2.7	0.2/4.2
MULTIPLIER POWER DENSITY (MW/m <sup>3</sup> )	} refer to breeder power density	
MIN./MAX. AT MIDPLANE:		
MIN./MAX. AT TOP/BOTTOM:		
DECAY HEAT AT SHUT DOWN (MW):	NA	

\* without carbon armor

\*\* volume-averaged value considering volume fraction  
(Li<sub>2</sub>O-Be-SS-H<sub>2</sub>O)

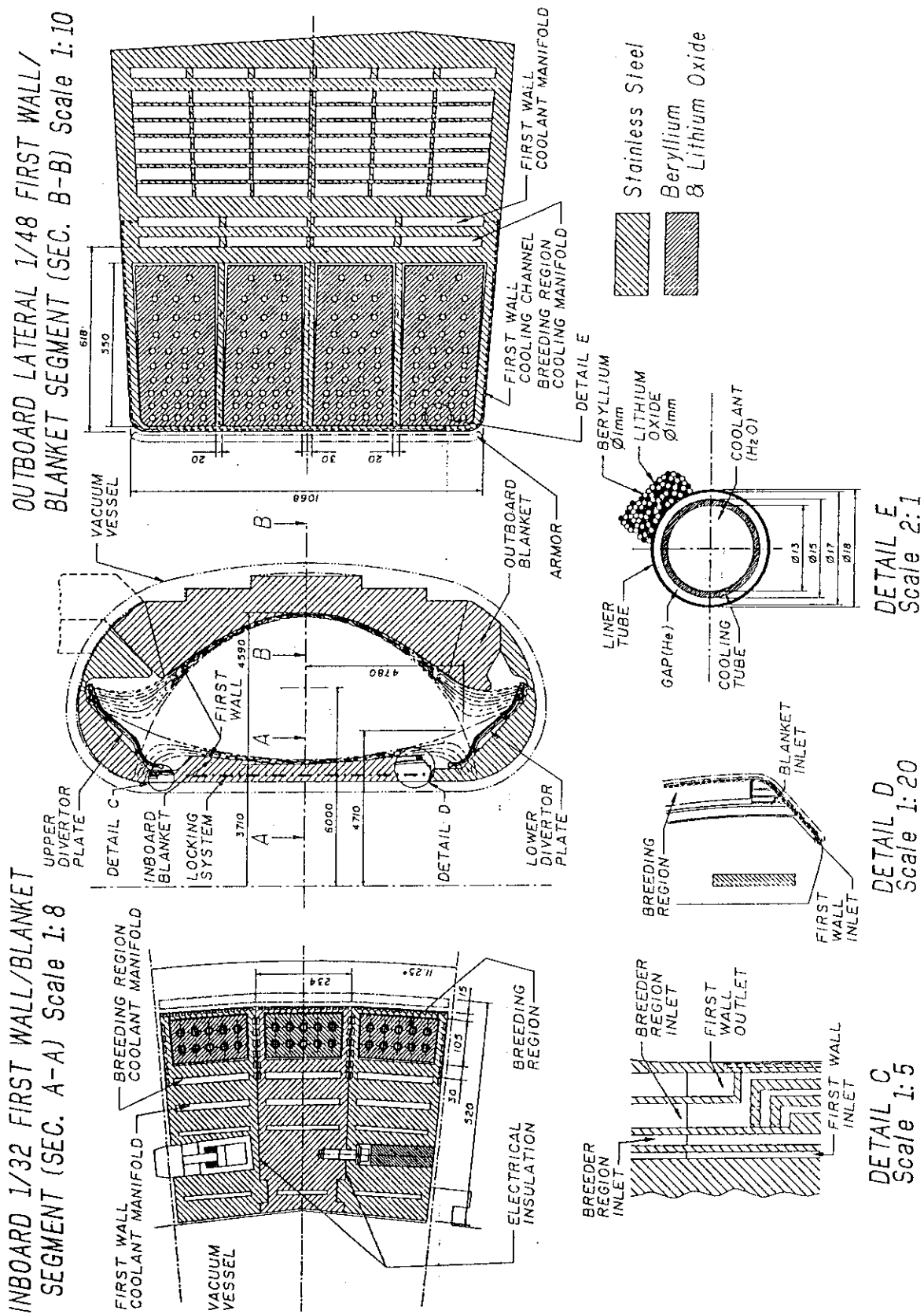


Fig. 2.3.1 Concept of the mixed pebble bed blanket



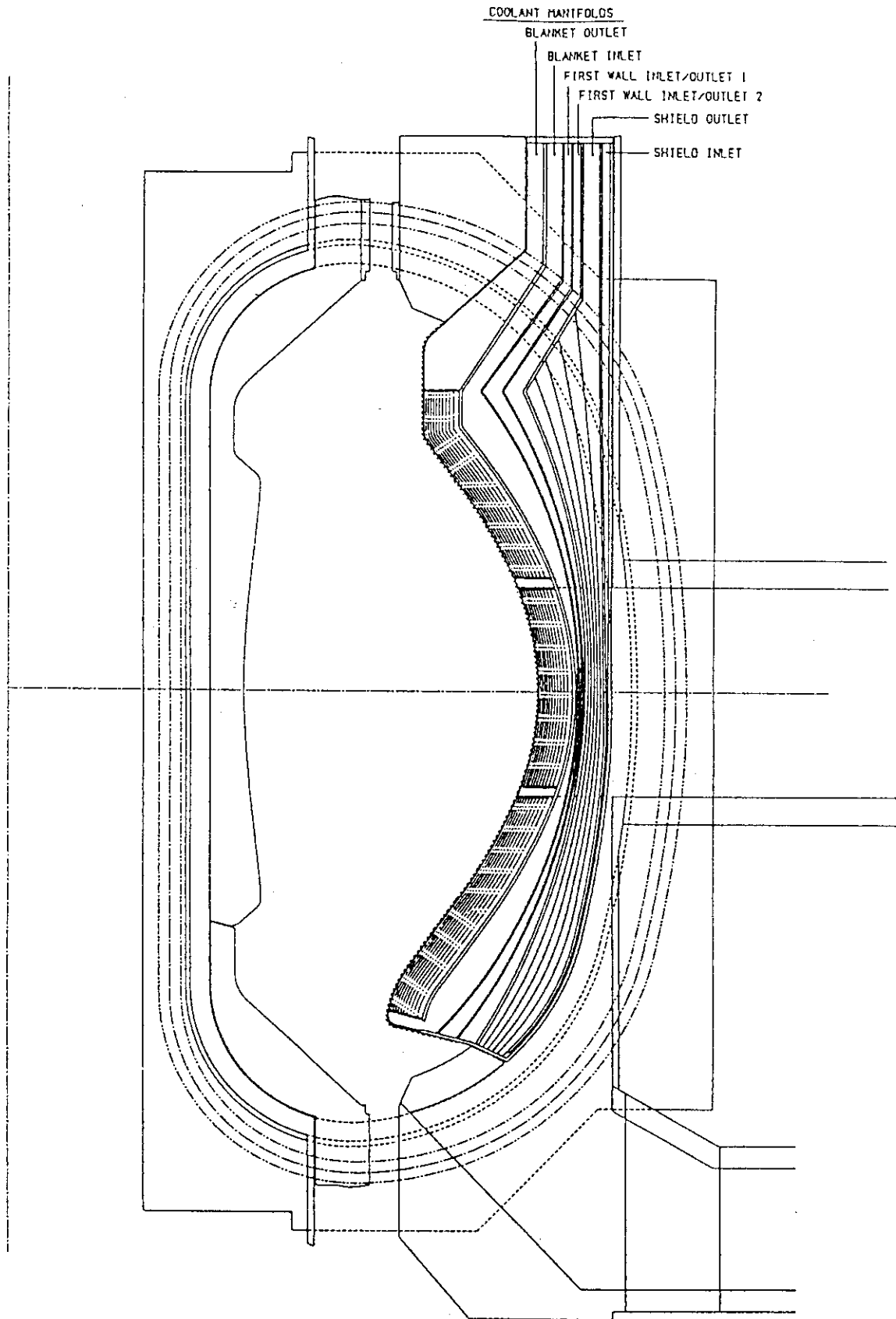


Fig. 2.3.2 Poloidal division of outboard side module for the mixed pebble bed blanket

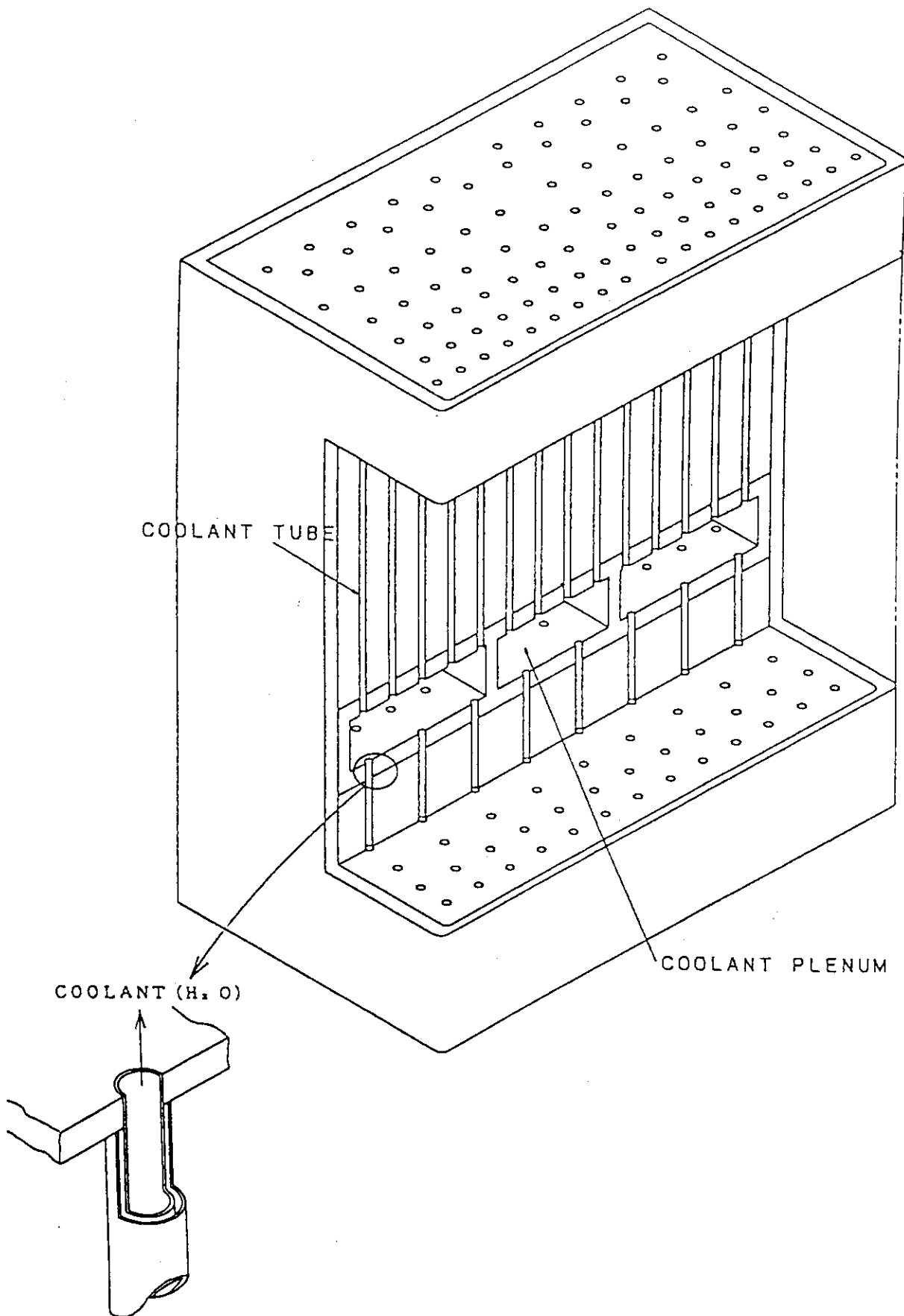


Fig. 2.3.3 Manifold concept for poloidally divided outboard side module of the mixed pebble bed blanket

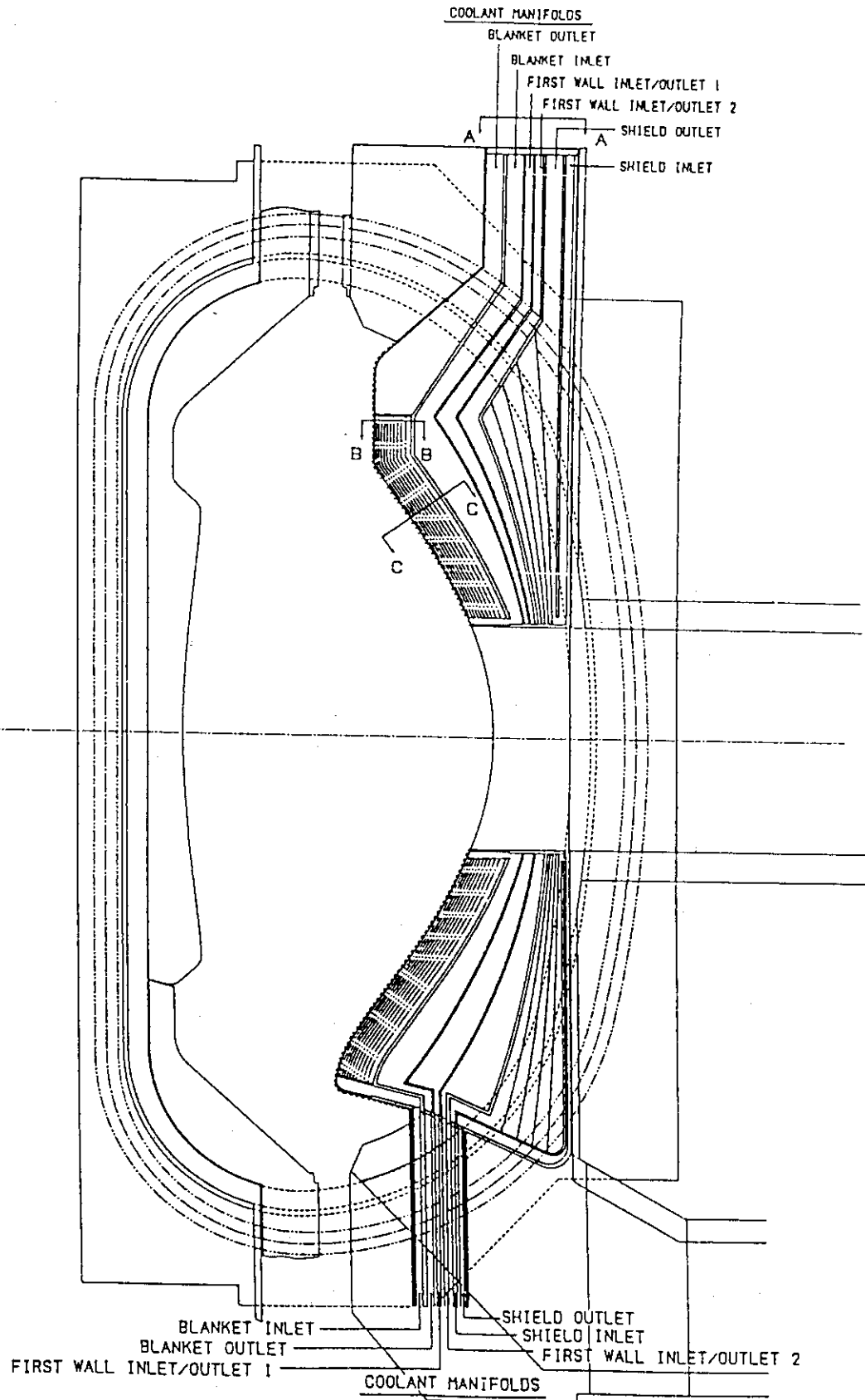


Fig. 2.3.4 Elevation view of outboard central module (mixed pebble blanket)

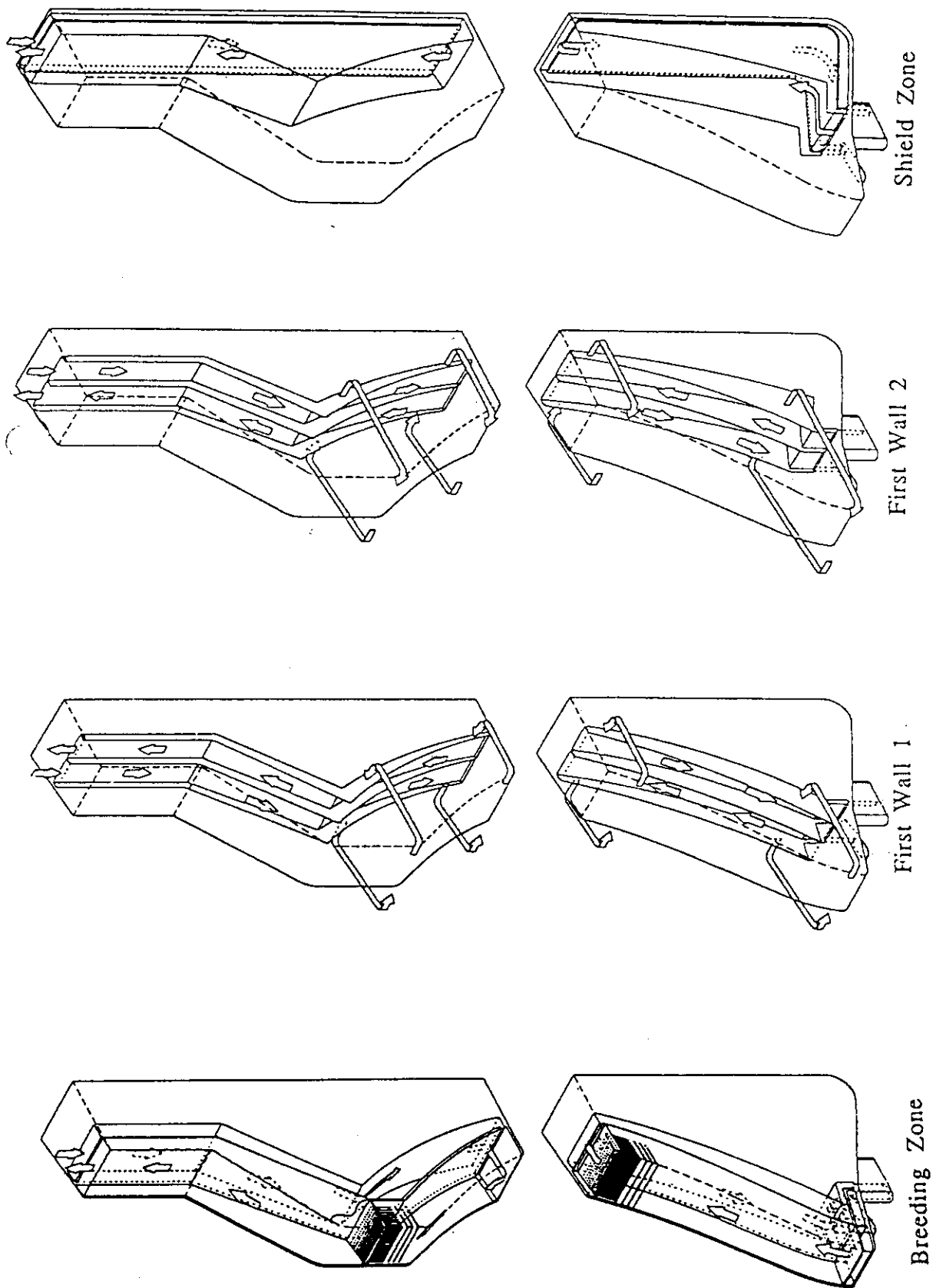


Fig. 2.3.5 Manifolding and coolant flow concepts (outboard central module)

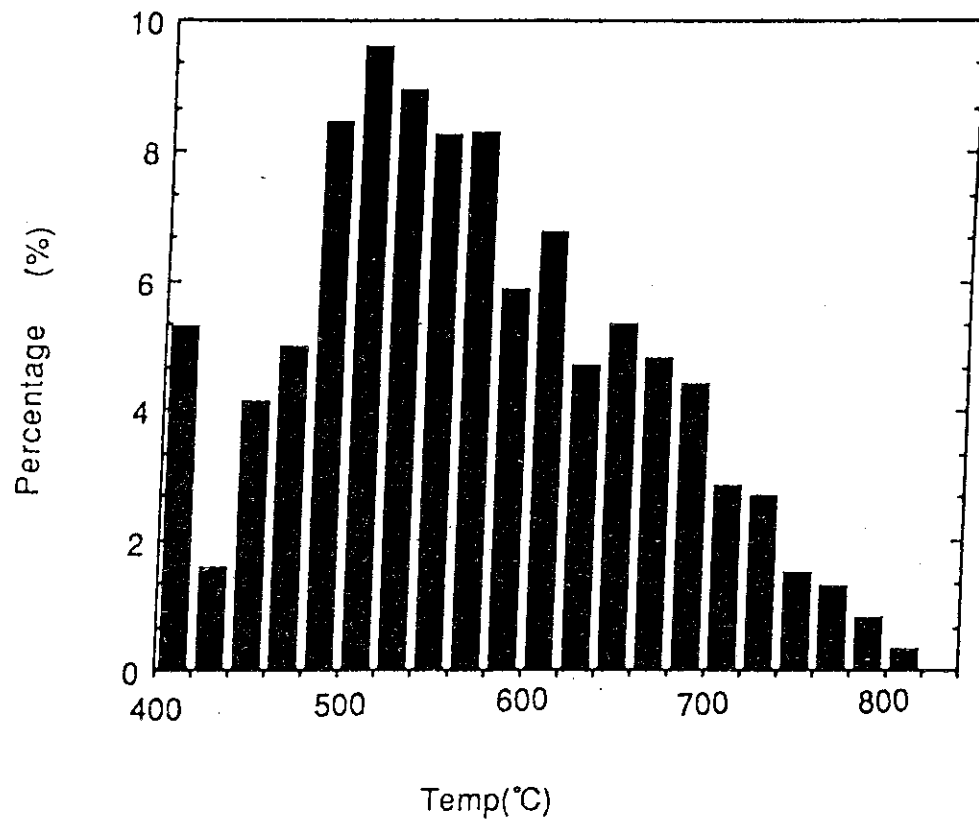


Fig. 2.3.6 Temperature spectrum in the mixed pebble bed blanket

### 3. Materials Selection

Type 316 stainless steel has been selected as the structural material in terms of its abundant data base with experiences of fission reactor operations. Low temperature ( $\leq 100^\circ\text{C}$ ) and low pressure (1-1.5 MPa) water coolant has been chosen with respect to reliability of the reactor.

As for the breeder, ceramic materials have been selected as the first option for ITER. Thermophysical properties of ceramic breeders are summarized in Table 3.1 [1]. Thermal conductivities and tritium release characteristics of these materials are also shown in Figs 3.1 and 3.2, respectively [1]. Among these ceramic breeders, lithium oxide ( $\text{Li}_2\text{O}$ ) has the highest thermal and tritium release performances as seen from the Table and the Figures, which are very important in the blanket design in order to have a wider design window and quicker in-situ tritium recovery. Tritium breeding ratio (TBR) will be similar for all ceramic materials as long as they have  $^6\text{Li}$  enrichment and are used with a neutron multiplier. An attractive feature of  $\text{Li}_2\text{O}$  is that there is a possibility to achieve enough TBR without  $^6\text{Li}$  enrichment due to its highest Li atom content among the ceramic breeders. From above viewpoints,  $\text{Li}_2\text{O}$  has been selected as the breeder material in the design below. A qualitative comparison of  $\text{Li}_2\text{O}$  properties with other candidate ceramic breeders, data base status and key R&D needs for  $\text{Li}_2\text{O}$  are discussed in Appendix.

To obtain high TBR, the use of a neutron multiplier will be required. Candidates for the multiplier are beryllium (Be) and lead (Pb). Due to the higher atomic number density, the lower threshold energy of (n,2n) reaction and the higher melting temperature which brings a wider design window, the former has been chosen.

A pebble form of  $\leq 1$  mm in diameter has been considered for both the breeder and the multiplier based on the following attractive features:

- Prevention of thermal cracking of the materials which will significantly affect breeder temperature control.
- More predictability of thermal performance (effective thermal conductivity) in the breeding zone than solid block concepts that have thermal contact conductances between solid blocks of breeder/multiplier and liner/clad walls.

- Space preparation for volumetric expansion due to irradiation swelling of the breeder and the multiplier.
- Easier fabrication; atmospheric control will be required during fabrication in order to prevent reactions of  $\text{Li}_2\text{O}$  and moisture, and possibly of Be and air. Pebbles will be filled into the blanket at the very last stage of the fabrication, thus problems accompanying with the atmospheric control will be eased.

On the other hand, a block form of the multiplier will lead to a simpler design of a blanket if the thermal contact conductance is kept high enough and well-predicted. The number of breeder/multiplier layers and the blanket thickness required to achieve enough TBR could be reduced due to higher thermal conductivity of Be block than that of a pebble bed. Therefore a concept using Be blocks also as a thermal resistant layer between the breeder and coolant is investigated in this design study.

#### Reference

- [1] D.L.Smith et al., U.S. contributions to the ITER Blanket Homework Task of Winter 1990 Session, ITER-TN-BL-5-0-1, Jan.-Mar. 1990

Table 3.1 Thermophysical properties of ceramic breeder materials  
(80% dense and 90%  $^6\text{Li}$  enrichment) [1]

Property	$\text{Li}_2\text{O}$	$\text{Li}_4\text{SiO}_4$	$\text{Li}_2\text{ZrO}_3$	$\text{LiAlO}_2$
Li-6 Density, $\text{g/cm}^3$	0.587	0.346	0.235	0.172
$T_{\text{melt}}$ , $^{\circ}\text{C}$	1432	1255	1616	1610
$T_{\text{phase}}$ , $^{\circ}\text{C}$	none	655	1100	none
$(\Delta V/V_0)_{\text{phase}}$ , %	none	0	+13	none
Thermal Conductivity at $600^{\circ}\text{C}$ , $\text{W/m-K}$	3.54	1.73	1.43	1.92
Thermal Diffusivity at $600^{\circ}\text{C}$ , $\text{mm}^2/\text{s}$	0.857	0.419	0.341	0.679
Thermal Expansion at $600^{\circ}\text{C}$ , %	1.50	1.38	0.57	0.64
$T_{\text{min}}$ ( $^{\circ}\text{C}$ ) for 1-day Tritium Residency Time	320	400 ( $\pm 25$ )	320	525 ( $\pm 25$ )
In-Reactor Volume Change <sup>(a)</sup>	high	intermediate	low	low
Incompatibility and Li Mass Transport <sup>(a)</sup>	high	intermediate	low	low
Activation and Afterheat <sup>(a)</sup>	low	intermediate	high	intermediate
Mechanical Response <sup>(a)</sup>	intermediate	poor	good	intermediate

(a) - relative ranking.



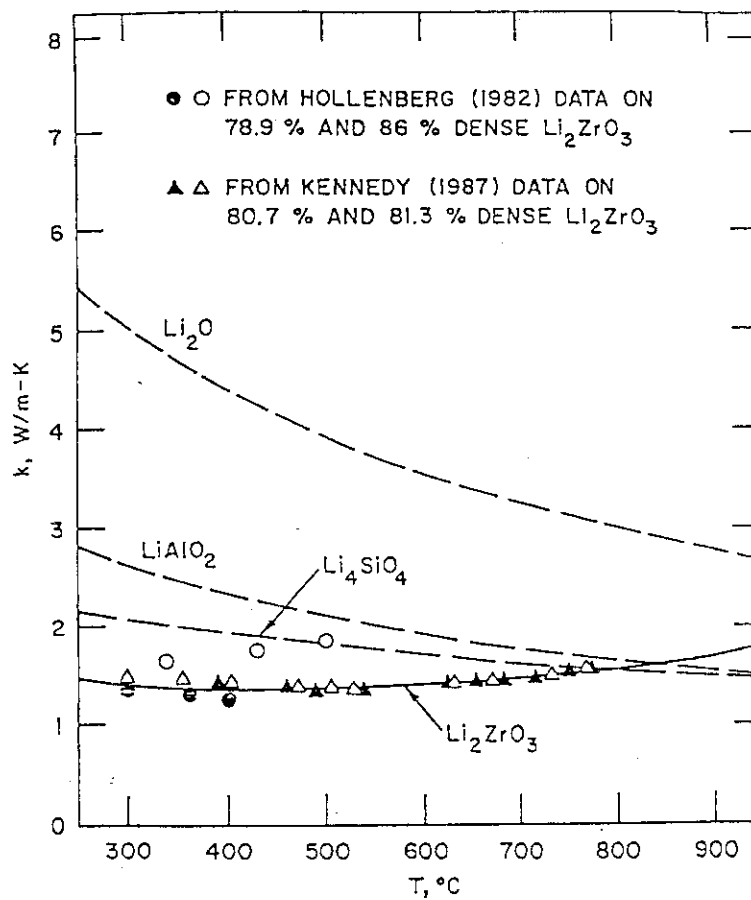


Fig. 3.1 Comparison of thermal conductivities of solid breeders at 80% dense[1]

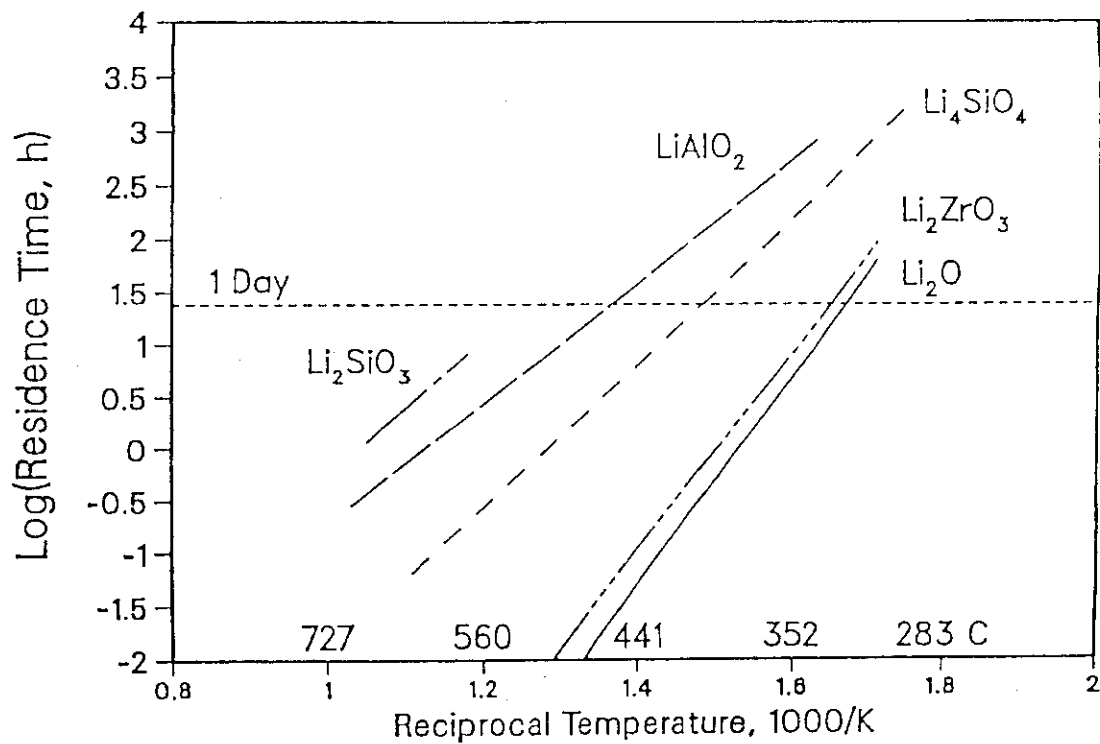


Fig. 3.2 Tritium residence times comparison[1]

#### 4. Mechanical Design of First Wall/Blanket/Shield

Three types of blankets have been considered as mentioned in Chapter 1. However, mechanical designs for segmentation into modules and integration with first wall/shield are basically common to all three blankets. The former is described in Section 4.1 and the latter in Section 4.2. Internal structures and major design parameters of individual blanket are represented in Section 4.3. Brief conclusions derived from this study of mechanical design are summarized in Section 4.4. Among three types of blankets studied, the mixed pebble bed and the layered pebble bed concepts are proposed as reference designs in Japanese contribution. The pebble and block concept is considered as a compromised design of Japan and US blankets for ITER and only preliminary investigated here.

##### 4.1 Blanket Segmentation

Outboard blanket is equally divided into three modules per sector, thus 48 modules in the full torus. Side modules extend poloidally the full length of the outboard region while a central blanket is divided into an upper and lower modules. Test modules and other service penetrations are located at midplane in the central blanket position.

Inboard blanket is equally divided into two modules per sector, thus 36 modules in the full torus. One module consists of three submodules which are joined in terms of simpler assembly and maintenance, but insulated electrically with each other to reduce electromagnetic force during plasma disruptions. All inboard modules extend poloidally from the top of the lower divertor plate to the top of the reactor.

#### 4.2 Integrated Design of First Wall/Blanket/Shield

##### 4.2.1 Outboard module

Figure 4.2.1 shows the shape of outboard blanket modules. They are box structures in which the first wall, blanket and shield are all integrated. Figure 4.2.2 shows the cross-section of a side module at midplane. The first wall is made of stainless steel (SS) with rectangular coolant channels of 5 mm × 10 mm. The thickness of the first wall is 15 mm; front SS layer is 3 mm thick, and rear SS layer 7 mm thick. The coolant channel is oriented toroidally. Each alternate coolant channel is connected to an independent cooling loop, thus a double cooling circuit is prepared for the first wall

in order to increase reliability under a LOCA in one cooling circuit. The flow of water coolant through a channel is designed to be in an opposite direction to those of adjacent channels. (During the ITER joint work from July to November, 1990, it was agreed that the influence of a single cooling circuit on reliability would not be so much different from that of a double cooling circuit taking into account of complexities of configurations and systems for the double cooling circuit. Therefore, a single cooling circuit will be pursued for the first wall in the next design work.) Manifolds of the independent first wall coolants are located behind a manifold of breeding zone coolant, which is located behind the breeding zone. The manifolds are oriented poloidally and vary in radial width from 30 mm (minimum) at midplane.

A shield zone is defined as a region behind the first wall manifolds. It consists of SS plates to obtain enough shielding performance and to separate cooling passages of inlet and outlet manifolds. In all manifolds for the first wall, blanket and shield, SS stiffening plates are placed to withstand the water coolant pressure of 1.5 MPa. Holes are drilled into each stiffening plate.

The concept of the upper and lower central modules are similar to that of the side module described above.

Elevation views of outboard side and central modules are shown in Figs 4.2.3 and 4.2.4, respectively. Cooling connections are prepared at the top for side and upper central modules. Coolants of the breeding and shield zones flow downwards from the top through their inlet manifolds, turn at the bottom of modules, and flow upwards through the breeding and shield zones. Coolants of the first wall also flow downwards from the top through inlet manifolds, toroidally through the first wall coolant channels, then upwards through outlet manifolds. Cooling connections for the lower central modules are prepared at the bottom as shown in Fig. 4.2.4. Coolants for the breeding and shield zones flow upwards through each zone, turn at the top of modules, and flow downwards through their outlet manifolds. The concepts of the manifolds and coolant flows are illustrated in Figs 4.2.5 and 4.2.6.

Layouts of coolant pipes at the top and on the bottom are shown in Figs 4.2.7 and 4.2.8, respectively. Sizes of the coolant pipes from each module

are summarized in Table 4.2.1.

Passive coil in the form of 5 mm thick copper plate is attached to upper and lower portions of side modules, and also to upper and lower central modules. The copper plates are on the inside at the first wall and on the outside on the other three sides as shown in Fig. 4.2.9.

#### 4.2.2 Inboard module

An elevation view and the cross-section at midplane of the inboard module are shown in Figs 4.2.10 and 4.2.11, respectively. An inboard submodule is a similar box structure to those of outboard modules, in which the first wall, blanket and shield are integrated. One inboard module consists of three submodules assembled by welding or bolting in the back region, i.e. shield zone.

The first wall consists of SS plate with rectangular coolant channels of 5 mm  $\times$  10 mm. The thickness of the first wall is 15 mm with 3 mm thick front SS layer and 7 mm thick rear SS layer. A double cooling circuit is also prepared for the first wall. (As mentioned above, a single cooling circuit will be employed in the next design.) Flow direction of the first wall coolant is, however, poloidal due to the limited inboard space to provide coolant manifolds for toroidal cooling.

Manifolds of the blanket and first wall coolants are also oriented poloidally and located behind the breeding zone. Detail concepts of manifolds are shown in Figs 4.2.12 through 4.2.14. All coolants for the first wall, blanket and shield flow downwards from the top through their inlet manifolds, turn at the bottom, and flow upwards through each zone.

Three submodules are fully integrated at the upper recess region; virtually their manifolds are integrated into one cooling passage for each zone. Figure 4.2.15 shows the concept of submodule integration. Piping layout at the top for inboard modules is indicated in Fig. 4.2.16 based on the numbers and sizes of pipes summarized in Table 4.2.1.

Table 4.2.1 Estimates of heat load distribution/coolant flow rate/pipe diameter (for assumed fusion power: 1300 MW)

Region	Heat Load		Coolant Temp. [°C]		No. of Modules/ Circuits	Flow Rate*1		Pipe Dia.*2 [mm]	Velocity [m/s]	No. of Inlet+Outlet Manifolds	
						[t/h]	[m³/s] per Module			per Module	per Sector
		Sur-face	Nuclear	Total	In-Out	ΔT					top/bottom
Inboard											
First wall	26	66	92	60-100	40	32/2	986	0.00882	50/60	2+2/-	64+64/-
Blanket	-	183	183	60-100	40	32/1	3920	0.0351	100/110	1+1/-	32+32/-
Shield*3	-	110	110	60-100	40	32/1	2360	0.0211	80/90	1+1/-	32+32/-
Shield Plug*4	-	45	45	60-100	40	32/1	964	0.00863	50/60	-1+1	-/32+32
Inboard Total	26	404	430								
Outboard											
Side Module											
First Wall	52	169	221	60-100	40	32/2	2370	0.0212	80/90	2+2/-	64+64/-
Blanket	-	468	468	60-100	40	32/1	10000	0.0897	150/160	1+1/-	32+32/-
Shield	-	13	13	60-100	40	32/1	279	0.00249	50/60	1+1/-	32+32/-
Center/Top											
First Wall	8	25	33	60-100	40	16/2	354	0.00633	50/60	2+2/-	32+32/-
Blanket	-	75	75	60-100	40	16/1	1610	0.0288	90/100	1+1/-	16+16/-
Shield	-	3	3	60-100	40	16/1	64.3	0.00115	50/60	1+1/-	16+16/-
Center/Bottom											
First Wall	8	25	33	60-100	40	16/2	354	0.00633	50/60	-2+2	-/32+32
Blanket	-	75	75	60-100	40	16/1	1610	0.0288	90/100	-1+1	-/16+16
Shield	-	3	3	60-100	40	16/1	64.3	0.00115	50/60	-1+1	-/16+16
Port											
First Wall	10	25	35	(60-100)(40)	(40)	16/2	(375)	(0.00671)	(50/60)	2+2*6	32+32*6
Shield Plug*5	-	65	65	(60-100)(40)	(40)	16/1	(1390)	(0.0249)	(80/90)	1+1*6	16+16*6
Outboard Total	78	946	1024								
Divertor Plate											
Upper	78	32	110	50-65	15	32/1	6320	0.0565	120/130	2+2/-	32+32/-
Lower	78	32	110	50-65	15	32/1	6320	0.0565	120/130	-2+2	-/32+32
Divertor Total	156	64	220								
Vacuum Vessel											
		25	25			32/1					
Total	260	1440	1700							22+22 /8+8 (3+3*6)	352+352/ 128+128 (48+48*6)

#1: in one circuit	*2: 50 mm of minimum inner diameter to be cut and welded from inside	*3: including top shielding region
--------------------	--	------------------------------------

\*4: behind lower divertor plate \*5: TBD for specification of each port

also for specification of each port  
(test modules, heating/current drive devices etc.)

\*6: at middle part

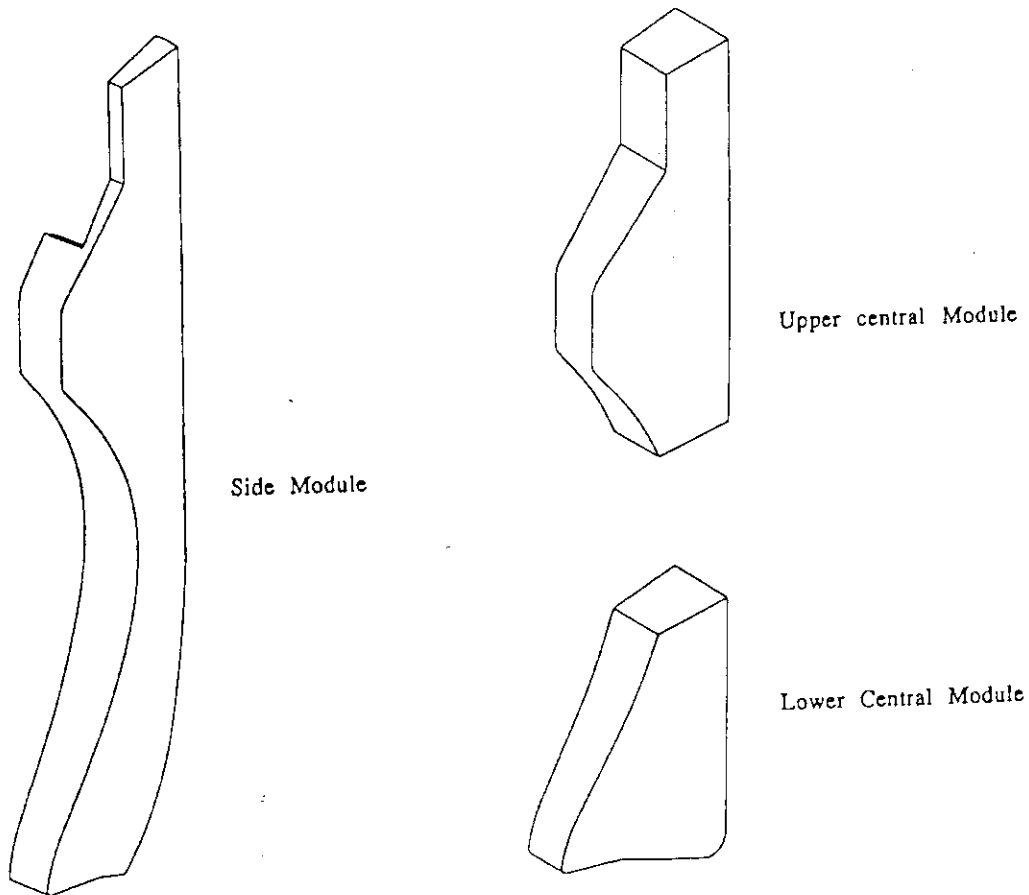


Fig. 4.2.1 Outboard blanket modules

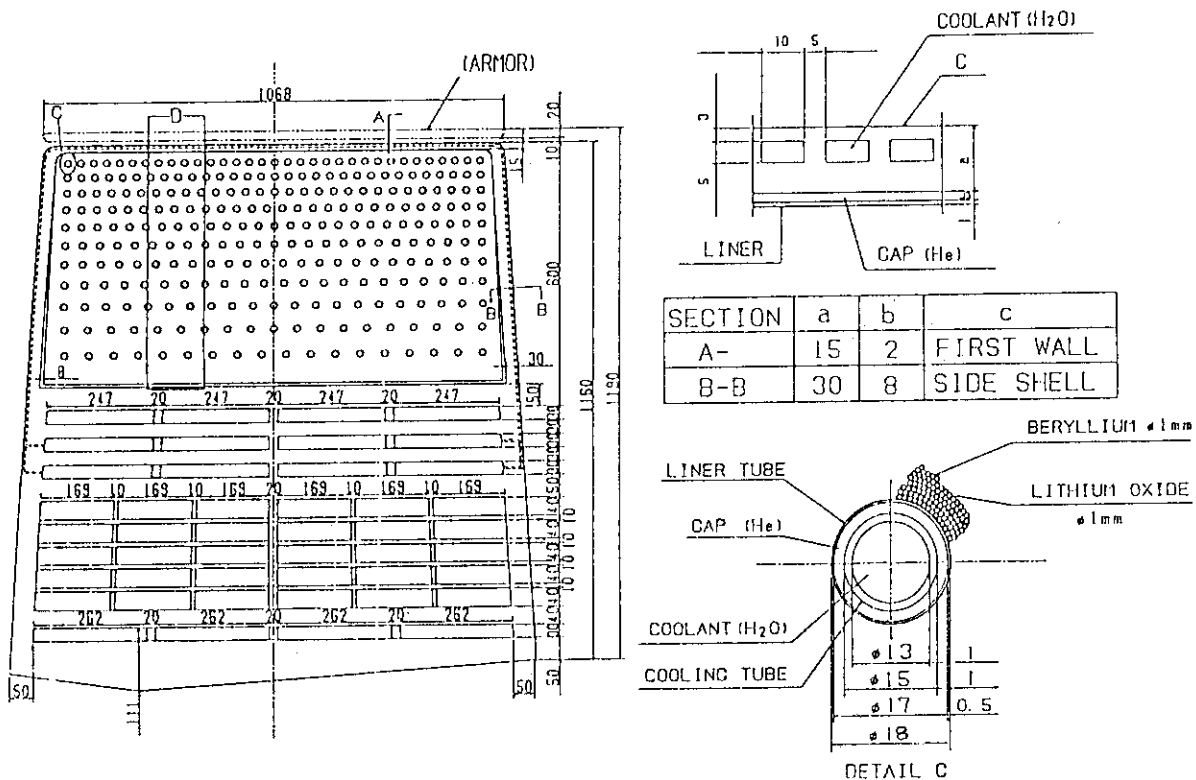


Fig. 4.2.2 Cross-sectional view of outboard side module at midplane (mixed pebble bed blanket)

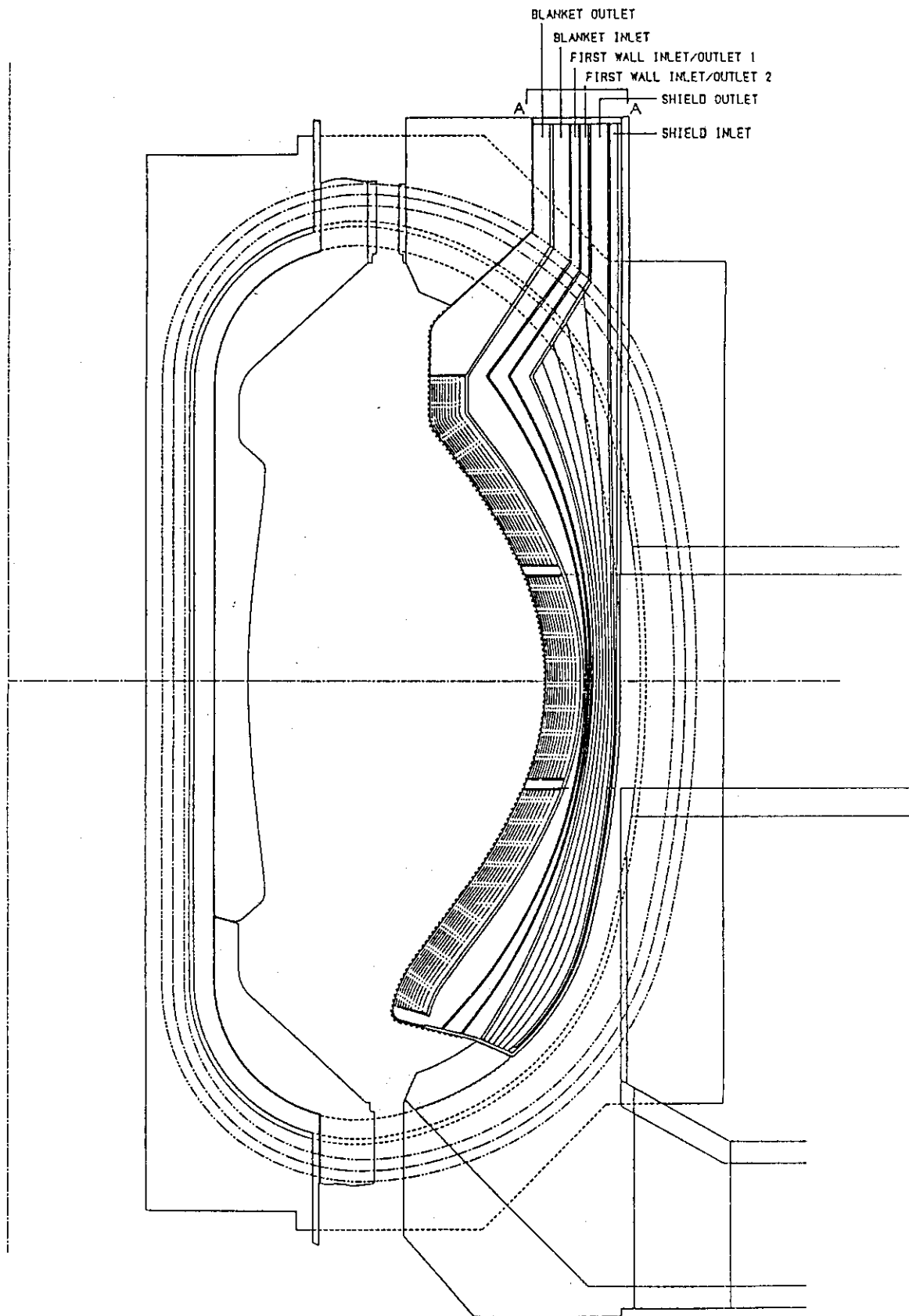


Fig. 4.2.3 Elevation view of outboard side module (mixed pebble bed blanket)

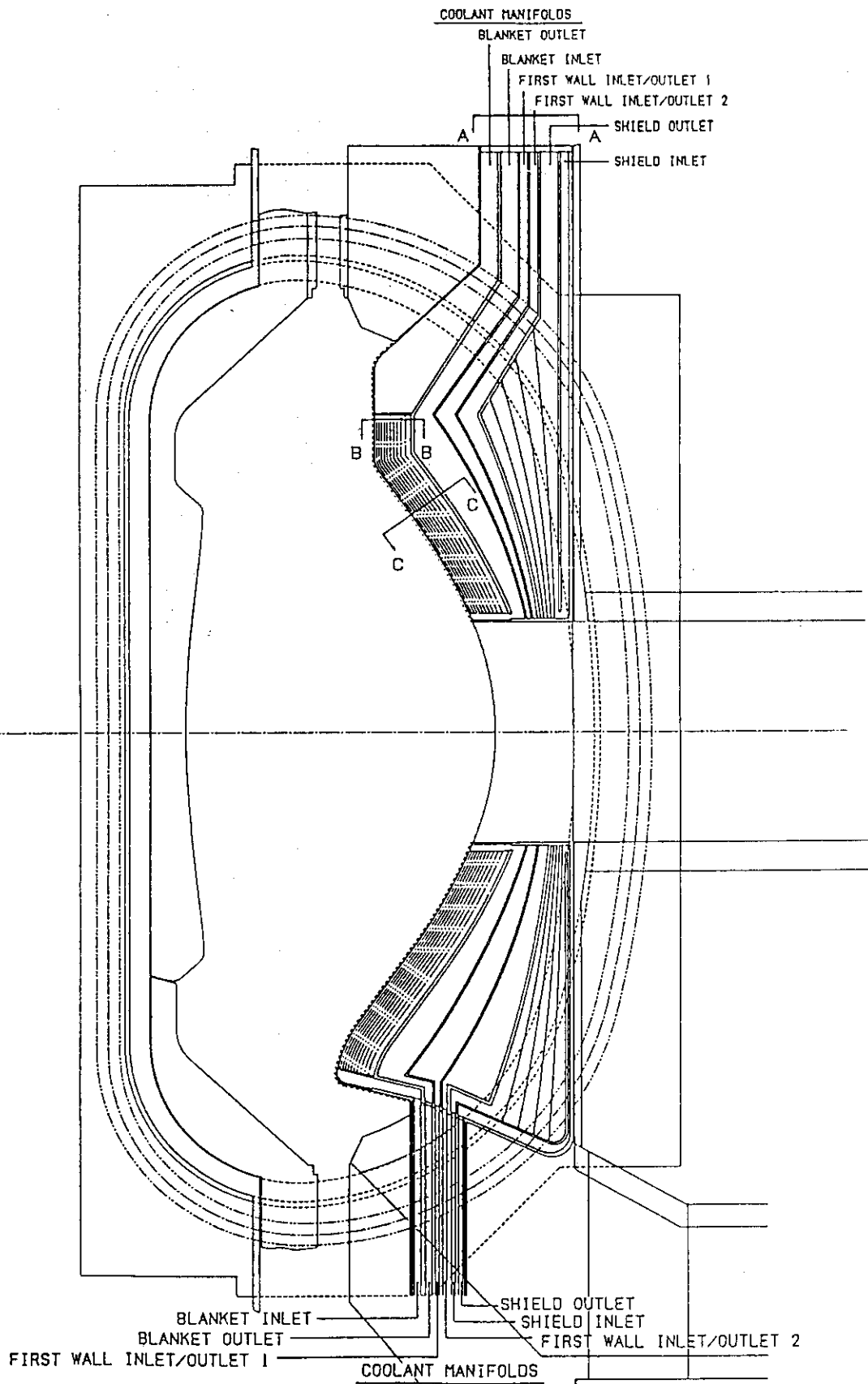


Fig. 4.2.4 Elevation view of outboard central module (mixed pebble bed blanket)



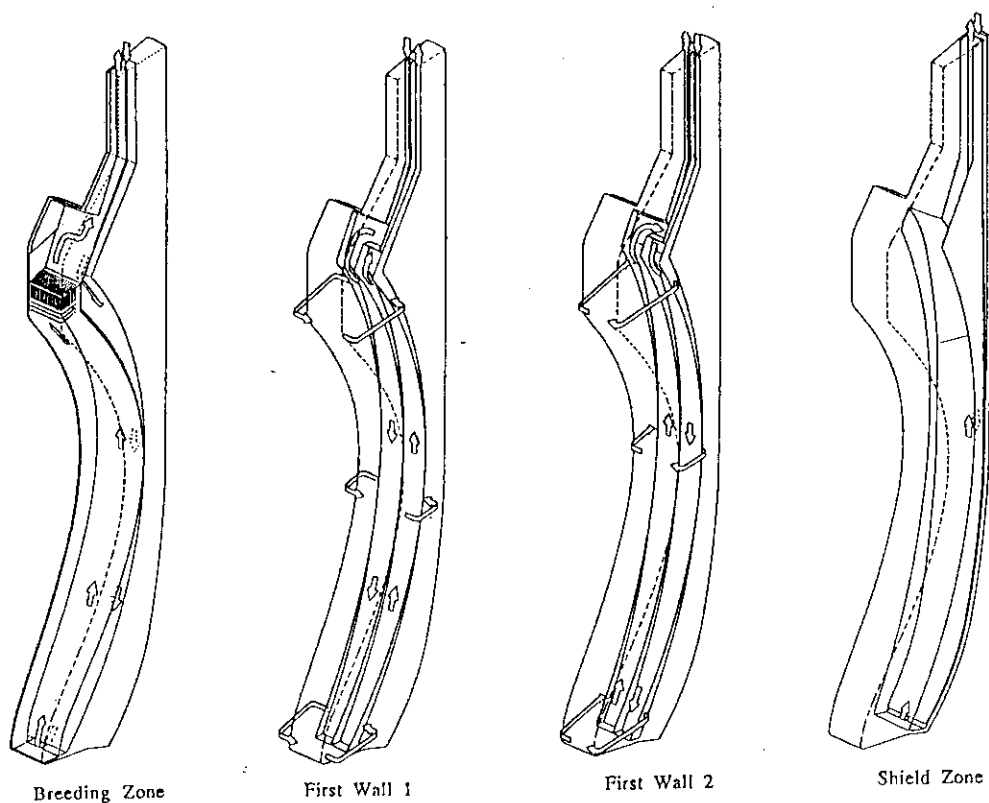


Fig. 4.2.5 Manifolding and coolant flow concepts for outboard side module (mixed pebble bed blanket)

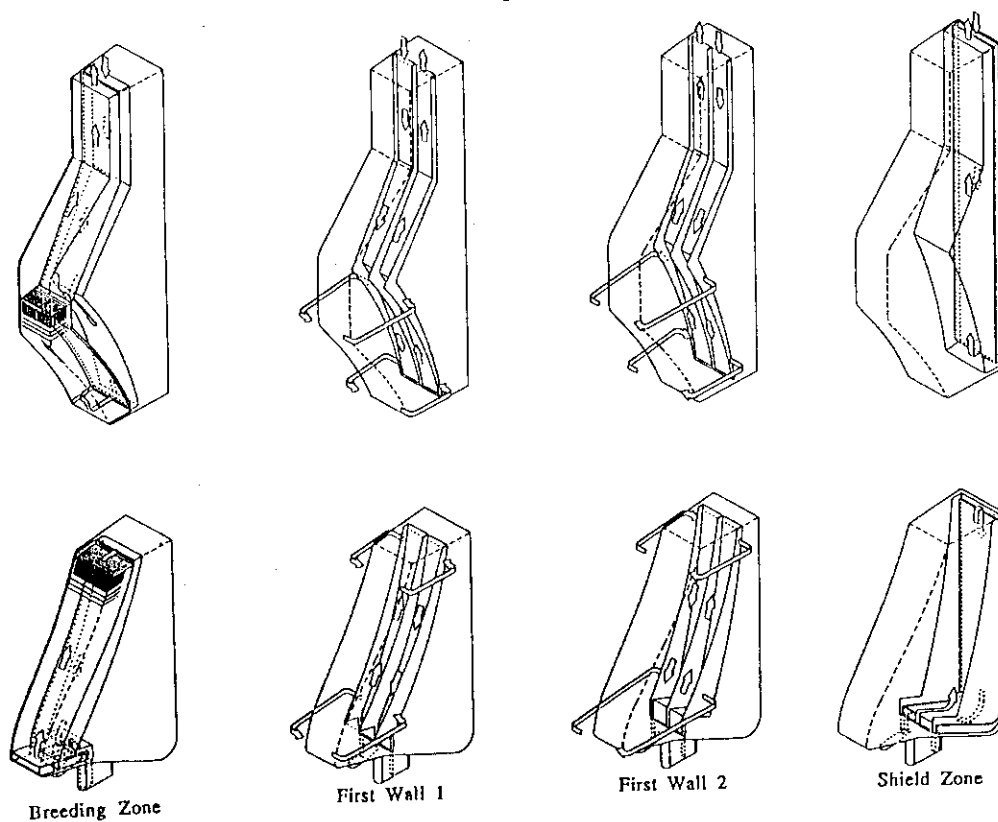


Fig. 4.2.6 Manifolding and coolant flow concepts for outboard central modules

# COOLANT PIPES

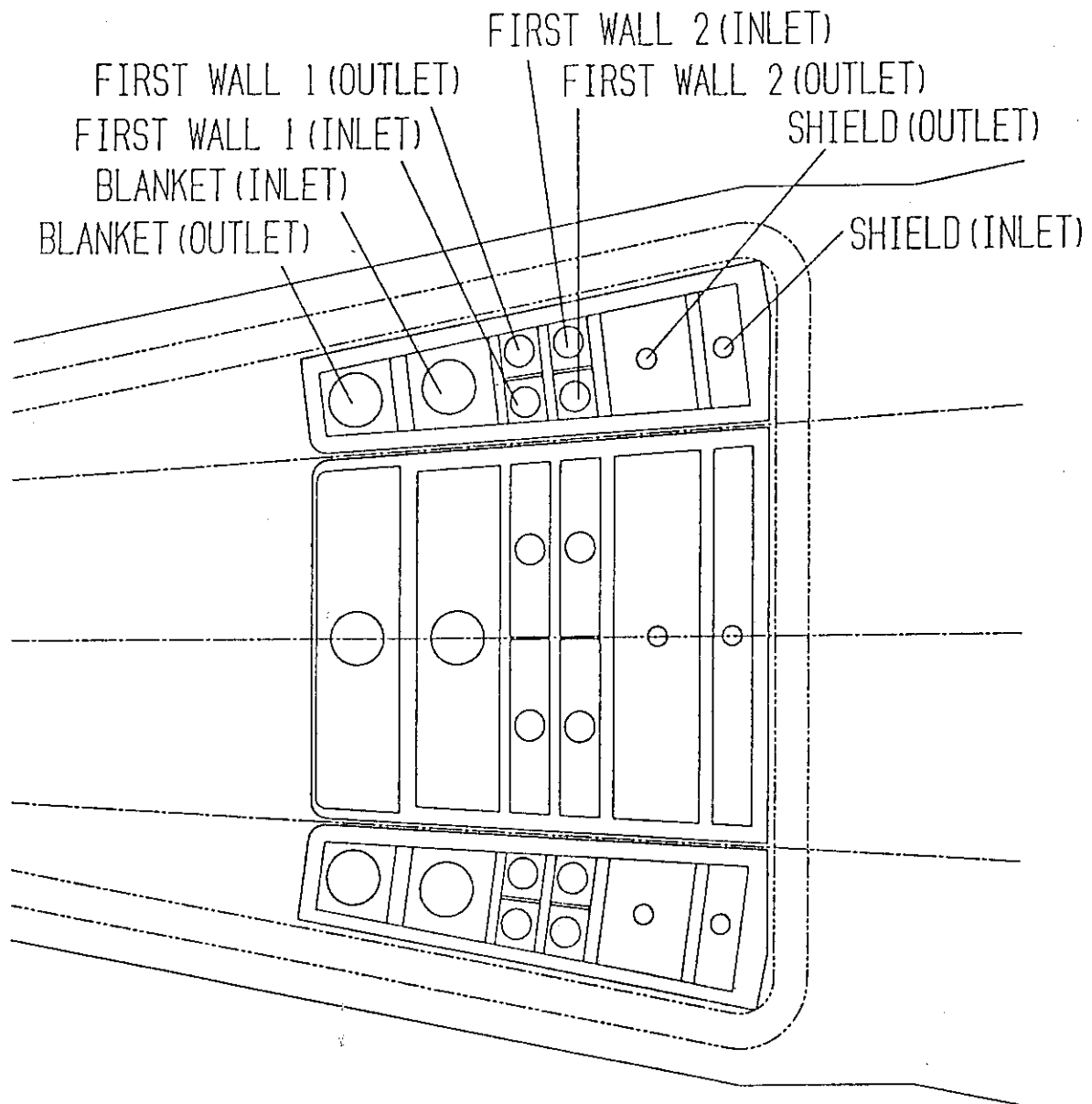


Fig. 4.2.7 Coolant pipes layout of outboard modules at the top (view A-A in Figs. 4.2.3 and 4.2.4)

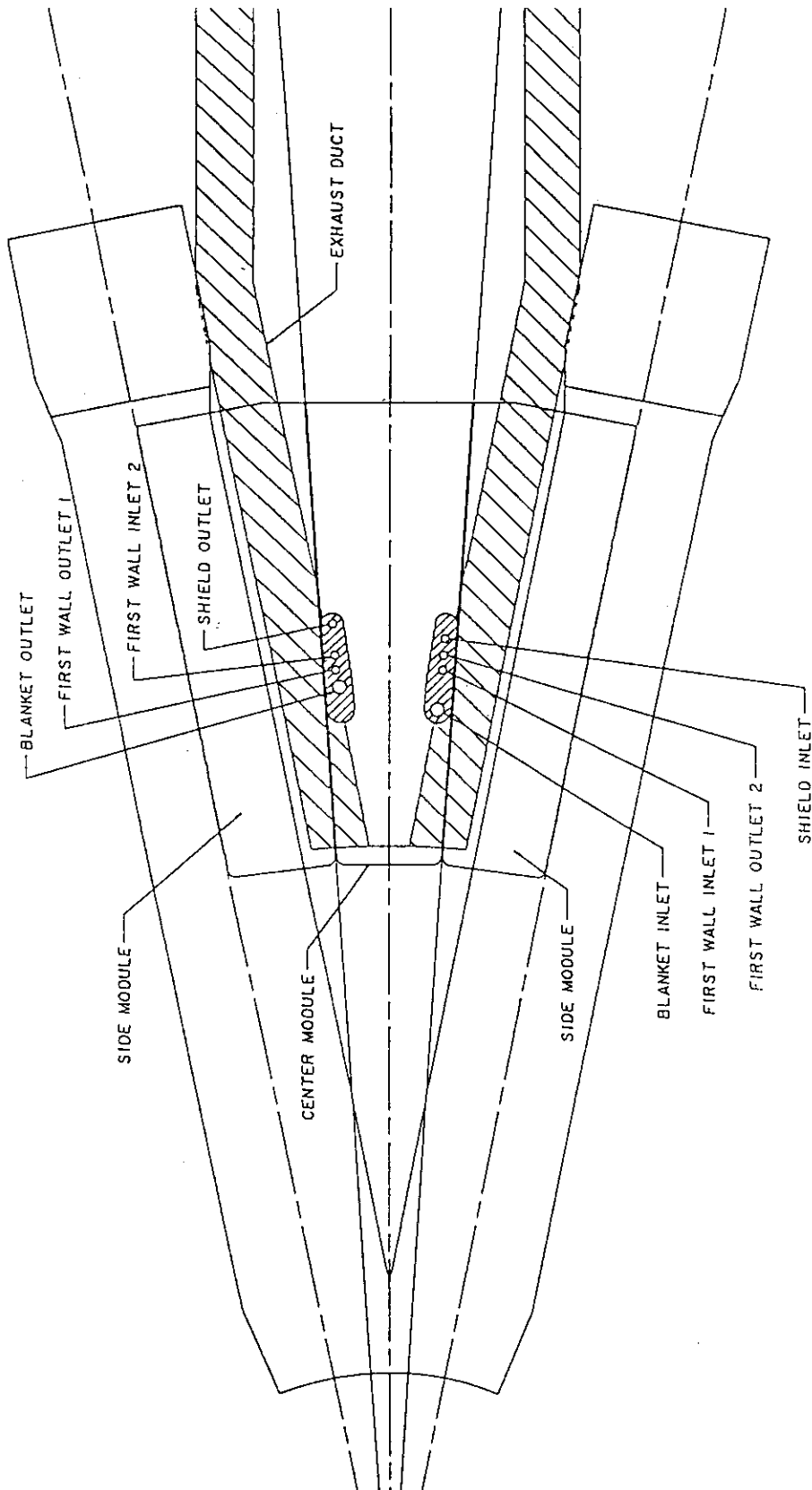


Fig. 4.2.8 Coolant pipes layout for outboard modules on the bottom

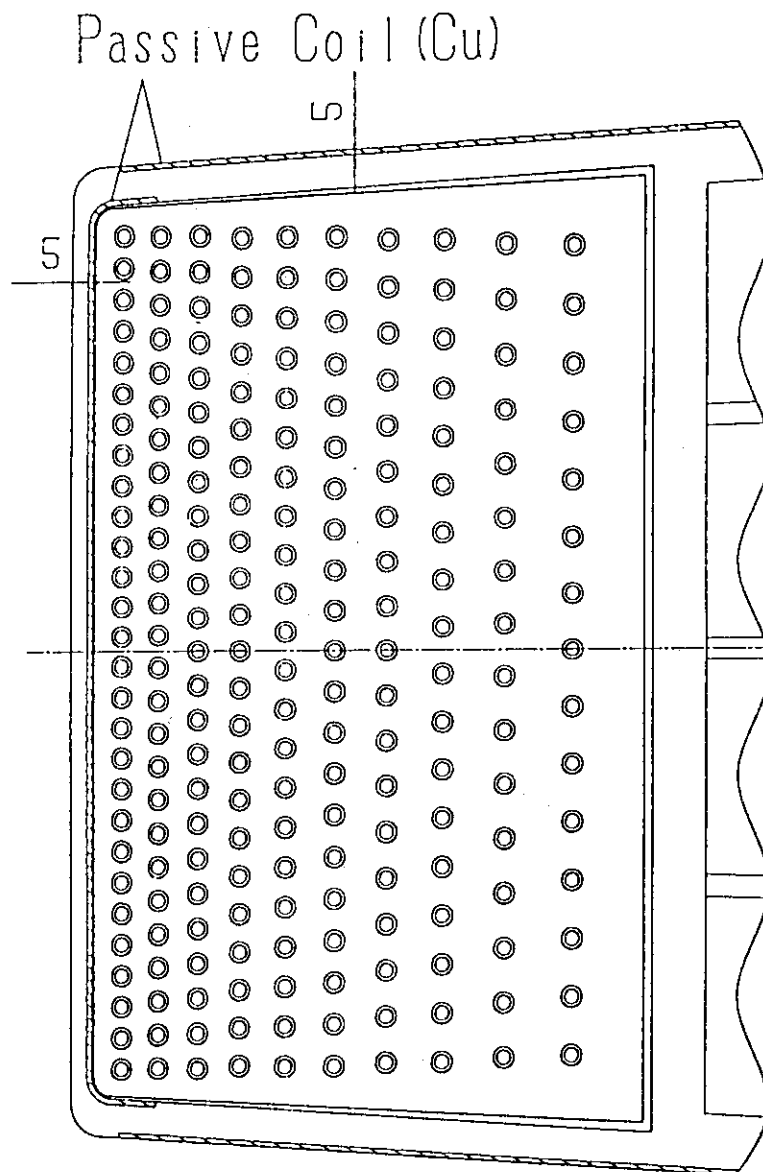


Fig. 4.2.9 Attachment of passive coil

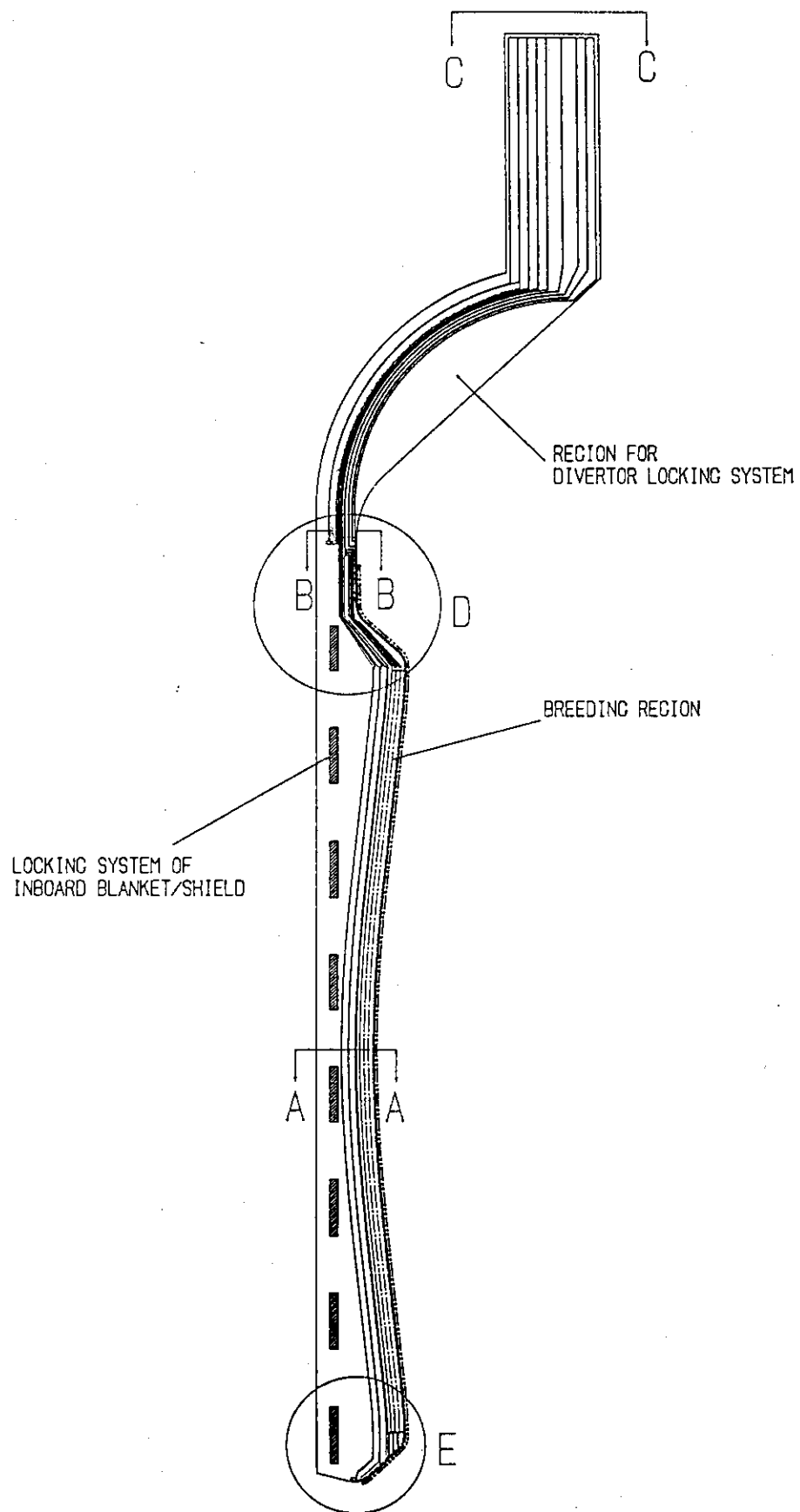


Fig. 4.2.10 Elevation view of inboard blanket (mixed pebble bed blanket)

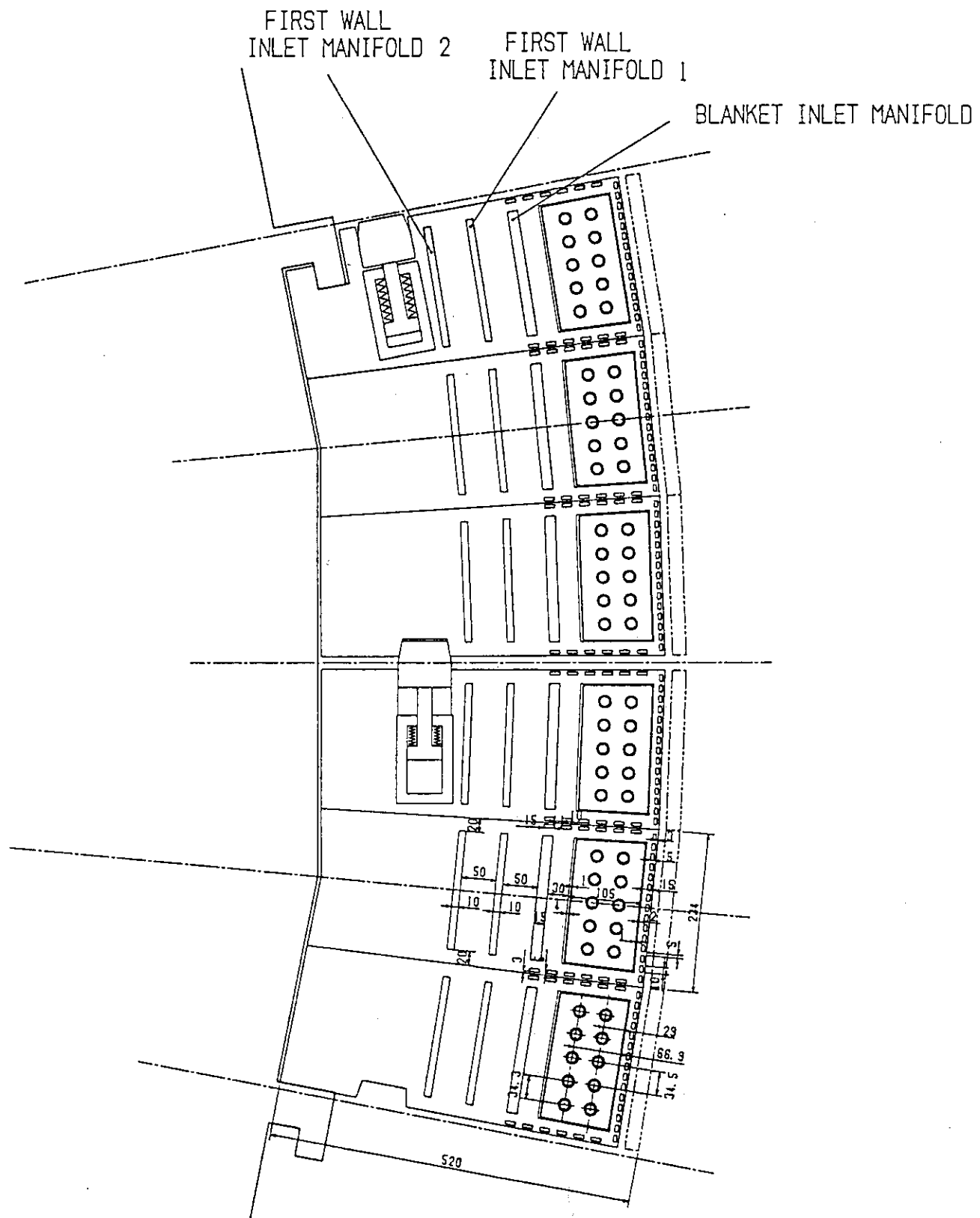


Fig. 4.2.11 Cross-sectional view of inboard blanket at midplane  
(mixed pebble bed blanket)

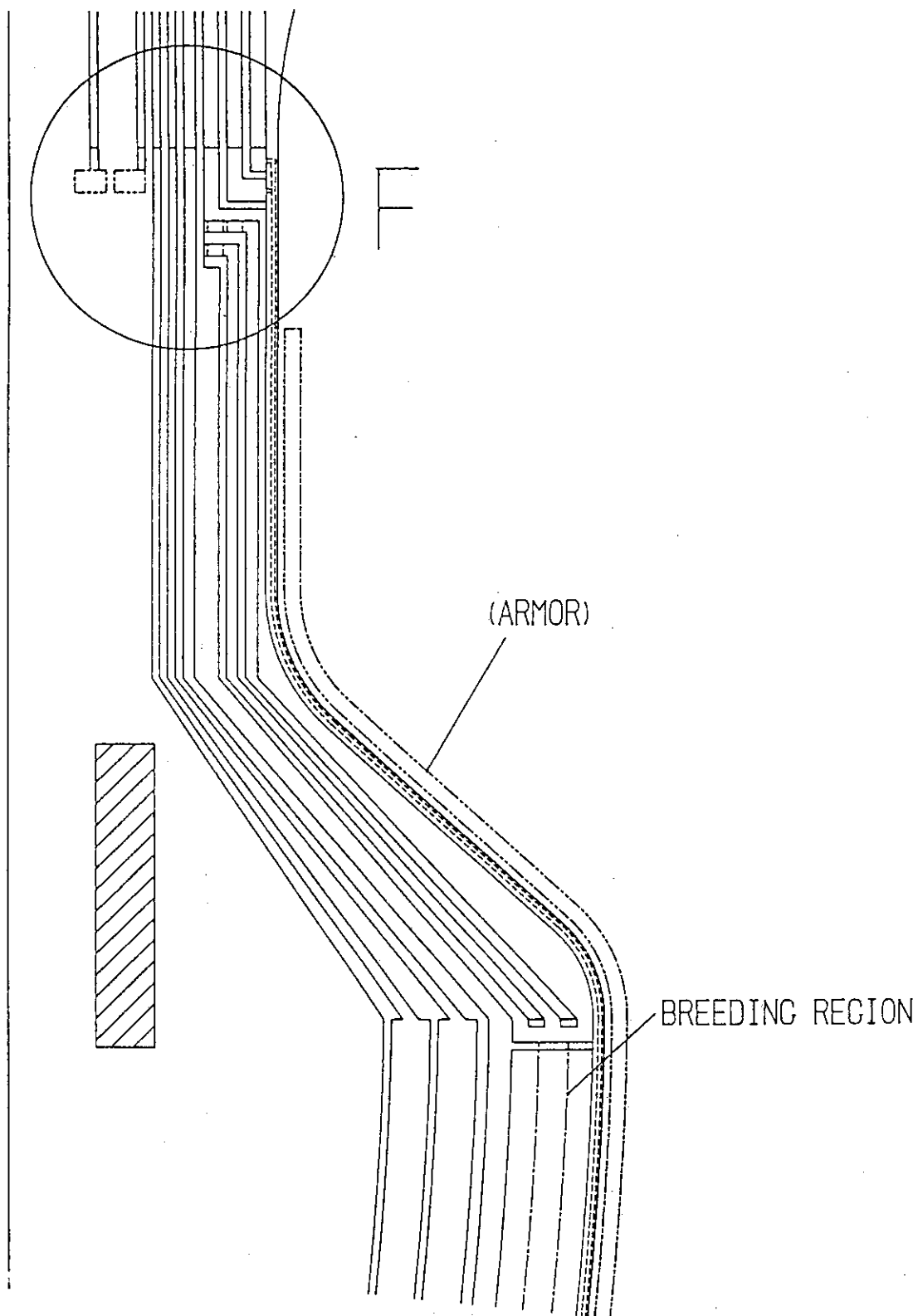


Fig. 4.2.12 Coolant manifolds at the top of inboard blanket  
(detail D in Fig. 4.2.10)

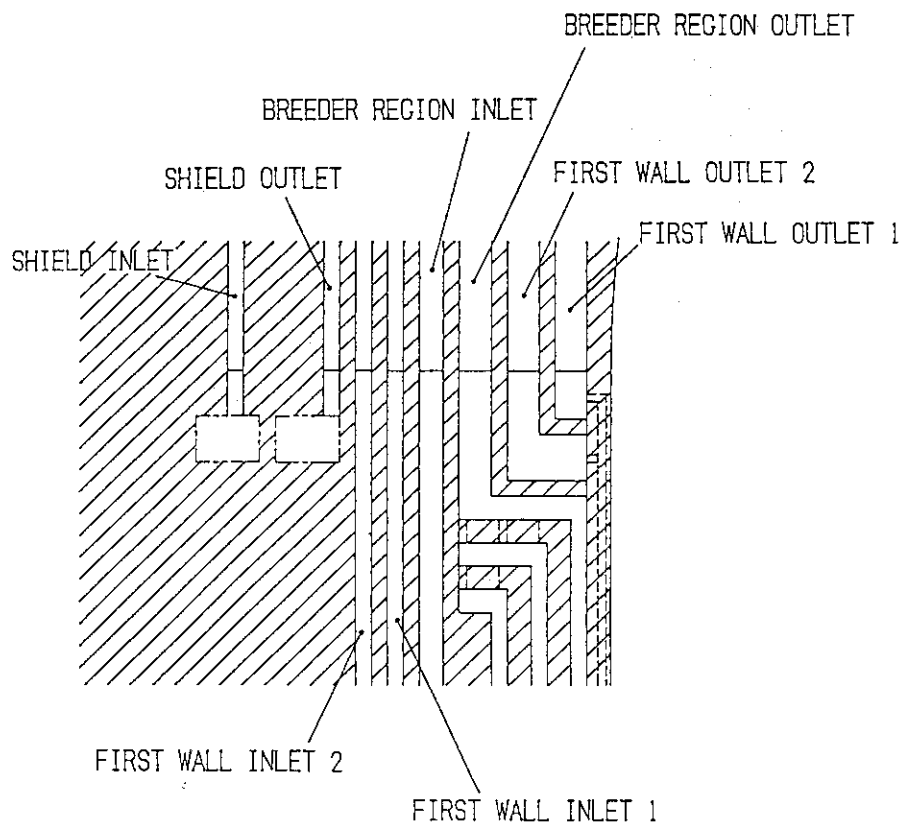


Fig. 4.2.13 Coolant manifolds at the top of inboard blanket  
(detail F in Fig. 4.2.12)

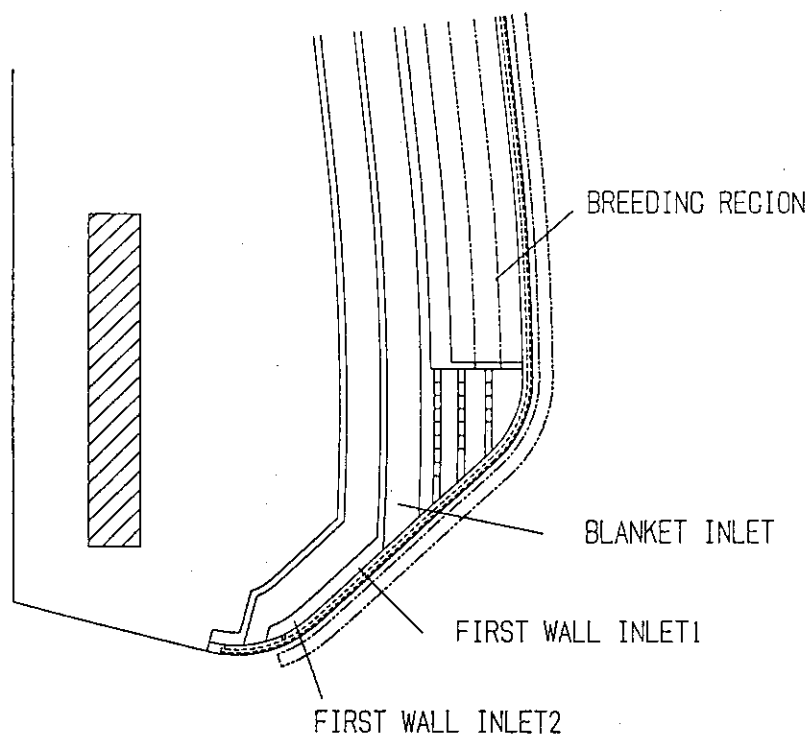


Fig. 4.2.14 Coolant manifolds on the bottom of inboard blanket  
(detail E in Fig. 4.2.10)



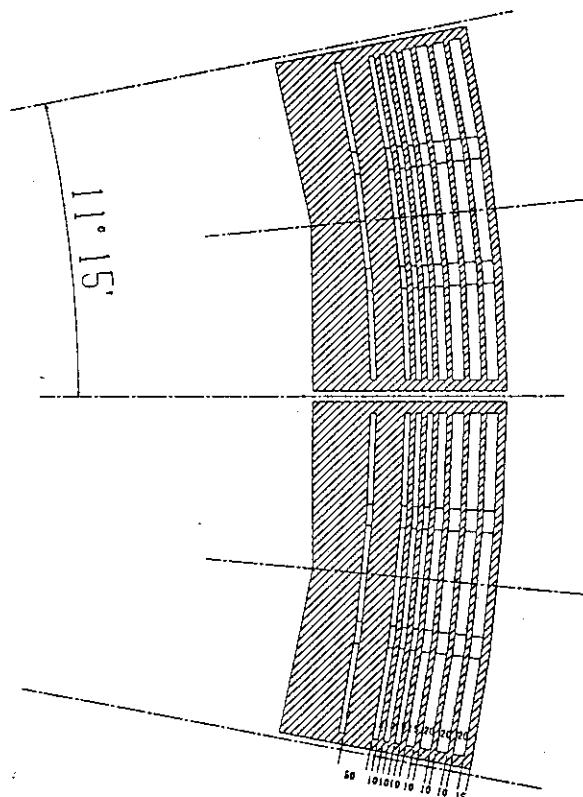


Fig. 4.2.15 Integration of inboard blanket submodules (section B-B in Fig. 4.2.10)

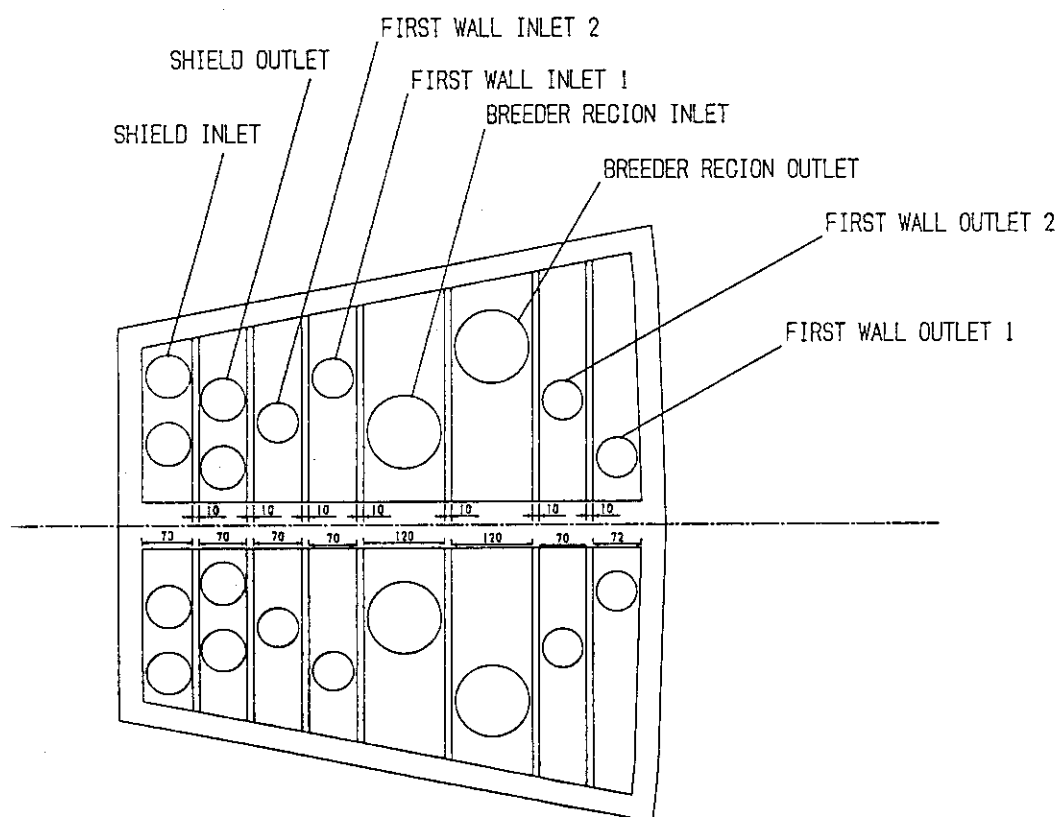


Fig. 4.2.16 Piping layout for inboard modules at the top (view C-C in Fig. 4.2.10)

### 4.3 Blanket Concepts

#### 4.3.1 Mixed pebble bed blanket

A concept of the mixed pebble bed blanket for an outboard module is shown in Fig. 4.3.1. The breeder-out of-tube (BOT) concept is adopted for this design. Homogeneously mixed pebbles of  $\text{Li}_2\text{O}$  breeder and Be multiplier are filled in the box structure. Both pebbles of  $\text{Li}_2\text{O}$  and Be are in the form of small spheres of which the diameter is  $\leq 1$  mm. The mixing ratio of  $\text{Li}_2\text{O}/\text{Be}$  is optimized to be 25/75 % for this design. The homogeneous mixture of the breeder and the multiplier leads to an unnecessary of  $^6\text{Li}$  enrichment to have good tritium breeding performance, or capability to obtain high tritium breeding ratio (TBR) when  $^6\text{Li}$  is enriched. Design packing fraction of pebbles is conservatively chosen to be ~60 %.

The breeder temperature is maintained within a nominal range which is less than the allowable one (400-100°C) in order to have an accommodative capability to power variations. To remove heat generated in the blanket and keep the maximum nominal temperature of the breeder, circular cooling tubes oriented poloidally are arranged according to the nuclear heating rates attenuating in the blanket. To keep the minimum nominal temperature of the breeder for effective tritium recovery from the blanket, helium (He) thermal gap is prepared around the cooling tubes and also inside the blanket walls. The gap widths are 1-3 mm around cooling tubes, 2 mm behind the first wall and 8 mm in front of the back wall at midplane. The thickness of outboard blanket is 60 cm including 15 mm thick first wall and 50 mm thick back wall.

To accommodate the dimensional change and the distribution of wall loading in poloidal direction, an outboard side module blanket is poloidally divided into three sections as shown in Fig. 4.3.2. The lengths of upper and lower sections are the same as those of upper and lower outboard central modules shown in Fig. 4.3.3, respectively. A concept of the coolant manifold between the poloidal sections in outboard side module is illustrated in Fig. 4.3.4. A coolant tube arrangement in the blanket at top region is shown in Fig. 4.3.5.

For inboard blanket, the same concept as that of the outboard blanket is applied. However the thickness of the blanket is reduced to 15 cm including 15 mm thick first wall and 30 mm thick back wall as shown in Fig. 4.3.6.

An elevation view of an inboard module is shown in Fig. 4.3.7. Poloidal division, such as for the outboard side module, would not be needed for the inboard blanket.

Major design parameters of the mixed pebble bed blanket are summarized in Table 4.3.1. Details of performances and characteristics will be mentioned in Chapters below.

#### 4.3.2 Layered pebble bed blanket

A concept of the layered pebble bed blanket is shown in Fig. 4.3.8. The BOT concept is adopted for this blanket. The breeding region consists of Be pebble bed interleaved with  $\text{Li}_2\text{O}$  pebble bed layers and cooling panels oriented poloidally.

Diameters of  $\text{Li}_2\text{O}$  and Be pebbles are both  $\leq 1$  mm. The enrichment of  $^6\text{Li}$  of ~50 % will be required for effective tritium breeding performance. Six breeder pebble layers clad by 1 mm thick stainless steel are installed in the blanket. The gas gap between coolant and  $\text{Li}_2\text{O}$  breeder is not employed in this blanket since the Be pebble zone works also as a thermal resistant layer between them. Thicknesses of  $\text{Li}_2\text{O}$  and Be layers are increased in radial direction according to the attenuation of nuclear heating rates in the blanket, and also vary in poloidal direction in order to accommodate the distribution of neutron wall loading. Thus the blanket thickness varies in poloidal direction with the minimum thickness of 56.2 cm (including 15 mm thick first wall and 50 mm thick back wall) at midplane. Figure 4.3.9 shows the configuration at the top/bottom of which the thickness is increased to 86.3 cm including the first and back walls. Poloidal division of an outboard side module, such as for the mixed pebble bed type blanket, will not be required for this blanket. The cooling panel consists of stainless steel with rectangular coolant channels of 4 mm  $\times$  30 mm. The coolant panel has a uniform thickness of 10 mm from top to bottom; front and rear layers are both 3 mm thick. For the inboard blanket, the same concept can be applied as shown in Fig. 4.3.10.

Major design parameters of the layered pebble bed blanket are summarized in Table 4.3.2. Details of performances and characteristics will be mentioned in Chapters below.

#### 4.3.3 Pebble and block blanket

A concept of the pebble and block blanket is shown in Fig. 4.3.11. The BOT concept is also applied to this blanket. Two layers of  $\text{Li}_2\text{O}$  pebble, which are clad by 1 mm thick stainless steel, are embedded in a Be block zone. The breeder layers have a uniform thickness in poloidal and also in radial directions. On the other hand, the thickness of the Be layers varies both in poloidal and radial directions in order to accommodate the attenuation of nuclear heating rates in the blanket and the poloidal distribution of neutron wall loading.

Temperature differences between coolant and the breeder, which is required for in-situ tritium recovery from the blanket, are maintained by choosing appropriate thicknesses of Be blocks. In addition to that, density of Be blocks is reduced in radial direction to have less thermal conductivity in the region of reduced nuclear heating, i.e. back region, and to prevent the blanket from being too thick. The densities of Be blocks are 85 % of density factor (DF) in the front two rows and 65 % DF in the last two rows in this design. Manifolds of He purge gas are prepared at both toroidal ends of the breeder layer. The cooling panel consists of stainless steel with rectangular coolant channel of 3 mm  $\times$  30 mm. The total thickness of the cooling panel is 9 mm; front SS layer is 3 mm thick and rear SS layer also 3 mm thick.

Major design parameters of the pebble and block blanket are summarized in Table 4.3.3. Performances, especially neutronics and thermal performances, of this blanket will be discussed in Chapter 6 and Section 7.3, respectively.

#### 4.4 Conclusions

Mechanical configuration including module segmentation, integration with first wall/shield, and internal structures of three blanket concepts have been studied. All three blankets can be incorporated into ITER basic machine with the following individual features. The mixed pebble bed blanket, especially outboard side module, needs to be subsegmented into three poloidal sections in the blanket box to accommodate the poloidal distribution of wall loading. In the layered pebble bed blanket, thicknesses of  $\text{Li}_2\text{O}$  and Be pebble packed layers should be varied in poloidal direction for

accommodating the wall load distribution. The pebble and block blanket should also have varying thicknesses of  $\text{Li}_2\text{O}$  packed layer and Be block. For all blankets, a critical issue is to investigate and incorporate stiffening structures to withstand electromagnetic forces during plasma disruption and support structures of cooling channels (and  $\text{Li}_2\text{O}$  pebble packed layers). For the pebble and block blanket, it should be required to secure heat transfer (enough thermal contact) between the clad of  $\text{Li}_2\text{O}$  pebble packed layer and Be block, that reveals to be very difficult as discussed in Section 7.3.

Table 4.3.1 Major Design Parameters of Mixed Pebble Bed Blanket

Breeder	: $\text{Li}_2\text{O}$
Form	: pebble ( $\leq 1$ mm diameter)
Density	: 85-95 % DF
$^6\text{Li}$ enrichment	: natural
Neutron multiplier	: Be
Form	: Pebble ( $\leq 1$ mm diameter)
Density	: 100 % DF
Pebble mixing ratio	: $\text{Li}_2\text{O}/\text{Be} = 25/75$
Pebble packing fraction	: 60 %
Cooling channel	: Poloidal circular tube
Outer/inner tube radius	: 15/13 mm
Blanket thickness	: 60 cm outboard, 15 cm inboard including first wall and back wall
Temperature control of breeder	: He gap and cooling tube arrangement
Gap width	: 1-3 mm around cooling tube
Breeder nominal temperature	: 450-600 °C
Accommodation to power variation	: 20 % increase
Tritium breeding ratio*	
Outboard local	: 1.45 at midplane 1.49 at upper and lower sections
Inboard local	: 0.55 at midplane
Outboard net	: 0.73
Inboard net	: 0.08
Total net	: 0.81
Coolant	: water
Inlet pressure	: 1.5 MPa
Inlet/outlet temperature	: 60/100 °C
Velocity	: $\leq 3$ m/s (outboard), $< 1.5$ m/s (inboard)
Pressure loss	: $\leq 37$ kPa (outboard), $< 20$ kPa (inboard)
Tritium recovery	: He purge gas
Purge gas flow rate	: 240 $\text{Nm}^3/\text{h}$
Pressure	: 0.1 MPa
Pressure loss	: 0.8 kPa
Hydrogen addition	: 0.01 % (H/T = 100)
Tritium inventory in Breeder	: 470 g
* without carbon armor	

Table 4.3.2 Major Design Parameters of Layered Pebble Bed Blanket

Breeder	: $\text{Li}_2\text{O}$
Form	: pebble ( $\leq 1$ mm diameter)
Density	: 85-95 % DF
$^6\text{Li}$ enrichment	: 50 %
Clad thickness	: 1 mm
Neutron multiplier	: Be
Form	: pebble ( $\leq 1$ mm diameter)
Density	: 100 % DF
Pebble packing fraction	: 60 %
Cooling channel	: poloidal cooling panel with rectangular channel
Panel thickness	: 10 mm
Channel size	: 4 mm $\times$ 30 mm
SS thickness	: 3 mm front layer, 3 mm in rear layer
Blanket thickness	: 56.2 cm outboard midplane 86.3 cm outboard top/bottom 15 cm inboard midplane including first wall and back wall
Temperature control of breeder	: thickness of Be pebble bed layer
Breeder nominal temperature	: 450-600°C
Accommodation to power variation	: 25 % increase
Tritium breeding ratio*	
Outboard local	: 1.35 at midplane 1.46 at upper and lower sections
Inboard local	: 0.54 at midplane
Outboard net	: 0.72
Inboard net	: 0.08
Total net	: 0.80
Coolant	: water
Inlet pressure	: 1.5 MPa
Inlet/outlet temperature	: 60/100 °C

\* without carbon armor

Table 4.3.2 (Cont'd)

Tritium recovery	: He purge gas
Purge gas flow rate	: 250 Nm <sup>3</sup> /h
Pressure	: 0.1 MPa
Pressure loss	: 10 kPa
Hydrogen addition	: 0.01 % (H/T = 100)
Tritium inventory in Breeder	: 93 g



Table 4.3.3 Major Design Parameters of Pebble and Block Blanket

Breeder	: $\text{Li}_2\text{O}$
Form	: pebble ( $\leq 1$ mm diameter)
Density	: 85-95 % DF
$^6\text{Li}$ enrichment	: 95 %
Clad thickness	: 1 mm
Pebble packing fraction	: 60 %
Neutron multiplier	: Be
Form	: block
Density	: 85 % DF in front region 65 % DF in rear region
Cooling channel	: toroidal cooling panel with rectangular channel
Panel thickness	: 9 mm
Channel size	: 3 mm $\times$ 30 mm
SS thickness	: 3 mm front layer, 3 mm rear layer
Blanket thickness	: 51.5 cm outboard midplane including first wall and back wall
Temperature control of breeder	: thickness of Be block
Tritium breeding ratio	
Outboard local	: 1.31 at midplane (with 2 cm thick carbon in front of blanket)
Coolant	: water
Inlet pressure	: 1.5 MPa
Inlet/outlet temperature	: 60/100 °C
Tritium recovery	: He purge gas
Pressure	: 0.1 MPa
Hydrogen addition	: 0.01 % (H/T = 100)

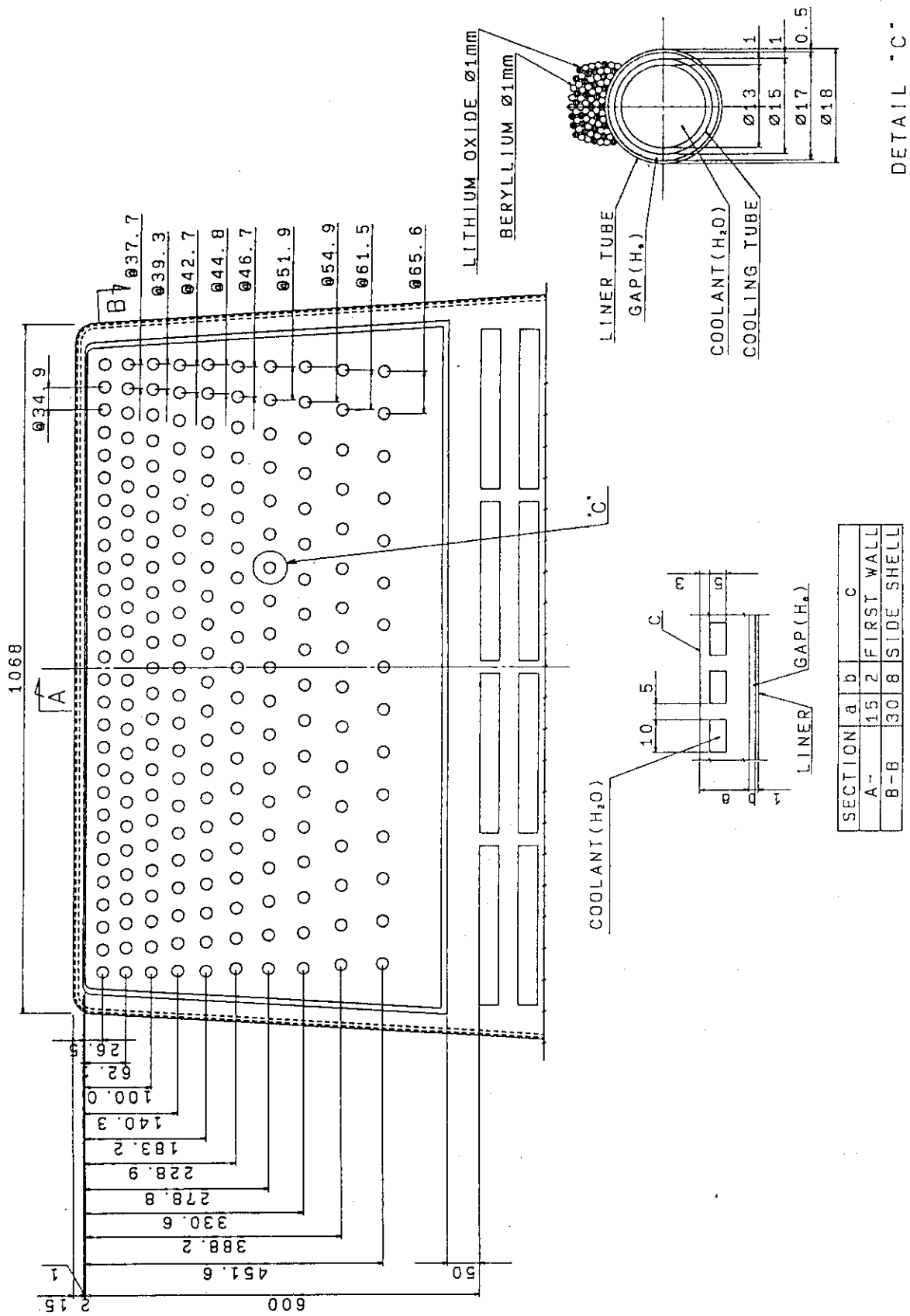


Fig. 4.3.1 Concept of the mixed pebble bed blanket (cross-sectional view of outboard side module at midplane)

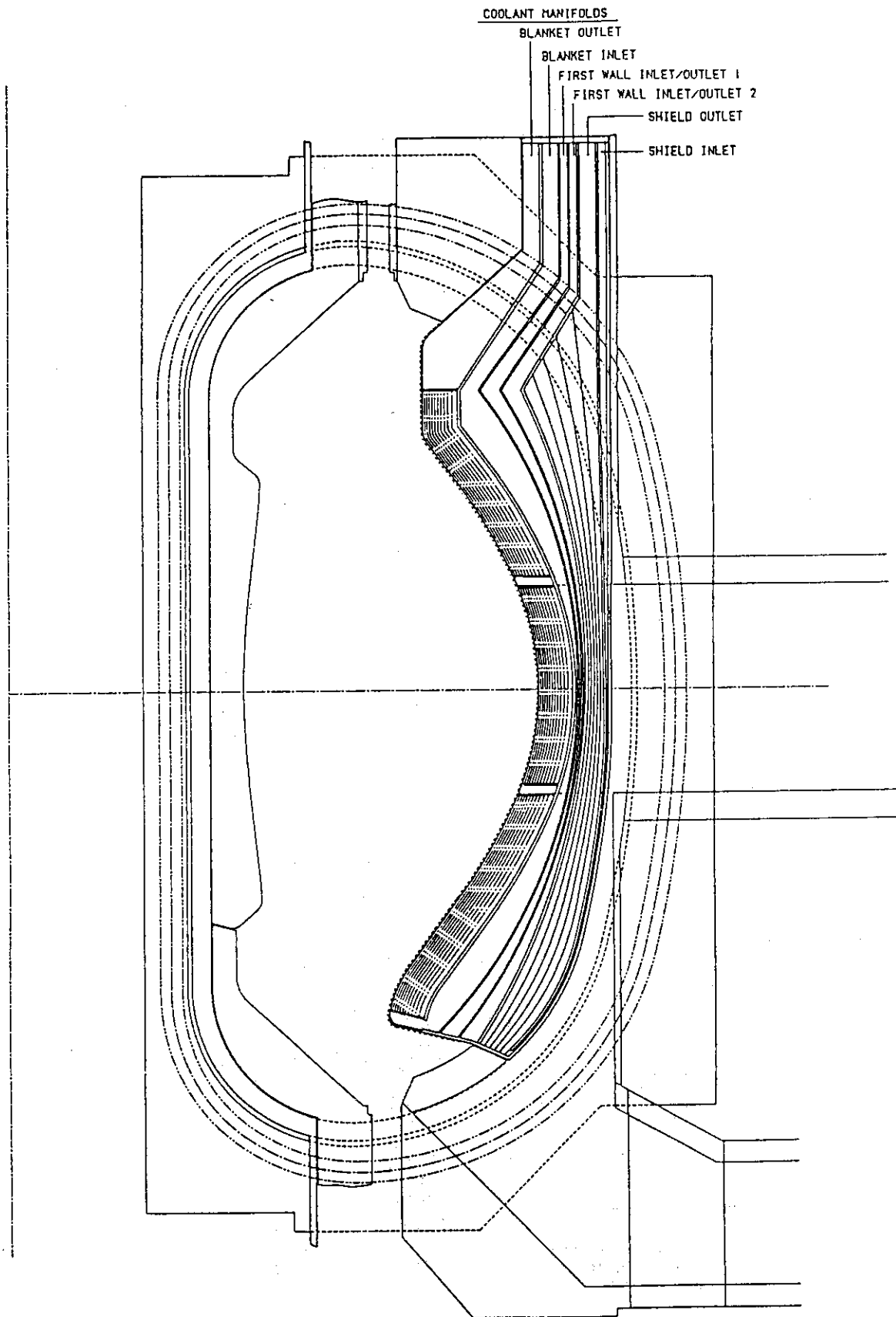


Fig. 4.3.2 Poloidal division for outboard side module of the mixed pebble bed blanket

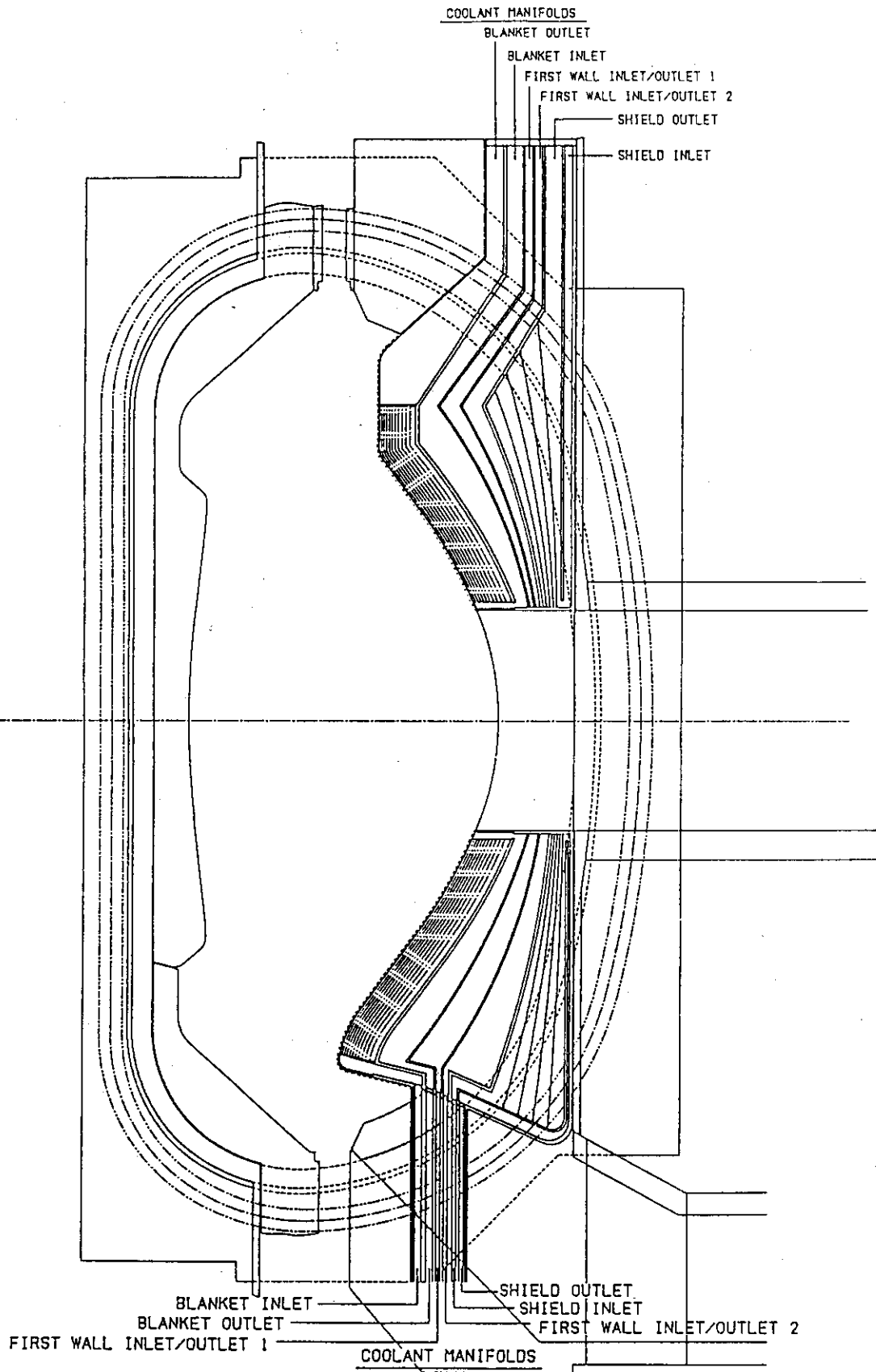


Fig. 4.3.3 Poloidal segmentation of outboard central modules  
(mixed pebble bed blanket)

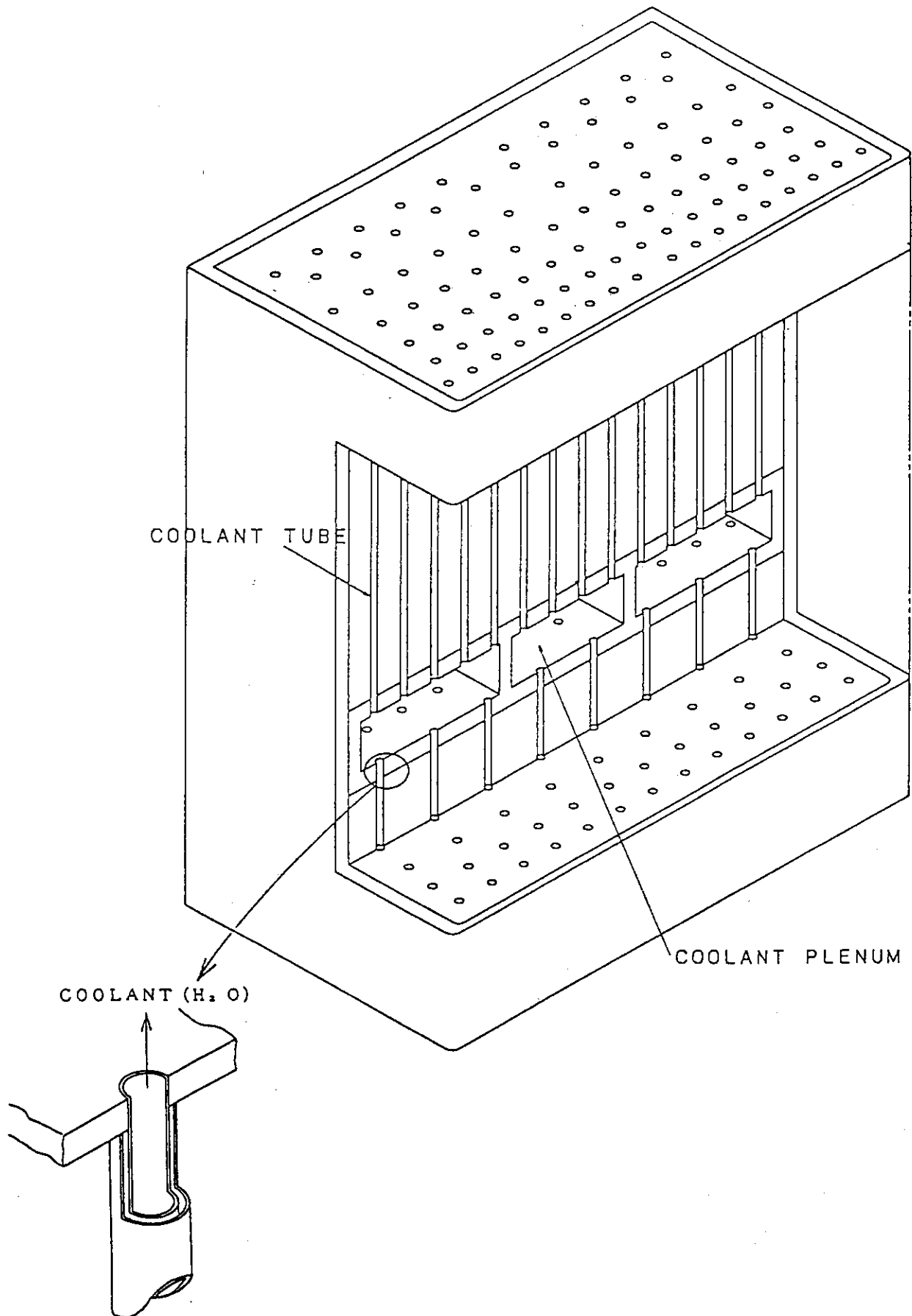


Fig. 4.3.4 Manifold concept for poloidally divided outboard side module of the mixed pebble bed blanket

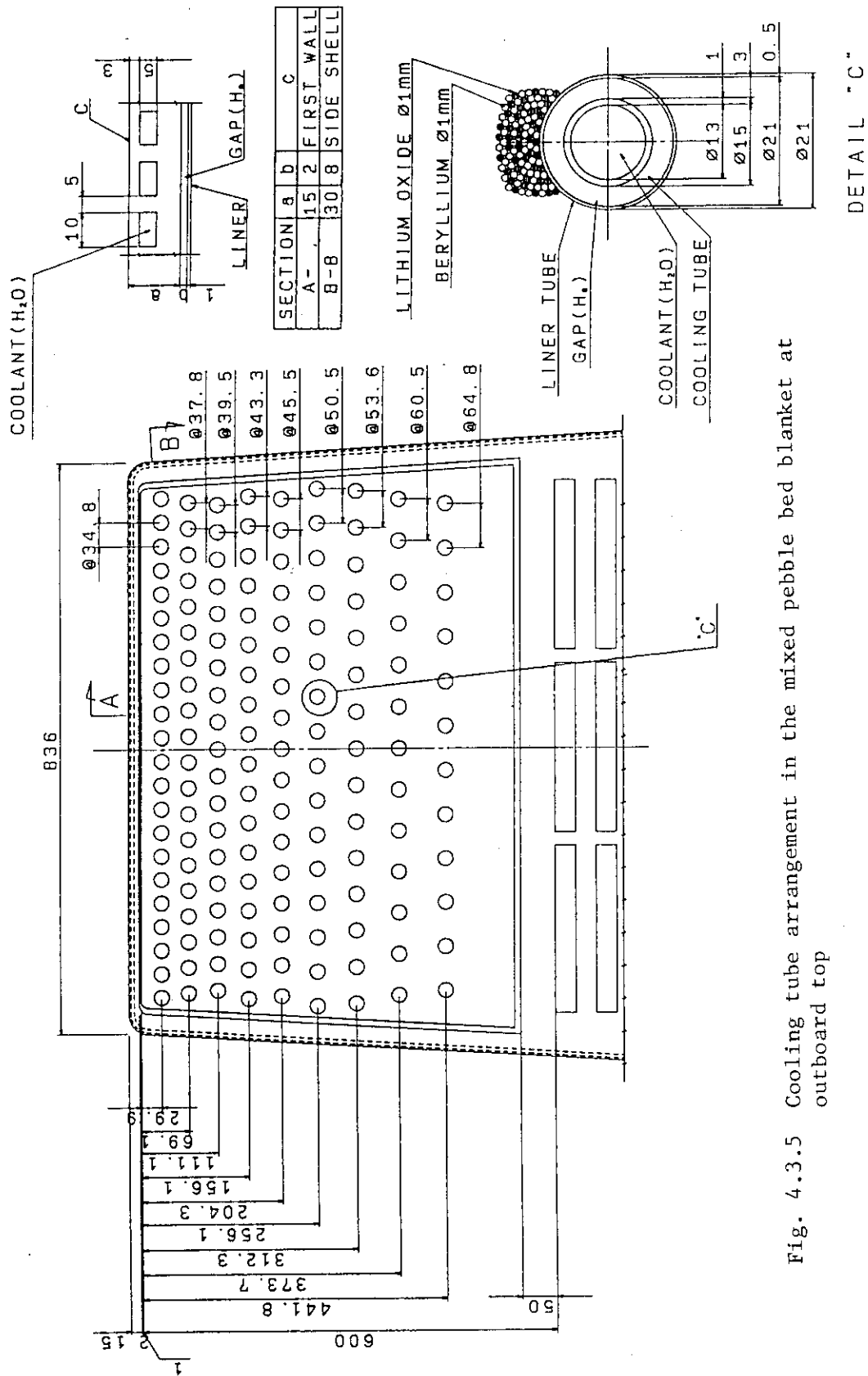


Fig. 4.3.5 Cooling tube arrangement in the mixed pebble bed blanket at outboard top

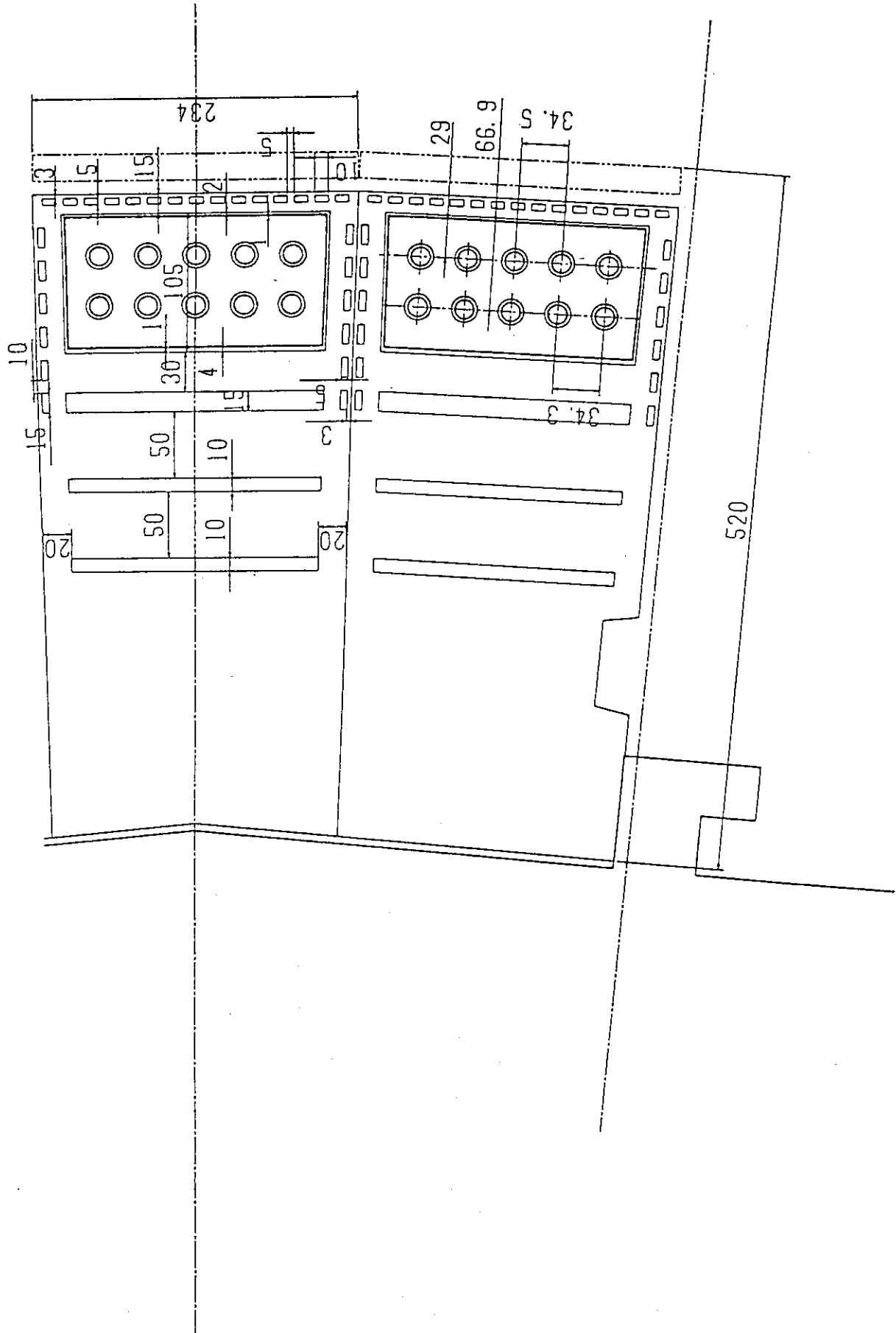


Fig. 4.3.6 Cross-sectional view of the mixed pebble bed blanket at inboard midplane

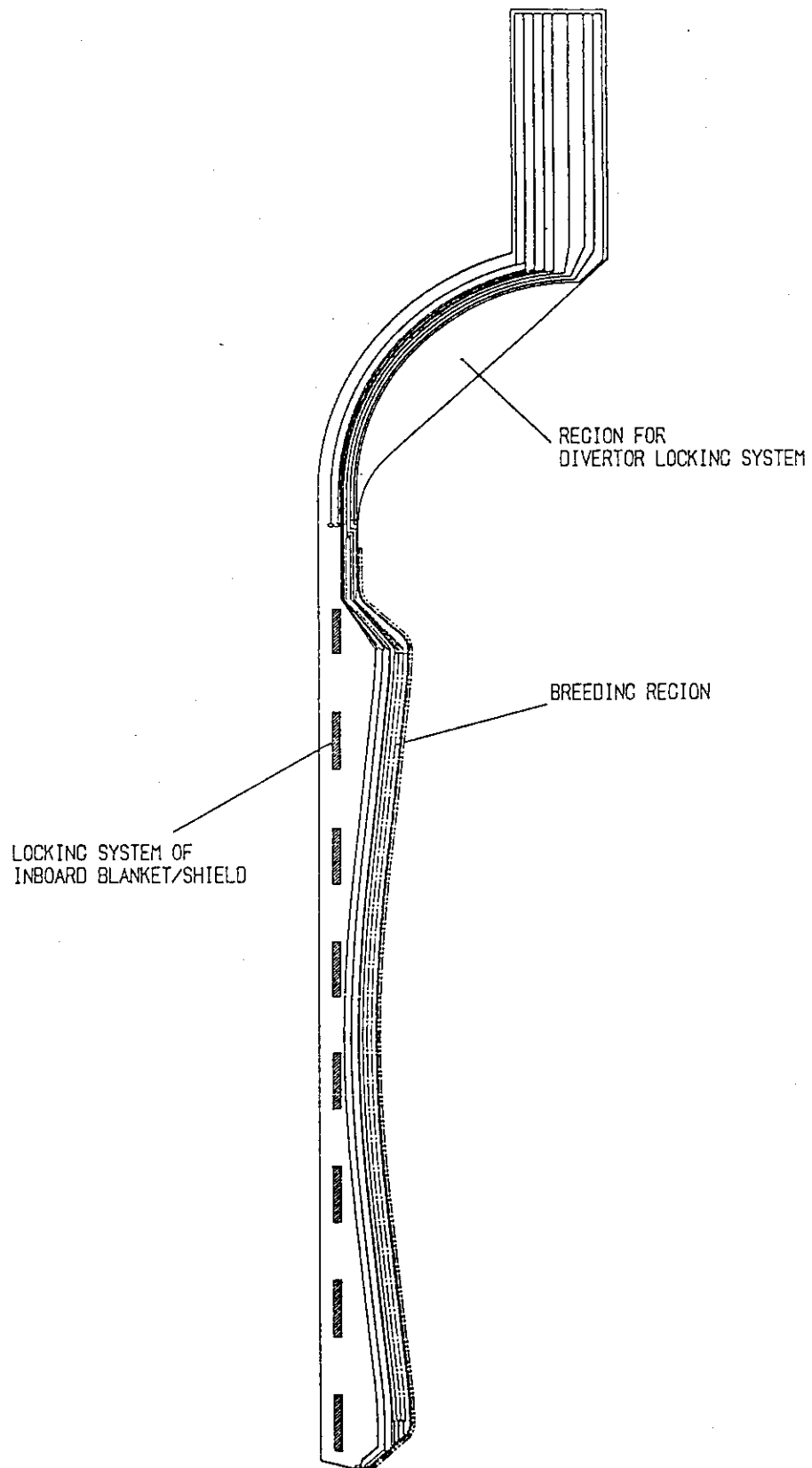


Fig. 4.3.7 Elevation view of inboard mixed pebble bed blanket



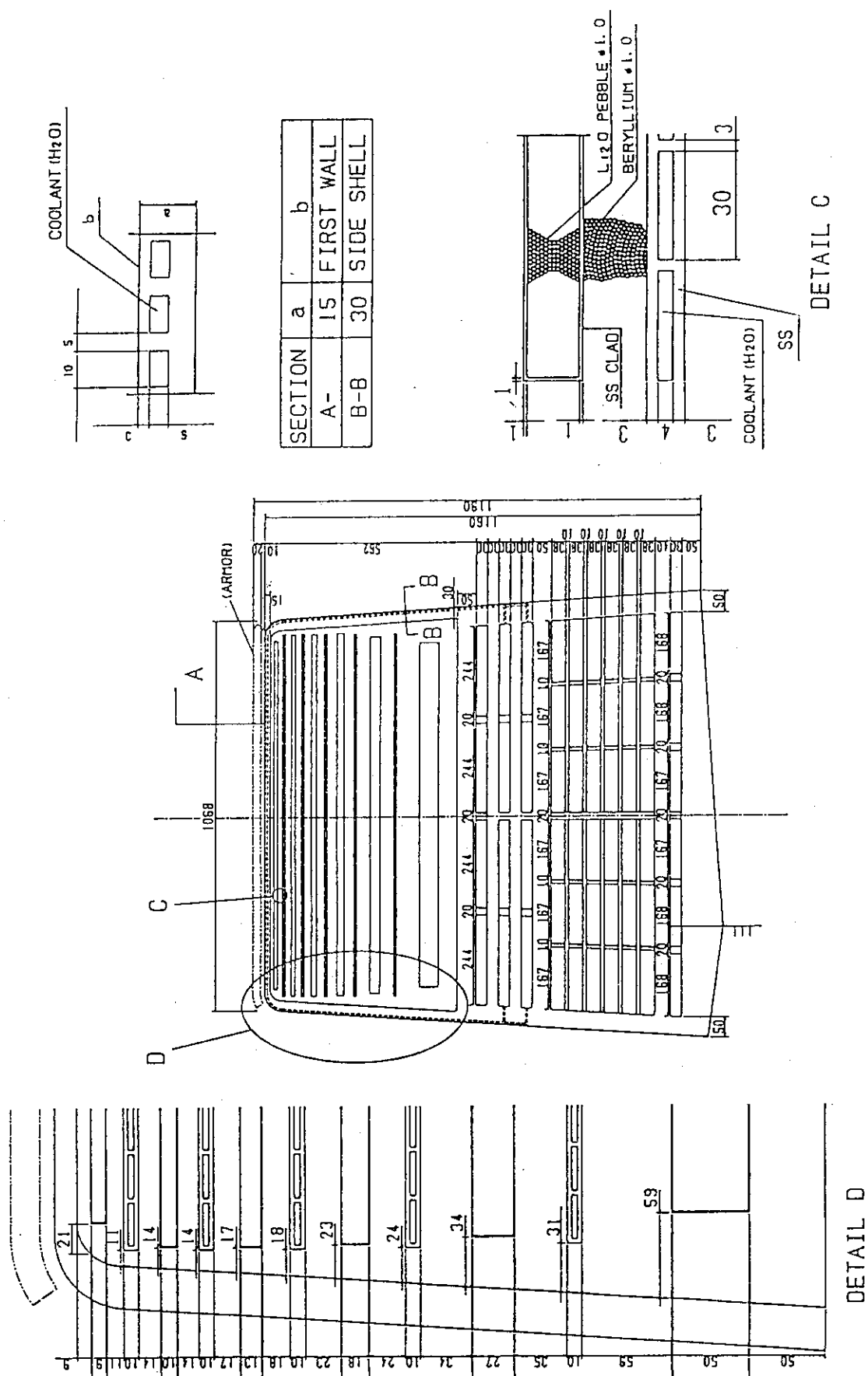


Fig. 4.3.8 Concept of the layered pebble bed blanket (cross-sectional view of outboard side module at midplane)

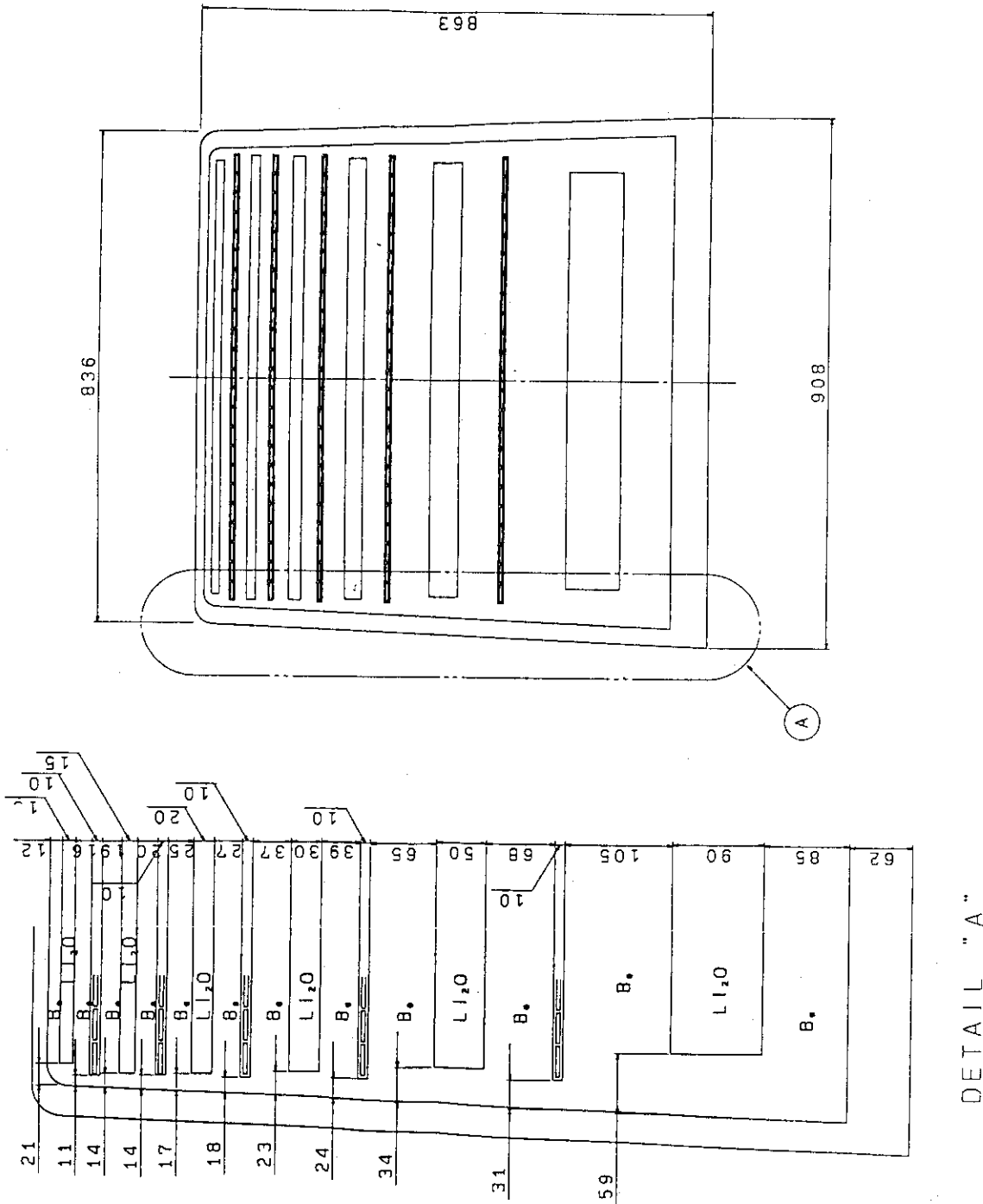


Fig. 4.3.9 Layer arrangement in the layered pebble bed blanket at outboard top

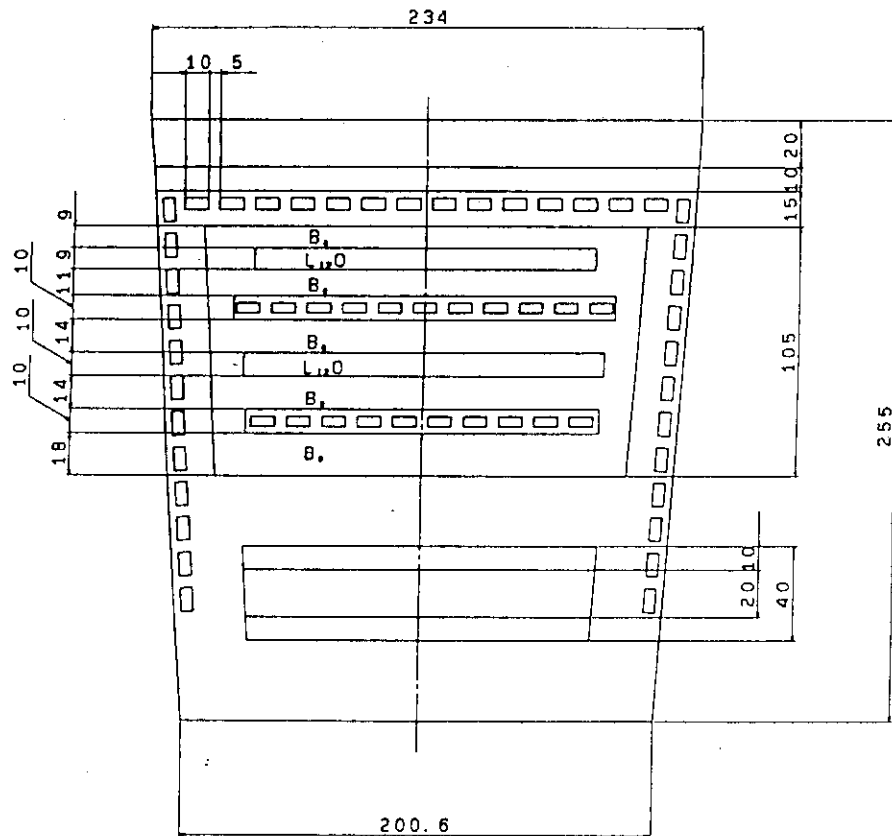


Fig. 4.3.10 Layer arrangement in the layered pebble bed blanket at inboard midplane

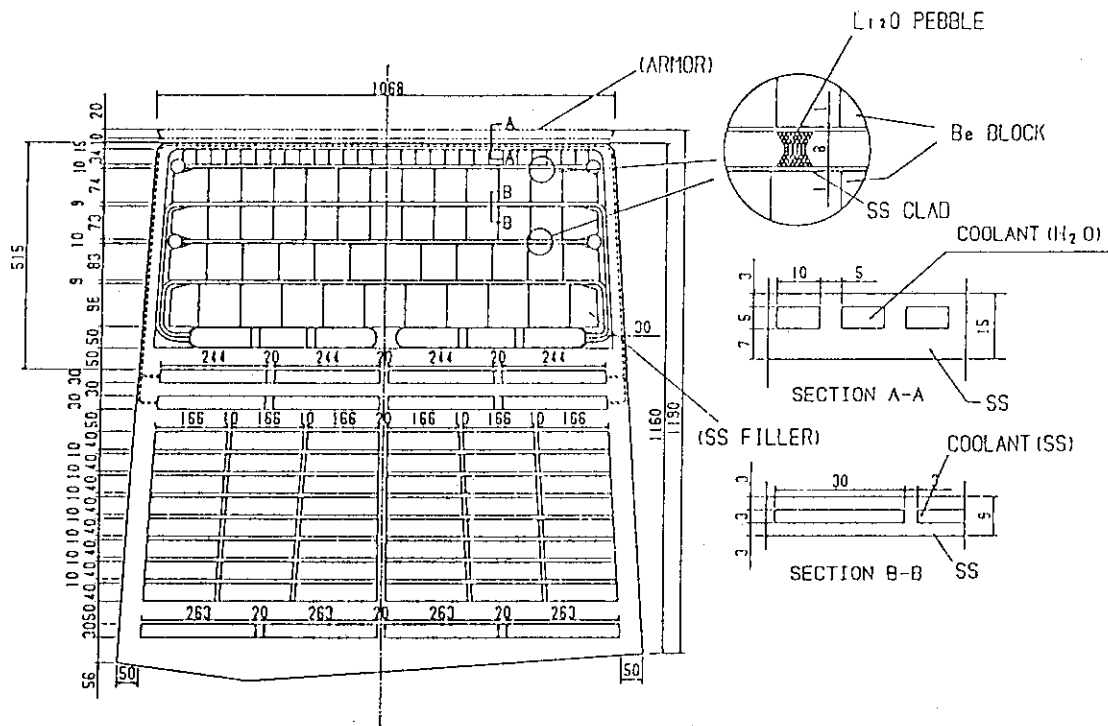


Fig. 4.3.11 Concept of the pebble and block blanket (cross-sectional view of outboard side module at midplane)

## 5. Fabrication and Assembly of First Wall/Blanket/Shield

Fabrication and assembly procedures of the mixed pebble bed blanket and layered pebble bed blanket have been preliminary investigated, which are described in Sections 5.1 and 5.2, respectively. A pebble production method of ceramic breeder which is one of key technologies for the fabrication of pebble type blanket is shown in Section 5.3.

### 5.1 Mixed Pebble Bed Blanket

Fabrication procedure of the mixed pebble bed blanket is shown in Fig. 5.1.1. The blanket is divided into four main parts; 1) first wall and side wall (including copper shell and wall liner), 2) cooling tube bundle (including tubesheets and plenum box), 3) back wall and top/bottom wall (including wall liner), 4) breeder and multiplier pebbles. They are assembled after those parts are fabricated or produced and tested separately.

Two bent plates and rectangular tubes are bonded by three-dimensional joint technique by HIP to form the first wall/side walls of the top, middle, and bottom units (see Fig. 5.1.2). The copper shell plate is fixed to the inner surface of the first wall and outer surface of the side wall by brazing, explosion bonding or diffusion bonding. Then protruding spacer pins are attached to the inner surface of the first wall/side wall (or copper shell). Wall liner plates for breeder temperature control are attached on the protruding spacer pins except internal plenum region by spot welding or mechanical attachment (see Fig. 5.1.3).

The back wall and the top/bottom walls are fabricated in the same manner as the first wall. Openings for breeder/multiplier pebble packing are provided in the back wall.

Tube bundle is composed of double walled cooling tubes and tubesheets. The tubesheet is the part of inlet/outlet headers or internal plenums (see Fig. 5.1.4). It also functions as spacer for cooling tubes.

The first wall/side wall and the tube bundle are assembled by welding the first wall/side wall and the internal plenum box (see Fig. 5.1.4 and 5.1.5). Finally, the back wall and the top/bottom walls are welded.

Before breeder/multiplier pebbles are packed in the blanket vessel. pressure and leak tests of the vessel and cooling tubes will be conducted with the openings for pebble packing being closed temporarily.

The breeder/multiplier pebbles are packed from the openings in the back wall on a shaking table in inert gas atmosphere (see Fig. 5.1.6).

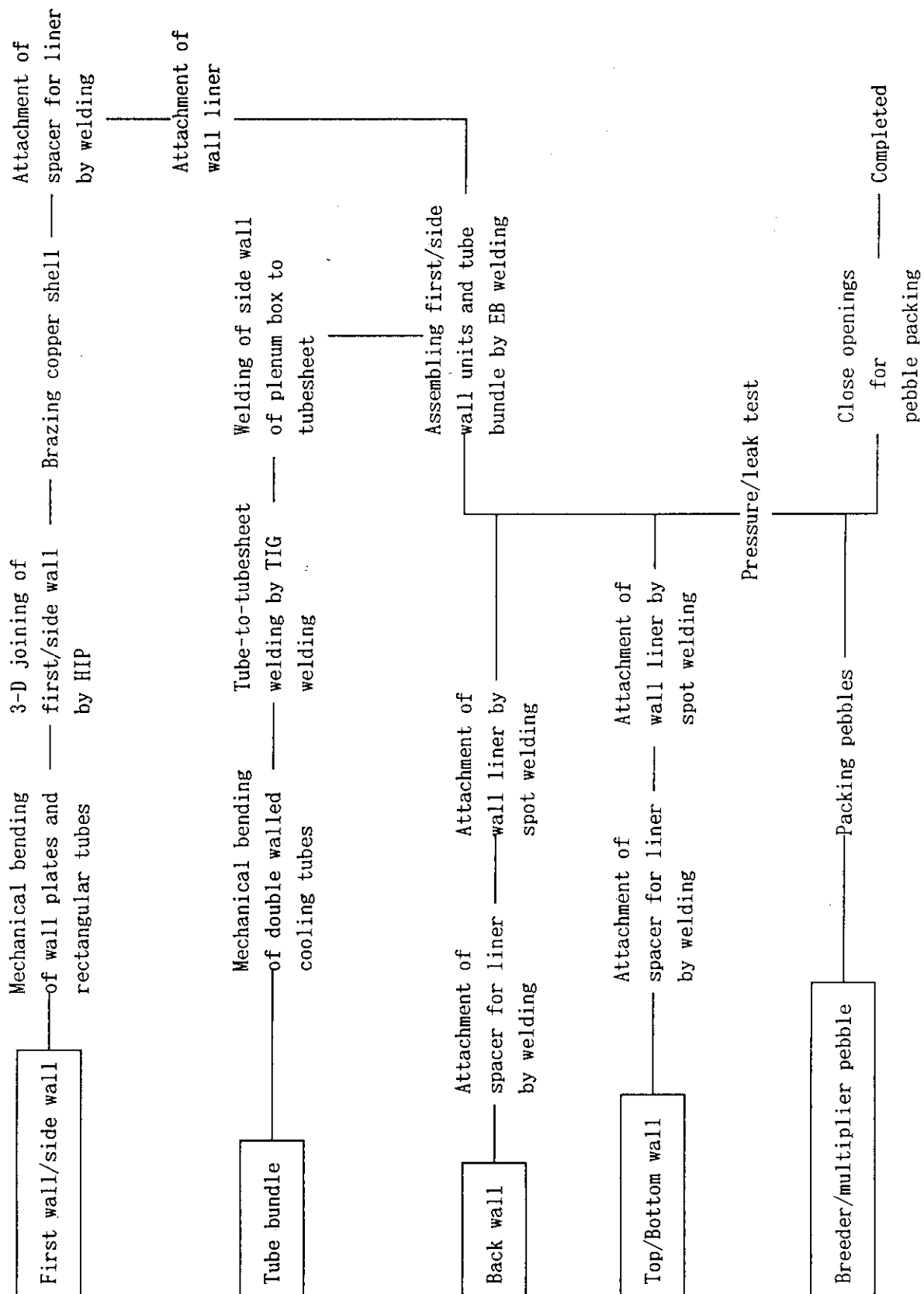


Fig. 5.1.1.1 Fabrication procedure for the mixed pebble bed blanket

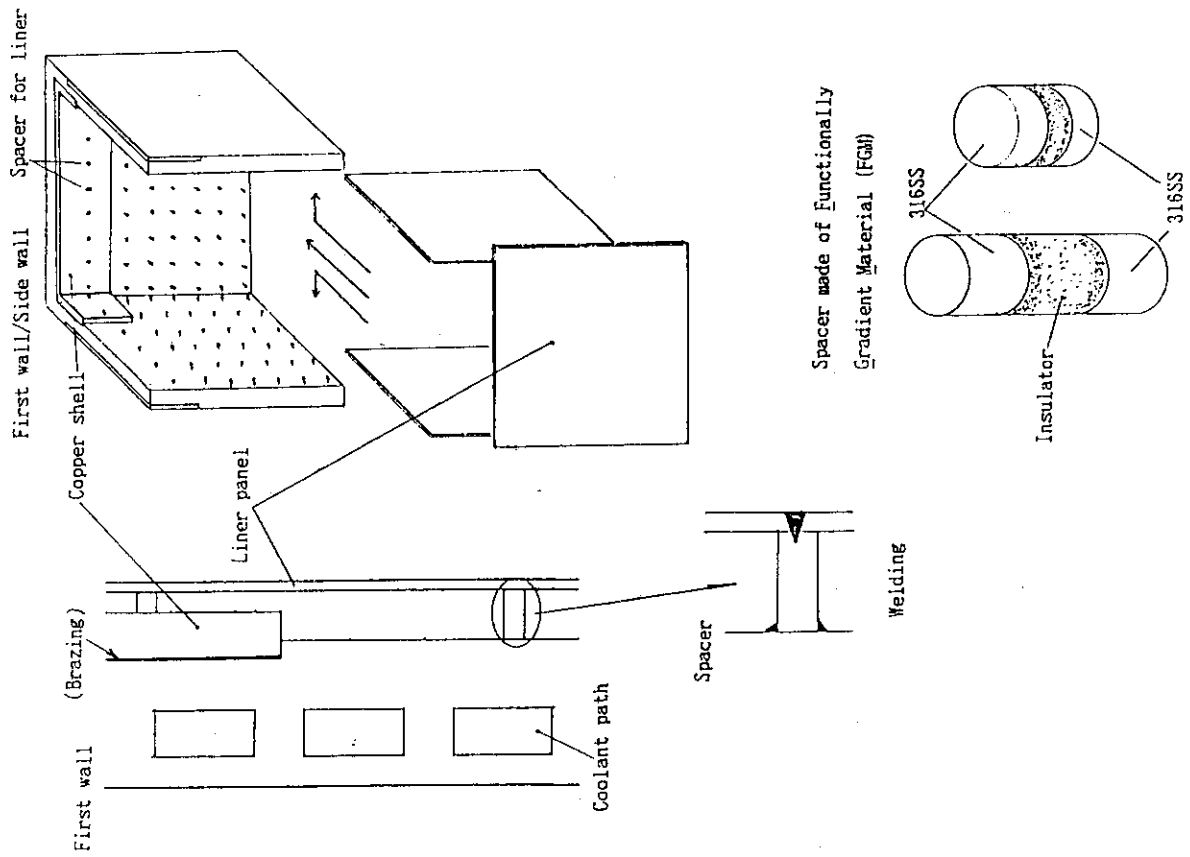


Fig. 5.1.3 Concept of liner attached on blanket walls for breeder temperature control

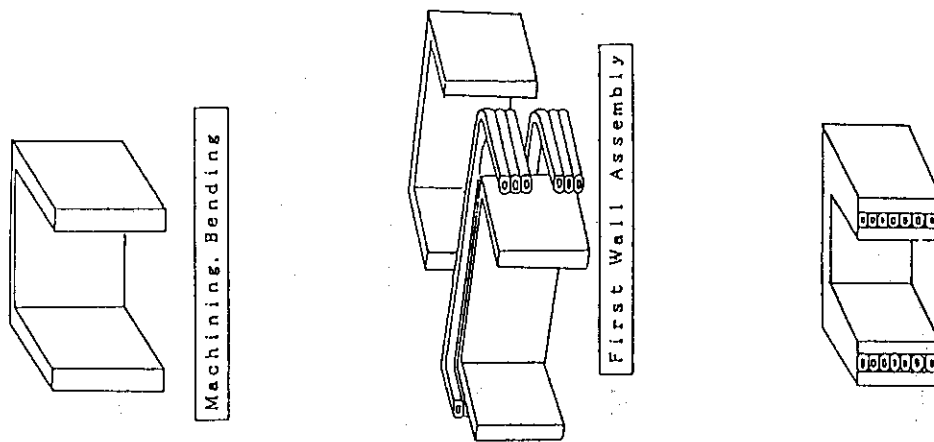


Fig. 5.1.2 Assembling procedure of first wall/side wall units

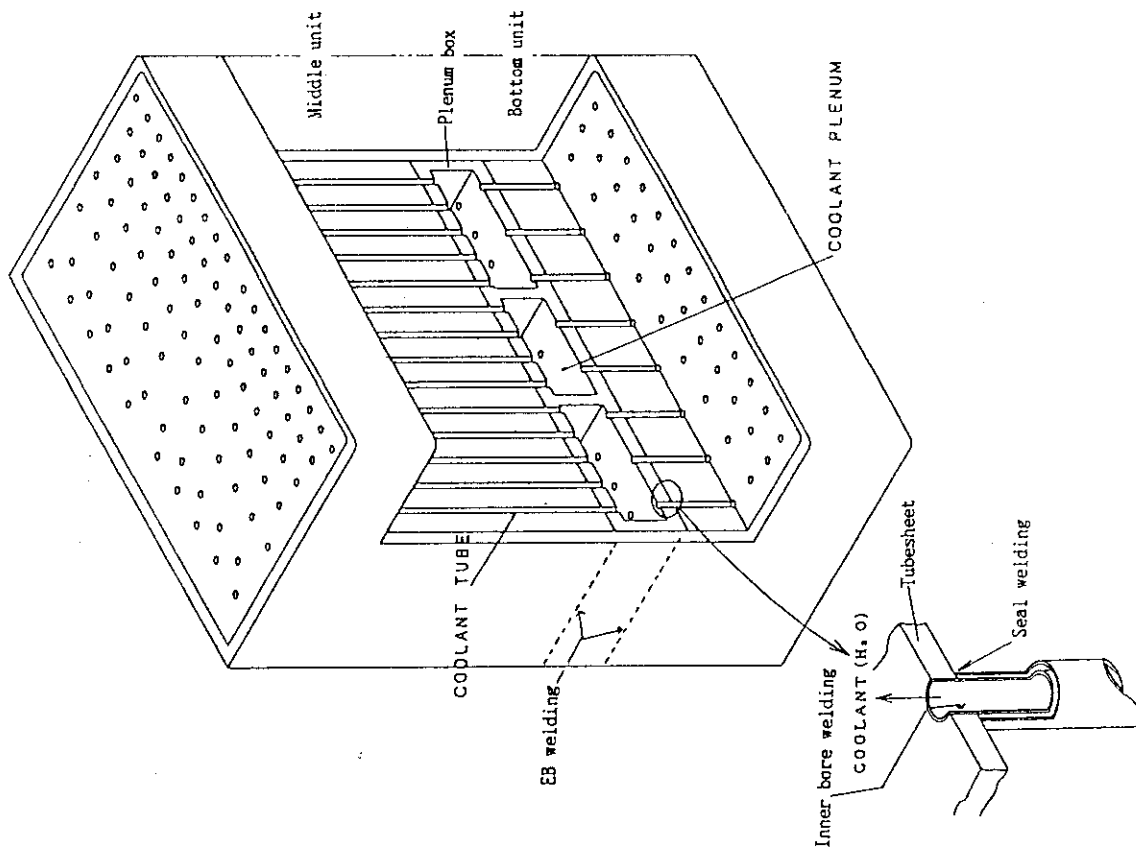


Fig. 5.1.5 Concept of internal coolant plenum

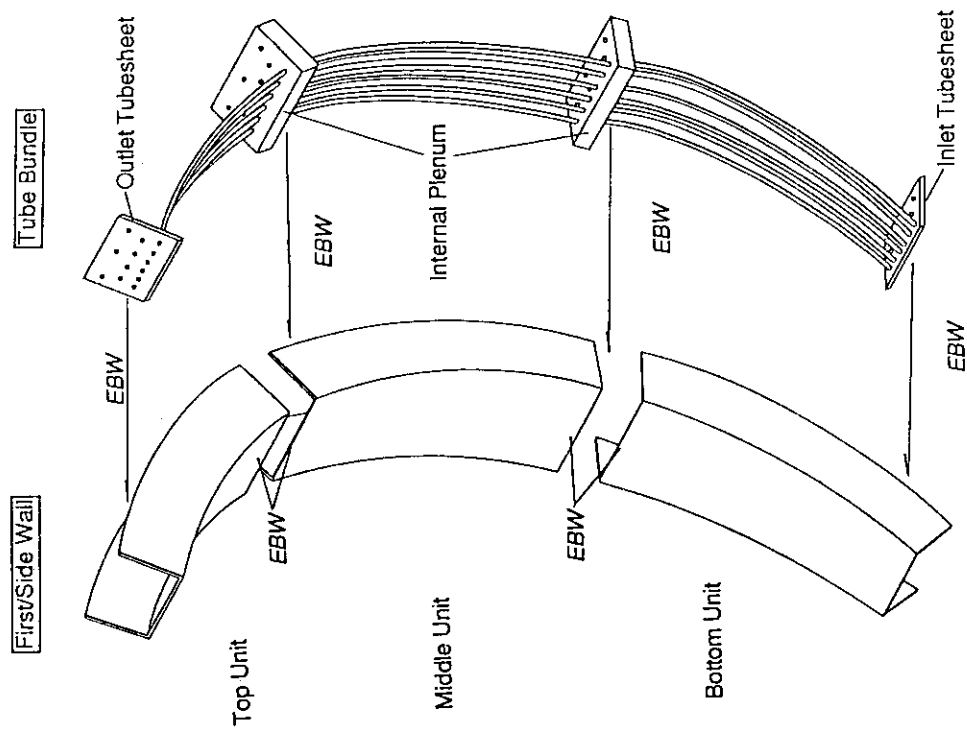


Fig. 5.1.4 Assembling of blanket vessel and tube bundle



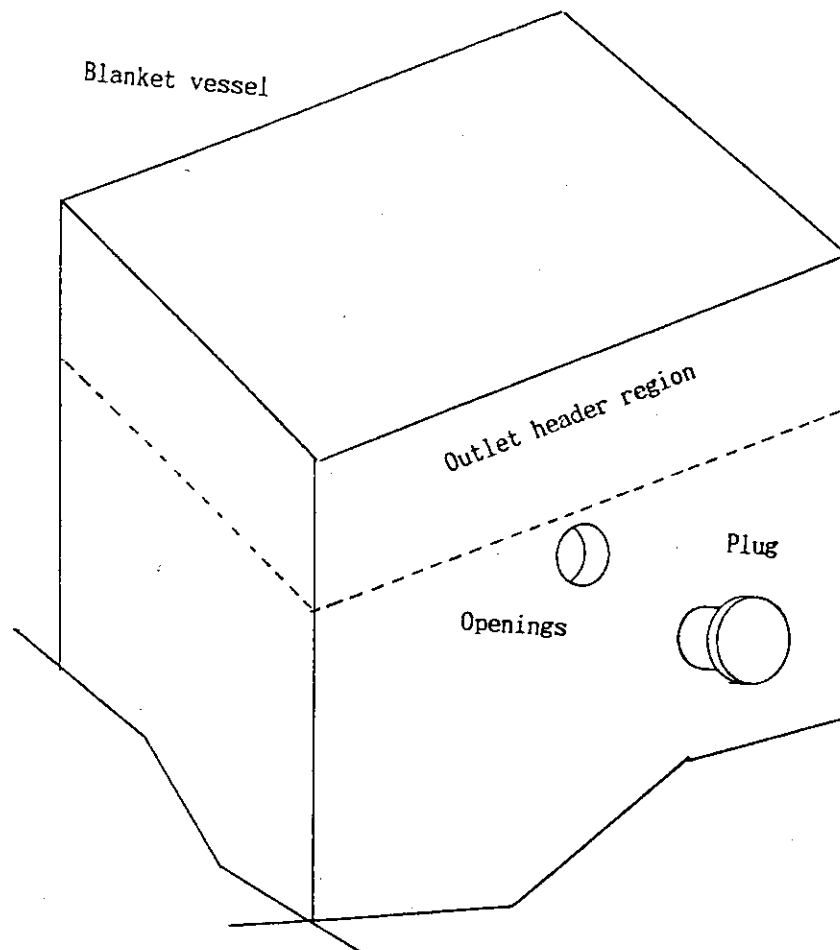


Fig. 5.1.6 Opening in back wall of blanket vessel for pebble insertion

## 5.2 Layered Pebble Bed Blanket

Fabrication procedure of the layered pebble bed blanket is shown in Fig. 5.2.1. The first wall/side wall part is assembled in the same manner as the pebble bed blanket except that the liner wall is not necessary in this blanket.

Breeder cans in which breeder pebbles are packed in advance are fixed to the side wall with mechanical attachment (see Fig. 5.2.2). Cooling panels are also placed in the proper place and are fixed to the side wall with mechanical attachment. The breeder can and the cooling panel are alternately attached.

The inlet header wall is welded to the cooling panels at the bottom of the blanket and then the back wall and the bottom wall are welded to the first wall/side wall.

Beryllium pebbles are inserted from the top of the blanket on a shaking table.

Finally, the outlet header wall and the top wall are welded to the blanket vessel at the top of the blanket.

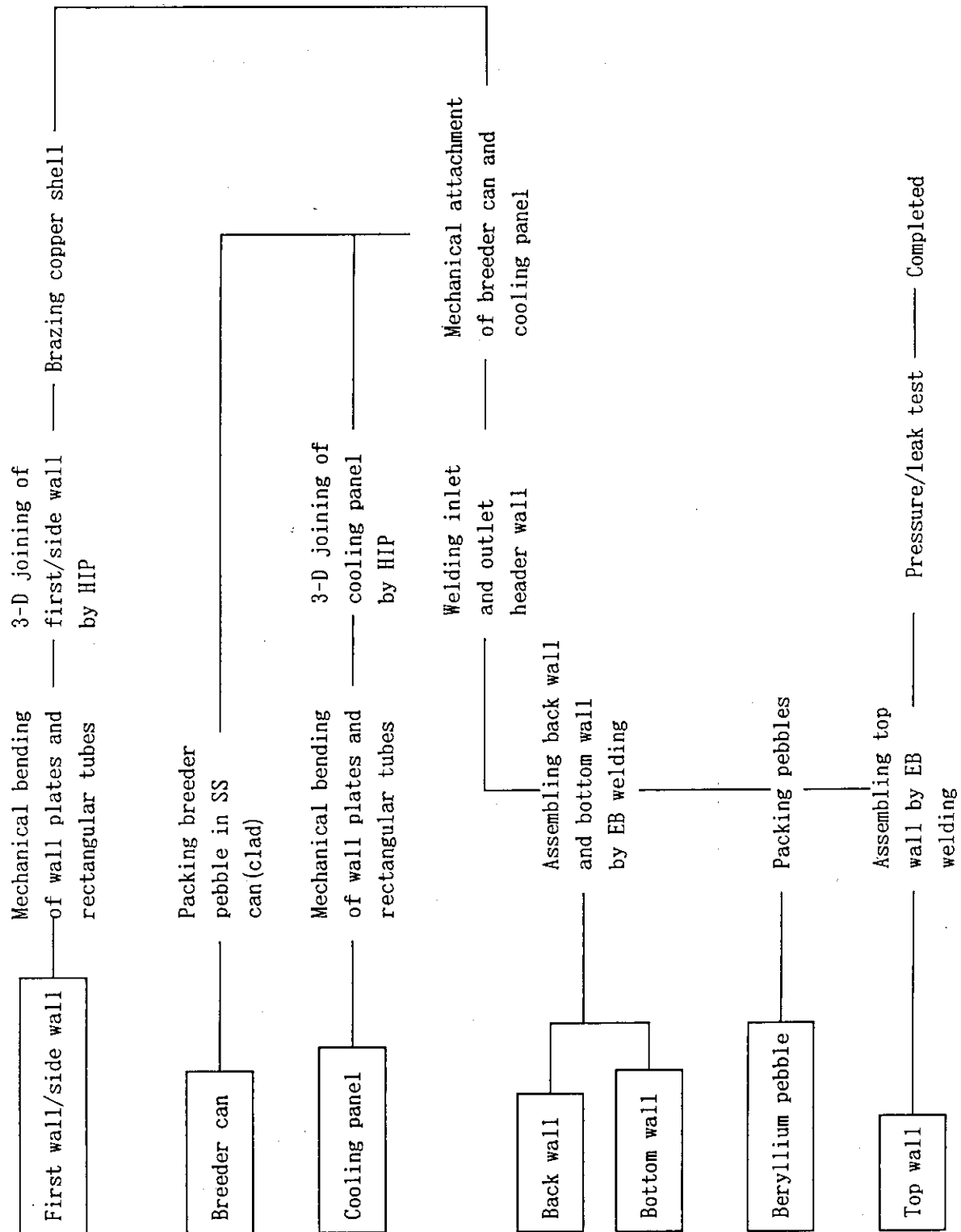


Fig. 5.2.1 Fabrication procedure for the layered pebble bed blanket

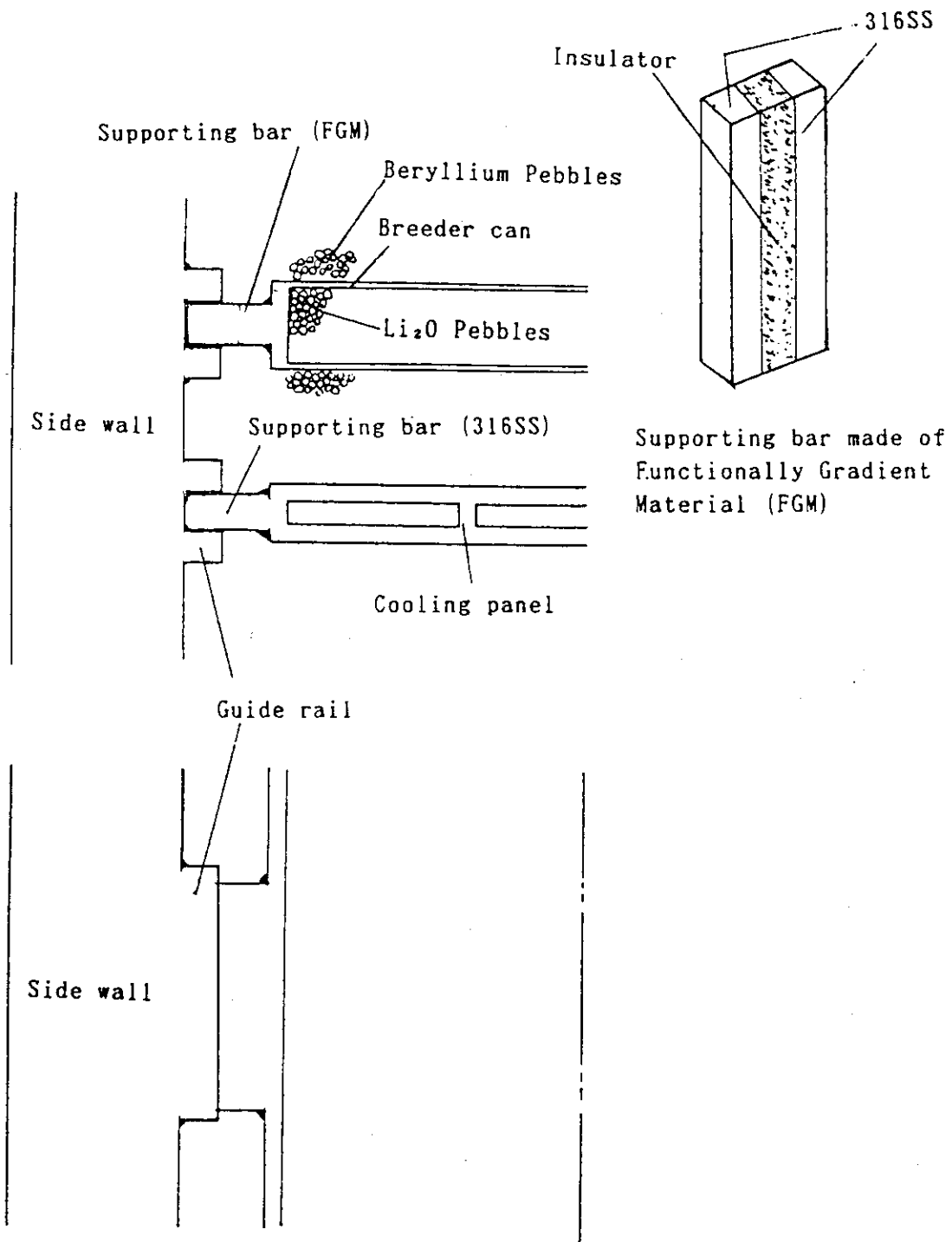


Fig. 5.2.2 Supporting concept of breeder can and cooling panel

### 5.3 Pebble Production

A rotating-granulation/sintering method has been developed[1,2] to produce a large amount of small pebbles (~1 mm-diameter). Fabrication process by this method is indicated in Fig. 5.3.1, and the concept of the fabrication test apparatus is schematically shown in Fig. 5.3.2.

The major process is as follows:

- ① Remove impurities in raw material powder ( $\text{Li}_2\text{O}$ ) by thermal treatment under vacuum
- ② Prepare fine powder from the raw material
- ③ Disperse the powder with binder (e.g. ethyl alcohol) in the rotating/granulation apparatus to produce nuclei of which diameter are about 0.3 mm
- ④ Extract the nuclei from the apparatus and classify them according to their sizes
- ⑤ Load the nuclei into the apparatus and disperse the powder and the binder to form 'green pebbles'
- ⑥ Sinter green pebbles under vacuum at high temperature

Appearance of pebbles produced is shown in Fig. 5.3.3. Major properties of the pebble is summarized in Table 5.3.1. Density and integrity of the pebbles are satisfactory.

Table 5.3.1 Major properties of  $\text{Li}_2\text{O}$  pebbles produced by rotating-granulation/sintering method

Size	1 mm $\phi$
Average Density	91 % T.D.*
Specific Surface Area	0.137 m <sup>2</sup> /g (BET method)
Average Grain Size	44 $\mu\text{m}$
Compressive Stress	250 kg/cm <sup>2</sup> at R.T.

\* Theoretical density : 2.01 g/cm<sup>3</sup>

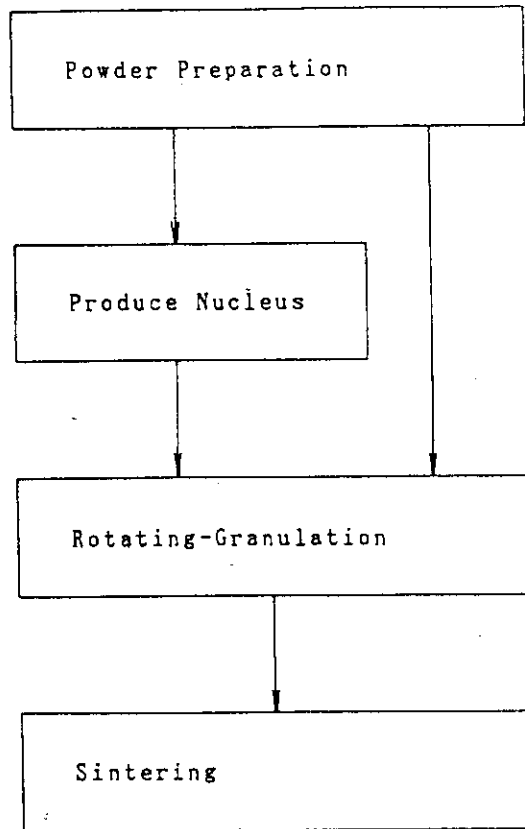


Fig. 5.3.1 Pebble fabrication process by rotating/granulating method

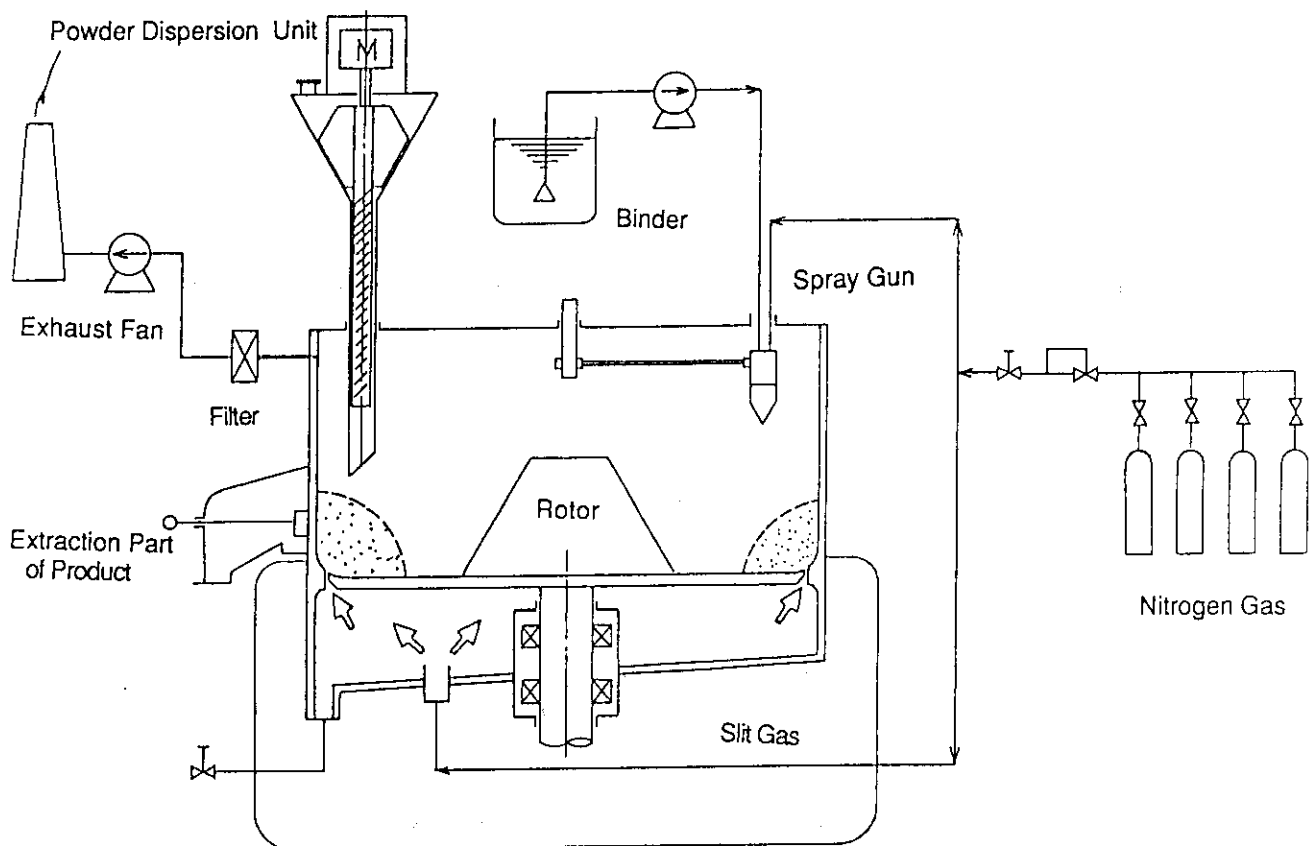


Fig. 5.3.2 Concept of rotating/granulating apparatus

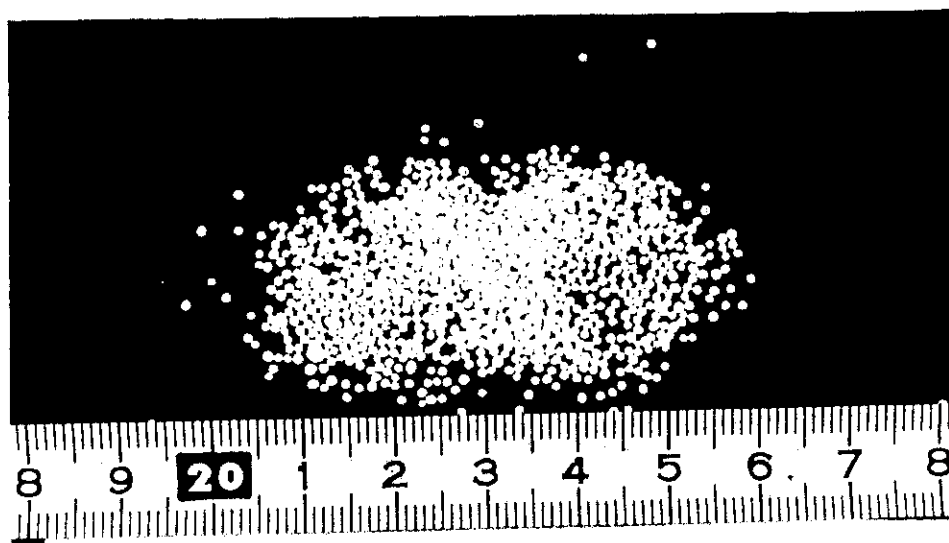


Fig. 5.3.3 Appearance of breeder pebbles

#### 5.4 Conclusions

Basic procedure for fabrications of the mixed pebble bed blanket and the layered pebble bed blanket are described. Further investigations will be required for incorporating stiffening structures for electromagnetic disruption forces, effective packing methods of breeder/multiplier pebbles, supporting integrity and achievable accuracy of placing cooling tubes/panels, fabrication of large components, and so forth. Especially for the mixed pebble bed blanket (or blanket with gas gaps for the breeder temperature control), examinations of fabricability and reliability under thermal cycling for double-walled cooling tubes and wall liners with precise gap width should be pursued.

From the test of pebble manufacturing, it can be resulted that the rotating/granulating technique will be a promising method for mass production of small pebbles of ceramic breeders.

#### References

- [1] Suzuki, T., et al., Development of Production Technique for Solid Breeder of Tritium Breeding Blanket, H17, 1990 Annual Meeting of the Atomic Energy Society of Japan (1990)
- [2] Kobayashi, T., p310, Fusion Technology, Vol. 17, Mar. 1990



## 6. Neutronics

In neutronic analysis, tritium breeding ratios (TBR) and nuclear heating rates are estimated and discussed for three types of blanket, which are mixed pebble bed, layered pebble bed, and pebble and block blankets. One-dimensional calculation models (poloidal model) for local TBR's of these blankets are represented in Section 6.1.1. In Section 6.1.2, the scheme of net (three-dimensional) TBR estimation from these local TBR's are discussed based on the experience of net TBR estimation from two-dimensional TBR's, which was previously established with the following calculations and evaluations of several effects.

- 1) TBR by two-dimensional RZ poloidal model (torus model),
- 2) effect of port on TBR by two-dimensional XY model,
- 3) effect of blanket side wall on TBR by two-dimensional XY model,
- 4) effects of blanket side wall and stiffening rib on TBR by two-dimensional XY model.

Results of local TBR's, tritium production rate distributions, nuclear heating rate distributions and net TBR's are represented and discussed in Section 6.2.

### 6.1 Calculational Model and Method

#### 6.1.1 One-dimensional cylindrical model

Atomic number densities used in the following calculations are shown in Table 6.1.1. One-dimensional transport code ANISN is used. Adopted nuclear group constant set is FUSION-J3[1] based on JENDL-3[2]. Applied Legendre polynomial order in scattering cross section and the order of angle dividing number in space are P5 and the isotropic division of S8, respectively.

For the mixed pebble bed blanket, local TBR's at the outboard mid-plane, the outboard top and the inboard mid-plane are calculated by one-dimensional cylindrical models as illustrated in Figs 6.1.1, 6.1.2 and 6.1.3, respectively. The number of radial meshes in the first two outboard models are 68 and that in the inboard model 48. Lithium oxide and beryllium pebbles are mixed in the ratio of 1 to 3 in each breeder zone. The packing ratio of pebbles is 60 %. Natural lithium is adopted for lithium oxide.

For the layered pebble bed blanket, local TBR's at the outboard midplane and the outboard top are calculated by one-dimensional cylindrical models as shown in Figs 6.1.4 and 6.1.5, respectively. The number of radial meshes in the former is 94 and that in the latter 112. Lithium oxide pebble layers are sandwiched between beryllium pebble layers. The packing ratio of each pebble is 60 %. Fifty percent enriched lithium-6 is adopted for lithium oxide.

Local TBR at the outboard midplane is calculated for the pebble and block blanket by one-dimensional cylindrical model as shown in Table 6.1.2. carbon armor is not included in the model. Lithium-6 in lithium oxide is enriched to 95 %.

#### 6.1.2 Scheme of net (three dimensional) TBR estimation

When a tritium breeding ratio based on a two-dimensional poloidal model (RZ torus model),  $TBR_0$ , is known, a net TBR can be obtained by a scheme shown in Fig. 6.1.6. In this scheme, three-dimensional effects of breeding region coverage on the net TBR are considered, i.e., a port effect,  $F_1$ , a side wall effect,  $F_2'$ , and a side wall and rib effect,  $F_2''$ . They were previously evaluated for ITER joint work in 1989 as  $F_1=0.914$ ,  $F_2'=0.870$  and  $F_2''=0.835$ [3]. The factor  $F$  means an outboard fraction of TBR in the two-dimensional poloidal model. With these factors, the net TBR is obtained by the following equation.

$$TBR = TBR_0 \times [(1-F) \times 0.870 + F \times 0.914 \times 0.835]$$

When only local TBR's based on one-dimensional cylindrical models (poloidal model) are available,  $TBR_0$  corresponding to TBR calculated with two-dimensional model is estimated by a scheme shown in Fig. 6.1.7, which includes the effect of poloidal distribution of neutron wall loading.

Table 6.1.1 Atomic number densities used in the calculation

No.	Material	Element	Number Density
1	Plasma 241 ~ 246	$^2\text{H}$ 7 ~ 12	$1.0 \times 10^{-10}$
2	Carbon 247 ~ 252	C 55 ~ 60	$8.023 \times 10^{-2}$
3	SS 253 ~ 258	Fe 151 ~ 156 Cr 139 ~ 144 Ni 163 ~ 168 Mo 187 ~ 192 Mn 145 ~ 150	$5.727 \times 10^{-2}$ $1.575 \times 10^{-2}$ $9.848 \times 10^{-3}$ $1.255 \times 10^{-3}$ $1.819 \times 10^{-3}$
4	H <sub>2</sub> O 259 ~ 264	H 1 ~ 6 O 67 ~ 72	$6.700 \times 10^{-2}$ $3.350 \times 10^{-2}$
5	Li <sub>2</sub> O 265 ~ 270 (natural Li)	$^6\text{Li}$ 25 ~ 30 $^7\text{Li}$ 31 ~ 36 O 67 ~ 72	$5.118 \times 10^{-3}$ $6.385 \times 10^{-2}$ $3.4484 \times 10^{-2}$
5'	Li <sub>2</sub> O 265 ~ 270 ( $^6\text{Li}$ 50% enriched)	$^6\text{Li}$ 25 ~ 30 $^7\text{Li}$ 31 ~ 36 O 67 ~ 72	$3.4484 \times 10^{-2}$ $3.4484 \times 10^{-2}$ $3.4484 \times 10^{-2}$
5''	Li <sub>2</sub> O 265 ~ 270 ( $^6\text{Li}$ 95% enriched)	$^6\text{Li}$ 25 ~ 30 $^7\text{Li}$ 31 ~ 36 O 67 ~ 72	$6.552 \times 10^{-2}$ $3.4484 \times 10^{-3}$ $3.4484 \times 10^{-2}$
6	Be 271 ~ 276	Be 37 ~ 42	$1.236 \times 10^{-1}$

Table 6.1.2 One-dimensional calculation model for the pebble and block blanket (outboard midplane)

Zone	Material	Thickness (cm)
First wall layer		
First wall	316SS	0.3
Coolant	Water	0.5
Back wall	316SS	0.7
Blanket		
Multiplier (1)	Be (0.85 DF)	3.4
Clad	316SS	0.1
Breeder (I)	Li <sub>2</sub> O *(0.6 PF)	0.8
Clad	316SS	0.1
Multiplier (2)	Be (0.85 DF)	7.4
Coolant channel	316SS	0.3
Coolant	Water	0.3
Coolant channel	316SS	0.3
Multiplier (3)	Be (0.65 DF)	7.3
Clad	316SS	0.1
Breeder (II)	Li <sub>2</sub> O *(0.6 PF)	0.8
Clad	316SS	0.1
Multiplier (4)	Be (0.65 DF)	8.3
Coolant channel	316SS	0.3
Coolant	Water	0.3
End wall	316SS	5.0

\* 85 % theoretical density, 95 % <sup>6</sup>Li enrichment

DF = Density Factor, PF = Packing Fraction

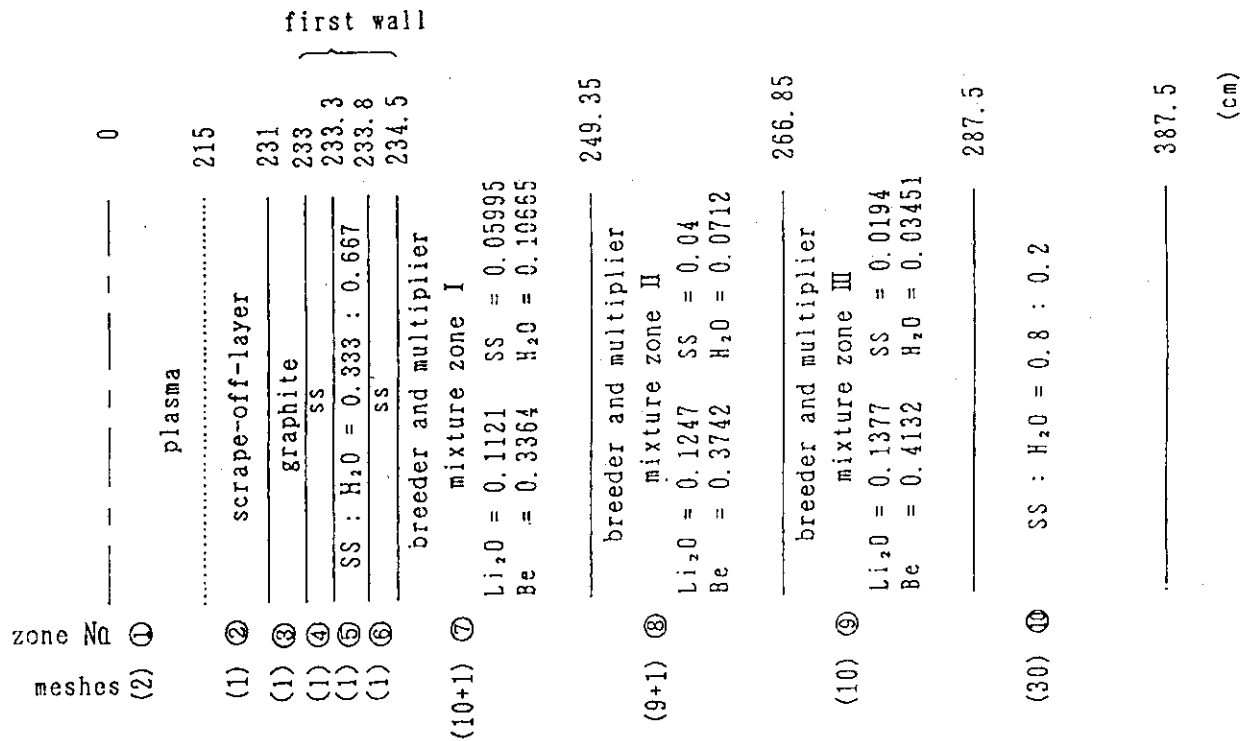


Fig. 6.1.1 One-dimensional cylindrical model of the mixed pebble bed blanket at outboard midplane for ANISN code (first wall loading:  $1.2 \text{ MW/m}^2$ , natural lithium)

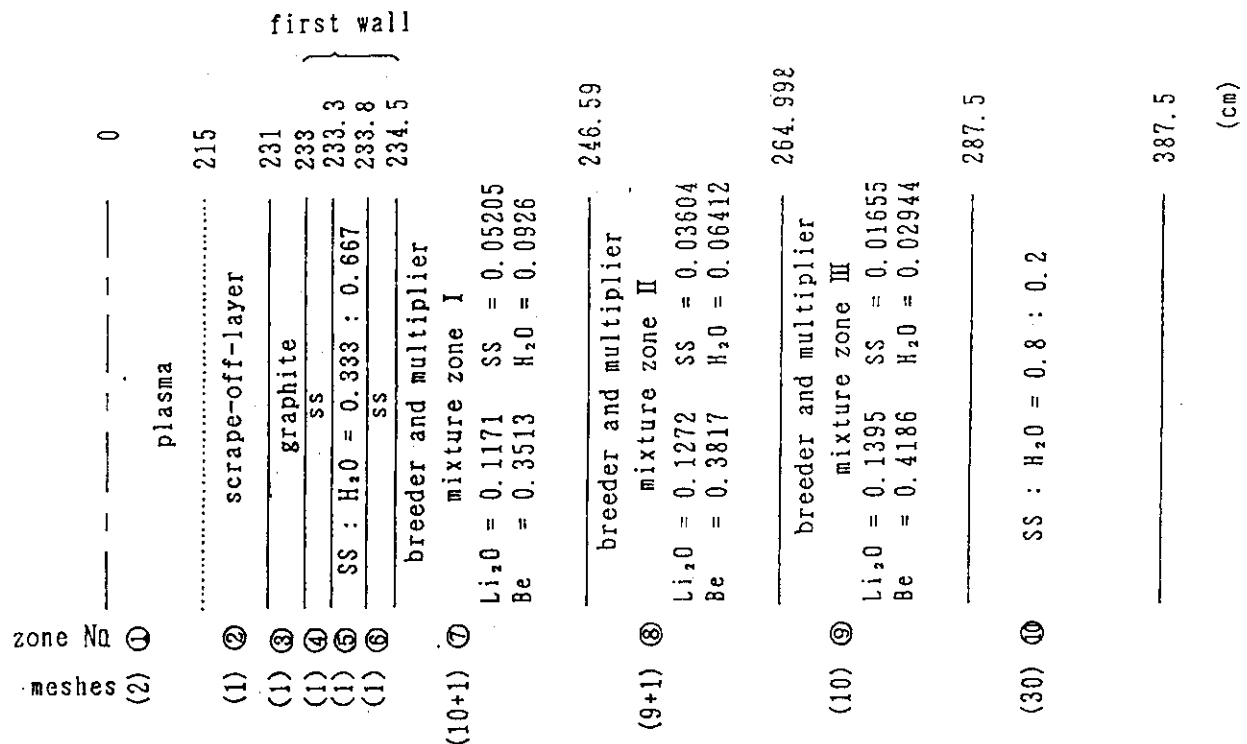


Fig. 6.1.2 One-dimensional cylindrical model of the mixed pebble bed blanket at outboard top for ANISN code (first wall loading:  $0.6 \text{ MW/m}^2$ , natural lithium)

zone No	meshes	materials	radii (cm)
①	(2)	plasma	0
②	(1)	scrape-off-layer	215
③	(1)	graphite	231
④	(1)	SS	233
⑤	(1)	SS : H <sub>2</sub> O = 0.333 : 0.667	233.3
⑥	(1)	SS	233.8
⑦	(3+1)	breeder and multiplier mixture zone I Li <sub>2</sub> O = 0.1095 SS = 0.0642 Be = 0.3286 H <sub>2</sub> O = 0.11421	234.5
⑧	(6+1)	breeder and multiplier mixture zone II Li <sub>2</sub> O = 0.1140 SS = 0.05702 Be = 0.3420 H <sub>2</sub> O = 0.10144	237.969
⑨	(30)	SS : H <sub>2</sub> O = 0.8 : 0.2	245
			345

Fig. 6.1.3 One-dimensional cylindrical model of the mixed pebble bed blanket at inboard midplane for ANISN code (first wall loading:  $0.9 \text{ MW/m}^2$ , natural lithium)

zone No	meshes	materials	radii (cm)
①	(2)	plasma	0
②	(1)	scrape-off-layer	215
③	(1)	graphite	231
④	(1)	SS	233
⑤	(1)	SS : H <sub>2</sub> O = 0.333 : 0.667	233.3
⑥	(1)	SS	233.8
⑦	(1)	Be	234.5
⑧	(1)	SS	235.4
⑨	(2+1)	Li <sub>2</sub> O	235.5
⑩	(1)	SS	236.4
⑪	(1)	Be	236.5
⑫	(1)	SS	237.6
⑬	(1)	SS : H <sub>2</sub> O = 0.231 : 0.769	237.9
⑭	(1)	SS	238.3
⑮	(2)	Be	238.6
⑯	(1)	SS	240.0
⑰	(2+1)	Li <sub>2</sub> O	240.1
⑱	(1)	SS	241.1
⑲	(2)	Be	241.2
⑳	(1)	SS	242.6
㉑	(1)	SS : H <sub>2</sub> O = 0.231 : 0.769	242.9
㉒	(1)	SS	243.3
㉓	(2)	Be	243.6
㉔	(1)	SS	245.3
㉕	(2+1)	Li <sub>2</sub> O	245.4
㉖	(1)	SS	246.7
㉗	(2)	Be	246.8
㉘	(1)	SS	248.6
㉙	(1)	SS : H <sub>2</sub> O = 0.231 : 0.769	248.9
㉚	(1)	SS	249.3
㉛	(2)	Be	249.6
㉜	(1)	SS	251.9
㉝	(2+1)	Li <sub>2</sub> O	252.0
㉞	(1)	SS	253.8
㉟	(2)	Be	253.9
㊱	(1)	SS	256.3
㊲	(1)	SS : H <sub>2</sub> O = 0.231 : 0.769	256.6
㊳	(1)	SS	257.0
㊴	(1)	SS	257.3

Fig. 6.1.4 One-dimensional cylindrical model of the layered pebble bed blanket at outboard midplane for ANISN code (first wall loading:  $1.2 \text{ MW/m}^2$ , 50% enriched lithium)

		0	
zone No	meshes		
(2) ①		plasma	215
(1) ②		scrape-off-layer	231
(1) ③		graphite	233
(1) ④		SS	233.3
(1) ⑤		SS : H <sub>2</sub> O = 0.333 : 0.667	233.8
(1) ⑥		SS	234.5
first wall			
(2) ⑦		Be	235.7
(1) ⑧		SS	235.8
(2+1) ⑨		Li <sub>2</sub> O	237.1
(1) ⑩		SS	237.2
(2) ⑪		Be	238.8
(1) ⑫		SS	239.1
(1) ⑬		SS : H <sub>2</sub> O = 0.231 : 0.769	239.5
(1) ⑭		SS	239.8
(2) ⑮		Be	241.7
(1) ⑯		SS	241.8
(2+1) ⑰		Li <sub>2</sub> O	243.3
(1) ⑱		SS	243.4
(2) ⑲		Be	245.4
(1) ⑳		SS	245.7
(1) ㉑		SS : H <sub>2</sub> O = 0.231 : 0.769	246.1
(1) ㉒		SS	246.4
(2) ㉓		Be	248.9
(1) ㉔		SS	249.0
(2+1) ㉕		Li <sub>2</sub> O	251.0
(1) ㉖		SS	251.1
(3) ㉗		Be	253.8
(1) ㉘		SS	254.1
(1) ㉙		SS : H <sub>2</sub> O = 0.231 : 0.769	254.5
(1) ㉚		SS	254.8
(3) ㉛		Be	258.5
(1) ㉜		SS	258.6
(3+1) ㉝		Li <sub>2</sub> O	261.6
(1) ㉞		SS	261.7
(4) ㉟		Be	265.6
(1) ㊱		SS	265.9
(1) ㊲		SS : H <sub>2</sub> O = 0.231 : 0.769	266.3
(1) ㊳		SS	266.6

Fig. 6.1.5 One-dimensional cylindrical model of the layered pebble bed blanket at outboard top for ANISN code (first wall loading:  $0.6 \text{ MW/m}^2$ , 50% enriched lithium)

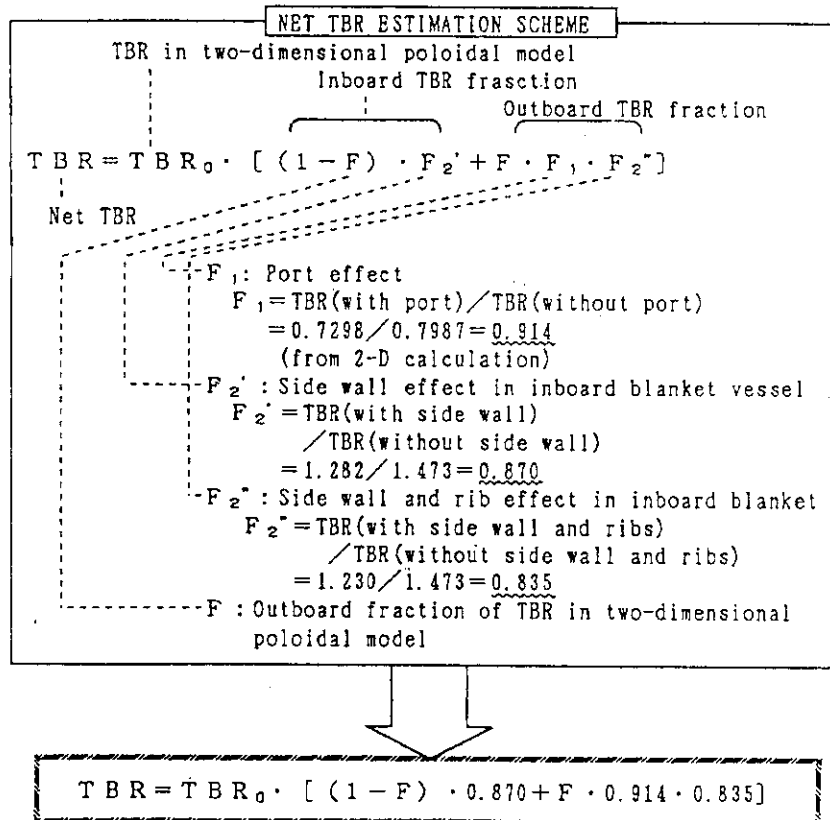


Fig. 6.1.6 Net tritium breeding ratio (3-D TBR) estimation scheme

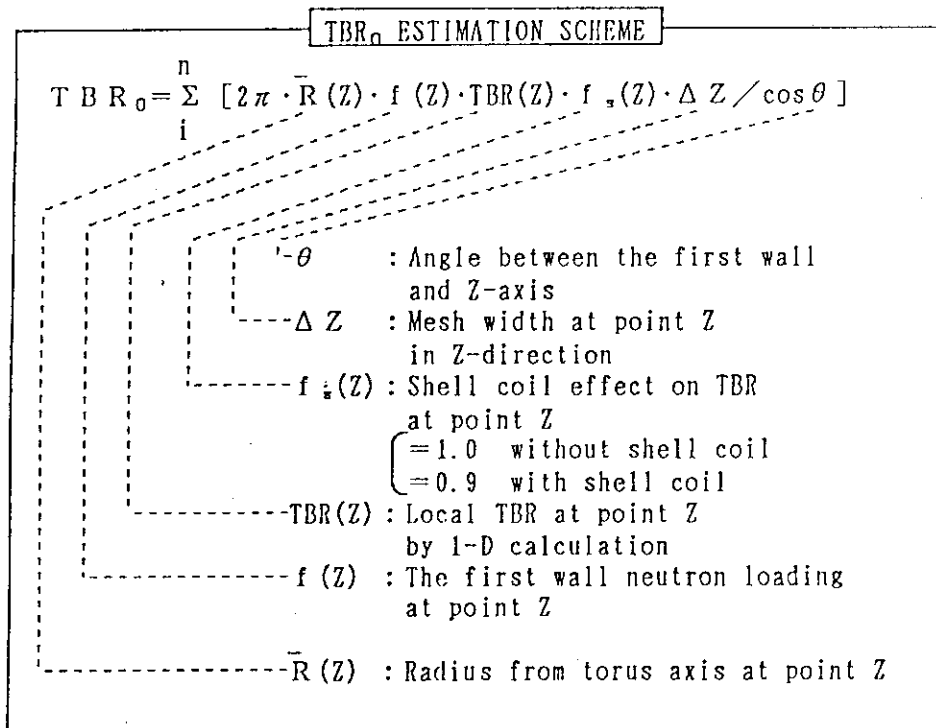


Fig. 6.1.7 TBR<sub>0</sub> (TBR in 2-D poloidal model) estimation scheme



## 6.2 Results of Calculations and Net TBR Estimates

The local TBR's at the outboard mid-plane, the outboard top and the inboard mid-plane are computed for the mixed pebble bed, the layered pebble bed, and the pebble and block blankets with and without carbon armor. In this section, these local TBR's and distributions of tritium production rate and nuclear heating rate are represented. Then net TBR's of the mixed pebble bed and the layered pebble bed blankets are estimated.

### 6.2.1 Mixed pebble bed blanket

Distributions of tritium production rate in the blanket at the outboard mid-plane, the outboard top and the inboard mid-plane are shown in Figs 6.2.1 to 6.2.3, respectively. These are the results for the blanket with carbon armor on the first wall surface. Those without carbon armor are shown in Figs 6.2.4 to 6.2.6. In these figures, the abscissa and the ordinate mean the distance from the plasma center and tritium production rate per one DT-neutron per  $\text{cm}^3$ , respectively.

Figures 6.2.7 to 6.2.12 show distributions of nuclear heating rate in the same parts of the blanket as those in the calculation of tritium production rate. In the first three figures, the distributions in the blankets with carbon armor are indicated, and those without carbon armor in the last three. At the outboard mid-plane, peak nuclear heating rates in the stainless steel first wall with and without 2 cm thick carbon armor are  $15 \text{ W/cm}^3$  and  $18 \text{ W/cm}^3$ , respectively.

Local TBR's obtained are as follows:

	With carbon armor	Without carbon armor
Outboard mid-plane	1.34	1.45
Outboard top-plane	1.37	1.49
Inboard mid-plane	0.55	0.57

### 6.2.2 Layered pebble bed blanket

Distributions of tritium production rate at the outboard mid-plane and the outboard top with carbon armor are shown in Figs 6.2.13 and 6.2.14, respectively. Those without carbon armor are shown in Figs 6.2.15 and 6.2.16. In these figures, the abscissa and the ordinate mean the distance

from the plasma center and tritium production rate per one DT-neutron per  $\text{cm}^3$ , respectively.

Figures 6.2.17 through 6.2.20 show distributions of nuclear heating rate in the same parts of the blanket as those in the above calculation. In the first two figures, the distributions in the blankets with carbon armor are indicated, and those without carbon armor in the last two. At the outboard mid-plane, peak nuclear heating rates in the first  $\text{Li}_2\text{O}$  layer for both of the first wall with and without carbon armor (2 cm thick) are  $25 \text{ W/cm}^3$ .

Local TBR's obtained are as follows:

	With carbon armor	Without carbon armor
Outboard mid-plane	1.25	1.35
Outboard top-plane	1.35	1.46
Inboard mid-plane	0.52	0.54

The TBR at the inboard mid-plane is estimated from the TBR's with the first two  $\text{Li}_2\text{O}$  layers of the outboard mid-plane taking into account the same breeder region thickness (10.5 cm).

### 6.2.3 Pebble and block blanket

Distribution of tritium production rate in the blanket is shown in Figs 6.2.21. Nuclear heating rates in beryllium,  $\text{Li}_2\text{O}$ , 316SS, and water in each layer are summarized in Tables 6.2.1 to 6.2.3. The maximum nuclear heating rates in the first wall (316SS) and  $\text{Li}_2\text{O}$  are  $18 \text{ W/cm}^3$  and  $48 \text{ W/cm}^3$ , respectively. Local TBR is calculated only at the outboard midplane without carbon armor. Contributions of  $^6\text{Li} (n, \alpha)$  and  $^7\text{Li} (n, n' \alpha)$  are 1.306 and 0.0008, respectively, resulting in the total TBR of 1.307.

### 6.2.4 Net tritium breeding ratio

Transformation factors from local TBR's to  $\text{TBR}_0$  for the outboard mixed pebble bed blanket, the outboard layered pebble bed blanket and both type of inboard blanket are summarized in Tables 6.2.4, 6.2.5 and 6.2.6, respectively. They are based on the neutron first wall loading distribution represented in Figs 6.2.22 and 6.2.23[4]. With these transformation factors,  $\text{TBR}_0$ 's can be estimated following the scheme shown in Fig. 6.1.7. Then a

net TBR can be obtained from  $TBR_0$ 's by applying the scheme shown in Fig. 6.1.6. Net TBR's obtained by these schemes are summarized in Table 6.2.7. From these results, it can be seen that there is no significant difference between TBR's of the mixed pebble bed and layered pebble bed blankets. With both type of blankets, net TBR of about 0.8 is obtained without carbon armor. The effect of 2 cm thick carbon armor on the net TBR is to decrease it by 0.05.

For the pebble and block blanket, only local TBR at the outboard mid-plane without carbon armor is calculated as mentioned above. The local TBR is 1.31 which is little smaller than those of other two blankets. However, the net TBR of this blanket could be similar to those of other two because the contribution from the inboard region is expected to be higher for this blanket than others.

Table 6.2.1 Nuclear heating rates in Be in the pebble and block blanket

Neutron Wall Load : 1.2 MW/m<sup>2</sup>

Distance from first wall (cm)		Neutron (W/cm <sup>3</sup> )	Gamma-ray (W/cm <sup>3</sup> )	Total (W/cm <sup>3</sup> )
First layer 1.5	2.067	4.67	1.13	5.8
	3.2	4.20	1.02	5.22
	4.333	3.79	0.943	4.73
Second layer 5.9	6.428	3.20	0.807	4.01
	7.486	2.94	0.762	3.70
	8.543	2.69	0.729	3.42
	9.6	2.47	0.716	3.19
	10.657	2.25	0.709	2.96
	11.714	2.05	0.716	2.77
Third layer 14.2	12.771	1.86	0.736	2.60
	14.721	1.17	0.488	1.66
	15.764	1.09	0.452	1.54
	16.807	1.03	0.422	1.45
	17.850	0.956	0.397	1.35
	18.893	0.892	0.376	1.27
Fourth layer 22.5	19.936	0.833	0.359	1.19
	20.978	0.775	0.344	1.12
	23.019	0.67	0.304	0.974
	24.056	0.624	0.293	0.917
	25.094	0.582	0.284	0.866
	26.131	0.541	0.278	0.819
	27.169	0.502	0.274	0.776
	28.206	0.465	0.271	0.736
	29.244	0.430	0.271	0.701
	30.281	0.394	0.273	0.667

Table 6.2.2 Nuclear heating rates in Li<sub>2</sub>O in the pebble and block blanketNeutron Wall Load : 1.2 MW/m<sup>2</sup>

Distance from first wall (cm)		Neutron (W/cm <sup>3</sup> )	Gamma-ray (W/cm <sup>3</sup> )	Total (W/cm <sup>3</sup> )
First layer 5	5.1	48.2	0.624	48.8
	5.3	33.5	0.618	34.1
	5.5	34.2	0.613	34.8
	5.7	58.3	0.609	58.9
Second layer 21.6	21.7	39.0	0.303	39.3
	21.9	17.8	0.301	18.1
	22.1	15.4	0.299	15.7
	22.3	21.9	0.297	22.2

Table 6.2.3 Nuclear heating rates in SS (first wall and clad) and H<sub>2</sub>O coolant in the pebble and block blanketNeutron Wall Load : 1.2 MW/m<sup>2</sup>

Distance from first wall (cm)		Neutron (W/cm <sup>3</sup> )	Gamma-ray (W/cm <sup>3</sup> )	Total (W/cm <sup>3</sup> )
First wall 0	0.25	9.18	9.18	18.4
	1.25	7.36	7.81	15.2
Li <sub>2</sub> O clad 4.9	4.95	3.81	7.09	10.9
	5.85	3.56	6.83	10.4
Coolant clad 13.3	13.45	1.88	6.09	7.97
	14.05	1.74	5.40	7.14
Coolant 13.6	13.675	4.23	0.612	4.84
	13.825	4.18	0.611	4.79
Li <sub>2</sub> O clad 21.5	21.55	0.891	3.61	4.50
	22.45	0.801	3.40	4.20
Coolant clad 30.8	30.95	0.454	2.82	3.27
Coolant 31.1	31.175	1.21	0.297	1.51
	31.325	1.20	0.297	1.50
Back wall 31.4	32.626	0.414	2.16	2.57
	37.53	0.201	1.08	1.28

Table 6.2.4 Neutron first wall loading distributions and transformation factor from outboard local TBR's to TBR<sub>0</sub> of 2-D RZ poloidal model for the mixed pebble bed blanket

$\Delta Z$ (m)	$\theta$ angle between the 1st wall and z-axis (deg.)	$\Delta L$ = $\Delta Z / \cos \theta$ (m)	f wall loading (MW/m <sup>2</sup> )	R <sup>†</sup> mean radius (m)	$\Delta p =$ $2\pi R^{\dagger} \Delta L f$ (MW)	$\Delta p /$ 348.495*	F <sub>t</sub> mid-plane and top or bottom transformation factor
0-1	0	1	1.18	8.3	61.54	0.1766	0.3006
1-1.7	20	0.745	1.14	8.1	43.22	0.1240	
1.86-3	30	1.316	1.01	7.65	64.89	0.1833	0.3854
3-4	35	1.221	0.81	7.0	43.50	0.1248	
4-5	35	1.221	0.56	6.3	27.07	0.0777	

\* Half of the total neutron power = 696.982/2 = 348.495 (MW)

Table 6.2.5 Neutron first wall loading distributions and transformation factor from outboard local TBR's to TBR<sub>0</sub> of 2-D RZ poloidal model for the layered pebble bed blanket

$\Delta Z$ (m)	$\theta$ angle between the 1st wall and z-axis (deg.)	$\Delta L$ = $\Delta Z / \cos \theta$ (m)	f wall loading (MW/m <sup>2</sup> )	$R^\dagger$ mean radius (m)	$\Delta p =$ $2\pi R^\dagger \Delta L f$ (MW)	$\Delta p /$ 348.495*	$F_t$ mid-plane and top or bottom transformation factor
0-1	0	1	1.18	8.3	61.54	0.1766	0.3495
1-2	20	1.064	1.14	8.1	60.27	0.1729	
2-3	30	1.155	1.01	7.65	56.07	0.1609	0.3634
3-4	35	1.221	0.81	7.0	43.50	0.1248	
4-5	35	1.221	0.56	6.3	27.07	0.0777	

\* Half of the total neutron power =  $696.989/2 = 348.495$  (MW)

Table 6.2.6 Neutron first wall loading distributions and transformation factor from inboard local TBR's to TBR<sub>0</sub> of 2-D RZ poloidal model for the mixed pebble bed and layered pebble bed blankets

$\Delta Z$ (m)	$\theta$ angle between the 1st wall and z-axis (deg.)	$\Delta L$ = $\Delta Z / \cos \theta$ (m)	f wall loading (MW/m <sup>2</sup> )	$R^\dagger$ mean radius (m)	$\Delta p =$ $2\pi R^\dagger \Delta L f$ (MW)	$\Delta p /$ 348.495*	$F_t$ mid-plane and top or bottom transformation factor
0-1	0	1	0.90	3.17	20.98	0.0602	0.1608
1-2	0	1	0.78	3.17	18.18	0.0522	
2-3	0	1	0.58	3.17	13.52	0.0388	
3-3.36	0	0.36	0.40	3.17	3.36	0.0096	

\* Half of the total neutron power =  $696.989/2 = 348.495$  (MW)

Table 6.2.7 Tritium breeding ratio of three types of blanket

TBR \ blanket type	Mixed pebble bed	Layered pebble bed	Pebble and block
WITH CARBON ARMOR			
<u>local TBR</u>			
outboard mid-plane	1.34	1.25	--
outboard upper	1.37	1.35	--
inboard	0.55	0.52	--
-----	-----	-----	-----
<u>Net TBR</u> outboard*	0.67	0.67	--
inboard	0.08	0.07	--
total	0.75	0.74	--
WITHOUT CARBON ARMOR			
<u>local TBR</u>			
outboard mid-plane	1.45	1.35	1.31
outboard upper	1.49	1.46	--
inboard	0.57	0.54	--
-----	-----	-----	-----
<u>Net TBR</u> outboard*	0.73	0.72	--
inboard	0.08	0.08	--
total	0.81	0.80	

\* outboard upper blanket with passive shell conductor (5mm thick copper)

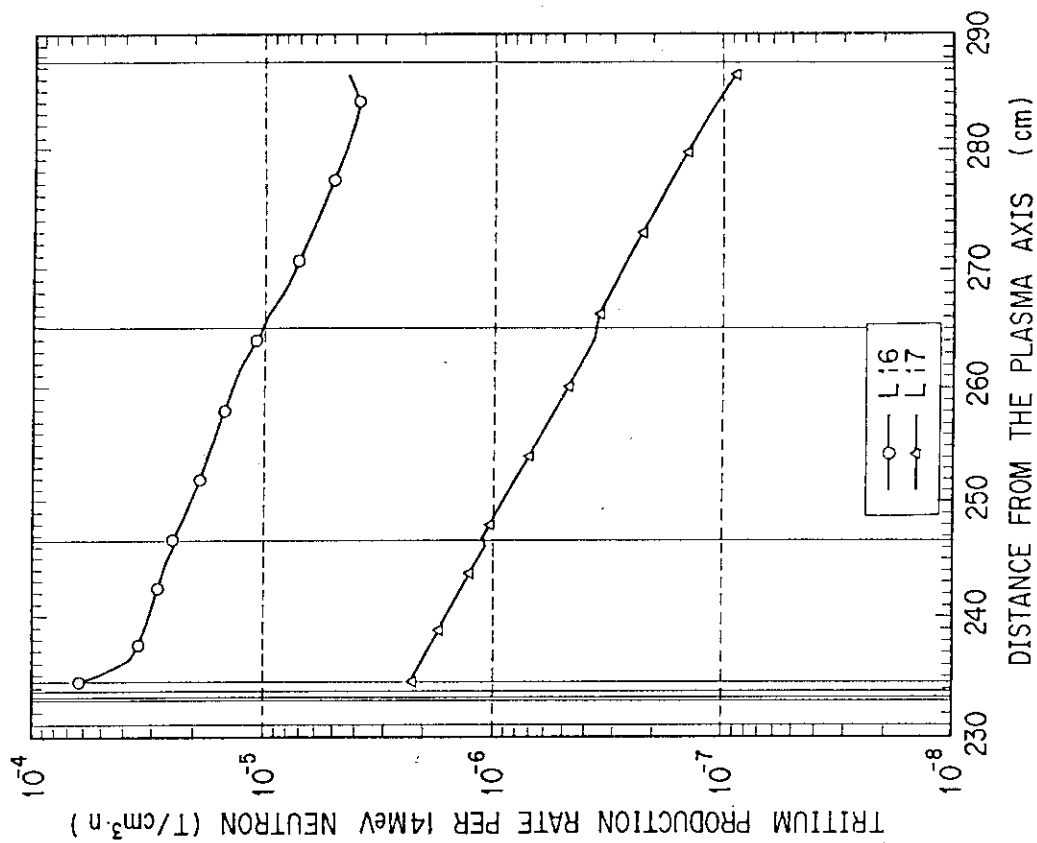


Fig. 6.2.1 Distribution of tritium production rate in the mixed pebble bed blanket at outboard midplane (with carbon armor)

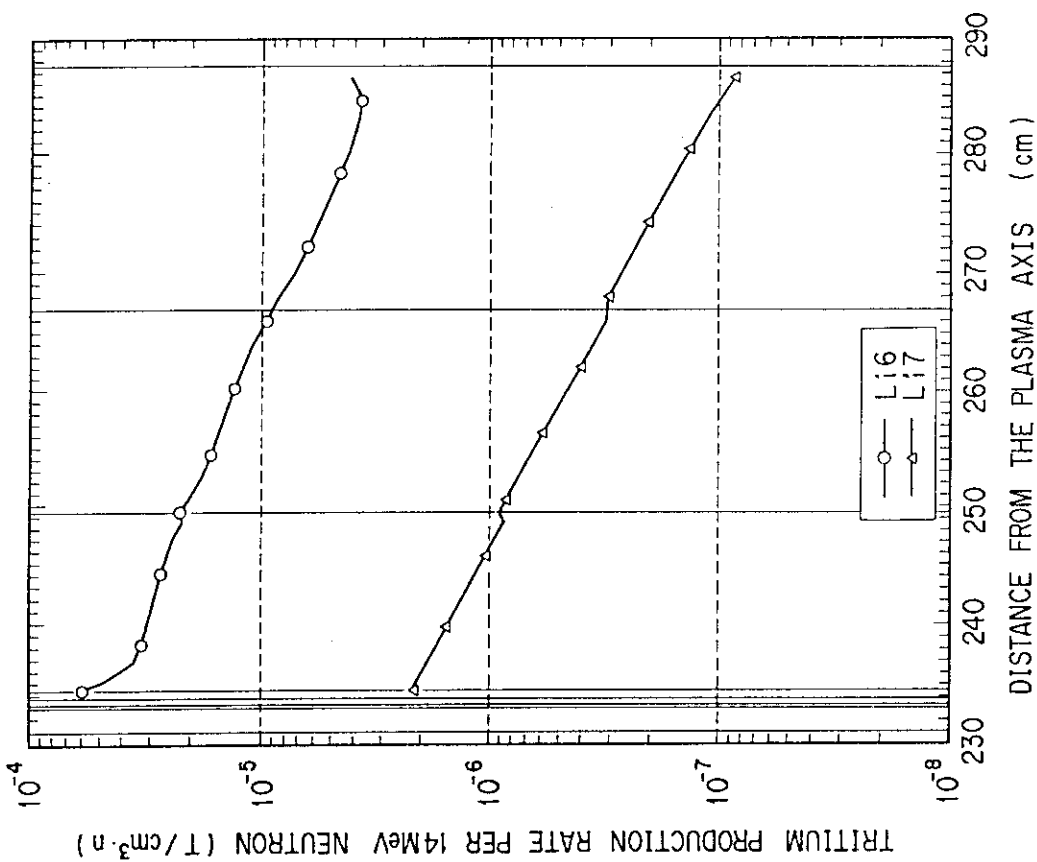


Fig. 6.2.2 Distribution of tritium production rate in the mixed pebble bed blanket at outboard top (with carbon armor)



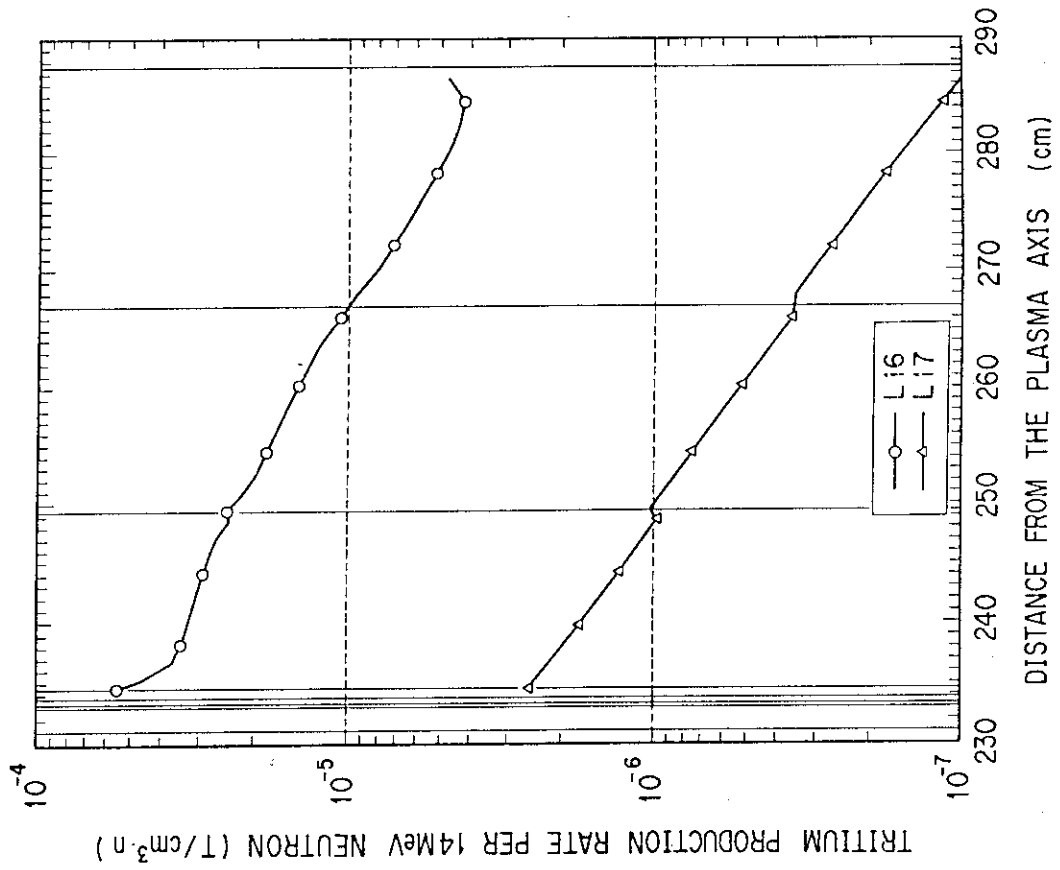


Fig. 6.2.3 Distribution of tritium production rate in the mixed pebble bed blanket at inboard midplane (with carbon armor)

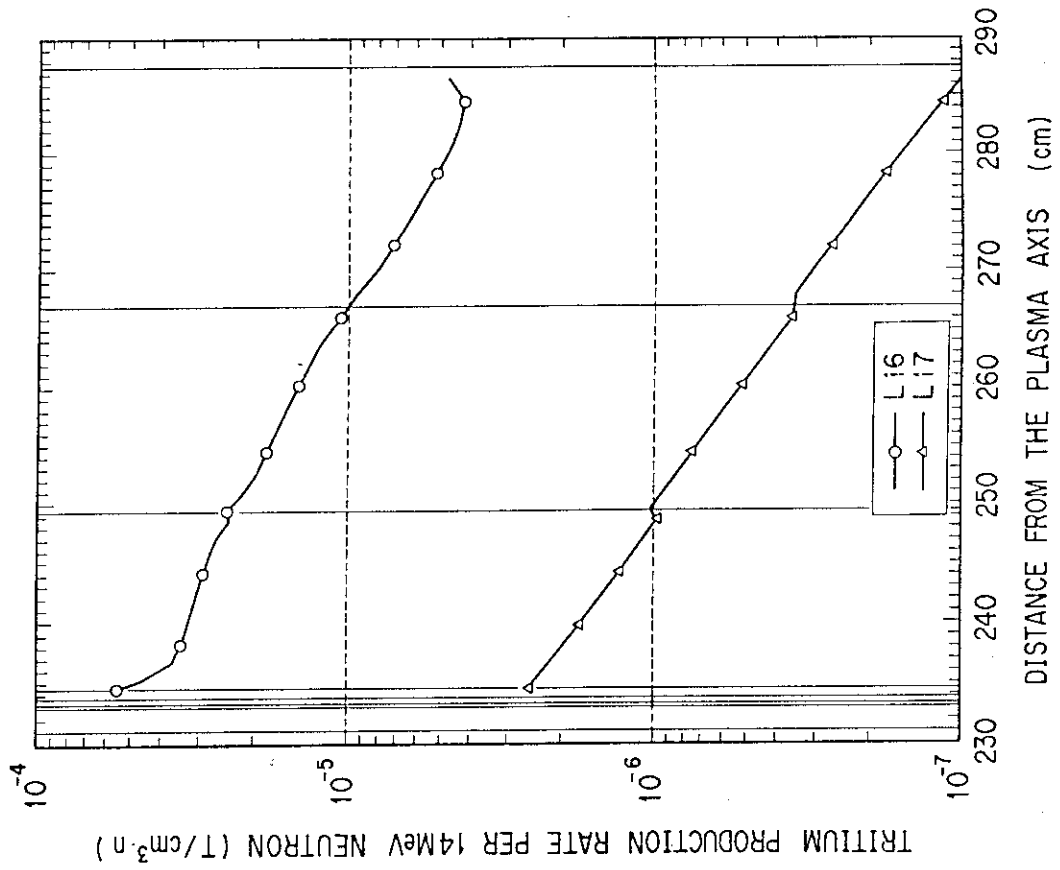


Fig. 6.2.4 Distribution of tritium production rate in the mixed pebble bed blanket at outboard midplane (without carbon armor)

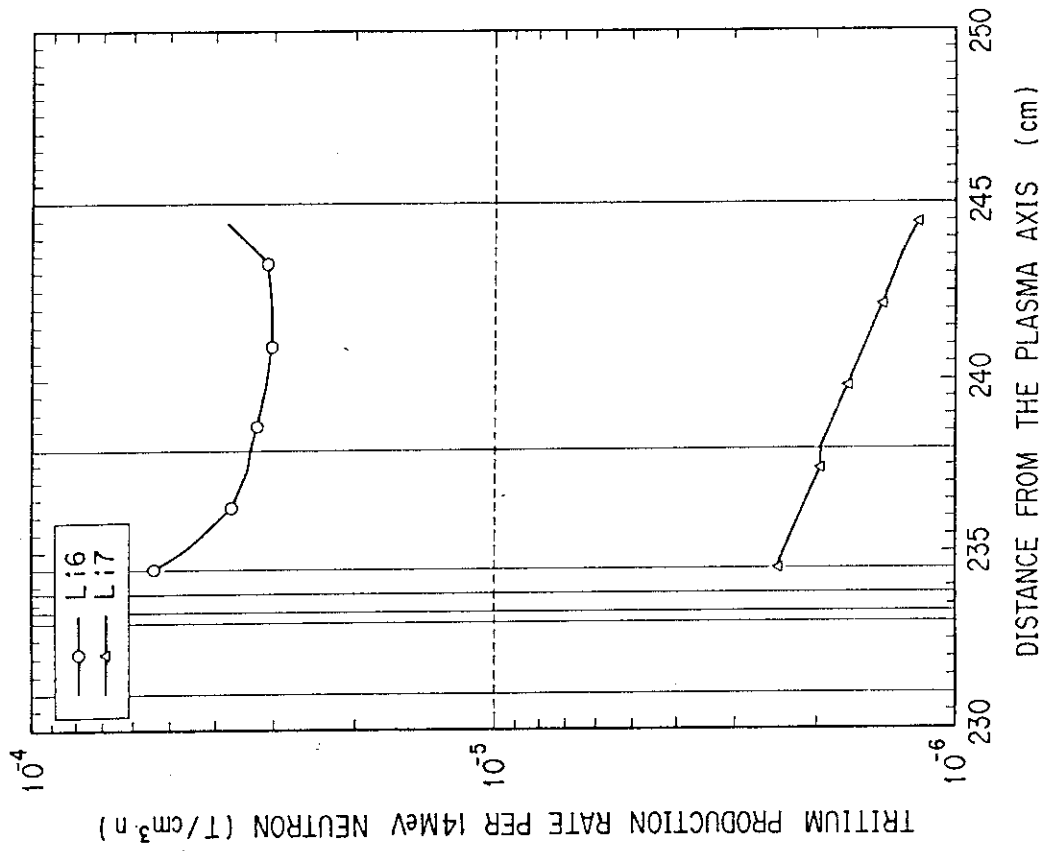


Fig. 6.2.5 Distribution of tritium production rate in the mixed pebble bed blanket at outboard top (without carbon armor)

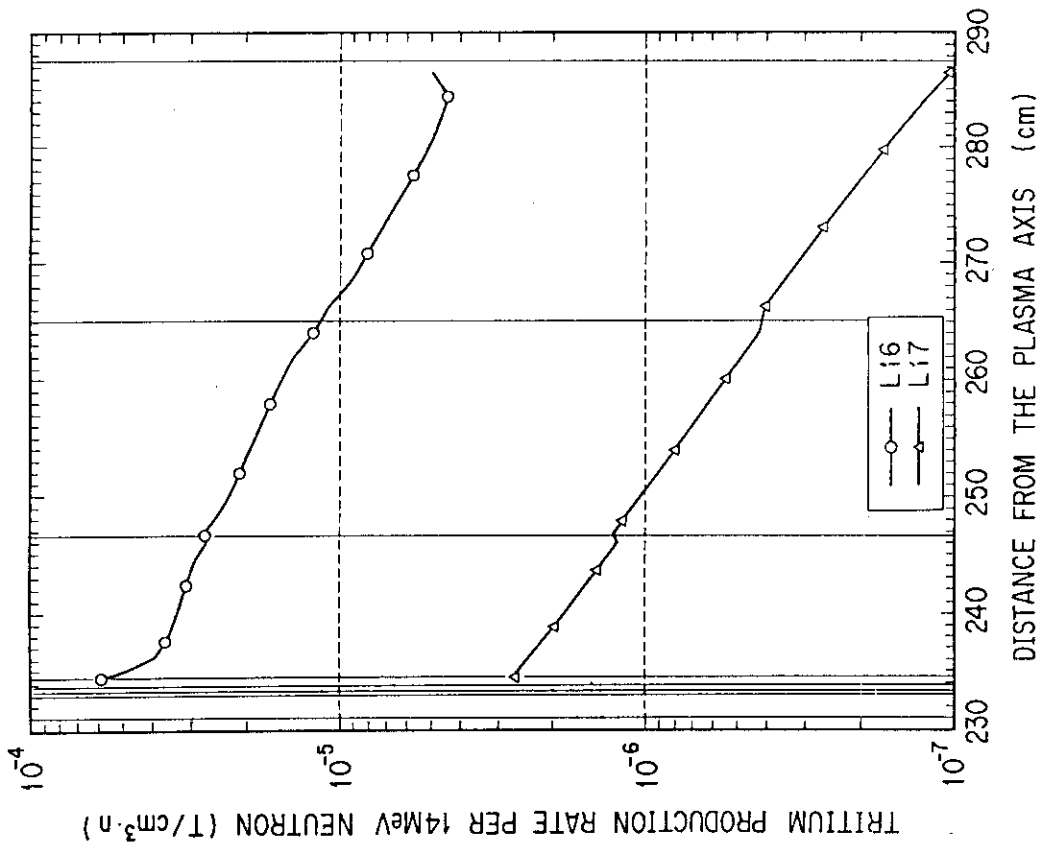


Fig. 6.2.6 Distribution of tritium production rate in the mixed pebble bed blanket at inboard midplane (without carbon armor)

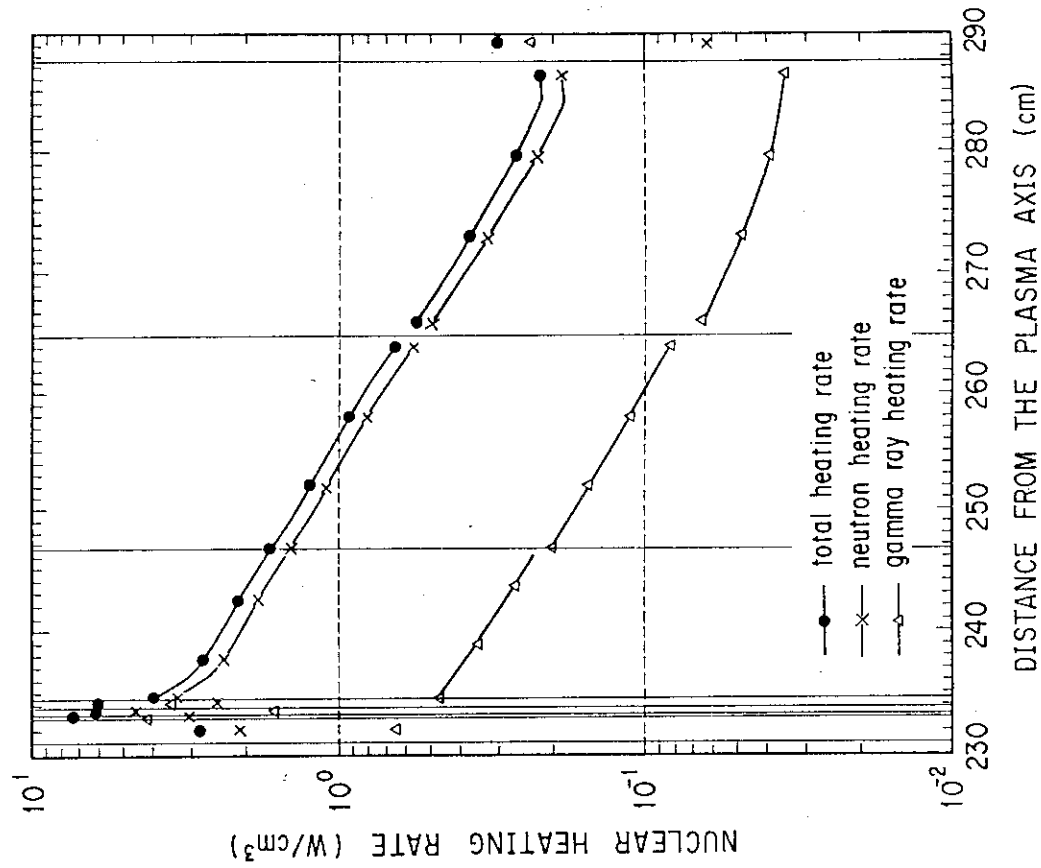


Fig. 6.2.8 Distribution of nuclear heating rate in the mixed pebble bed blanket at outboard top (with carbon armor)

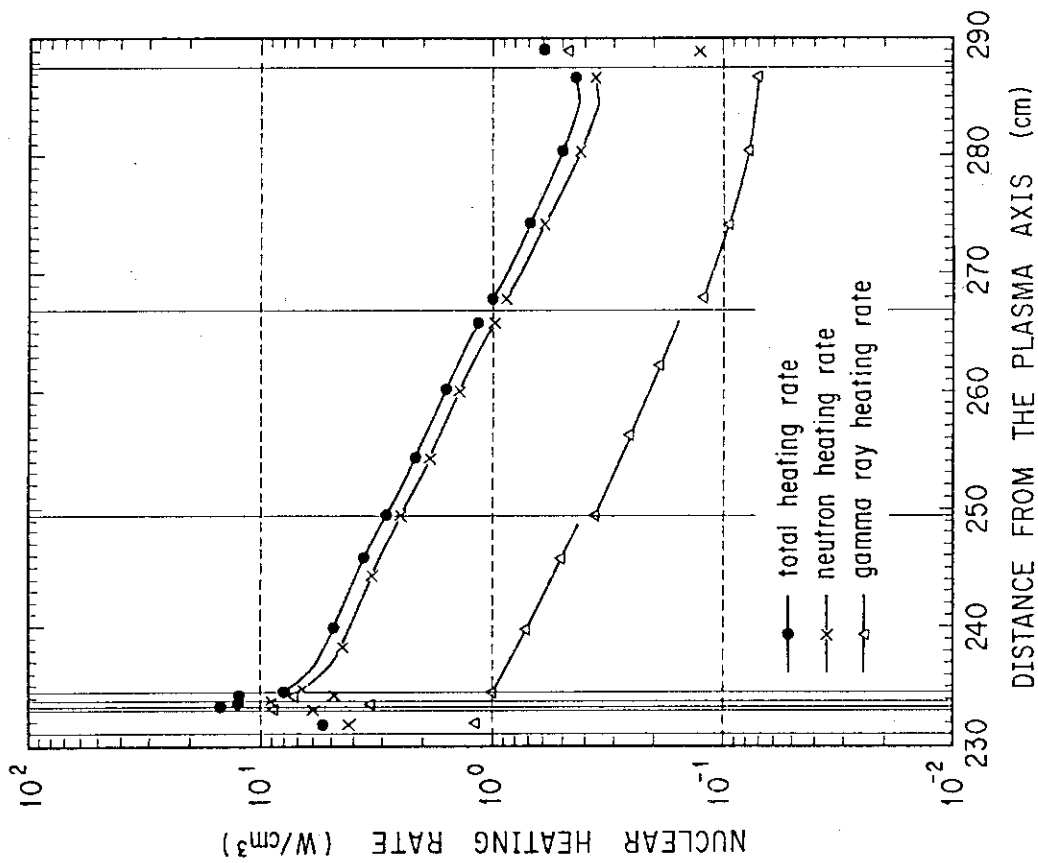


Fig. 6.2.7 Distribution of nuclear heating rate in the mixed pebble bed blanket at outboard midplane (with carbon armor)

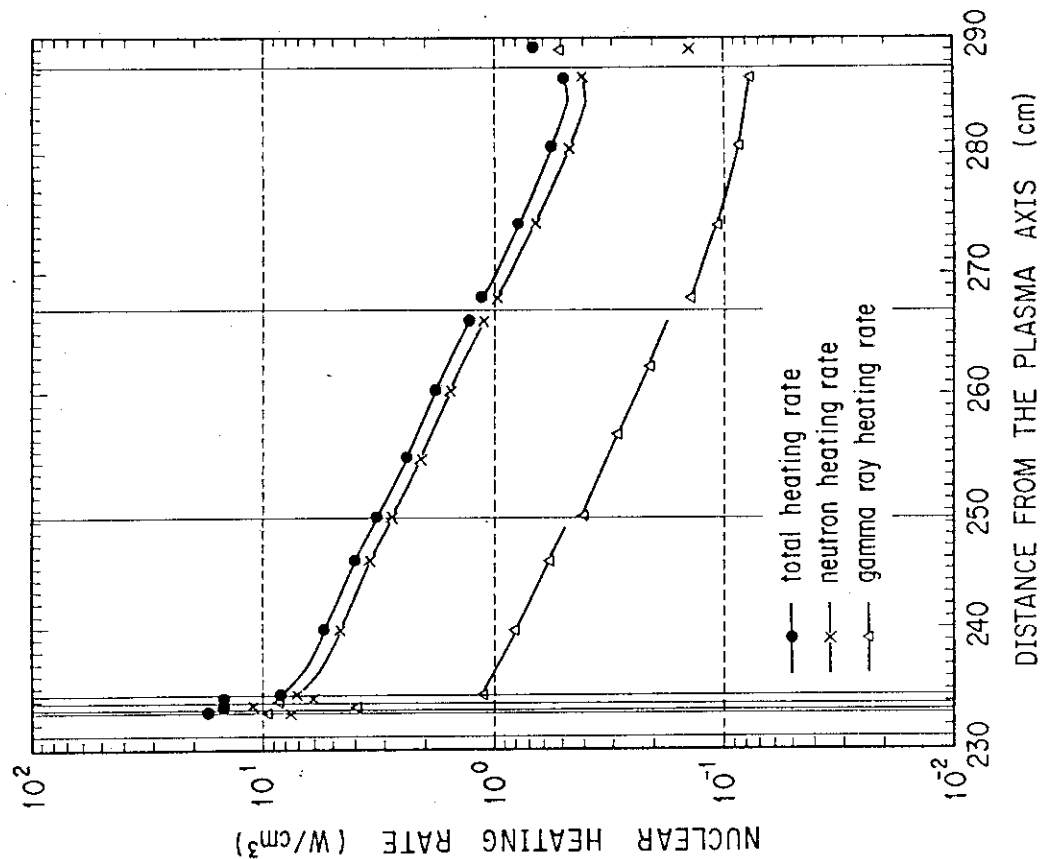


Fig. 6.2.9 Distribution of nuclear heating rate in the mixed pebble bed blanket at inboard midplane (with carbon armor)

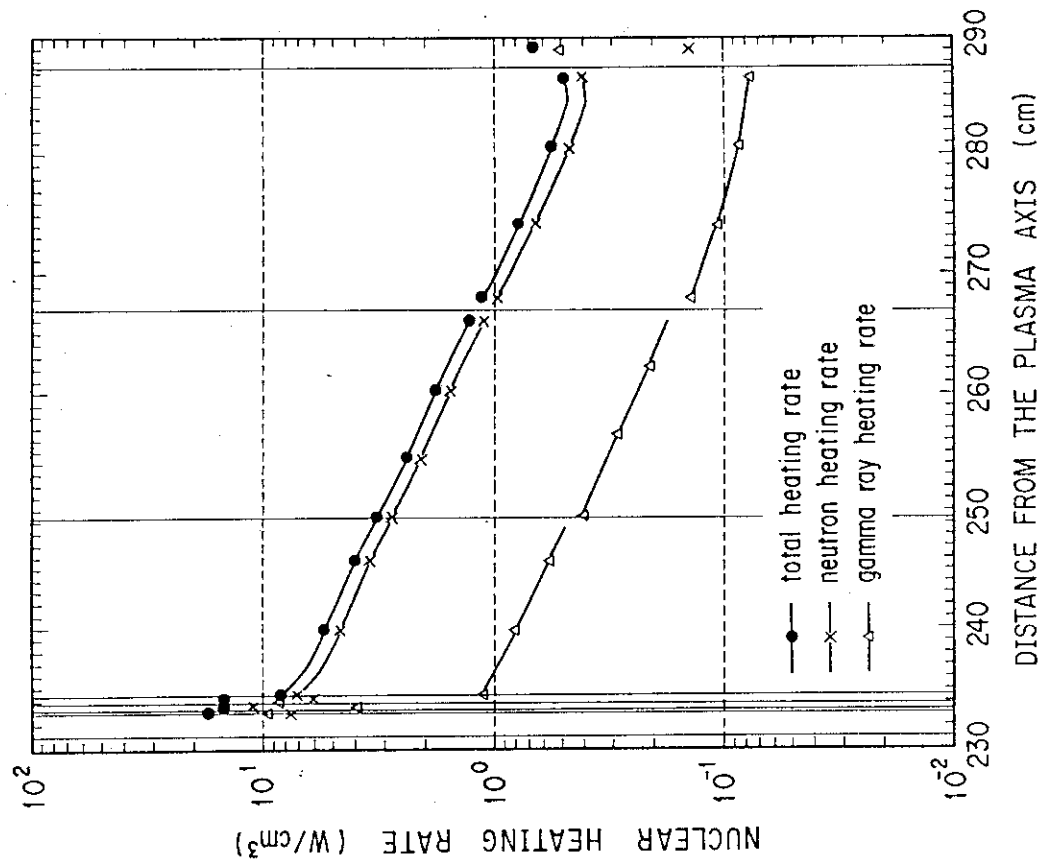


Fig. 6.2.10 Distribution of nuclear heating rate in the mixed pebble bed blanket at outboard midplane (without carbon armor)

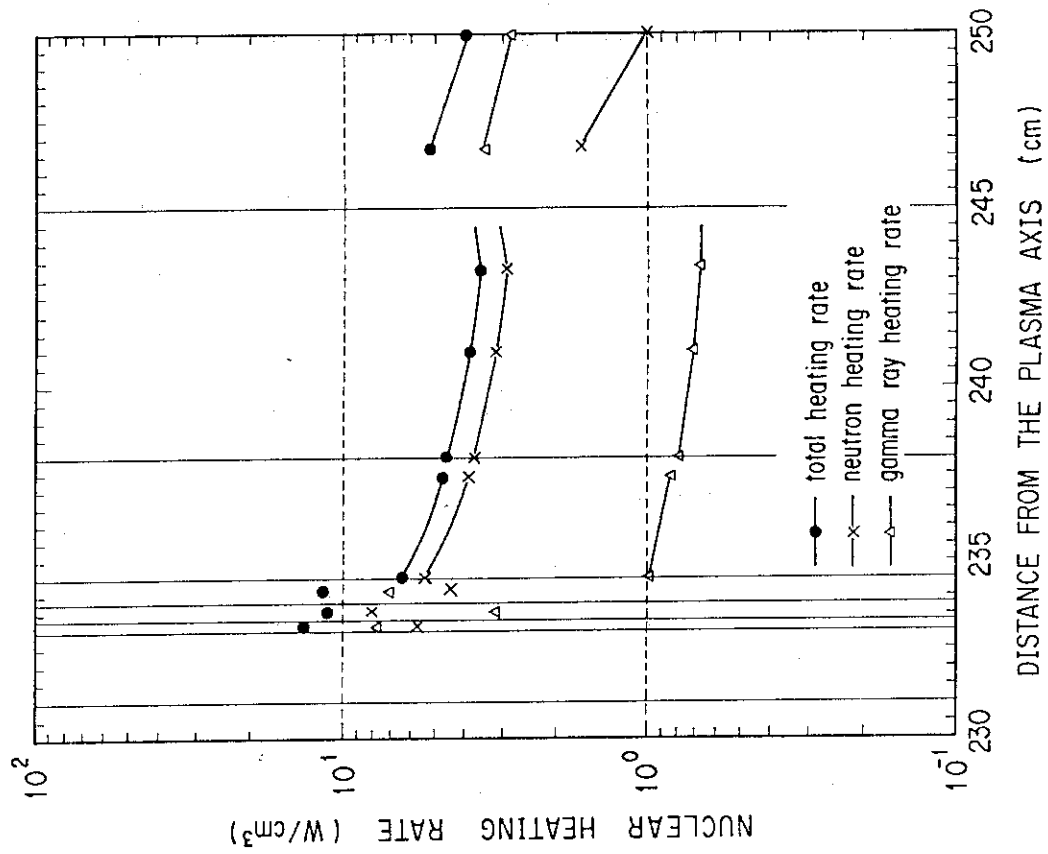


Fig. 6.2.12 Distribution of nuclear heating rate in the mixed pebble bed blanket at inboard midplane (without carbon armor)

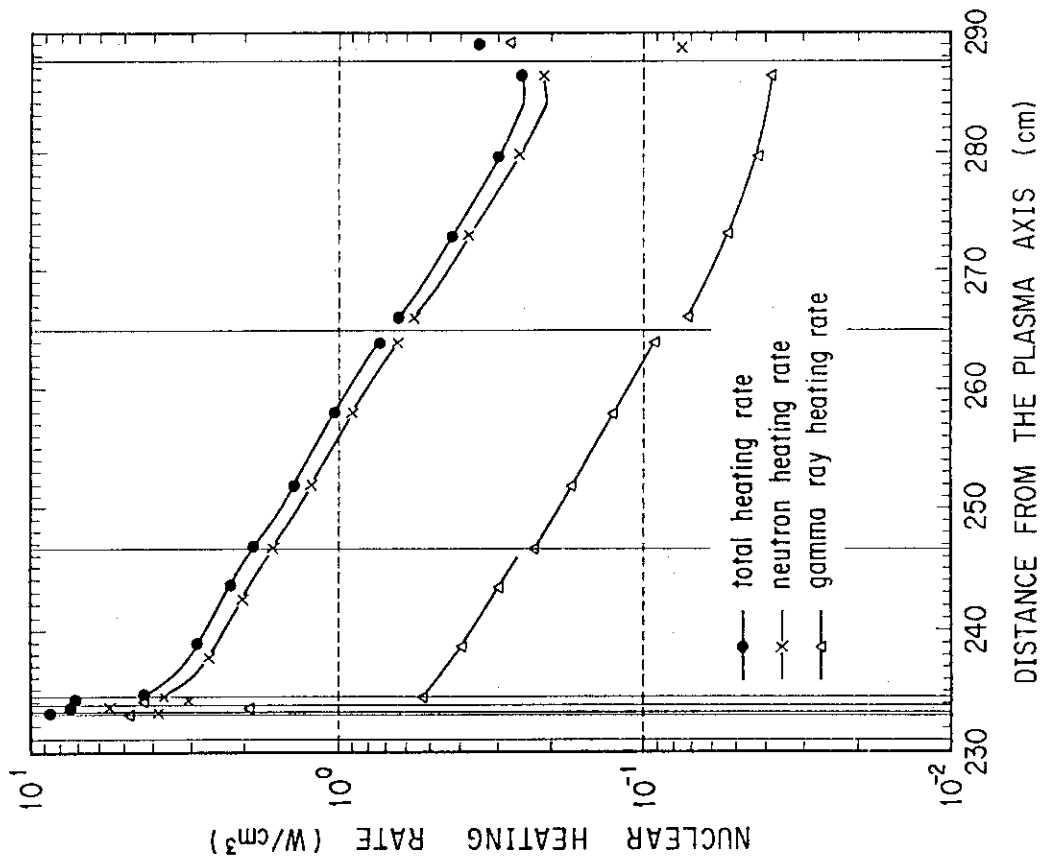


Fig. 6.2.11 Distribution of nuclear heating rate in the mixed pebble bed blanket at outboard top (without carbon armor)

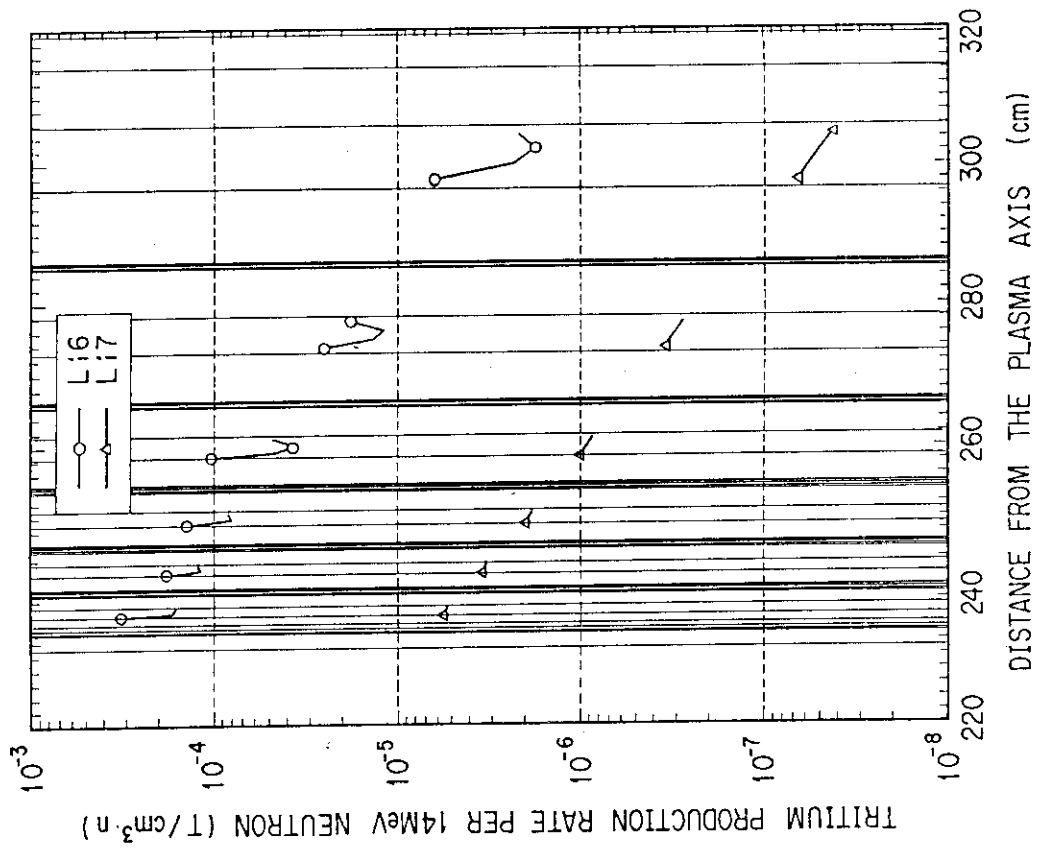


Fig. 6.2.14 Distribution of tritium production rate in the layered pebble bed blanket at outboard top (with carbon armor)

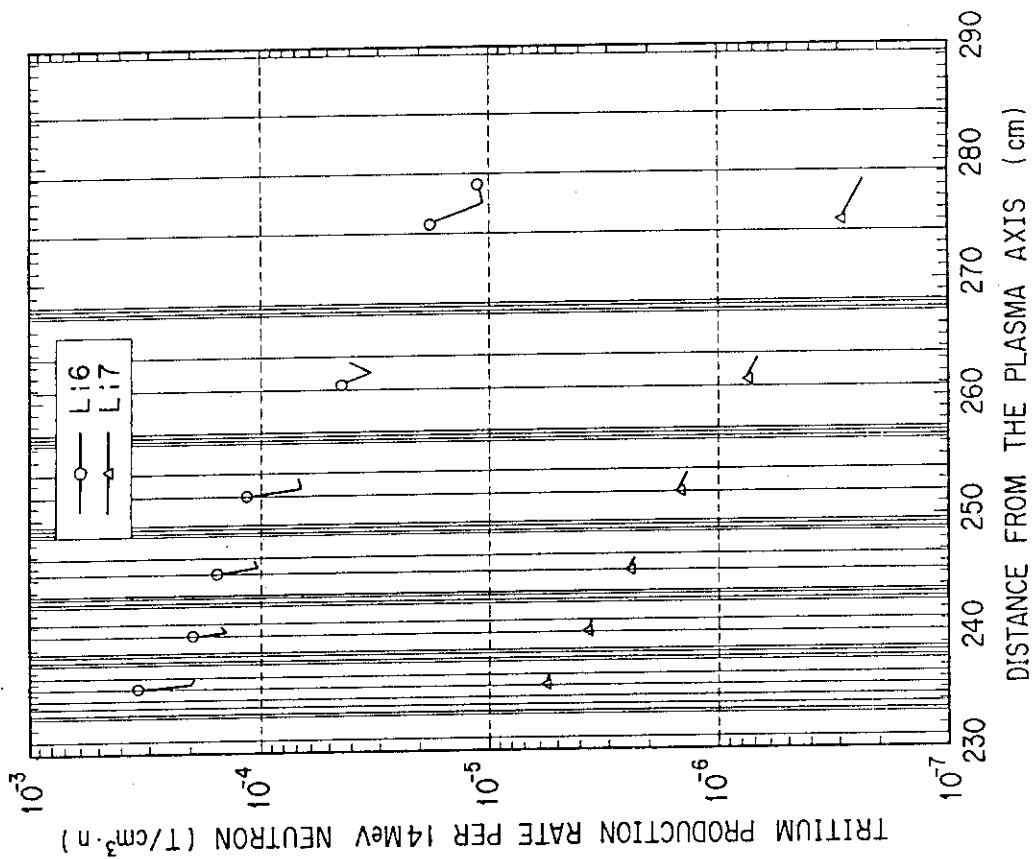


Fig. 6.2.13 Distribution of tritium production rate in the layered pebble bed blanket at outboard midplane (with carbon armor)

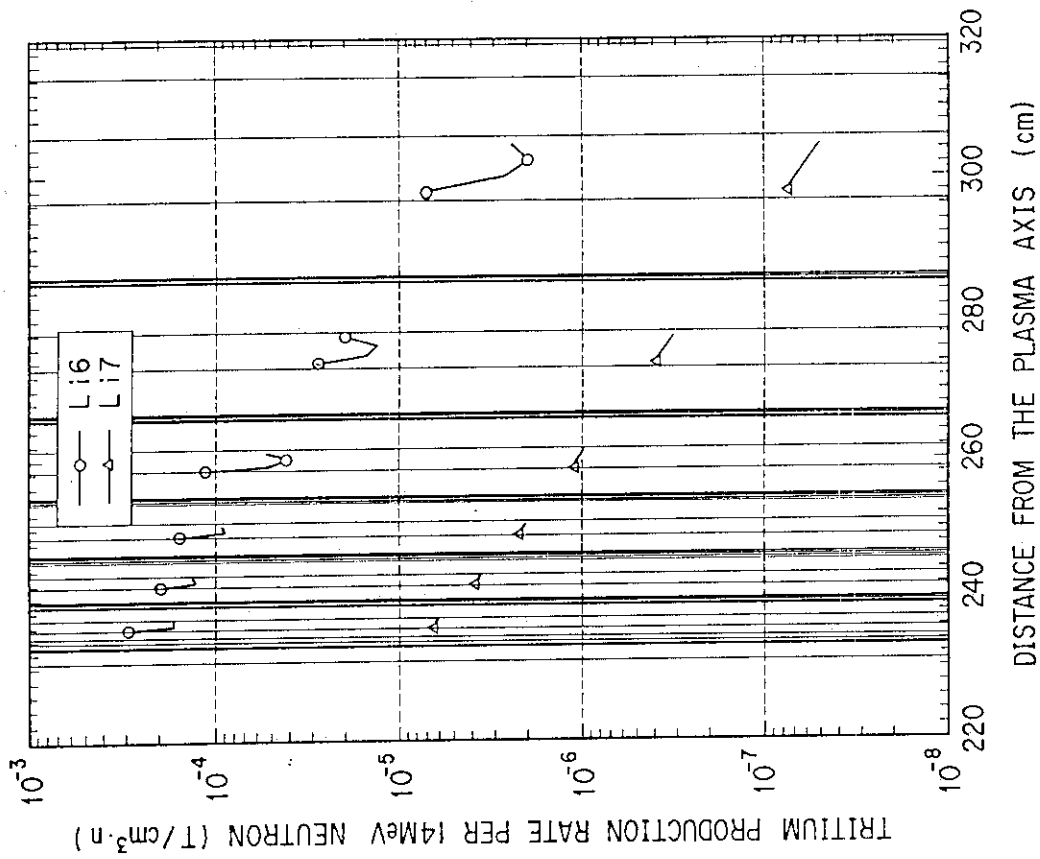


Fig. 6.2.16 Distribution of tritium production rate in the layered pebble bed blanket at outboard top (without carbon armor)

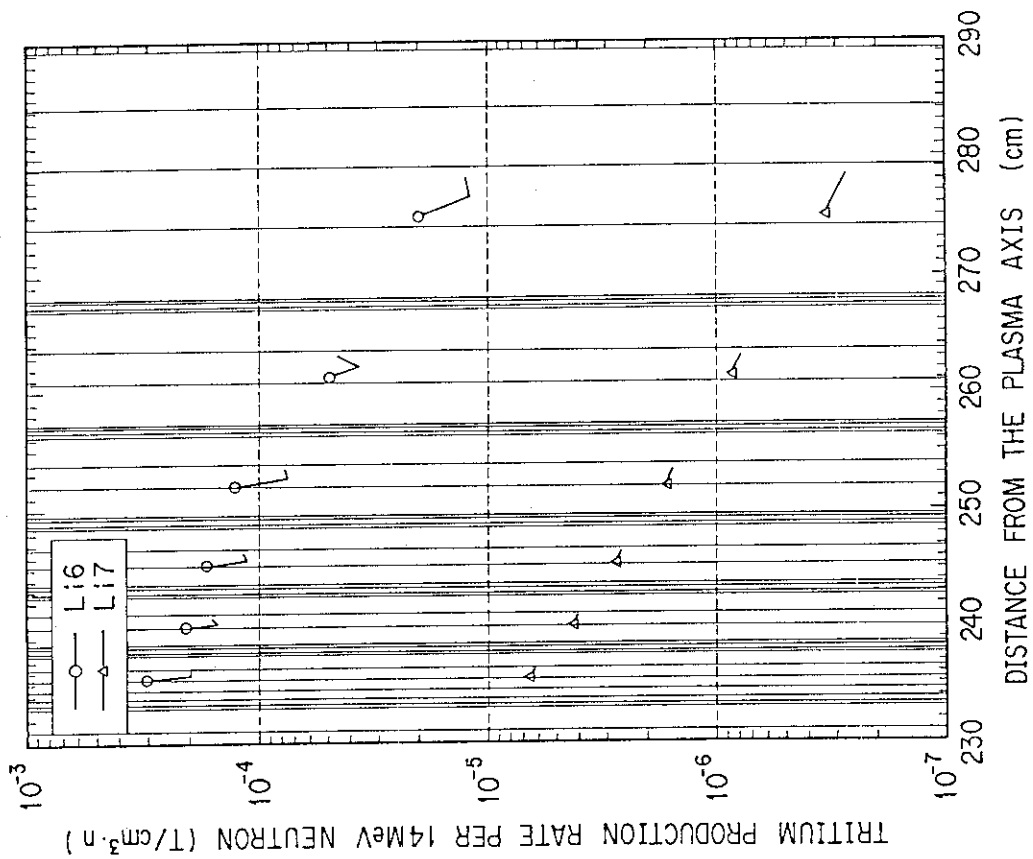


Fig. 6.2.15 Distribution of tritium production rate in the layered pebble bed blanket at outboard midplane (without carbon armor)

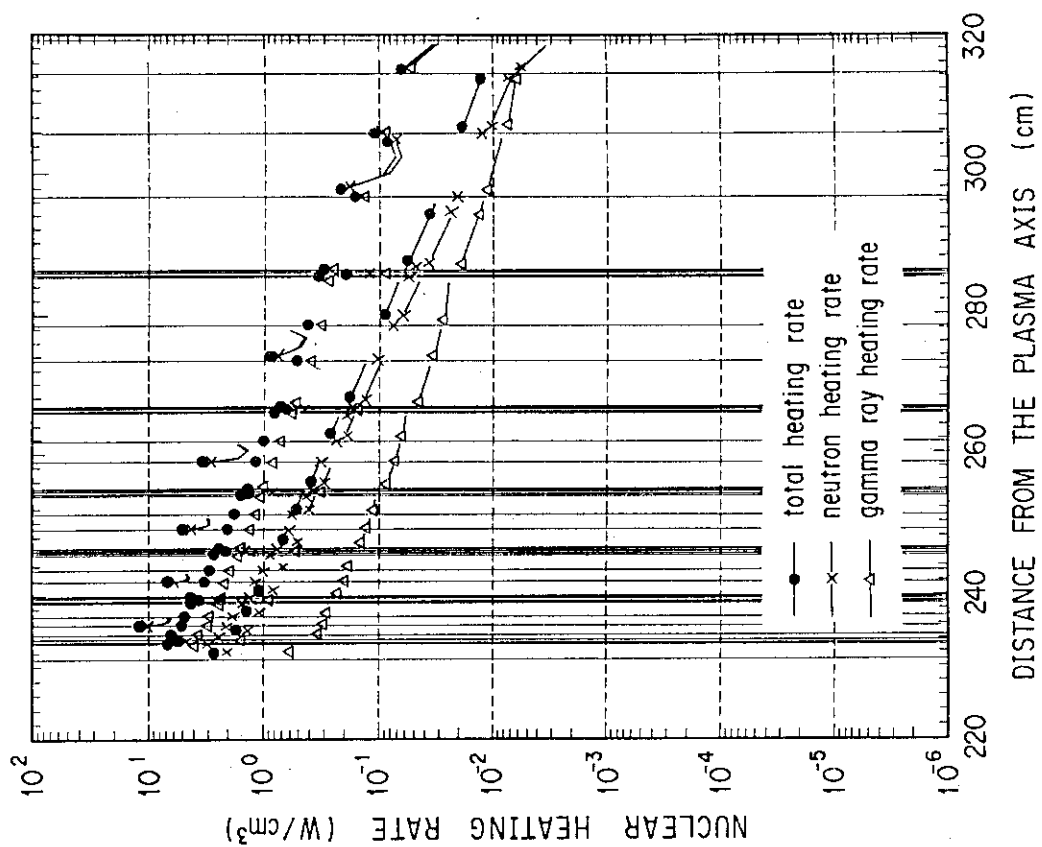


Fig. 6.2.17 Distribution of nuclear heating rate in the layered pebble bed blanket at outboard midplane (with carbon armor)

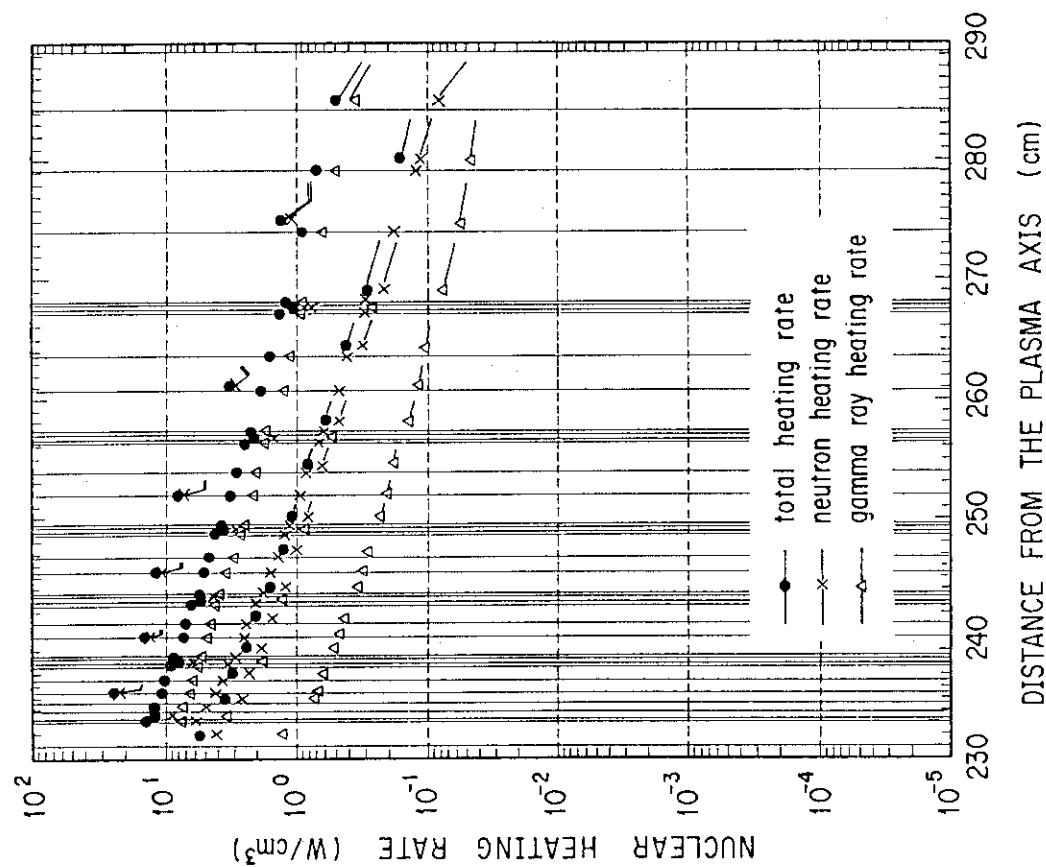


Fig. 6.2.18 Distribution of nuclear heating rate in the layered pebble bed blanket at outboard top (with carbon armor)



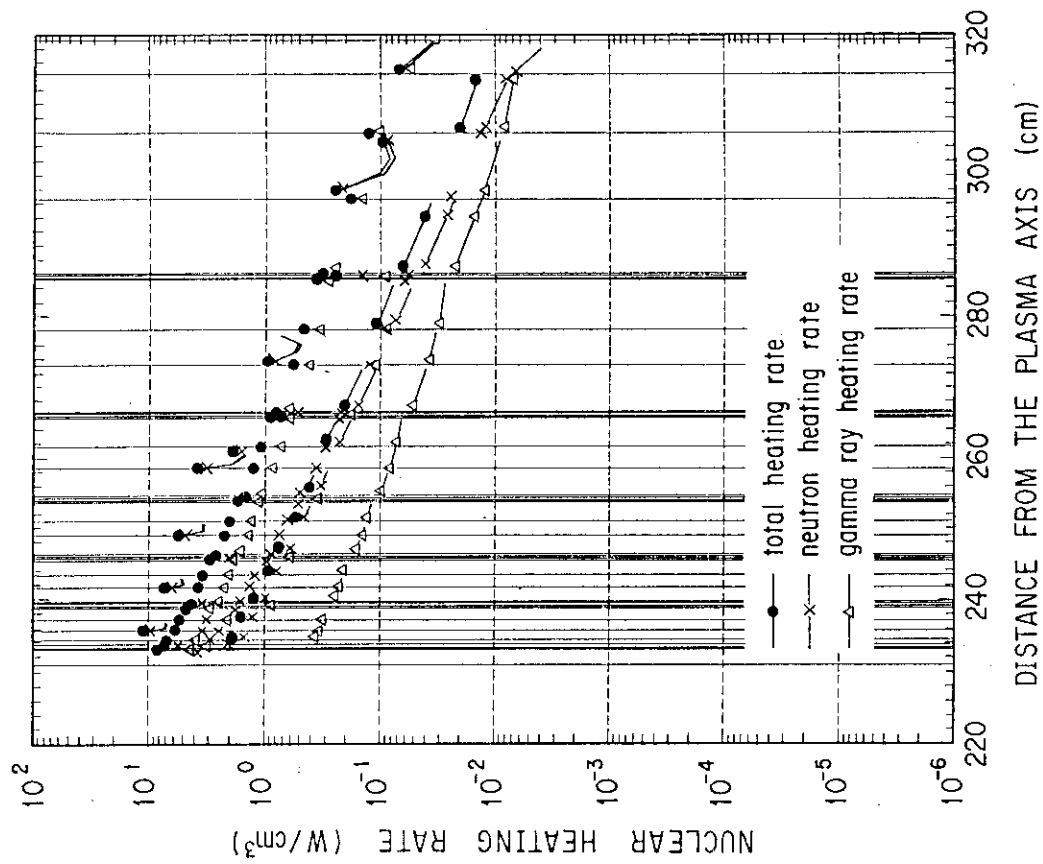


Fig. 6.2.20 Distribution of nuclear heating rate in the layered pebble bed blanket at outboard top (without carbon armor)

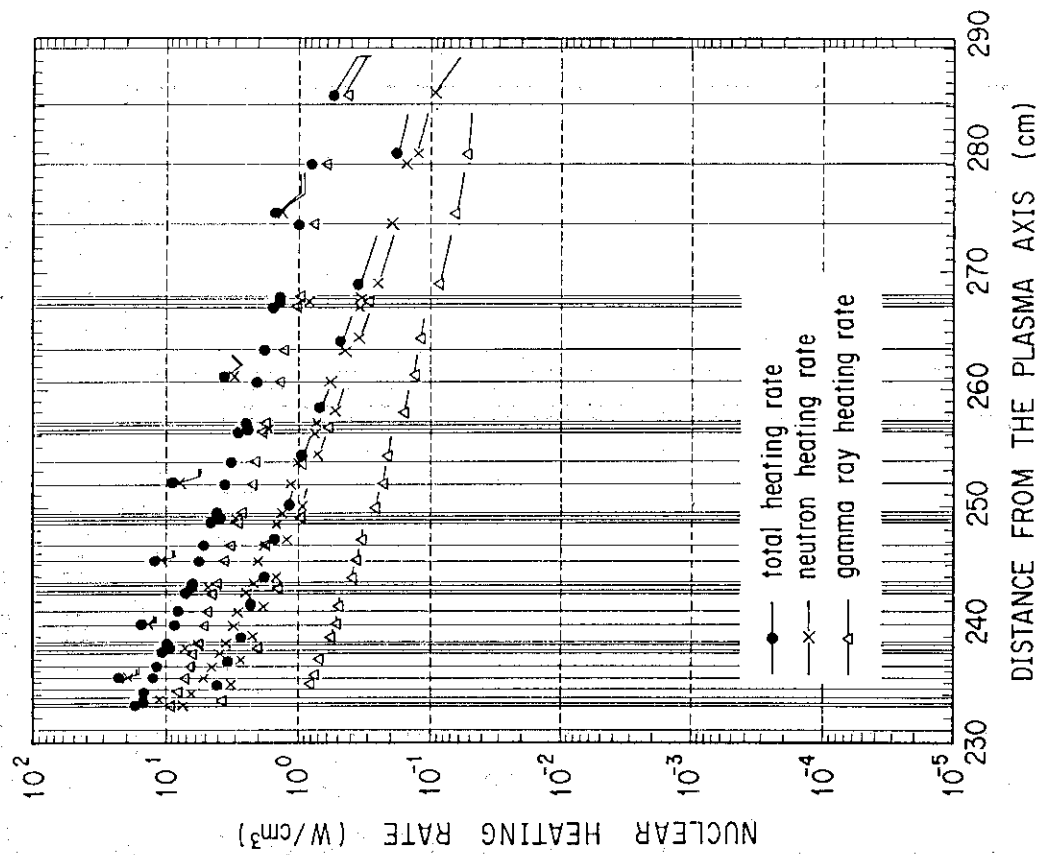


Fig. 6.2.19 Distribution of nuclear heating rate in the layered pebble bed blanket at outboard midplane (without carbon armor)

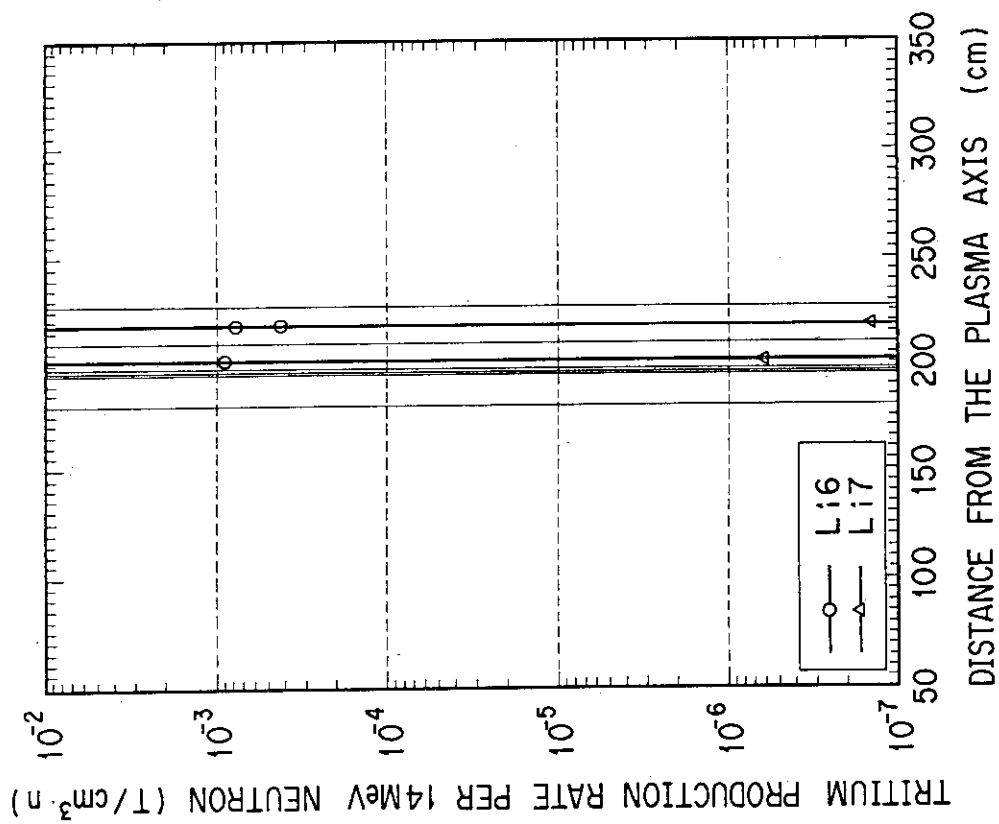


Fig. 6.2.21 Tritium production rate profile in the pebble and block blanket (without carbon armor)

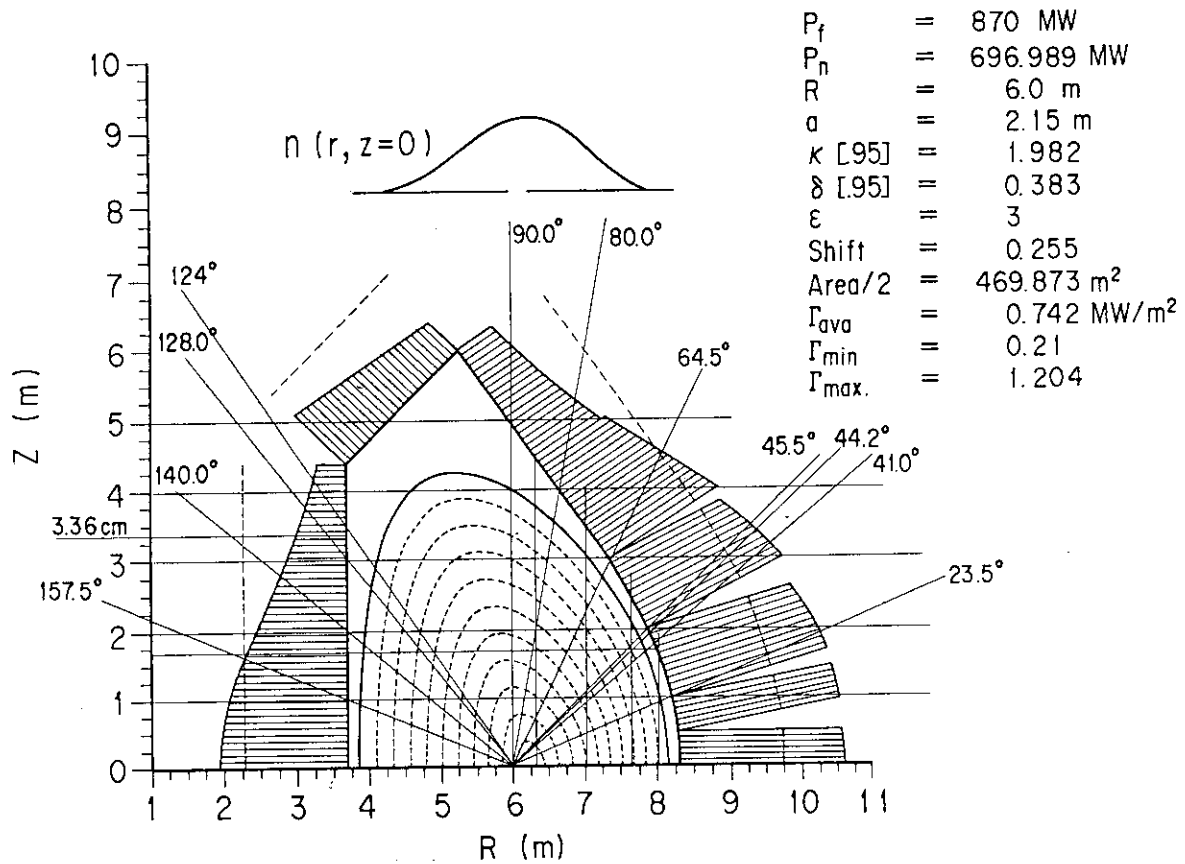


Fig. 6.2.22 Neutron well loading distribution for the Technology Phase

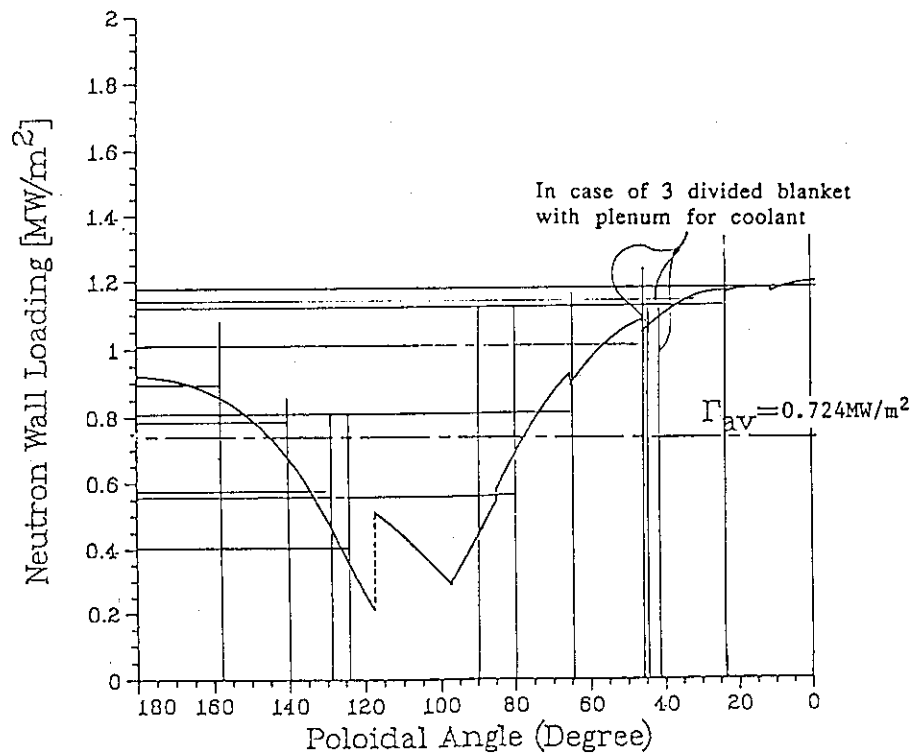


Fig. 6.2.23 Neutron wall loading distribution as a function of the poloidal angle for the Technology Phase

### 6.3 Conclusions

Neutronic analyses for three types of blanket have been performed. In these analyses, net TBR's are estimated based on local TBR's by one-dimensional calculations. Tritium production rates and nuclear heating rates are also computed. From the results of these analyses, the following conclusions are obtained.

- 1) Net TBR's of the mixed pebble bed and the layered pebble bed blankets have no significant difference. They are 0.80 without carbon armor and 0.75 with 2 cm thick carbon armor.
- 2) Carbon armor with 2 cm thickness in front of the breeding region decreases the net TBR by 0.05.
- 3) The local TBR of the pebble and block blanket without carbon armor is 1.31 which is little smaller than those of other blankets. However, the net TBR of this blanket is expected to be similar to those of others.
- 4) At the outboard midplane of the mixed pebble bed blanket, peak nuclear heating rates in the first wall stainless steel structure without and with 2 cm thick carbon armor are  $18 \text{ W/cm}^3$  and  $15 \text{ W/cm}^3$ , respectively.
- 5) At outboard midplane of the layered pebble bed blanket, peak nuclear heating rates in the first  $\text{Li}_2\text{O}$  layer with 2 cm thick carbon armor are  $25 \text{ W/cm}^3$ , which is almost the same as that without the carbon armor.

### REFERENCES

- [1] Maki, K., et al., : "Fusion Nuclear Group Constant Set FUSION-J3 and Shielding Properties for Fusion Experimental Reactor by FUSION-J3," 1990 Annual Meeting of the Atomic Energy Society of Japan F8 (April 1990).
- [2] Shibata K., et al., : "Japanese Evaluated Nuclear Data Library, Version-3 --JENDL-3--," JAERI 1319 (June, 1990).
- [3] Maki, K., et al., "Estimation of Tritium Breeding Ratio in ITER with Full Blanket," 1989 Summer Specialist Meeting on ITER Blanket and Shield, (1989).
- [4] Gohar, Y., et al., "U.S. Solid Breeder Blanket Design and Analyses," 1990 Winter Specialist Meeting on ITER Blanket, (Jan., 1990).

## 7. Thermal Analysis

Temperature distributions in two types of blanket, the mixed pebble bed and the layered pebble bed blankets, are preliminarily calculated. Breeder temperature control with a contact conductance between a clad of  $\text{Li}_2\text{O}$  pebble packed layer and a beryllium block in the pebble and block blanket is also investigated. Section 7.1 describes analytical models, calculational cases and results for the mixed pebble bed blanket. In terms of  $\text{Li}_2\text{O}$  temperature, permissible power variations are also discussed. Analytical models, calculational cases, results and discussions of permissible power variations for the layered pebble bed blanket are indicated in Section 7.2. Section 7.3 shows the discussions on breeder temperature control and thermal stress in a beryllium block in the pebble and block blanket.

### 7.1 Mixed Pebble Bed Blanket

#### 7.1.1 Design process

Since temperature control of the breeder in the mixed pebble bed blanket is realized by the cooling tube arrangement and gap width around the cooling tube, those two are the most important parameters for thermal design of this type of blanket. The process of thermal design is shown in Fig. 7.1.1.1. Solution is not unique and is achieved by various combinations of design parameters such as pitch of tubes, gap width, nominal temperature of breeder and so forth. In the present design, the following assumptions are taken into account.

- (1) A blanket module (outboard side module) is poloidally divided into three units in the blanket box. Neutron wall loads applied to them are as follows:

Upper unit	0.6-0.9 MW/m <sup>2</sup>
Middle unit	0.9-1.2 (at midplane) - 0.9 MW/m <sup>2</sup>
Lower unit	0.6-0.9 MW/m <sup>2</sup>

- (2) Cooling tubes are arranged at the point of the lowest wall load in each unit; 0.6 MW/m<sup>2</sup> for the upper and lower units, and 0.9 MW/m<sup>2</sup> for the middle unit.
- (3) Gap widths are changed in the poloidal direction and also in the radial direction.
- (4) The nominal design temperature range of the breeder is 450-600 °C, while the allowable operation temperature range is 400-1000 °C (for  $\text{Li}_2\text{O}$ ).

Tube arrangement and gap widths are computed with the procedure indicated in Fig. 7.1.2. Calculated tube arrangements in the selected poloidal cross-sections are summarized in Table 7.1.1 and described in Figs 7.1.3 and 7.1.4. Schematic views of the tubes and breeder pebbles are illustrated in Figs 7.1.5 to 7.1.8.

### 7.1.2 Analytical model and cases

The center part of the blanket cross-section is modeled as shown in Figs 7.1.9. Left and right boundaries of this model, which face helium gap on the first and back walls, are assumed to be at the constant temperature of 400 °C. Top and bottom boundaries are assumed to be adiabatic. Nonlinear thermal analyses have been performed with this model by the finite element analysis code, ABAQUS. Thermal conductivity of  $\text{Li}_2\text{O}$  pebble bed with packing fraction of 60 %, which is used in this analysis, is shown in Figs 7.1.10 as a function of temperature. Temperature-dependent thermal conductivity is used also for 316SS. Thermal conductivity of the gap layer is assumed to be that of helium gas at 0.1 MPa and 250 °C. Emissivity of 316SS in the gap layer is assumed to be 0.6. Nuclear heating rates in the  $\text{Li}_2\text{O}$  pebble bed and 316SS cooling tube are represented by the following exponential functions.

- In pebble bed:  $Q = 6.1 \cdot P \cdot \exp(-0.0544x)$ ,
- In 316SS:  $Q = 8.1 \cdot P \cdot \exp(-0.0465x)$ ,

where  $Q$  = nuclear heating rate [ $\text{W}/\text{cm}^3$ ],  $P$  = neutron wall load [ $\text{W}/\text{cm}^2$ ],  $x$  = distance from the first wall [cm]. Coolant temperature and heat transfer coefficient are assumed to be 90 °C and 10,000  $\text{W}/\text{m}^2\text{K}$ , respectively.

With the model mentioned above, the following six cases are calculated.

- Case A: Top part of the upper unit ( $P = 0.6 \text{ MW}/\text{m}^2$ )
- Case B: Bottom part of the upper unit ( $P = 0.9 \text{ MW}/\text{m}^2$ )
- Case C: Top part of the middle unit ( $P = 0.9 \text{ MW}/\text{m}^2$ )
- Case D: Midplane of the middle unit ( $P = 1.2 \text{ MW}/\text{m}^2$ )
- Case E: Midplane of the middle unit ( $P = 1.2 \text{ MW}/\text{m}^2$ )  
with increased gap width from 1 mm (Case D) to 2 mm
- Case F: Midplane of the middle unit with increased wall load  
from 1.2  $\text{MW}/\text{m}^2$  (Case D) to 1.44  $\text{MW}/\text{m}^2$

### 7.1.3 Results and discussions

Temperature distributions of the six cases are shown in Figs 7.1.11 to 7.1.16. Temperatures of almost all region are within the allowable range (400 - 1000 °C). Temperatures of small area around tubes near the back wall are below 400 °C (Case B, C and D). With wider gap width (2 mm), temperatures of this area rise above 400 °C (Case E), thus further careful optimization of gap widths are required to keep the breeder temperature above the lower temperature limit. The maximum temperature is still below 1000 °C even if the wall load is increased by 20 % (Case F). Further investigation is necessary to find the optimum design parameters, especially tube arrangements and gap widths including their poloidal and radial distributions, to keep the breeder temperature within the nominal design range and to obtain larger margin for power variations.

Table 7.1.1 Tube arrangement in the mixed pebble bed blanket

Top unit (Bottom unit)

Row No.	Number of tubes	Toroidal pitch (mm)		Distance from F/W liner (mm)	Gap thickness (mm)	
		Upper (Lower)	Lower (Upper)		Upper (Lower)	Lower (Upper)
1	22	34.8	39.1	29.9	3	1
2	20	37.8	42.8	69.1	3	1
3	19	39.5	44.9	111.1	3	1
4	18	43.3	49.6	156.1	3	1
5	17	45.5	52.3	204.3	3	1
6	16	50.5	58.6	256.1	3	1
7	15	53.6	62.4	312.3	3	1
8	13	60.5	70.9	373.7	3	1 (3)*
9	12	64.8	76.3	441.8	3	1 (3)

Middle unit

Row No.	Number of tubes	Toroidal pitch (mm)		Distance from F/W liner (mm)	Gap thickness (mm)	
		Upper & Lower	Midplane		Upper & Lower	Midplane
1	28	32.4	34.9	26.5	2	1
2	26	35.0	37.7	62.1	2	1
3	25	36.5	39.3	100.0	2	1
4	23	39.7	42.7	140.3	2	1
5	22	41.6	44.8	183.2	2	1
6	21	43.6	46.7	228.9	2	1
7	19	48.2	51.9	277.8	2	1
8	18	51.0	54.9	330.6	2	1
9	16	57.2	61.5	388.2	2 (3)*	1 (2)*
10	15	61.0	65.6	451.6	2 (3)*	1 (2)*

\* Gap thickness must be increased to rise temperature around cooling tubes.



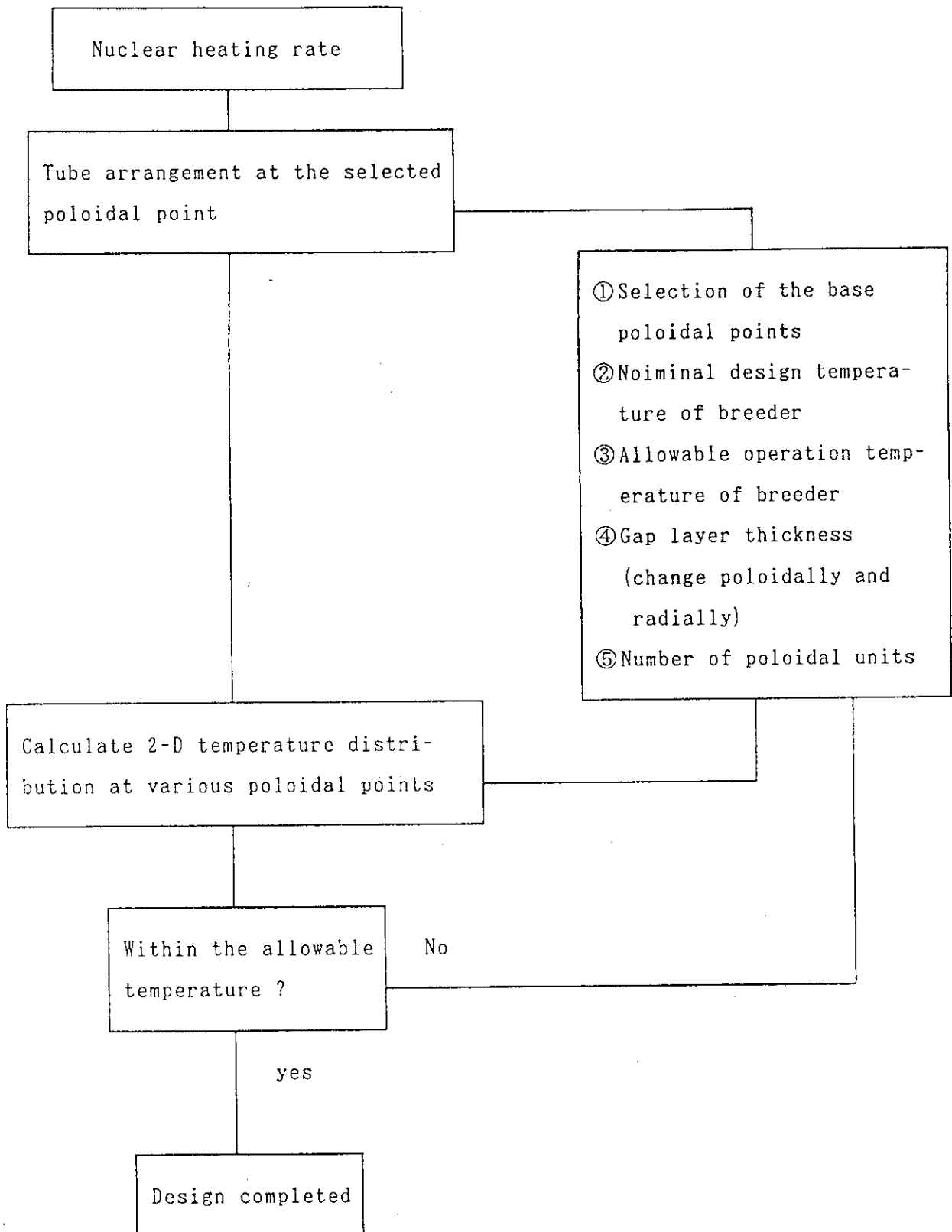


Fig. 7.1.1 Flowchart for thermal design of the mixed pebble bed blanket

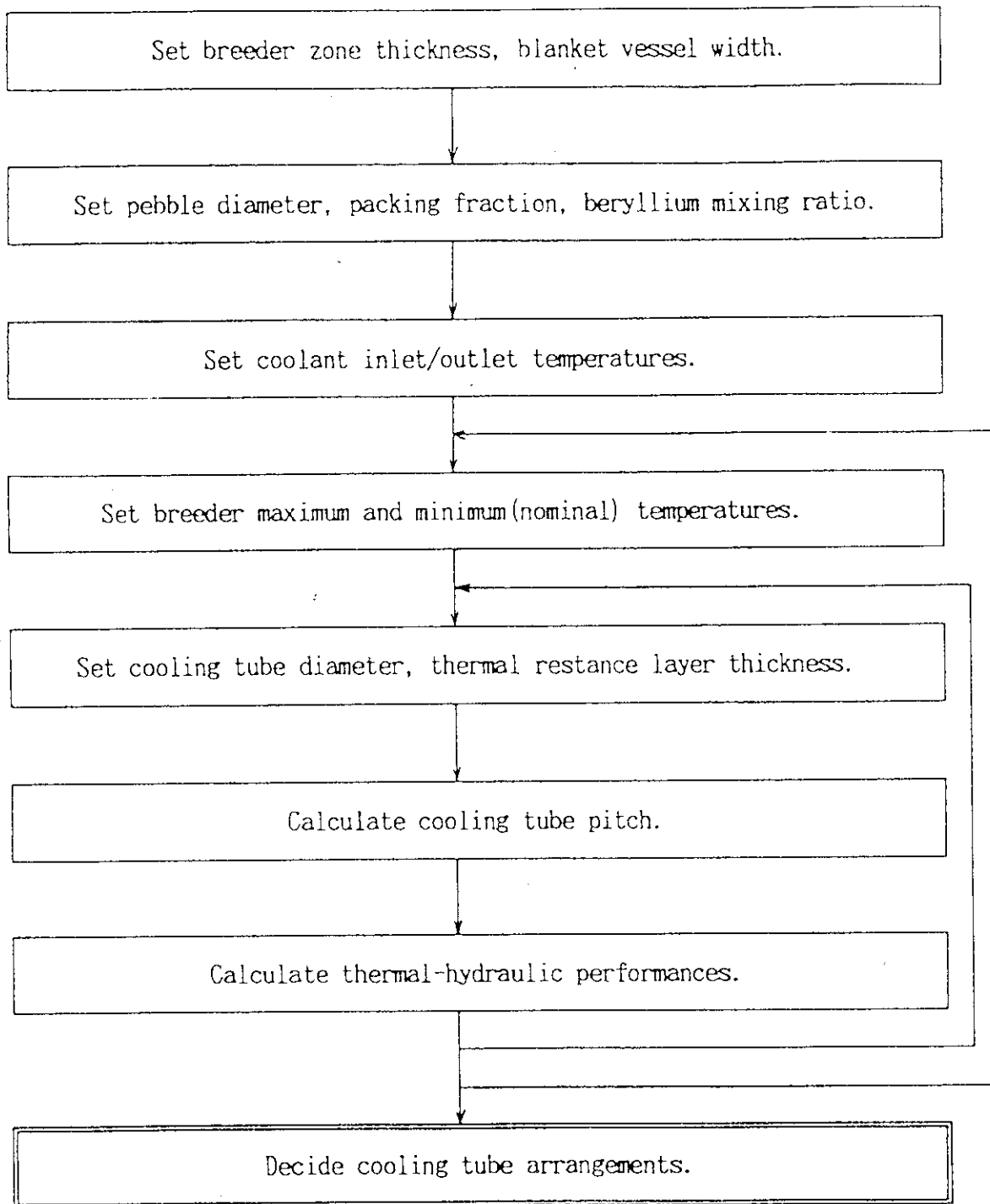


Fig. 7.1.2 Procedure for cooling tube arrangement

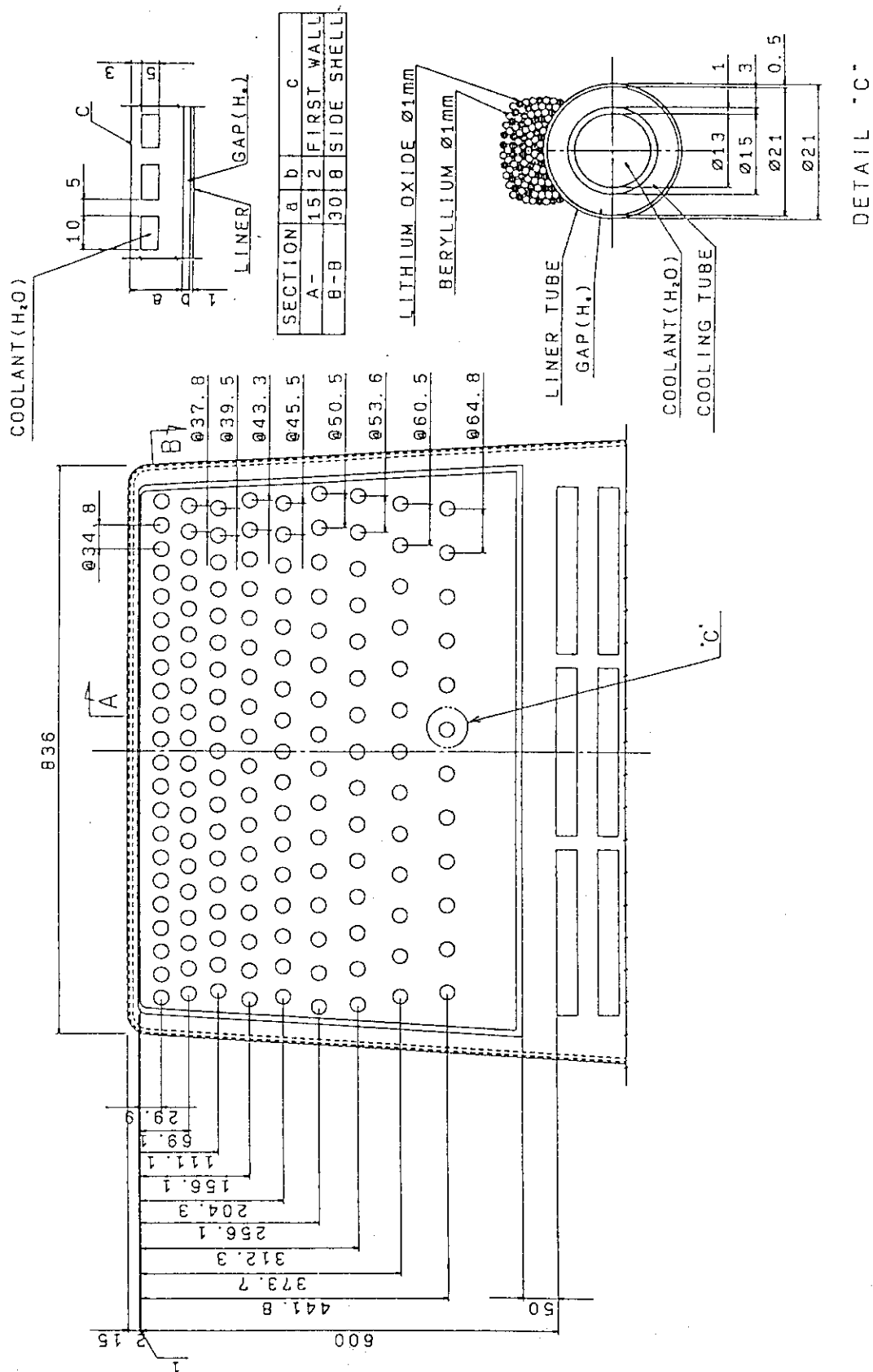


Fig. 7.1.3 Tube arrangement at top end of the upper unit

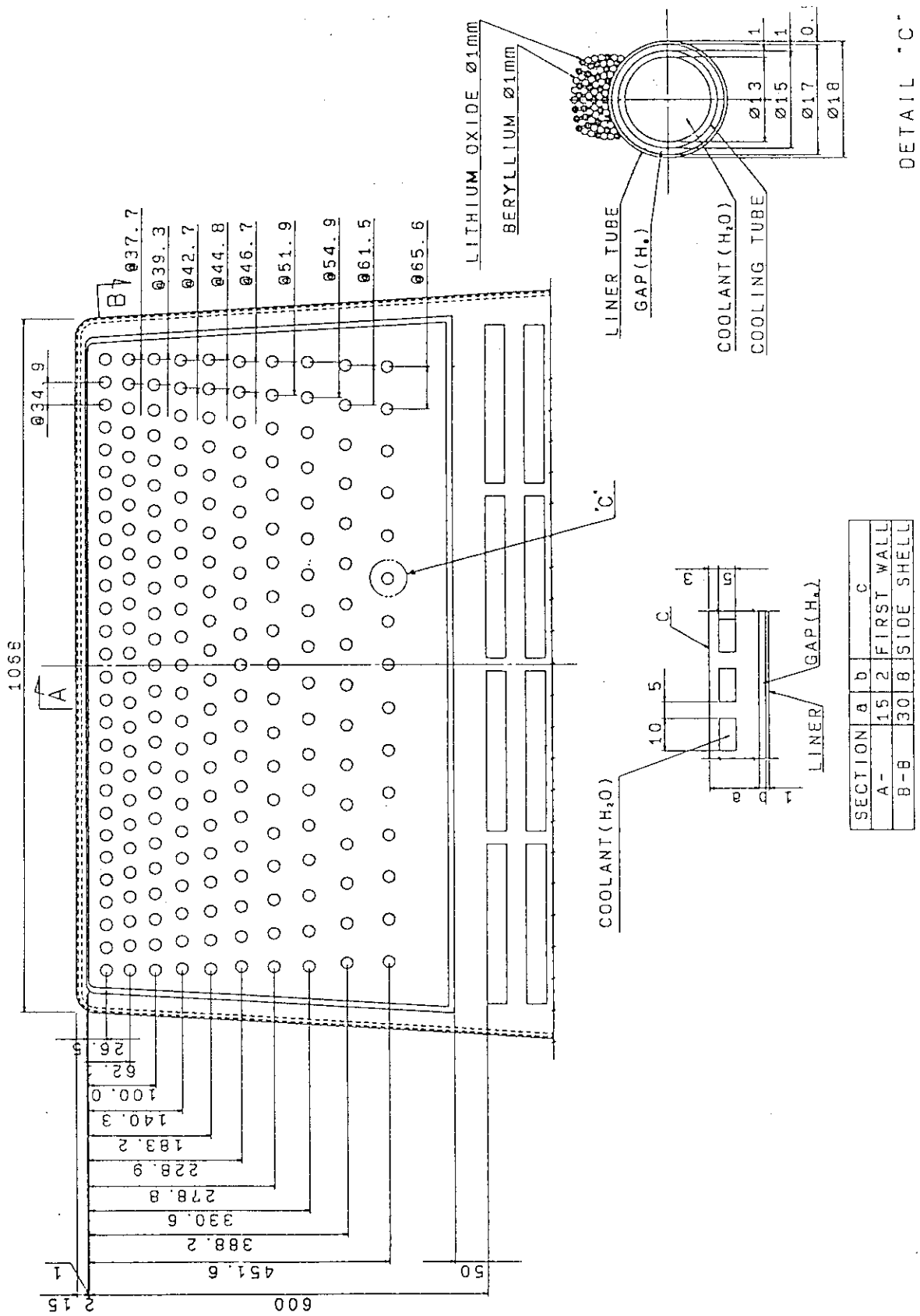


Fig. 7.1.4 Tube arrangement at midplane of hte middle unit

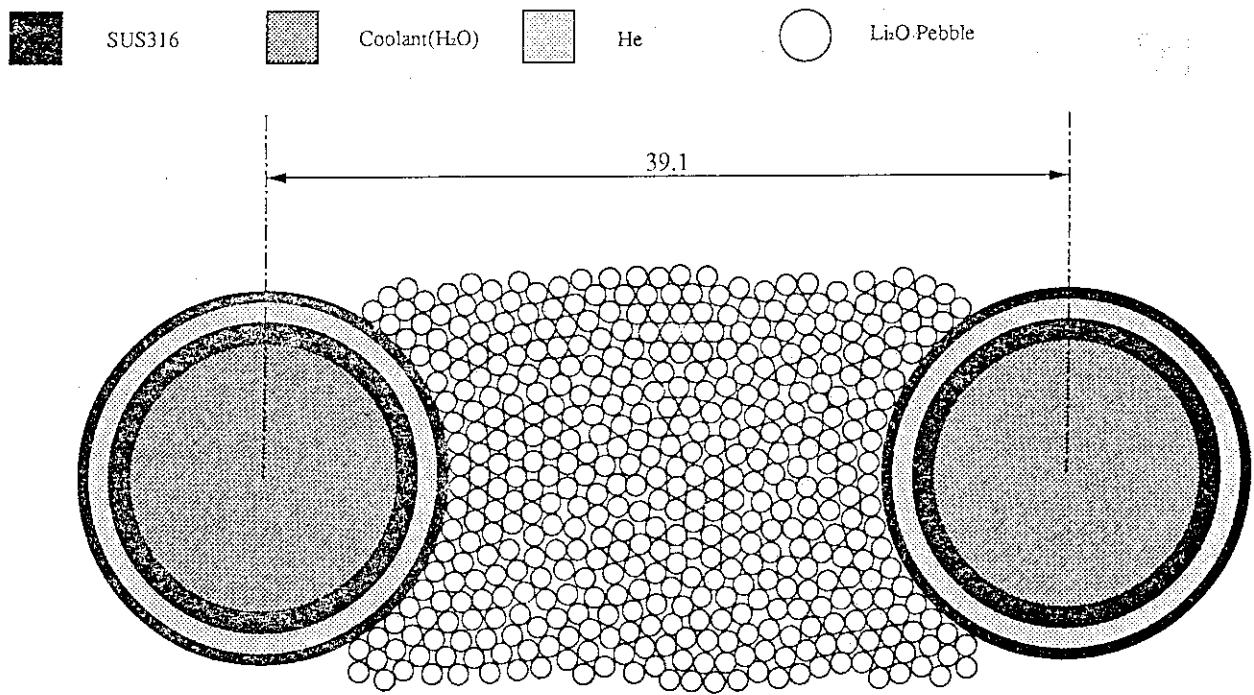


Fig. 7.1.5 Schematic view of coolant tubes and breeder pebbles (plasma side of the upper unit at outlet, tube outer/inner diameter: 15/13 mm, He gap: 1 mm, spacer tube thickness: 0.5 mm, inlet/outlet coolant temperature: 90/100°C)

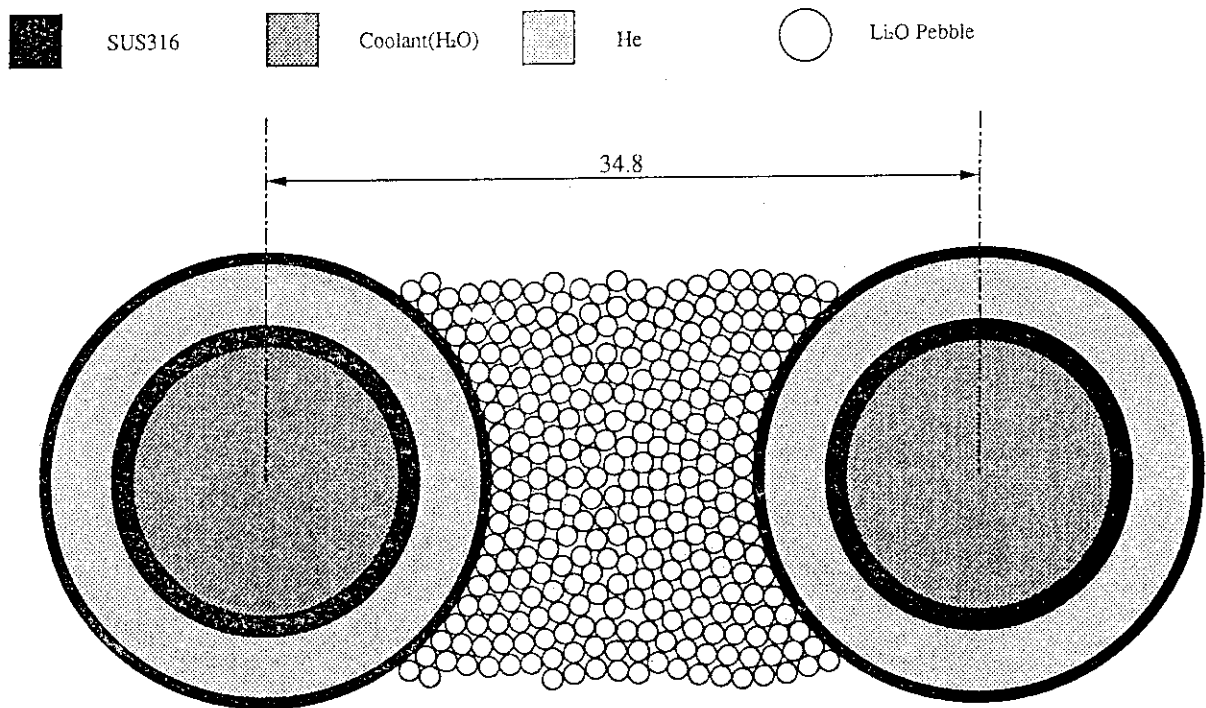


Fig. 7.1.6 Schematic view of coolant tubes and breeder pebbles (plasma side of the upper unit at outlet, tube outer/inner diameter: 15/13 mm, He gap: 3 mm, spacer tube thickness: 0.5 mm, inlet/outlet coolant temperature: 90/100°C)

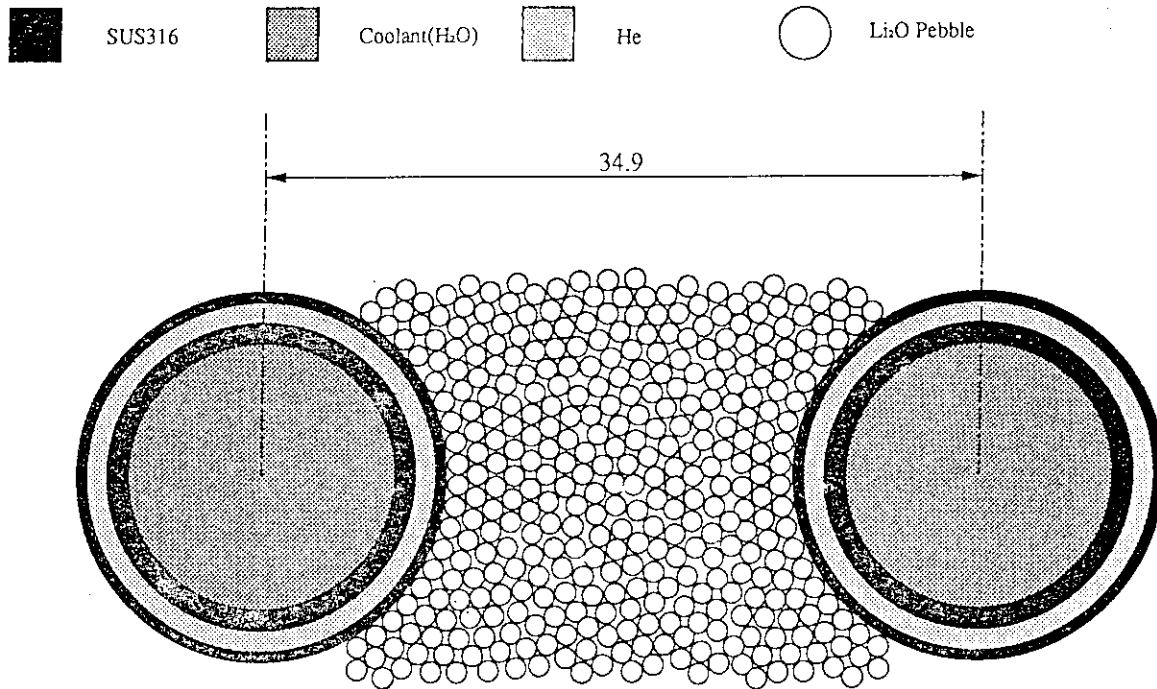


Fig. 7.1.7 Schematic view of coolant tubes and breeder pebbles (plasma side of the middle unit at midplane, tube outer/inner diameter: 15/13 mm, He gap: 1 mm, spacer tube thickness: 0.5 mm, inlet/outlet coolant temperature: 70/90°C)

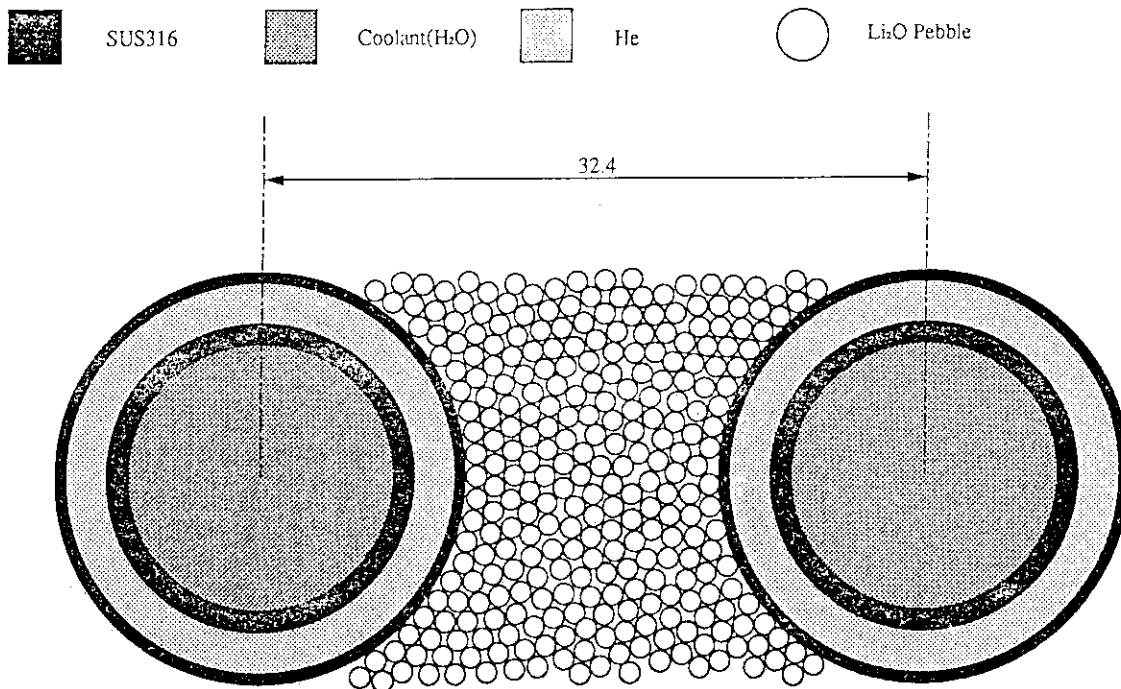


Fig. 7.1.8 Schematic view of coolant tubes and breeder pebbles (plasma side of the middle unit at outlet, tube outer/inner diameter: 15/13 mm, He gap: 2 mm, spacer tube thickness: 0.5 mm, inlet/outlet coolant temperature: 70/90°C)

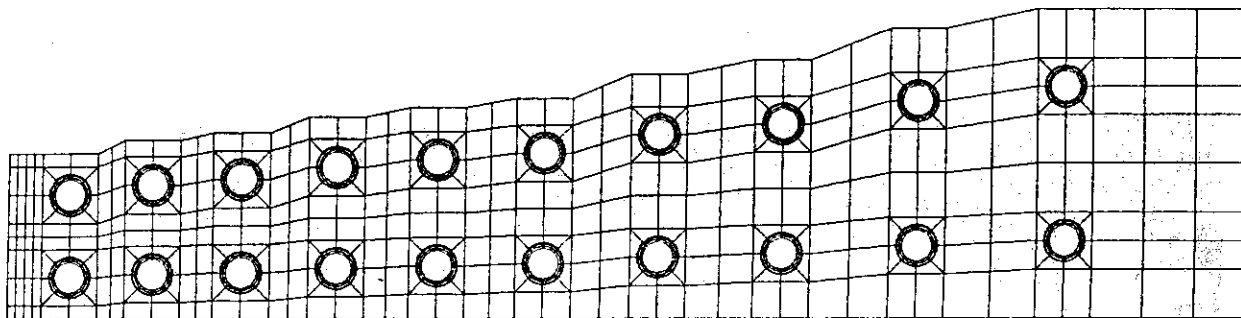


Fig. 7.1.9 Geometrical model  
for 2-D finite  
element thermal  
analysis

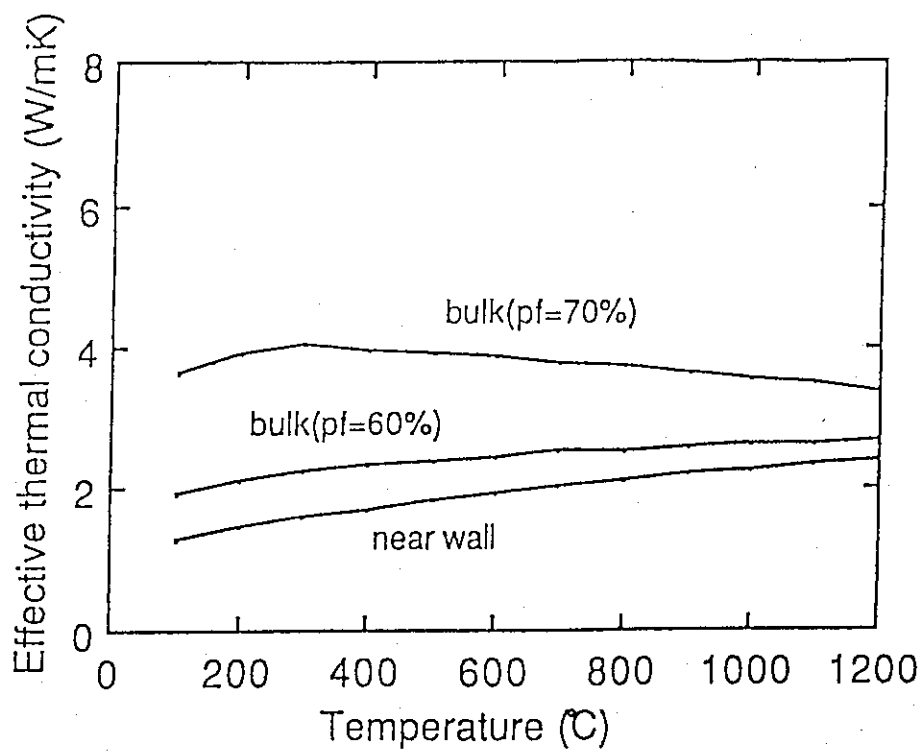


Fig. 7.1.10 Effective thermal conductivity of  
breeding zone ( $\text{Li}_2\text{O}$ : 25%, Be:75%,  
pebble diameter:1mm)

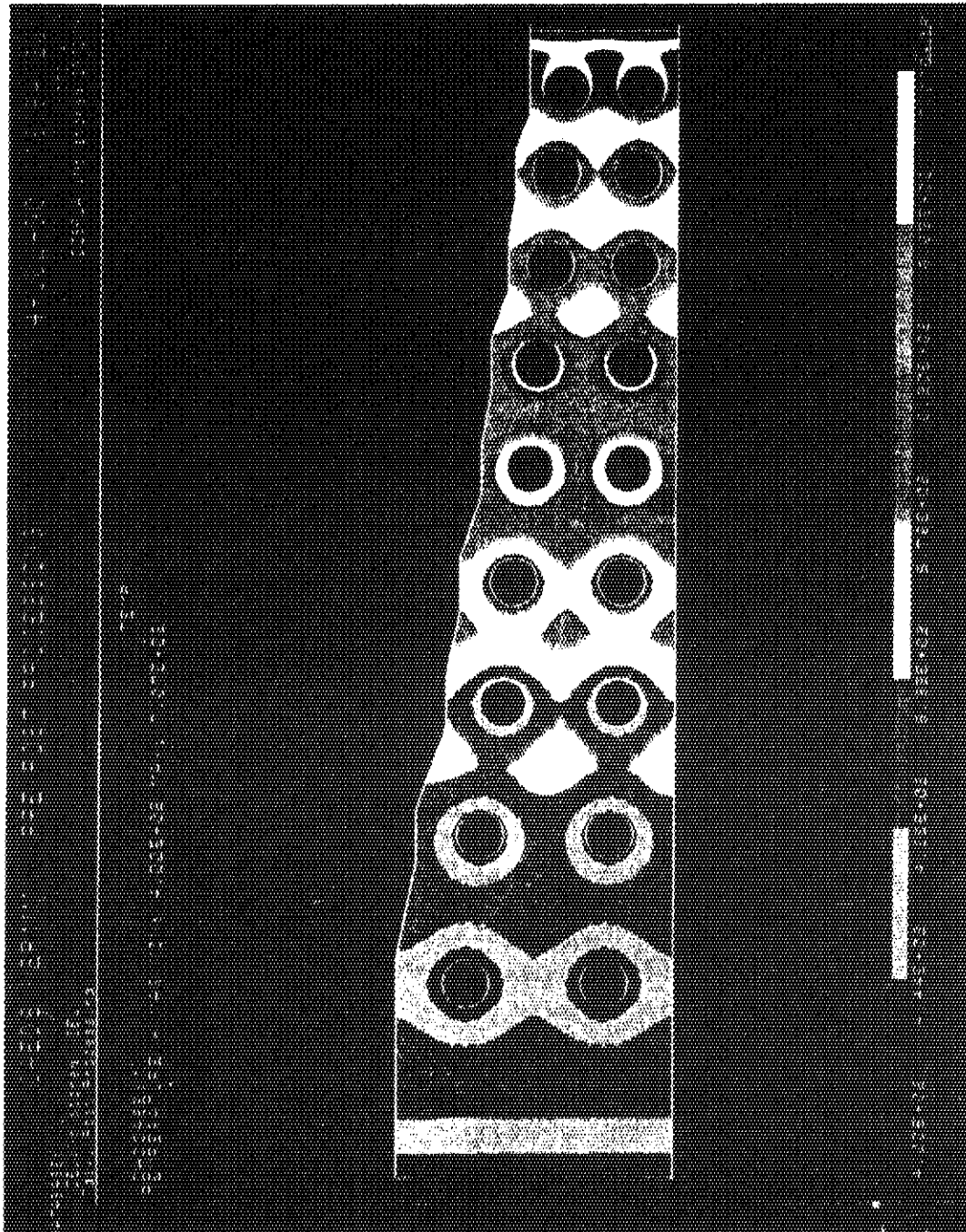


Fig. 7.1.11 Temperature distribution in the mixed pebble bed blanket  
(case A; top part of the upper unit with wall loading of  
 $0.6 \text{ MW/m}^2$ )



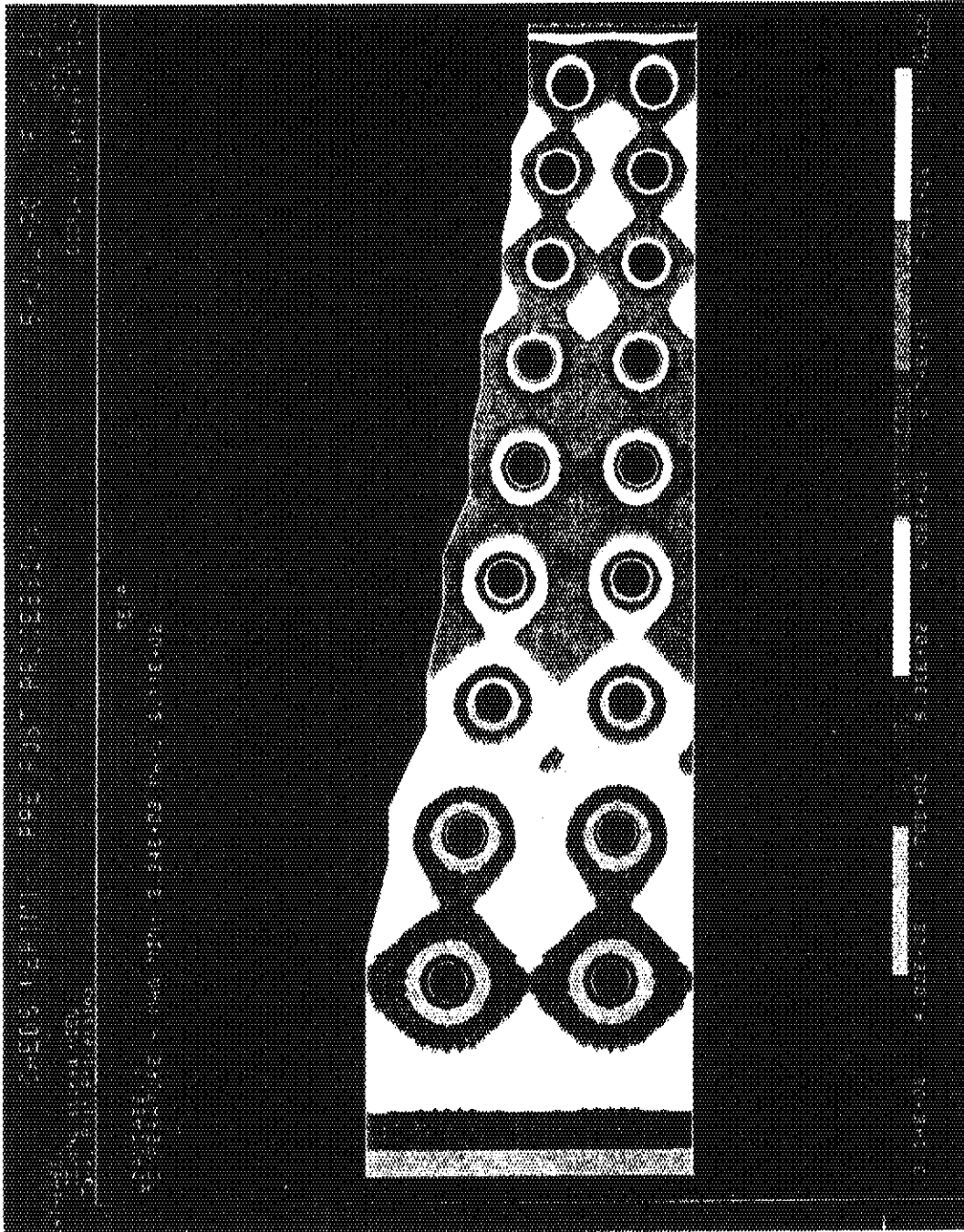


Fig. 7.1.12 Temperature distribution in the mixed pebble bed blanket  
 (case B; bottom part of the upper unit with wall loading of  
 $0.9 \text{ MW/m}^2$ )

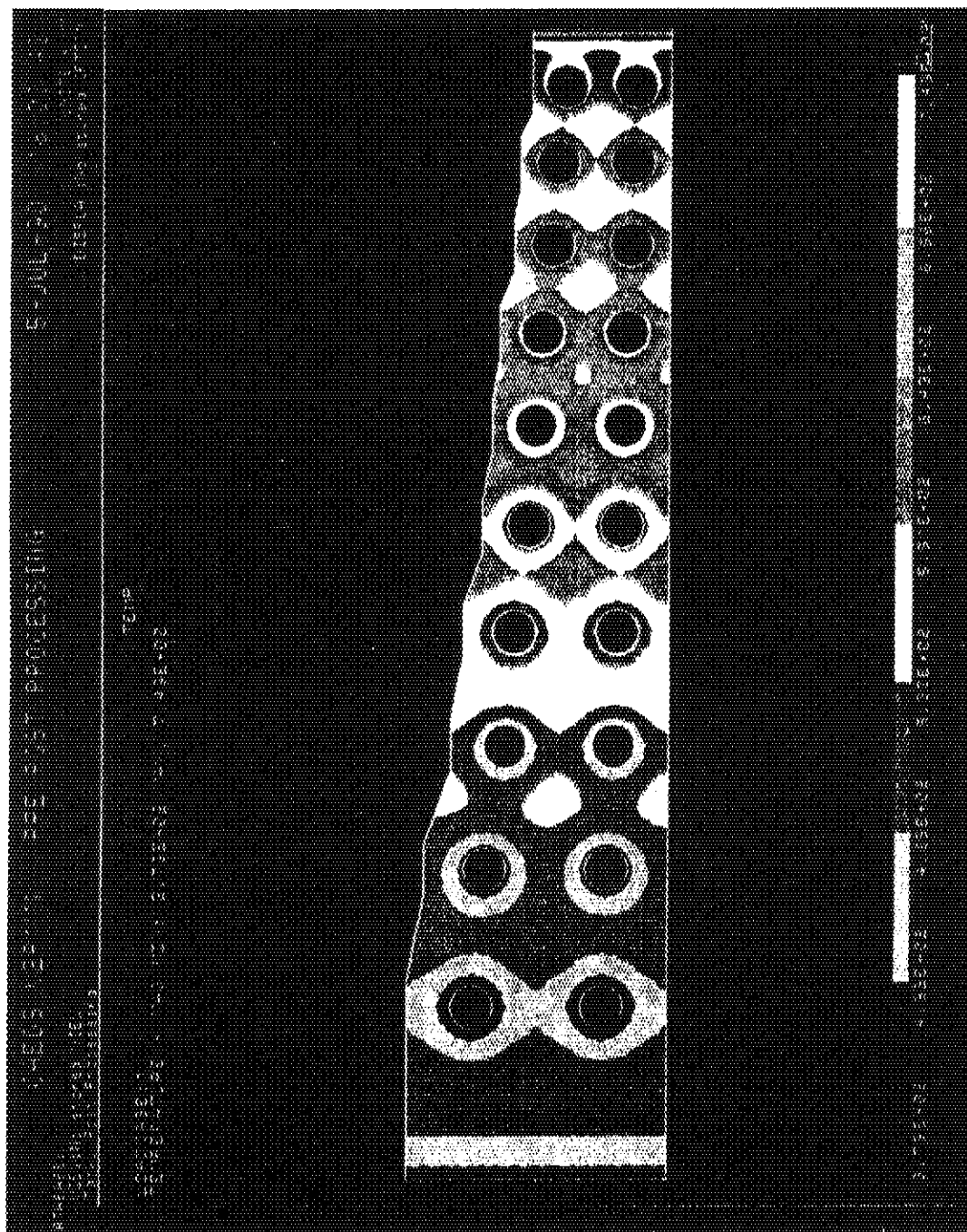


Fig. 7.1.13 Temperature distribution in the mixed pebble bed blanket  
(case C; top part of the middle unit with wall loading of  
 $0.9 \text{ MW/m}^2$ )

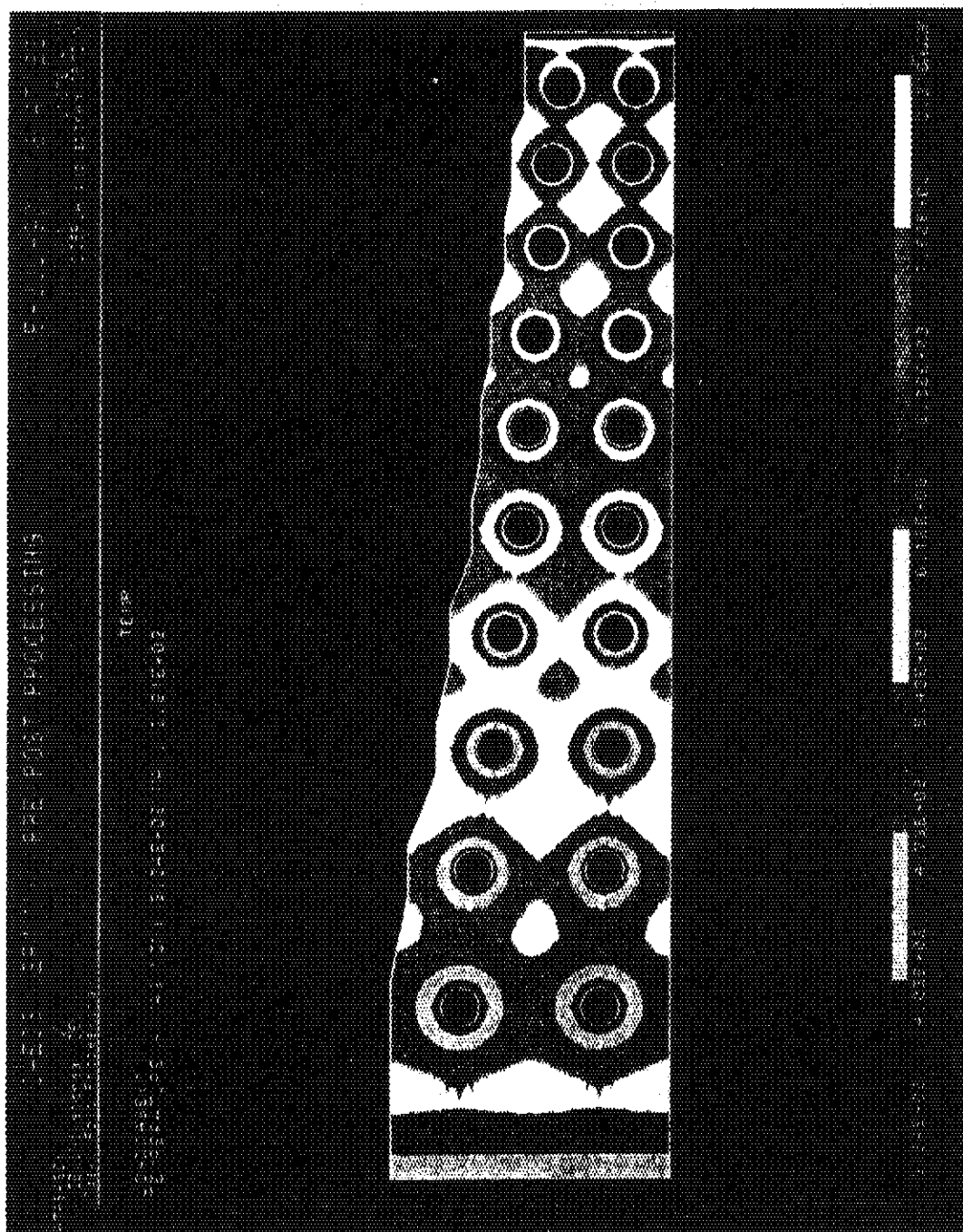


Fig. 7.1.14 Temperature distribution in the mixed pebble bed blanket  
 (case D; midplane of the middle unit with wall loading of  
 $1.2 \text{ MW/m}^2$  and He gap width of 1mm)

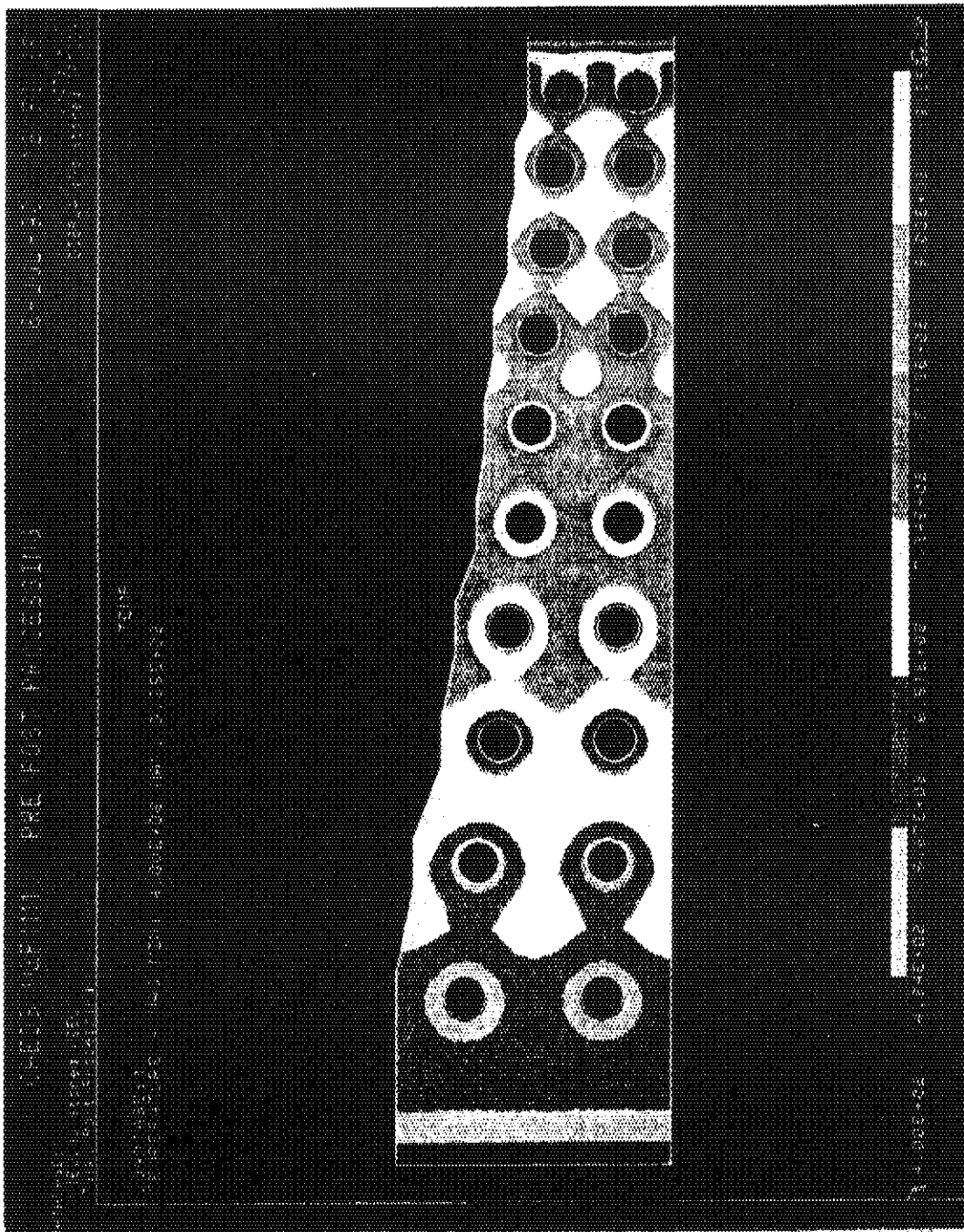


Fig. 7.1.15 Temperature distribution in the mixed pebble bed blanket  
(case E; midplane of the middle unit with wall loading of  
1.2 MW/m<sup>2</sup> and He gap width of 2mm)

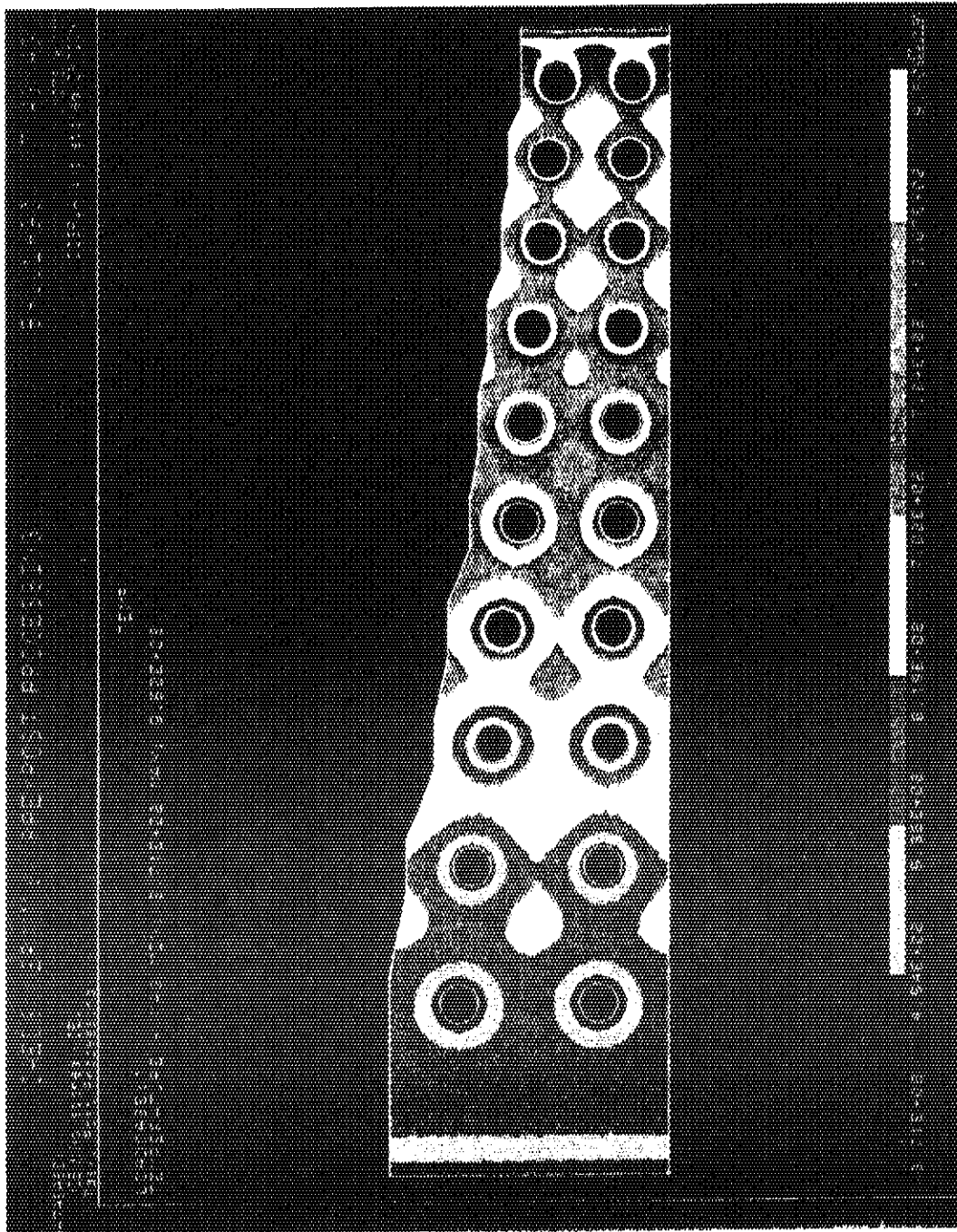


Fig. 7-1.16 Temperature distribution in the mixed pebble bed blanket  
(case F; midplane of the middle unit with wall loading of  
 $1.44 \text{ MW/m}^2$  and He gap width of 1mm)

## 7.2 Layered Pebble Bed Blanket

### 7.2.1 Design process

Temperature control of breeder in the layered pebble bed blanket is realized by thicknesses of beryllium pebble packed and breeder pebble packed layers. In the design process of this blanket, determination of each layer thickness, neutronics analysis to evaluate nuclear heating rates and thermal analysis to evaluate temperatures of each material should be iterated with an initial set of each layer thickness given as a first guess. In this section, the results of thermal analysis for the initial configuration by two-dimensional heat transfer analysis code with finite difference method, TAC-2D, are presented.

### 7.2.2 Analytical model and cases

The following four models are established for thermal analysis of the layered pebble bed blanket. Each model consists of six unit regions which have nine layers of coolant water, 316SS, beryllium pebbles, and  $\text{Li}_2\text{O}$  pebbles as shown in Figs 7.2.1 to 7.2.8.

Model 1: Top end of outboard blanket

Model 2: Improved thicknesses of regions 1, 2 and 6 from Model 1

Model 3: Midplane of outboard blanket

Model 4: Improved thicknesses of region 6 from Model 3

Calculations have been performed for each unit region independently. Temperature of water coolant is assumed to be constant at 80 °C. Adiabatic condition is assumed at top and bottom boundaries of the models. Nuclear heating rates in 316SS, beryllium and  $\text{Li}_2\text{O}$  pebble layers are shown in Figs 7.2.9 to 7.2.12 as a function of distance from the first wall. Detail distributions of nuclear heating rate in  $\text{Li}_2\text{O}$  layers are represented in Figs 7.2.13 and 7.2.14. Thermal conductivities of pebble bed layers used in the analyses are shown in Figs 7.2.15 and 7.2.16.

With above analytical models and assumptions, the following cases have been computed.

Case 1: Top end of outboard blanket (Model 1) with neutron wall loading of  $0.6 \text{ MW/m}^2$  given as the reference operation

- Case 2: Top end of outboard blanket (Model 1) with neutron wall loading of  $0.75 \text{ MW/m}^2$  which is increased by 25 % from the reference value
- Case 3: Top end of outboard blanket with modified layer thicknesses (Model 2) with neutron wall loading of  $0.6 \text{ MW/m}^2$
- Case 4: Top end of outboard blanket with modified layer thicknesses (Model 2) with increased neutron wall loading of  $0.75 \text{ MW/m}^2$
- Case 5: Midplane of outboard blanket (Model 3) with neutron wall loading of  $1.2 \text{ MW/m}^2$  given as the reference operation
- Case 6: Midplane of outboard blanket with modified layer thickness (Model 4) with neutron wall loading of  $1.2 \text{ MW/m}^2$

### 7.2.3 Results and discussions

Temperature distributions in the blanket resulted from the analyses are shown in Figs 7.2.17 to 7.2.22. Detail distributions of temperatures in individual unit regions are indicated in the following figures.

- Figs 7.2.23 to 7.2.28: Case 1 and 2
- Figs 7.2.29 to 7.2.34: Case 3 and 4
- Figs 7.2.35 to 7.2.40: Case 5
- Fig. 7.2.41 : Case 6

For the first guess of layer arrangements at top end of outboard blanket with reference neutron wall loading (Case 1), almost all  $\text{Li}_2\text{O}$  layers stay in temperature range of  $400 - 600^\circ\text{C}$  which satisfies the allowable operation temperature range for  $\text{Li}_2\text{O}$  ( $400 - 1000^\circ\text{C}$ ). Keeping  $\text{Li}_2\text{O}$  temperatures within the allowable range has no difficulty even with the neutron wall loading increased by 25 % as shown in Figs 7.2.23 to 7.2.27. Temperatures of the  $\text{Li}_2\text{O}$  layer in region 6 are below  $400^\circ\text{C}$  for both cases, therefore layer thicknesses in region 6 should be rearranged.

Though the allowable operation temperature range for  $\text{Li}_2\text{O}$  is  $400 - 1000^\circ\text{C}$ , it is desirable to keep a narrower range in order to leave a margin for possible power variations. Figures 7.2.29 to 7.2.34 show temperature distributions for improved layer thicknesses with the reference and increased wall loadings. Temperatures of  $\text{Li}_2\text{O}$  are maintained within a desirable nominal range of  $450 - 650^\circ\text{C}$  except for the region 6. With this nominal temperature range, wider power variations than  $-10\%$  to  $+25\%$  would be

permitted in terms of keeping  $\text{Li}_2\text{O}$  temperature within the allowable range. Though layer thicknesses in region 6 still need to be modified, it is expected that the modification will be incorporated rather easily.

For layer arrangements at outboard midplane,  $\text{Li}_2\text{O}$  temperatures are maintained within the allowable range with the improved thicknesses of region 6 as shown in Figs 7.2.35 to 7.2.41. These temperatures are resulted for neutron wall loading of  $1.2 \text{ MW/m}^2$ . Further modifications and optimizations of layer thicknesses, especially in back regions (regions 5 and 6), are required to leave a margin for power variations.



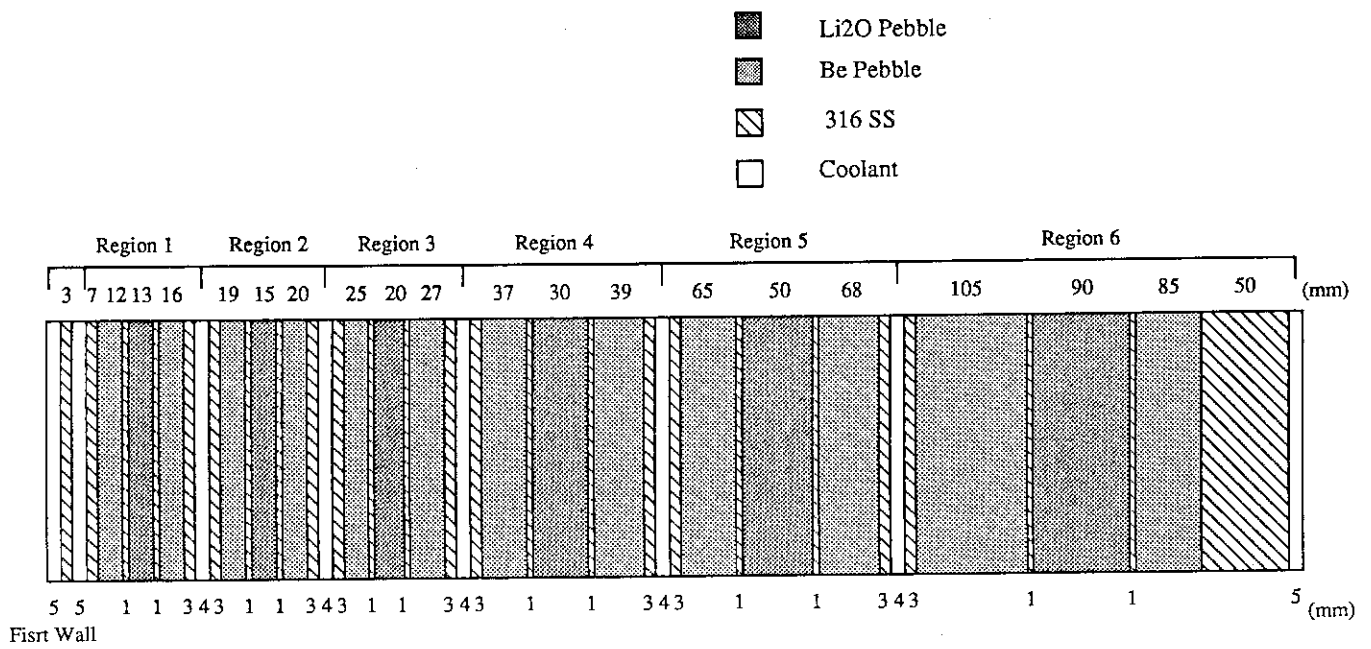


Fig. 7.2.1 Analytical model 1 (top end of outboard blanket)

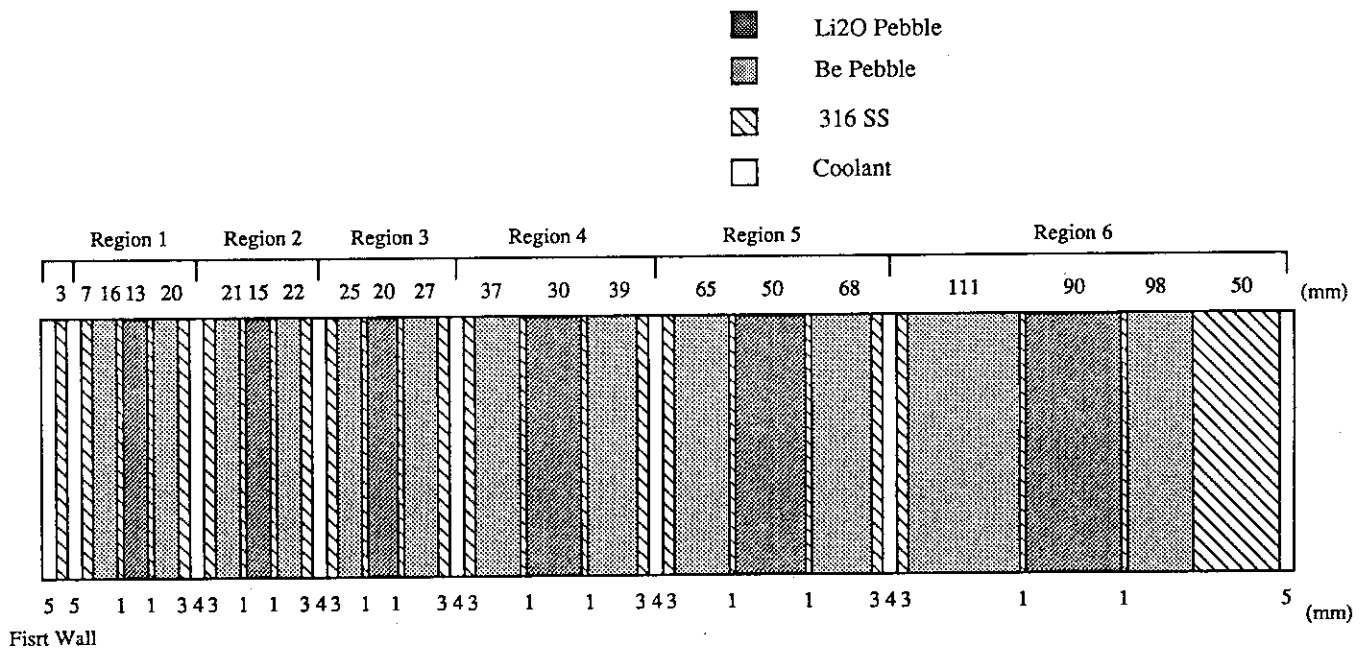


Fig. 7.2.2 Analytical model 2 (top end of outboard blanket with modified layer thickness)

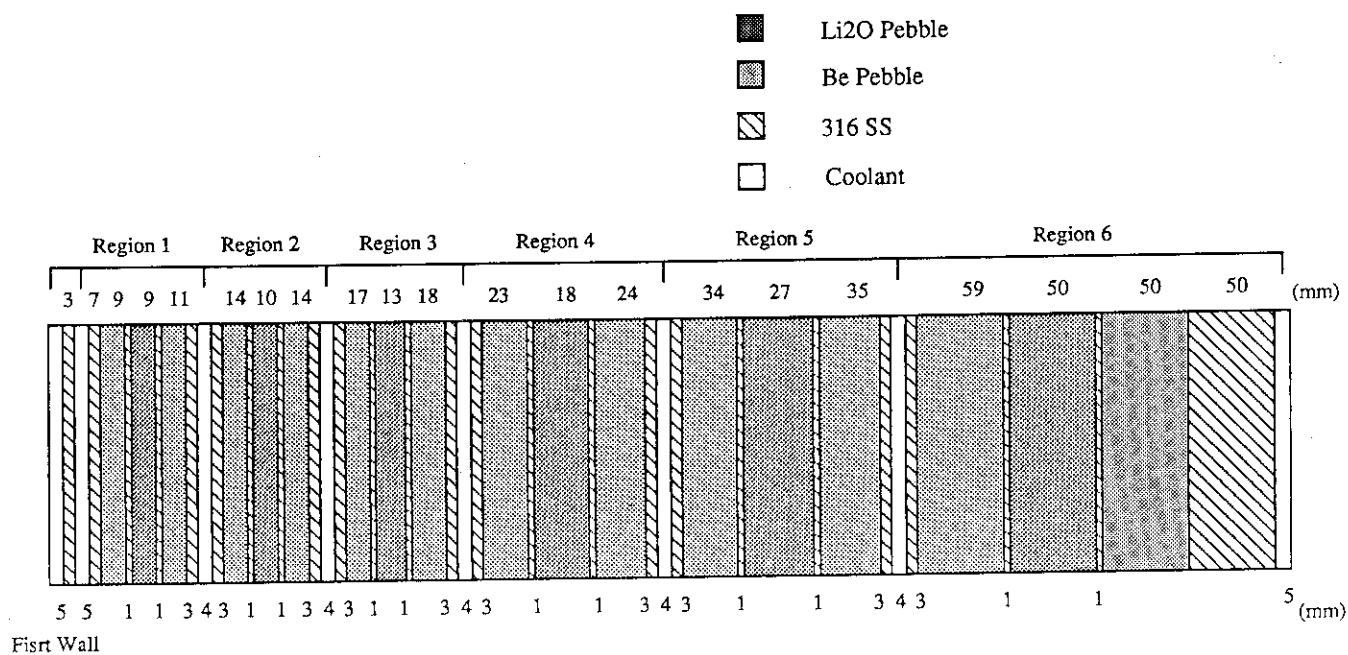


Fig. 7.2.3 Analytical model 3 (midplane of outboard blanket)

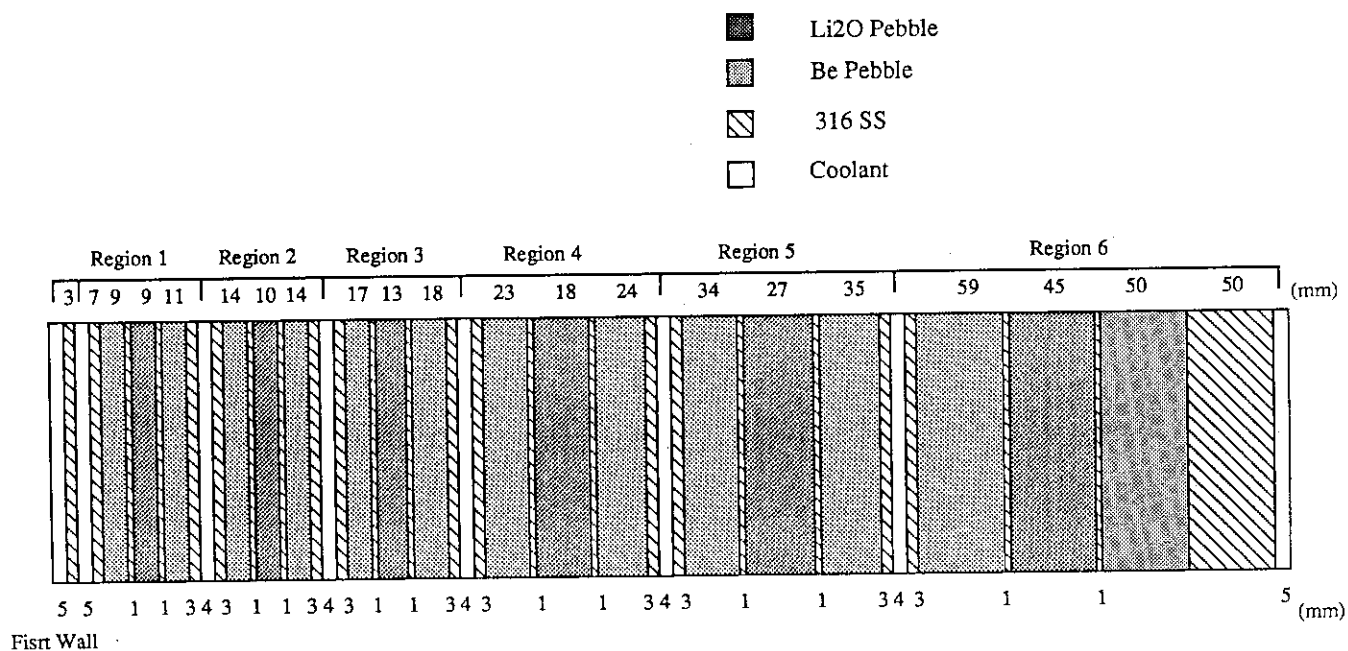


Fig. 7.2.4 Analytical model 4 (midplane of outboard blanket with modified layer thickness)

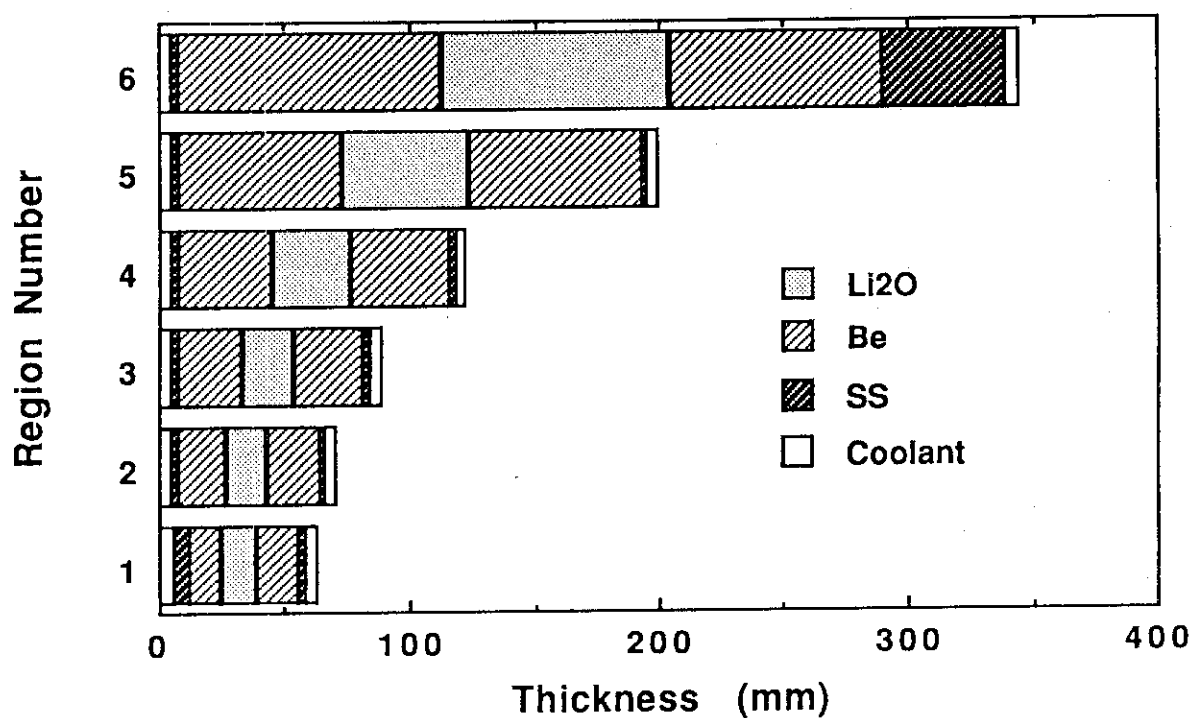


Fig. 7.2.5 Analytical model 1 with individual unit regions (top end of outboard blanket)

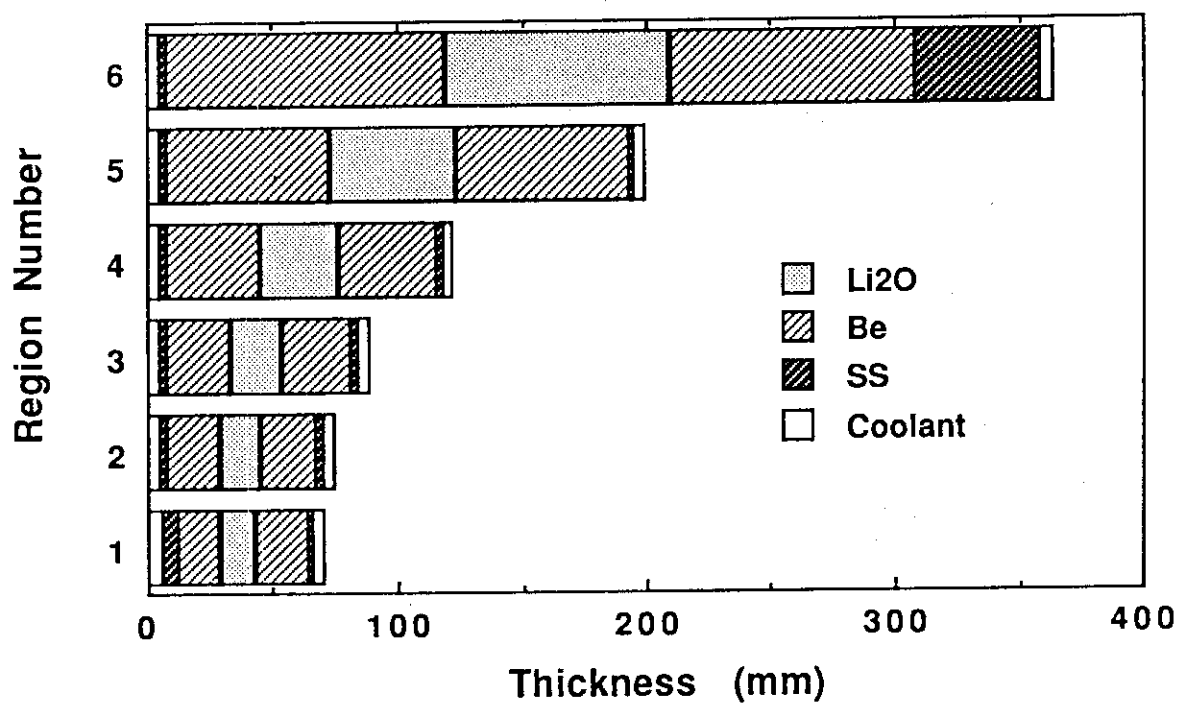


Fig. 7.2.6 Analytical model 2 with individual unit regions (top end of outboard blanket with modified layer thickness)

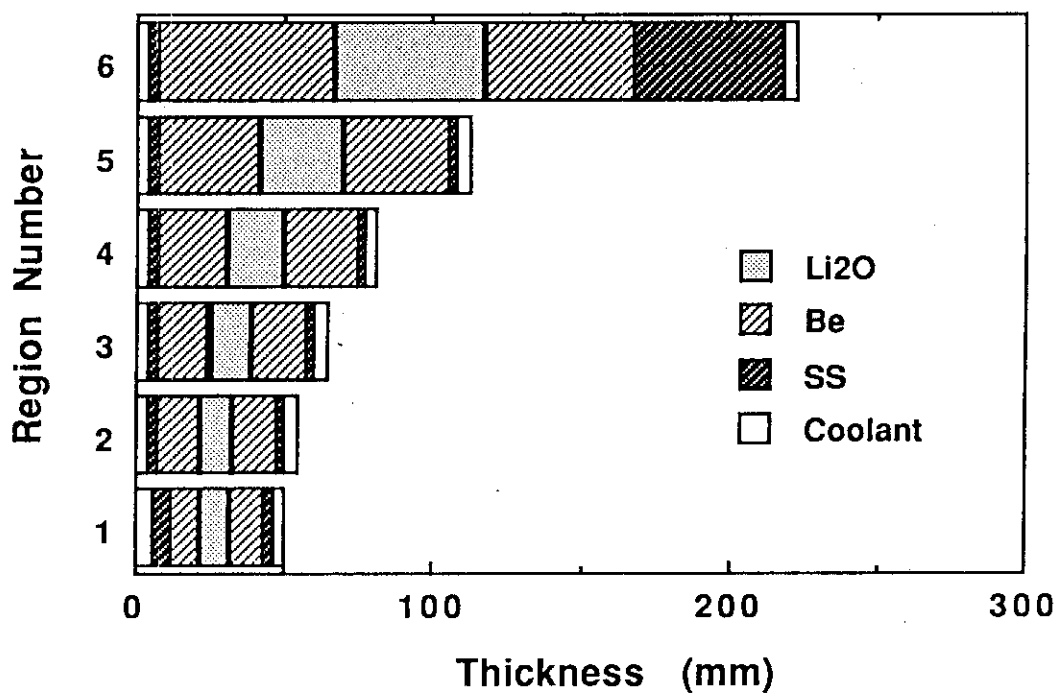


Fig. 7.2.7 Analytical model 3 with individual unit regions  
(midplane of outboard blanket)

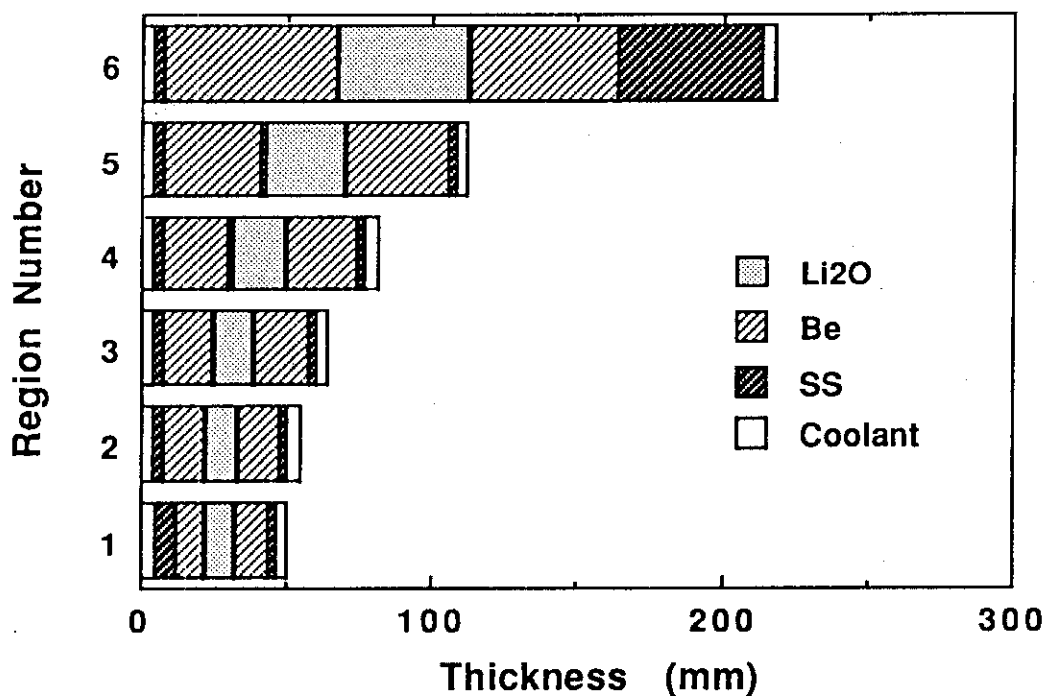


Fig. 7.2.8 Analytical model 4 with individual unit regions  
(midplane of outboard blanket with modified layer thickness)

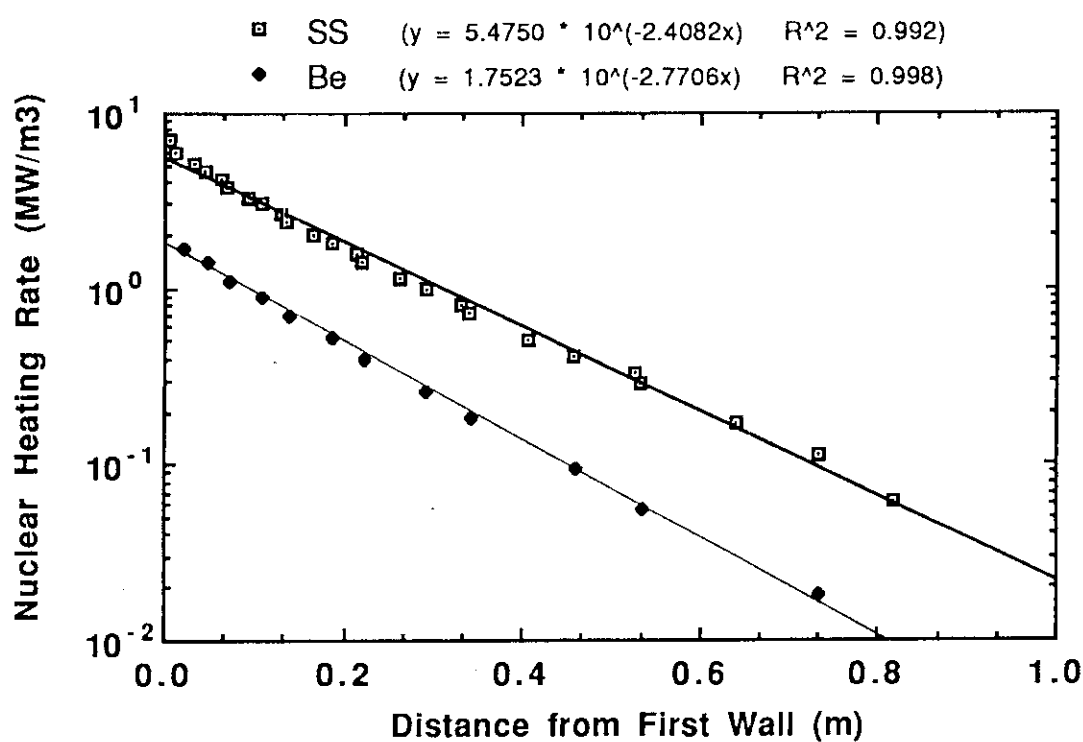


Fig. 7.2.9 Nuclear heating rates in SS and Be at top end of outboard blanket (for Models 1 and 2)

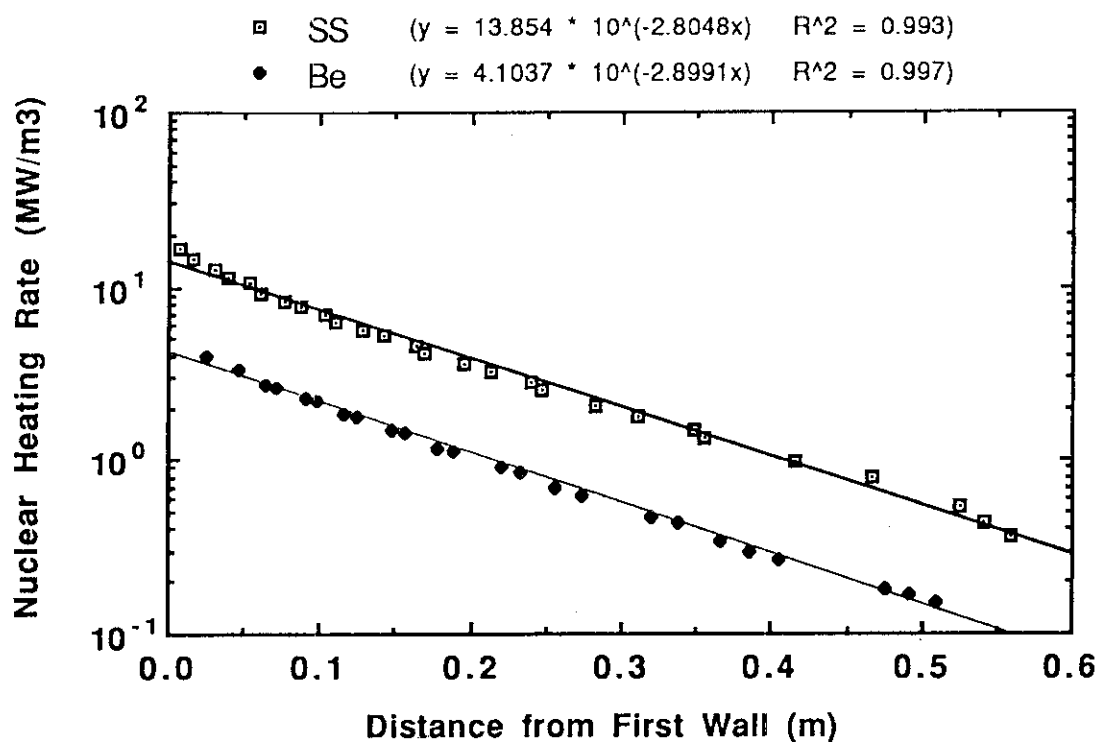


Fig. 7.2.10 Nuclear heating rates in SS and Be at midplane of outboard blanket (for Models 3 and 4)

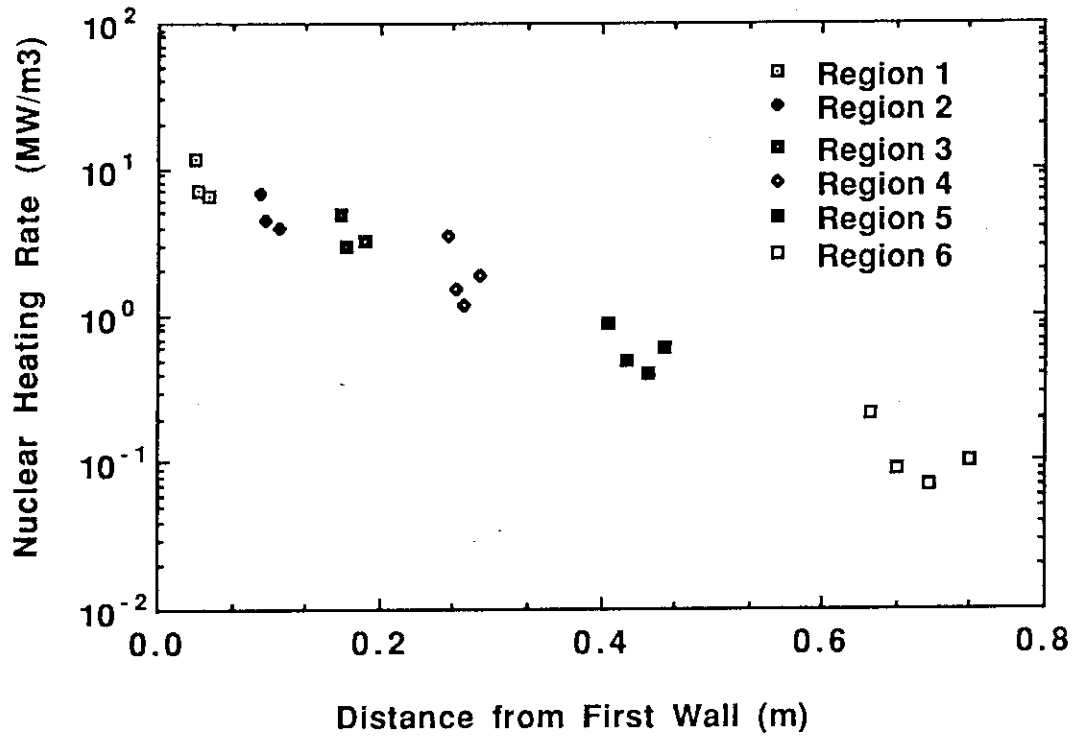


Fig. 7.2.11 Nuclear heating rates in Li<sub>2</sub>O at top end of outboard blanket (for Models 1 and 2)

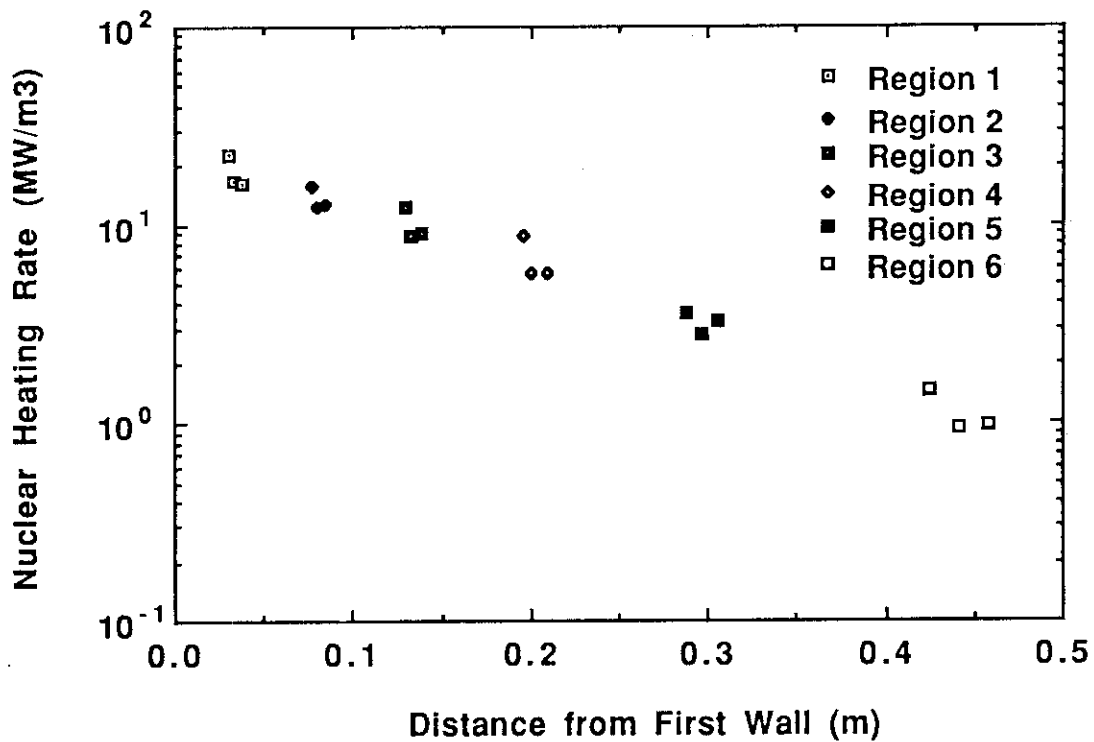
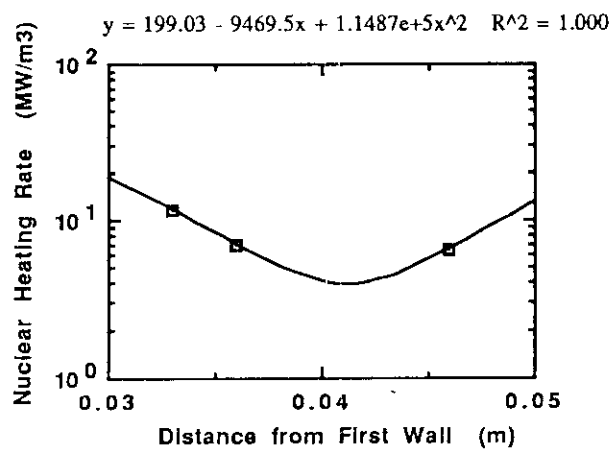
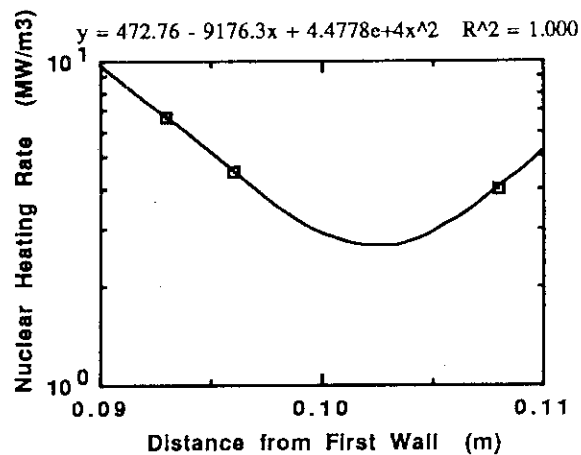


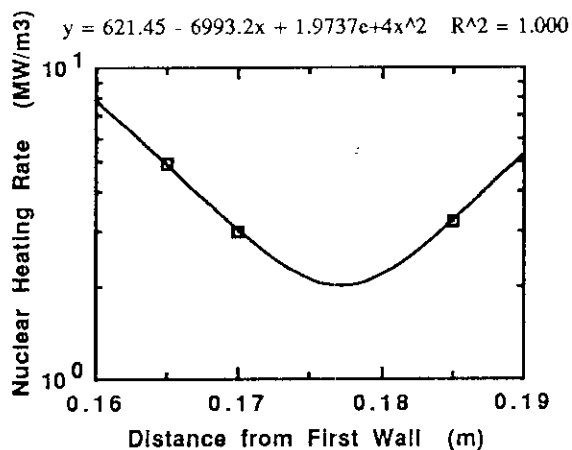
Fig. 7.2.12 Nuclear heating rates in Li<sub>2</sub>O at midplane of outboard blanket (for Models 3 and 4)



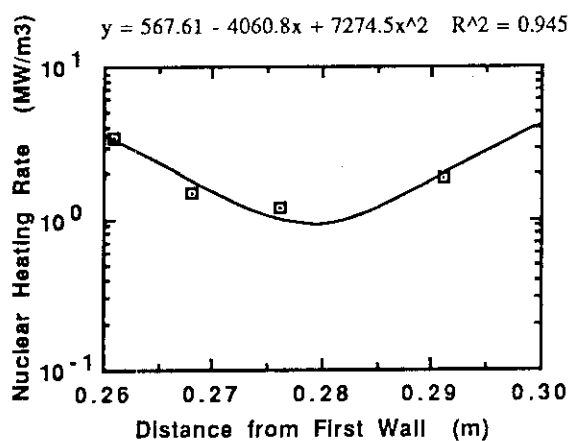
Region 1



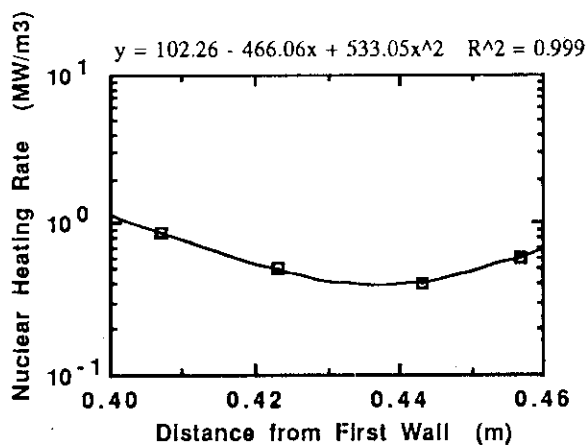
Region 2



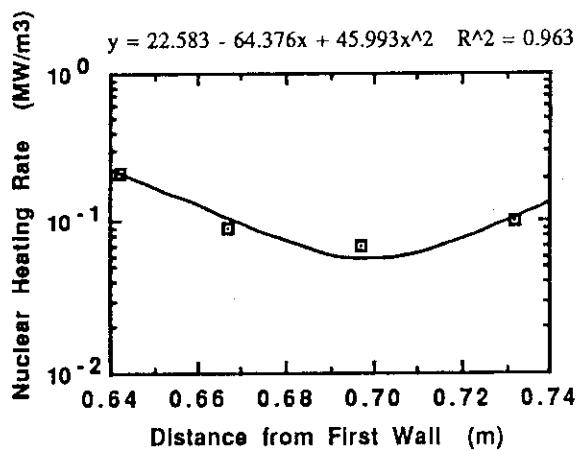
Region 3



Region 4

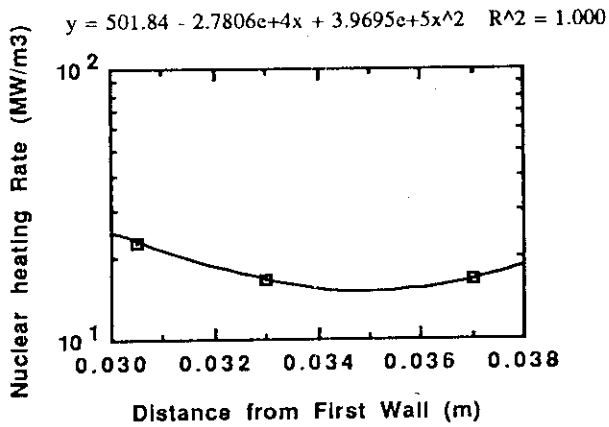


Region 5

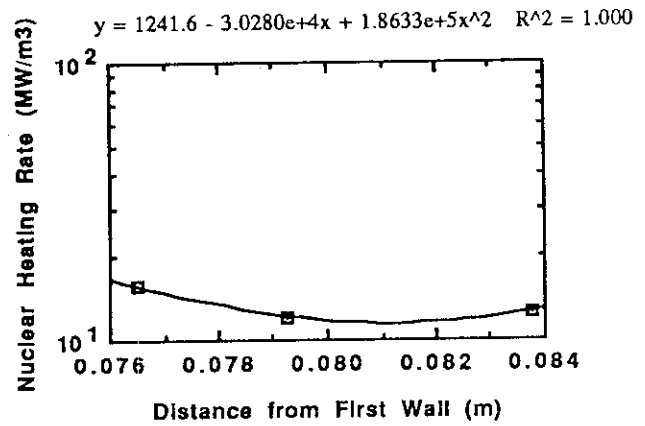


Region 6

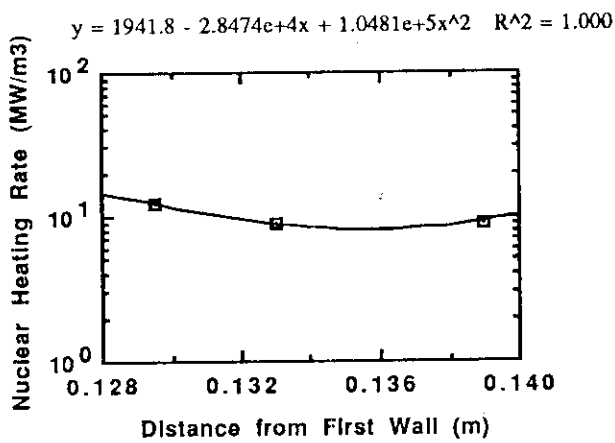
Fig. 7.2.13 Nuclear heating rate distribution in  $\text{Li}_2\text{O}$  pebble layers at top end of outboard blanket (for Models 1 and 2)



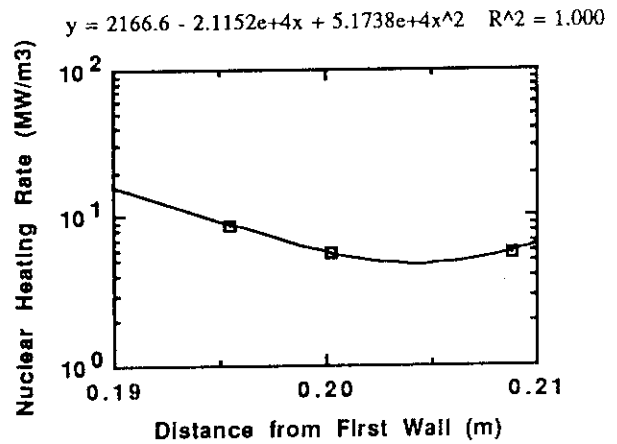
Region 1



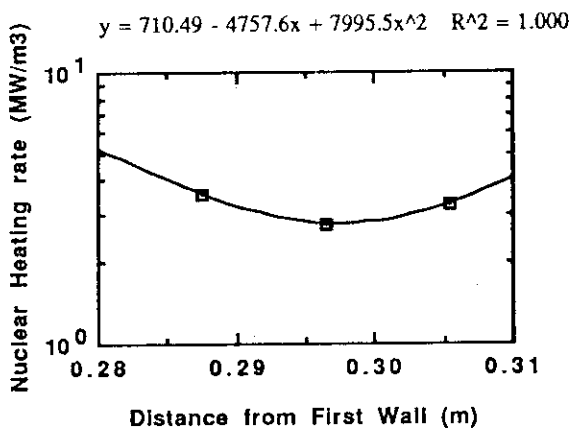
Region 2



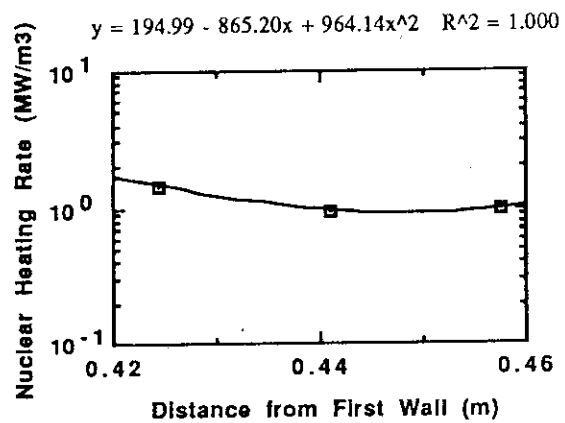
Region 3



Region 4



Region 5



Region 6

Fig. 7.2.14 Nuclear heating rate distribution in  $\text{Li}_2\text{O}$  pebble layers at midplane of outboard blanket (for Models 3 and 4)



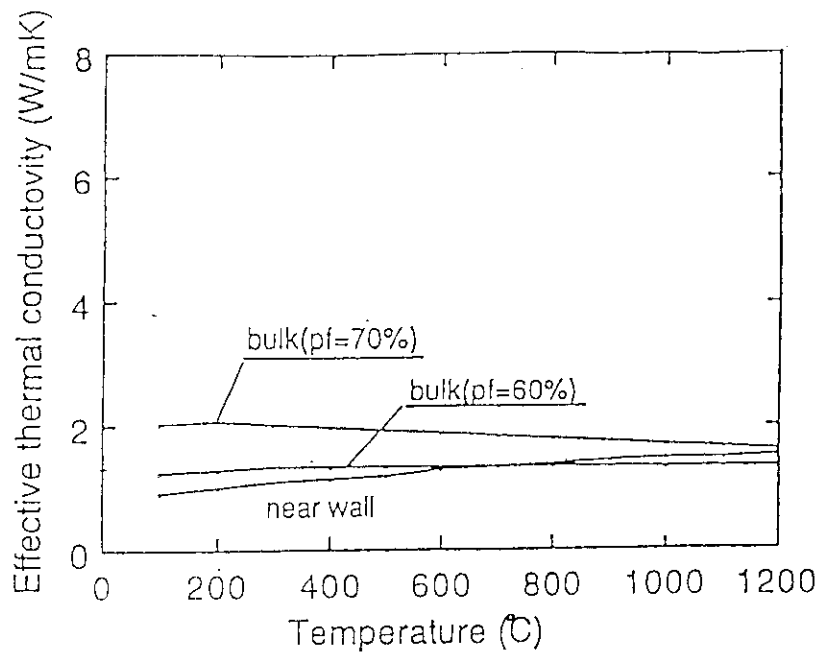


Fig. 7.2.15 Effective thermal conductivity of  $\text{Li}_2\text{O}$  pebble layer  
(pebble diameter: 1mm)

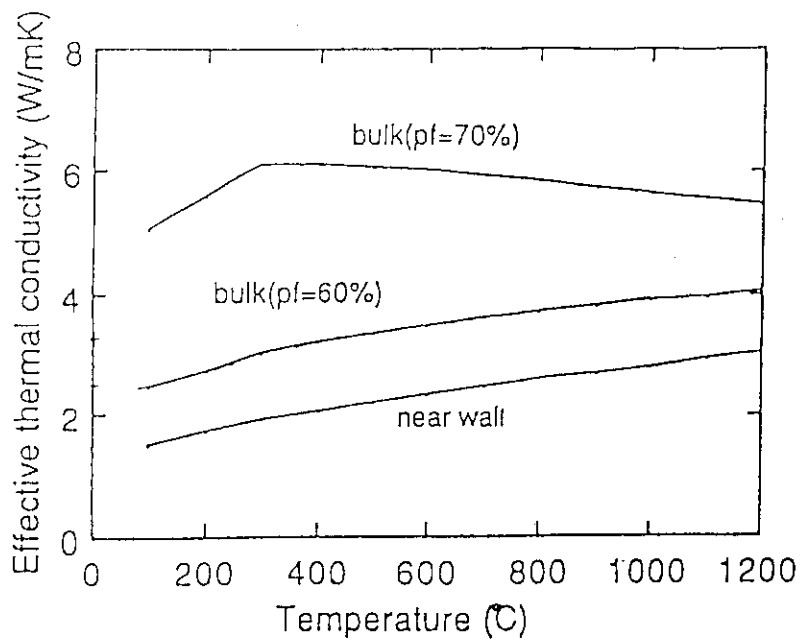


Fig. 7.2.16 Effective thermal conductivity of Be pebble layer  
(pebble diameter: 1mm)

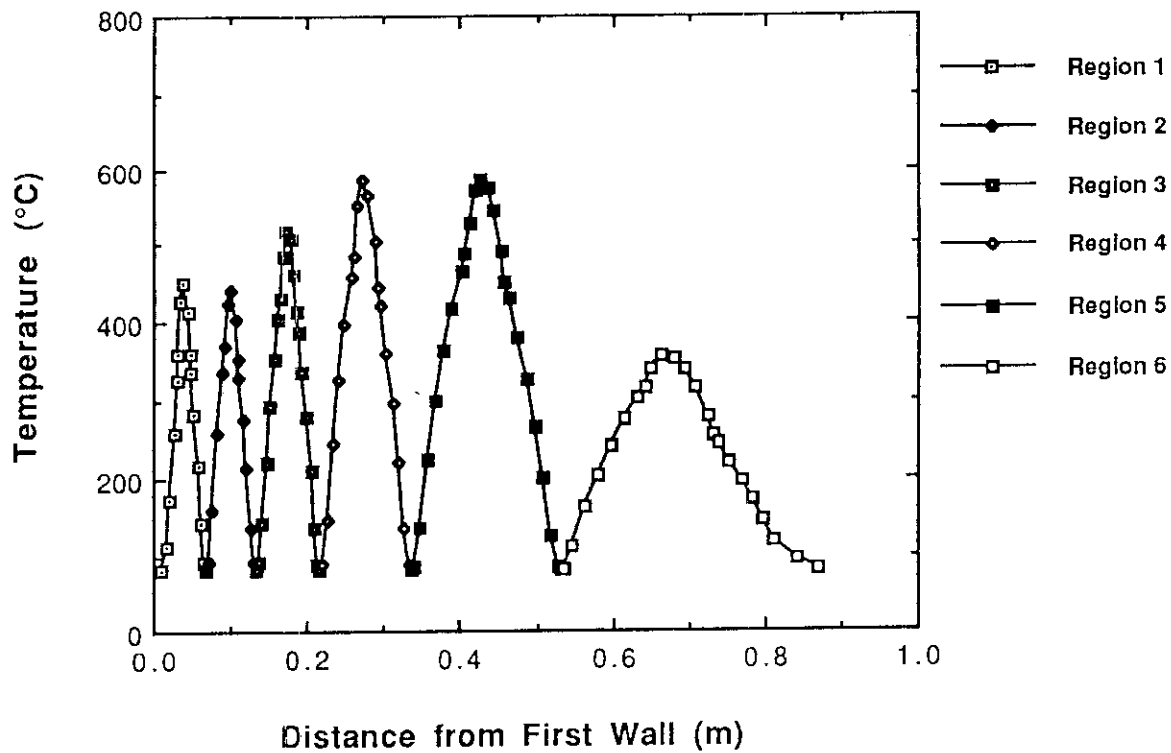


Fig. 7.2.17 Temperature profile in the layered pebble bed blanket (at outboard top with wall loading of  $0.6 \text{ MW/m}^2$ )

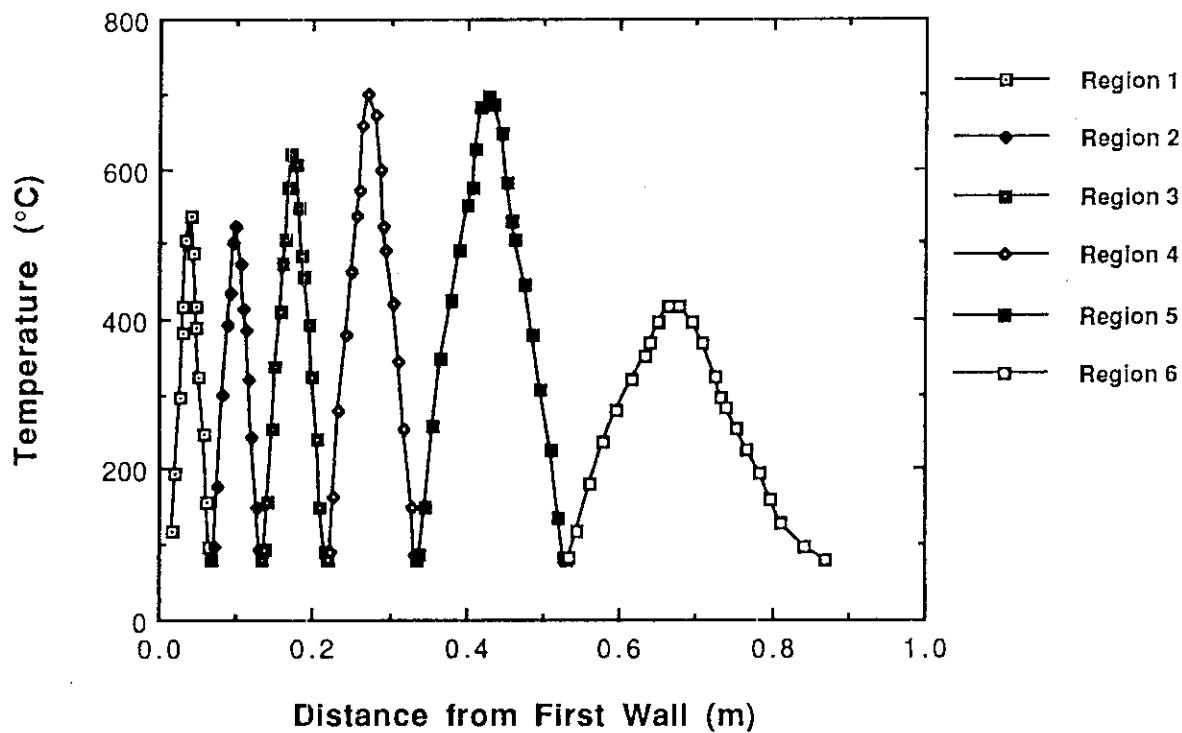


Fig. 7.2.18 Temperature profile in the layered pebble bed blanket (at outboard top with wall loading of  $0.75 \text{ MW/m}^2$ )

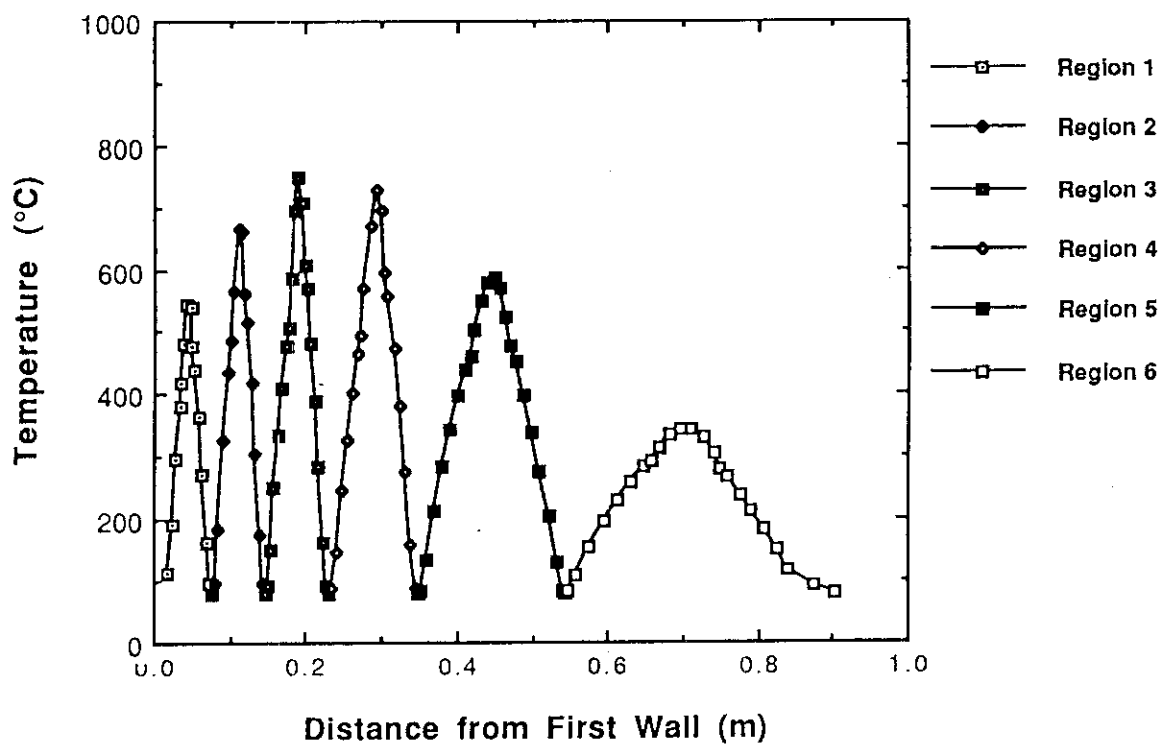


Fig. 7.2.19 Temperature profile in the layered pebble bed blanket (at outboard top with modified layer thickness and with wall loading of  $0.6 \text{ MW/m}^2$ )

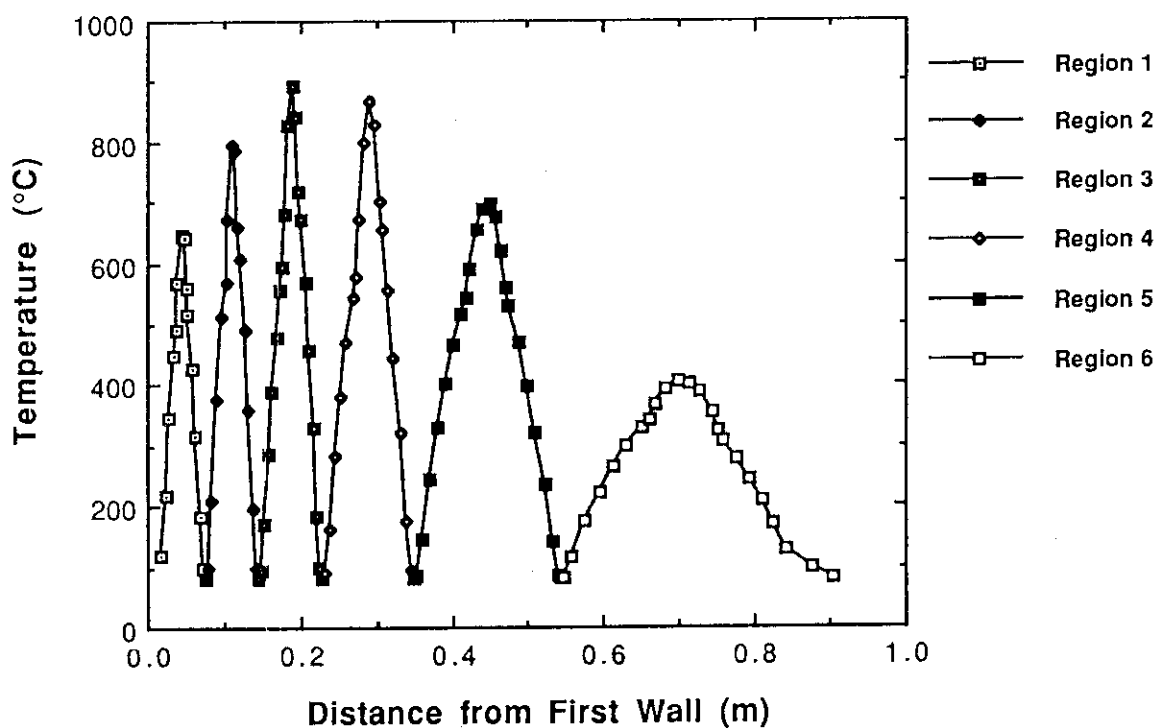


Fig. 7.2.20 Temperature profile in the layered pebble bed blanket (at outboard top with modified layer thickness and with wall loading of  $0.75 \text{ MW/m}^2$ )

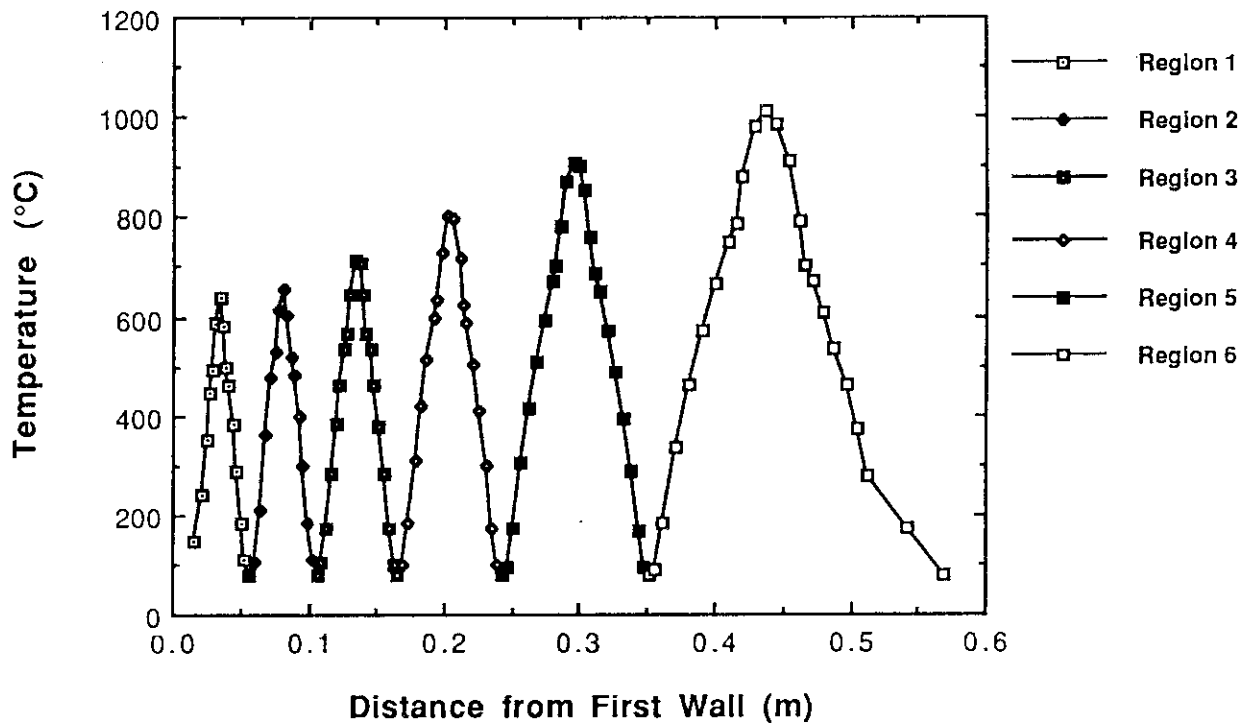


Fig. 7.2.21 Temperature profile in the layered pebble bed blanket (at outboard midplane with wall loading of  $1.2 \text{ MW/m}^2$ )

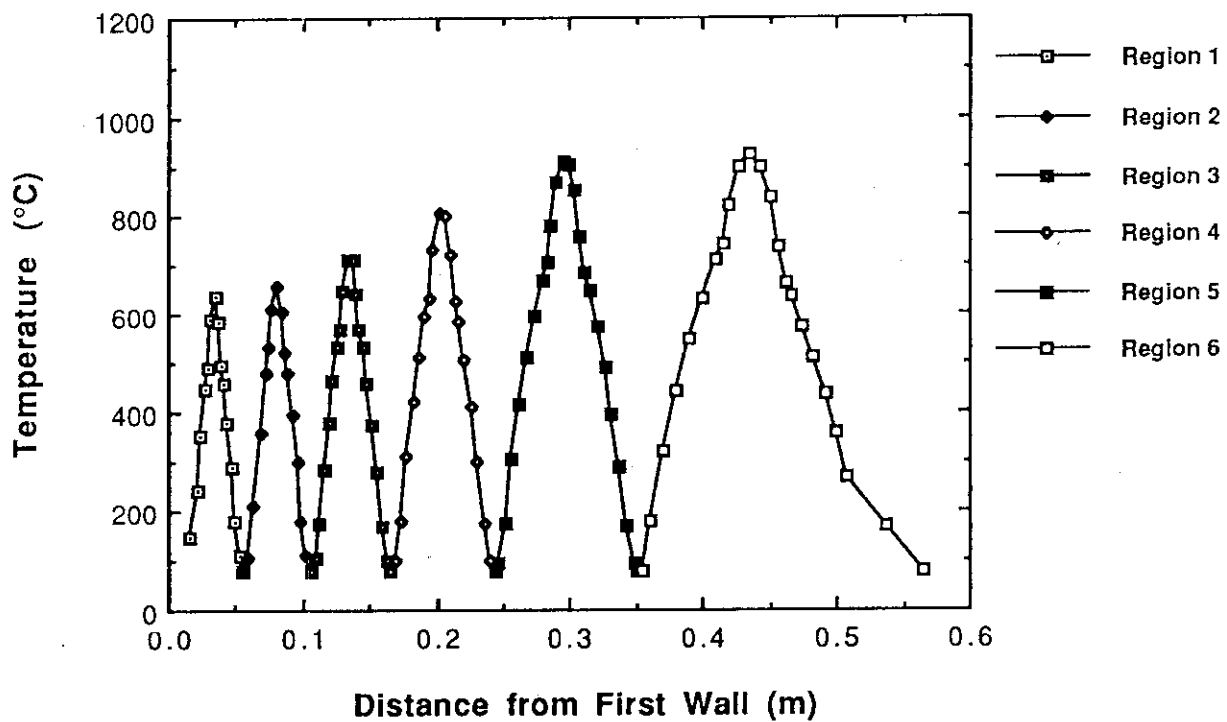


Fig. 7.2.22 Temperature profile in the layered pebble bed blanket (at outboard midplane with modified layer thickness and with wall loading of  $1.2 \text{ MW/m}^2$ )

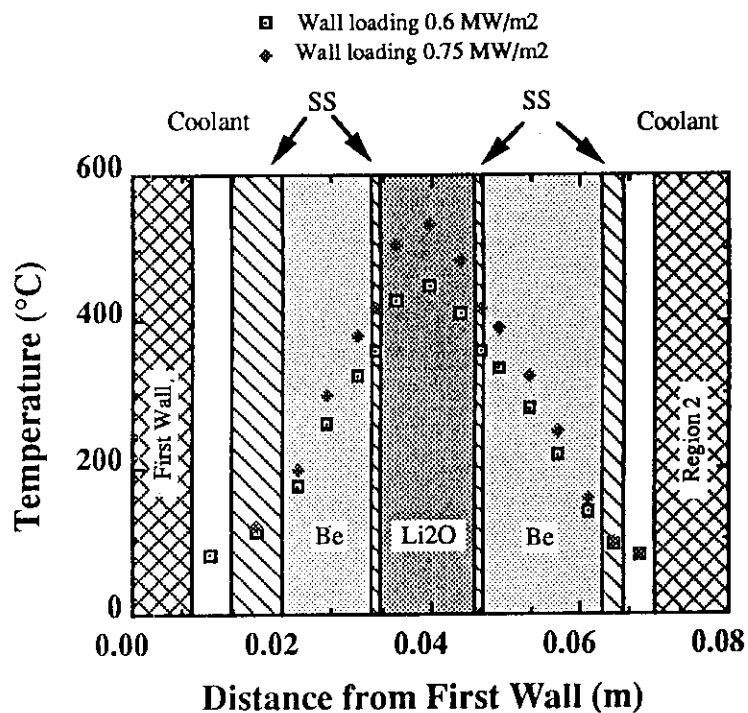


Fig. 7.2.23 Temperature profile in the unit region 1 at outboard top

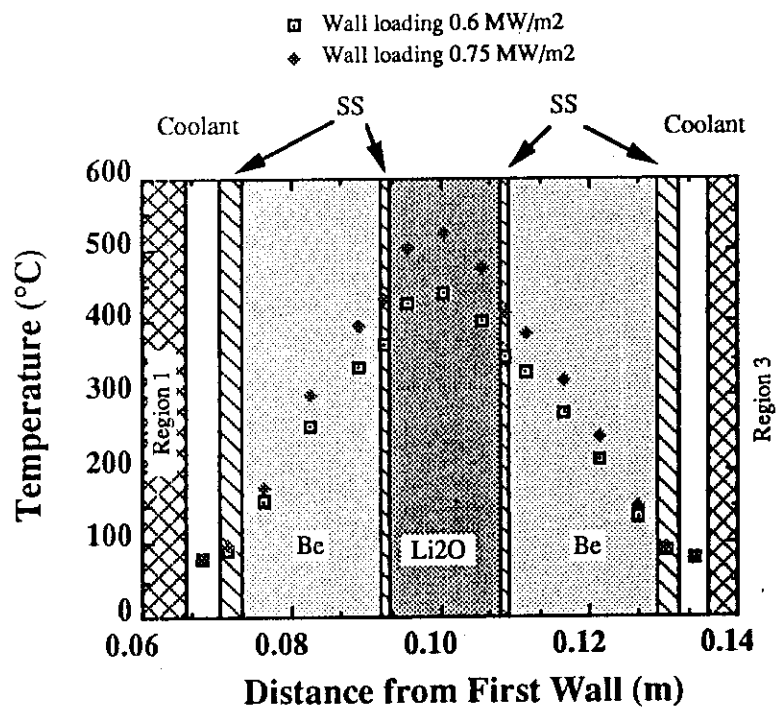


Fig. 7.2.24 Temperature profile in the unit region 2 at outboard top

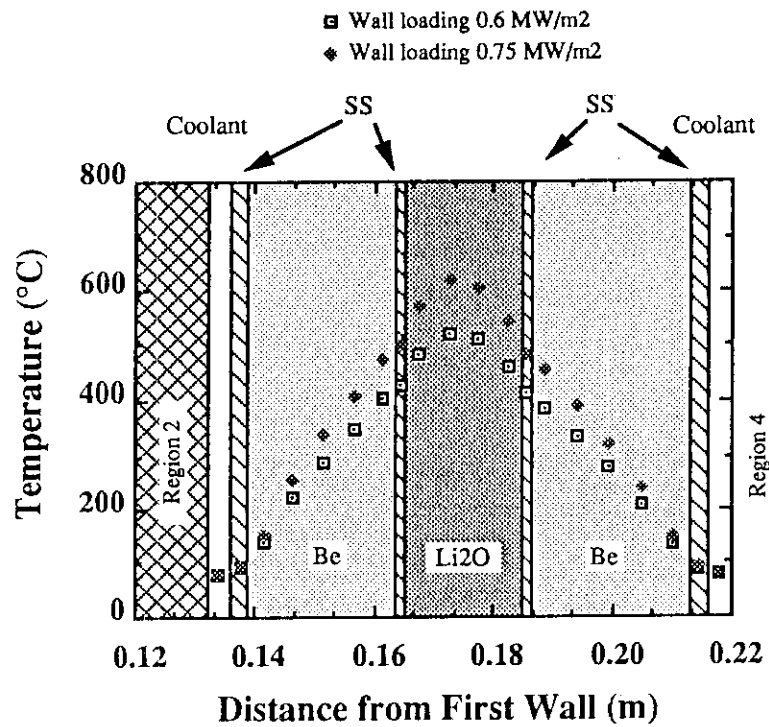


Fig. 7.2.25 Temperature profile in the unit region 3 at outboard top

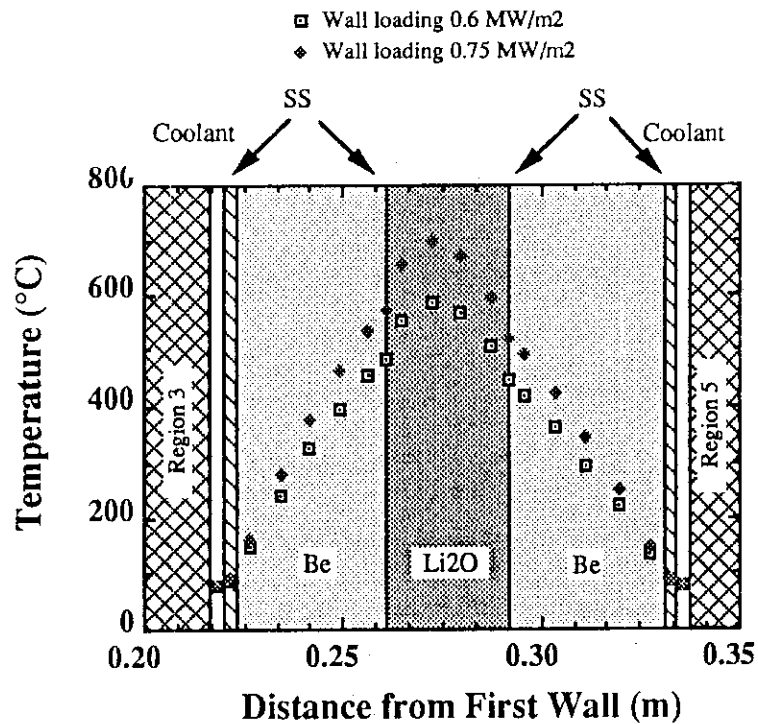


Fig. 7.2.26 Temperature profile in the unit region 4 at outboard top

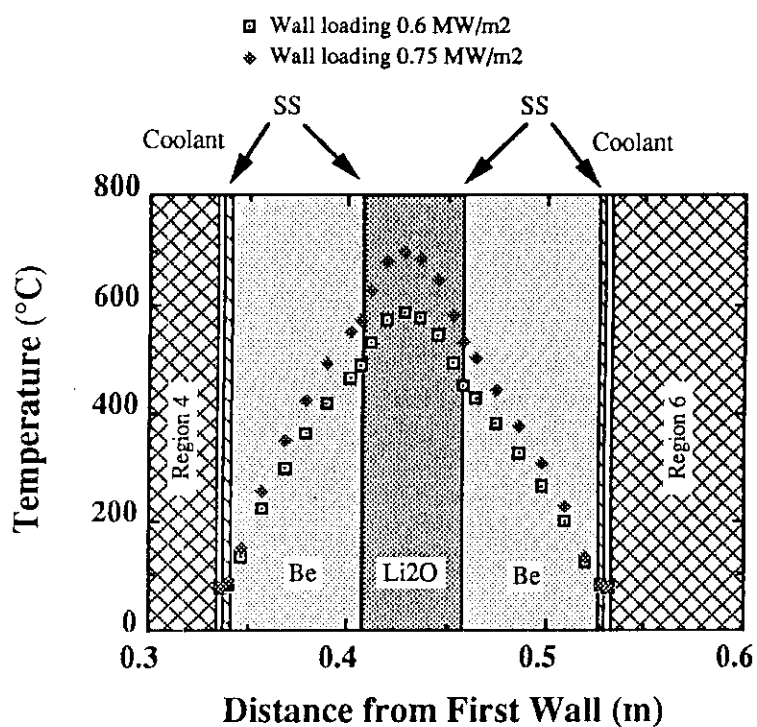


Fig. 7.2.27 Temperature profile in the unit region 5 at outboard top

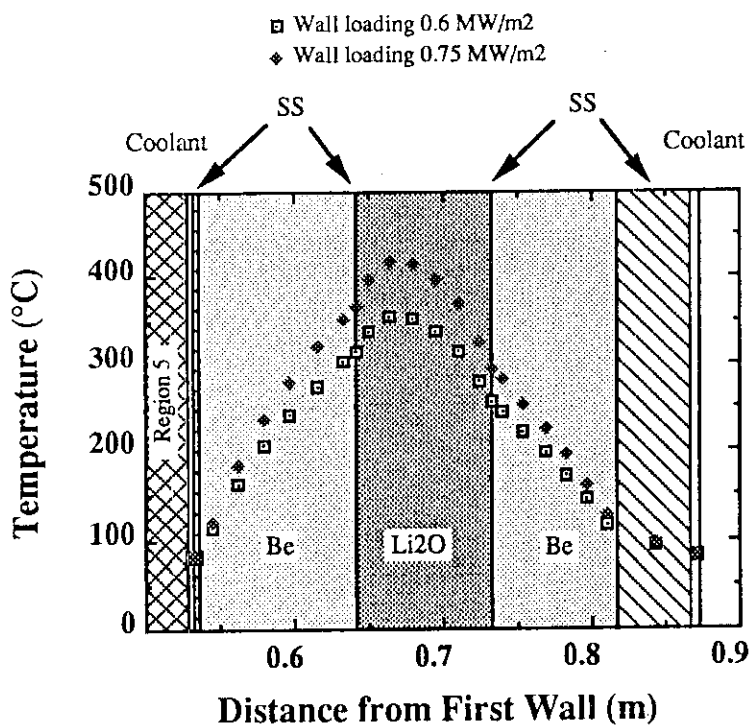


Fig. 7.2.28 Temperature profile in the unit region 6 at outboard top

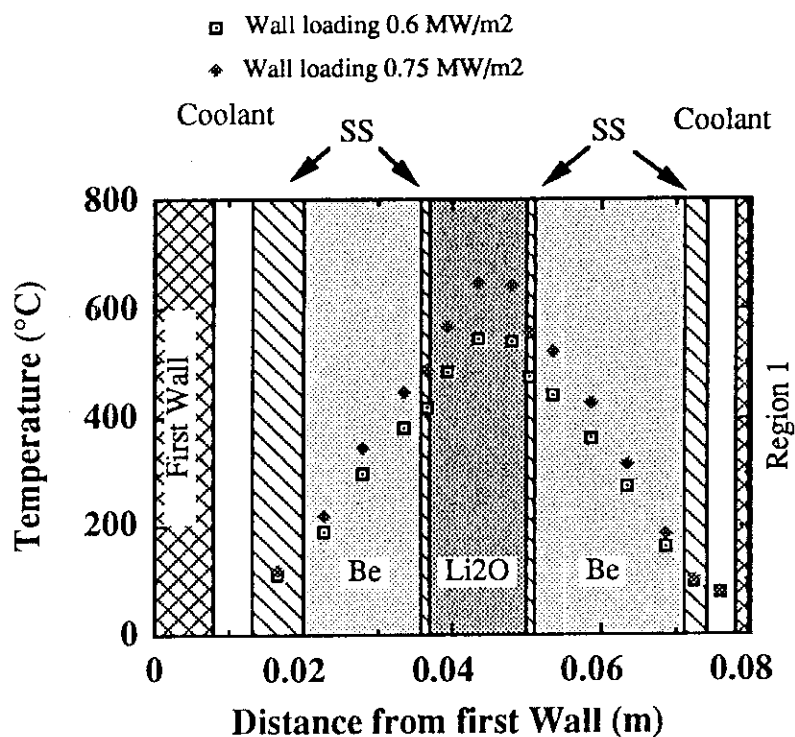


Fig. 7.2.29 Temperature profile in the unit region 1 at outboard top with modified layer thickness

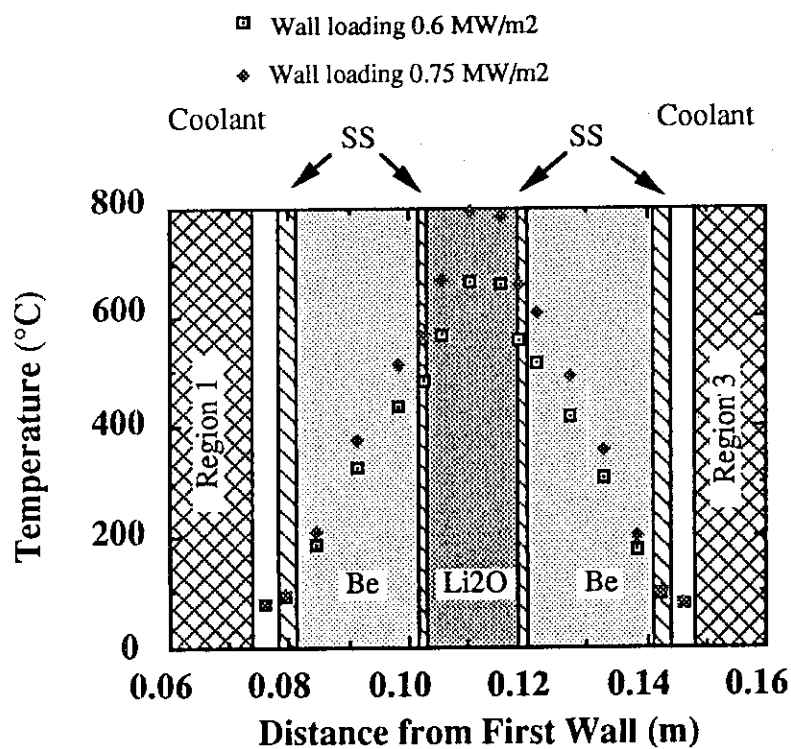


Fig. 7.2.30 Temperature profile in the unit region 2 at outboard top with modified layer thickness



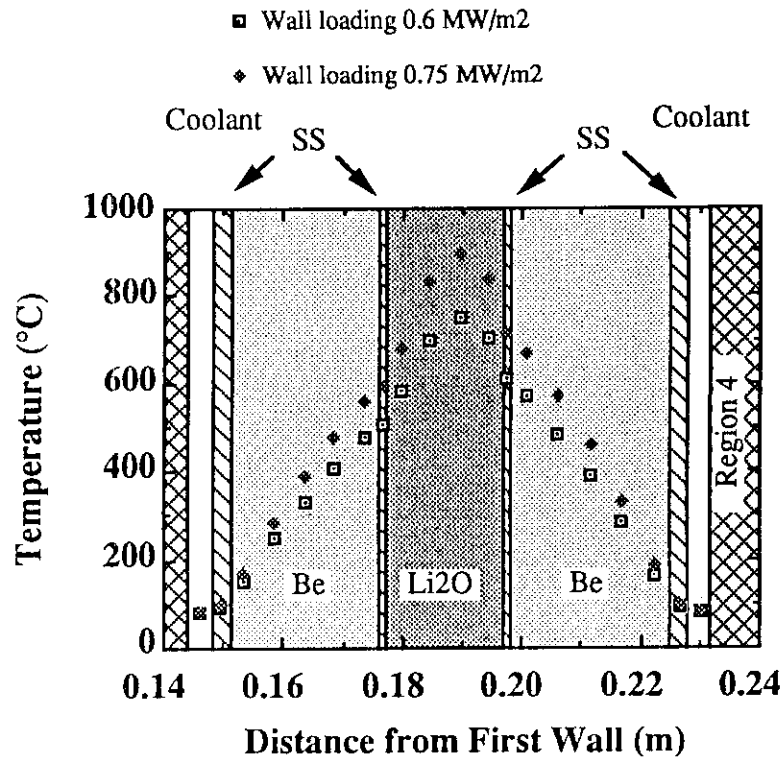


Fig. 7.2.31 Temperature profile in the unit region 3 at outboard top with modified layer thickness

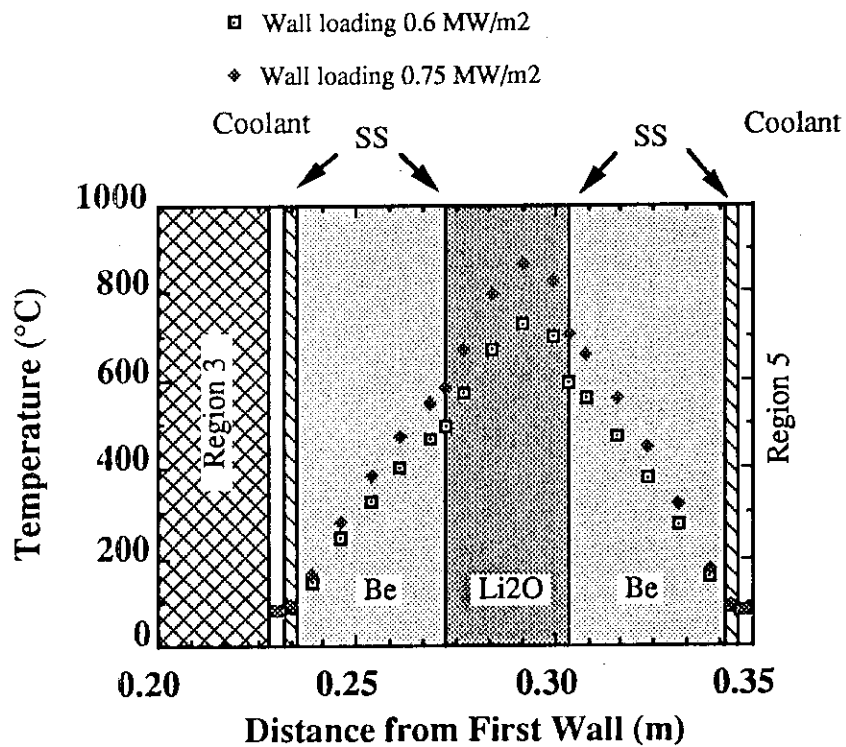


Fig. 7.2.32 Temperature profile in the unit region 4 at outboard top with modified layer thickness

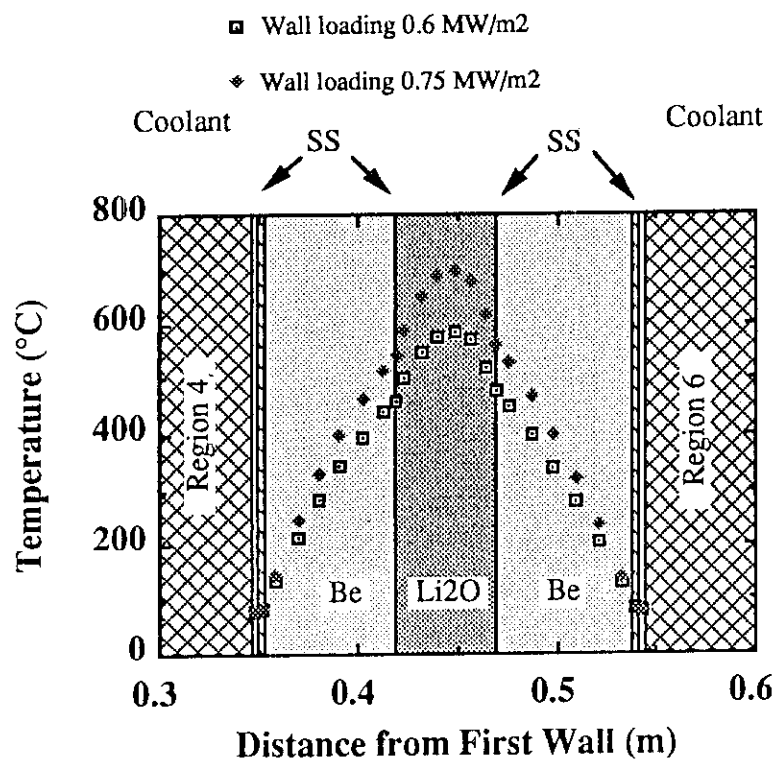


Fig. 7.2.33 Temperature profile in the unit region 5 at outboard top with modified layer thickness

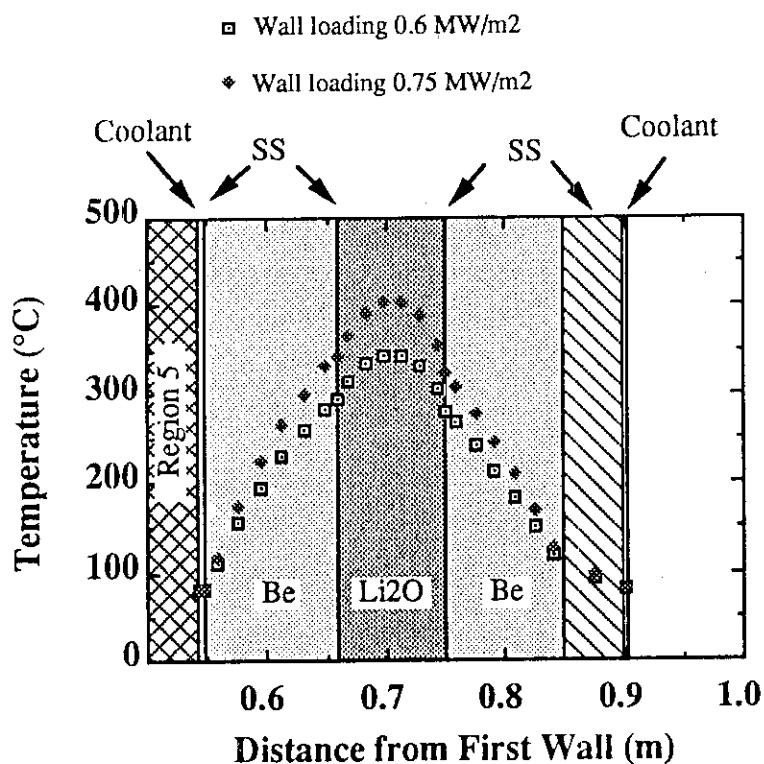


Fig. 7.2.34 Temperature profile in the unit region 6 at outboard top with modified layer thickness

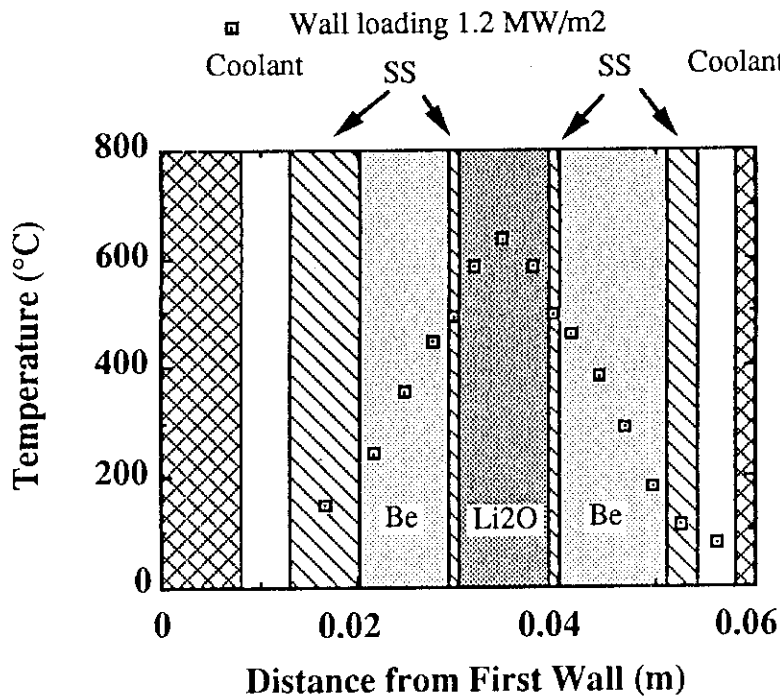


Fig. 7.2.35 Temperature profile in the unit region 1 at outboard midplane

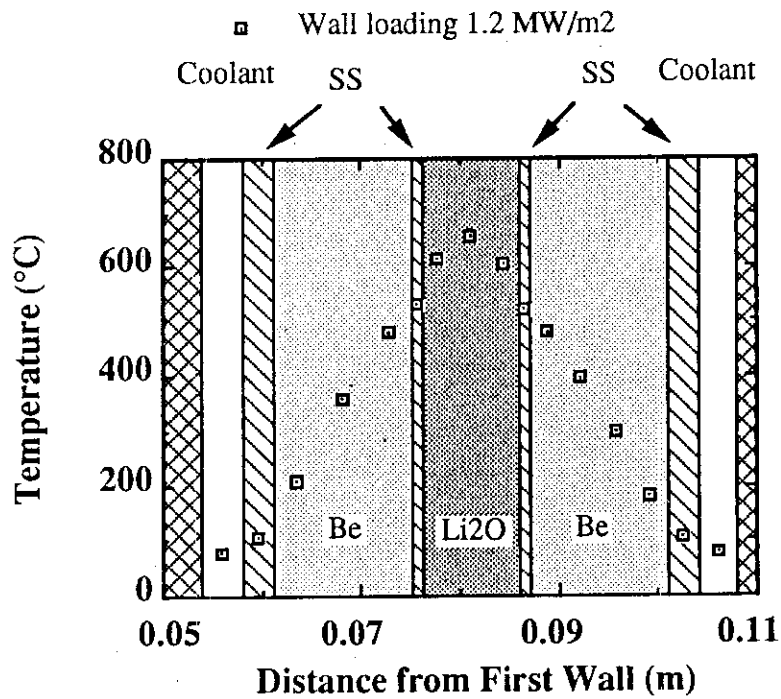


Fig. 7.2.36 Temperature profile in the unit region 2 at outboard midplane

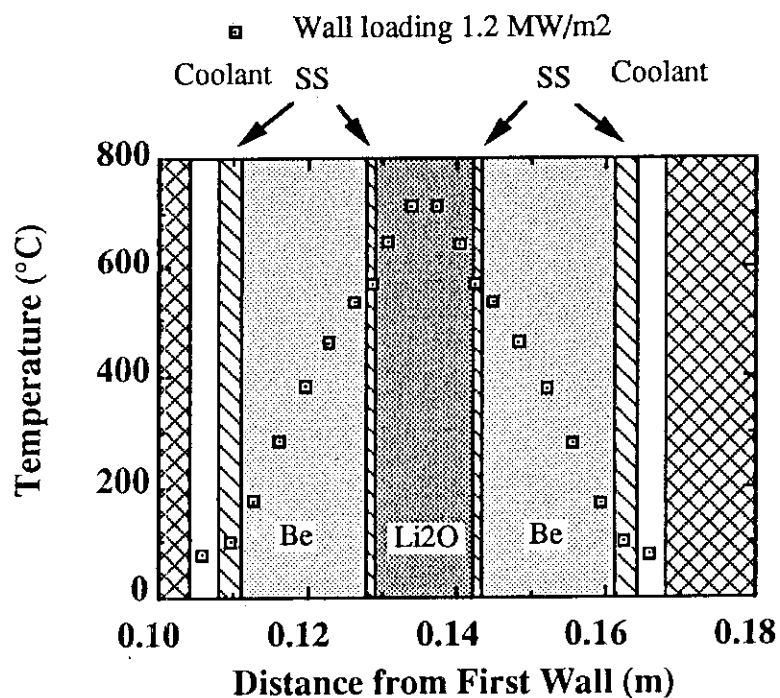


Fig. 7.2.37 Temperature profile in the unit region 3 at outboard midplane

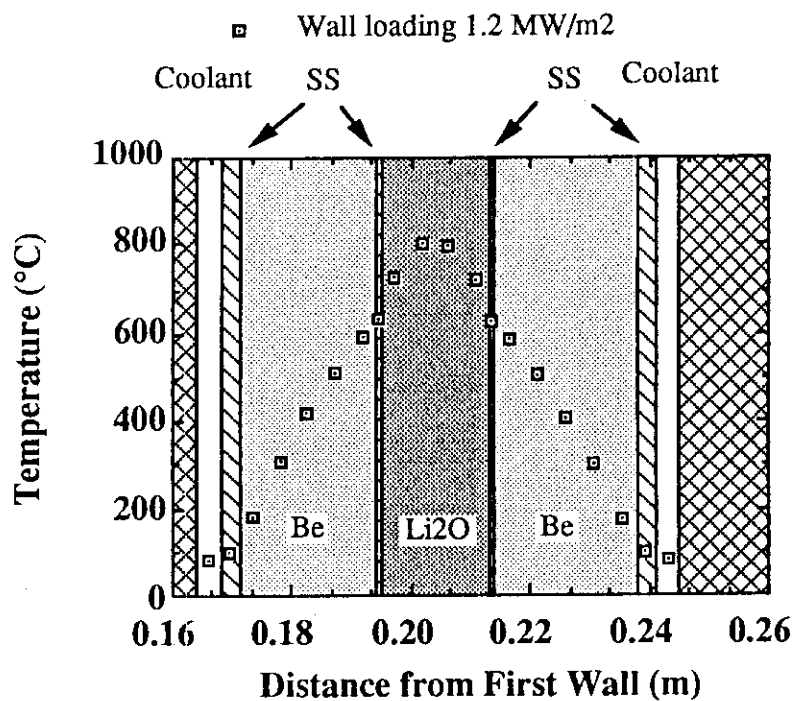


Fig. 7.2.38 Temperature profile in the unit region 4 at outboard midplane

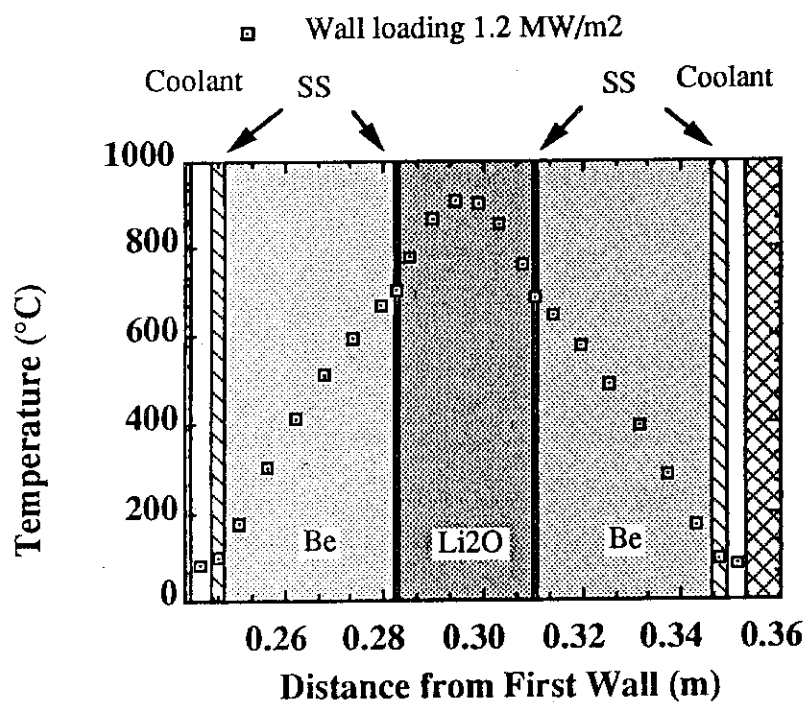


Fig. 7.2.39 Temperature profile in the unit region 5 at outboard midplane

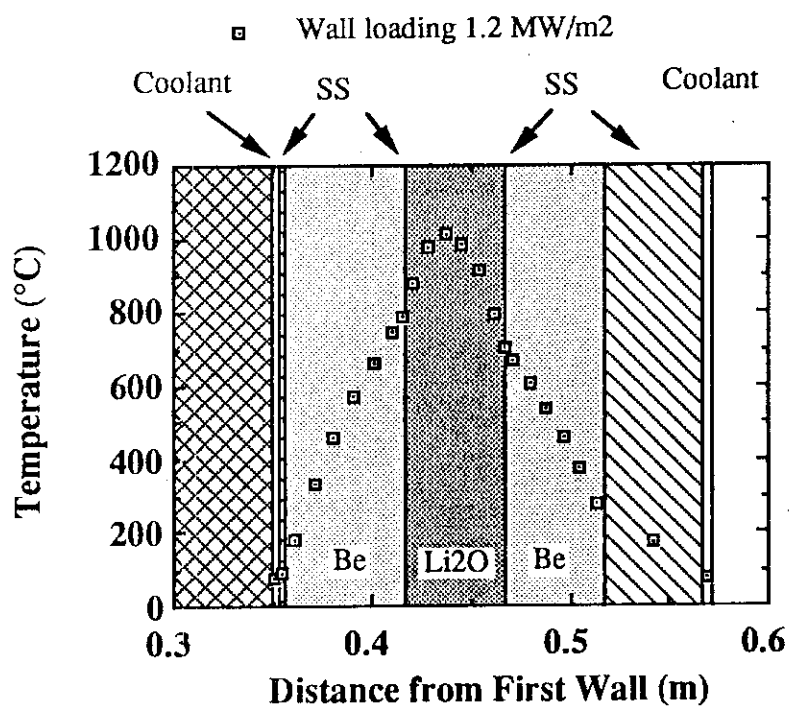


Fig. 7.2.40 Temperature profile in the unit region 6 at outboard midplane

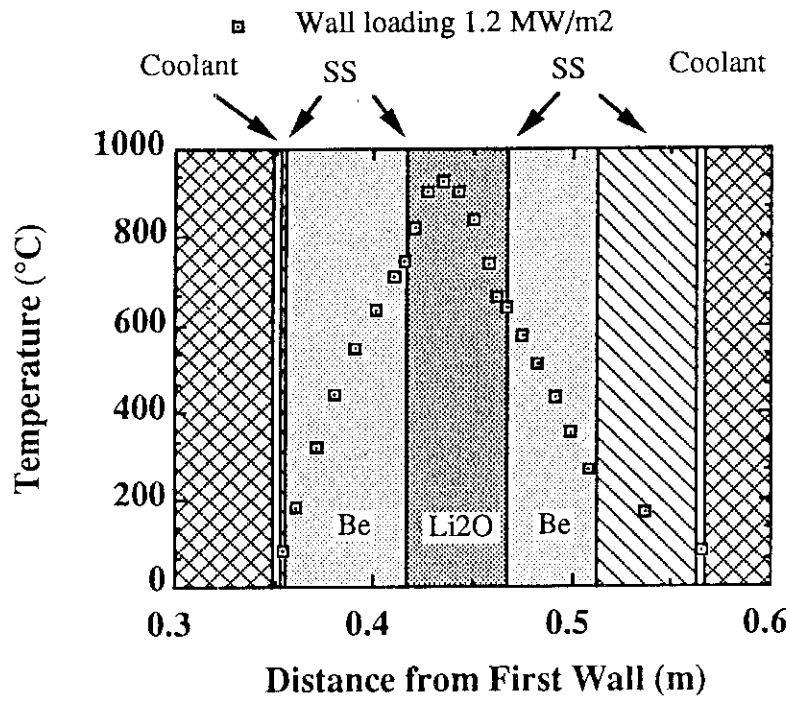


Fig. 7.2.41 Temperature profile in the unit region 6 at outboard midplane with modified layer thickness

### 7.3 Pebble and Block Blanket

#### 7.3.1 Critical issues for pebble and block blanket

In the pebble and block blanket, the minimum breeder temperature is kept higher than 400 °C with beryllium blocks located between cooling panels and breeder pebble layers. Since the heat transfer coefficient strongly depends on contact conditions of the beryllium block and the clad of breeder pebble layer, the change of the contact conditions might cause an impermissible variation of the breeder temperature. In this study, the variation was evaluated as the function of the contact conductance between beryllium block and clad. The beryllium block might be also damaged by thermal stress due to temperature difference within each block. The thermal stress has been roughly calculated to estimate the integrity of the beryllium blocks.

#### 7.3.2 Breeder temperature variation due to the change of contact conductance of beryllium block and clad

One-dimensional analytical model of the first breeder layer in the pebble and block blanket used in this study is shown in Fig. 7.3.1.

The maximum and minimum temperatures of breeder has been evaluated with the following equations.

$$T_{\min} = T_{\text{cool}} + \Delta T_f + \Delta T_{\text{ss}} + \Delta T_{\text{g1}} + \Delta T_{\text{Be}} + \Delta T_{\text{g2}} + \Delta T_{\text{cl}} \quad (7.3-1)$$

$$T_{\max} = T_{\text{cool}} + \Delta T_f + \Delta T_{\text{ss}} + \Delta T_{\text{g1}} + \Delta T_{\text{Be}} + \Delta T_{\text{g2}} + \Delta T_{\text{cl}} + \Delta T_{\text{Li2O}} \quad (7.3-2)$$

Here,  $T_{\text{cool}}$  : coolant temperature,

$\Delta T_f$  : film temperature drop,

$\Delta T_{\text{ss}}$  : temperature difference across stainless steel wall of cooling panel,

$\Delta T_{\text{g1}}$  : temperature difference across cooling panel side gap (gap 1),

$\Delta T_{\text{Be}}$  : temperature difference across beryllium block,

$\Delta T_{\text{g2}}$  : temperature difference across breeder layer side gap (gap 2),

$\Delta T_{\text{cl}}$  : temperature difference across stainless steel clad of breeder layer,

$\Delta T_{\text{Li2O}}$  : difference of the maximum and the minimum temperatures in breeder pebble ( $\text{Li}_2\text{O}$ ) packed layer.

Each term of these equations is evaluated as follows.

(i)  $T_{cool} + \Delta T_f + \Delta T_{ss}$

The surface temperature of the cooling panel is assumed to be 120°C.

(ii)  $\Delta T_{Be}$

$$\Delta T_{Be} = \frac{Q_{Be}}{2 \lambda_{Be}} t_{Be}^2 + \frac{(Q_{Li_2O} t_{Li_2O} + Q_{c1} t_{c1})}{\lambda_{Be}} t_{Be} = 104^\circ\text{C} \quad (7.3-3)$$

(iii)  $\Delta T_{c1}$

$$\Delta T_{c1} = \frac{Q_{c1}}{2 \lambda_{c1}} t_{c1}^2 + \frac{Q_{Li_2O} t_{Li_2O}}{\lambda_{c1}} t_{c1} = 10^\circ\text{C} \quad (7.3-4)$$

(iv)  $\Delta T_{Li_2O}$

$$\Delta T_{Li_2O} = \frac{Q_{Li_2O}}{2 \lambda_{Li_2O}} t_{Be}^2 = 271^\circ\text{C} \quad (7.3-5)$$

(v)  $\Delta T_{g1}$

$$\Delta T_{g1} = \frac{Q_{Li_2O} t_{Li_2O} + Q_{c1} t_{c1} + Q_{Be} t_{Be}}{h_{g1}} \quad (7.3-6)$$

(vi)  $\Delta T_{g2}$

$$\Delta T_{g2} = \frac{Q_{Li_2O} t_{Li_2O} + Q_{c1} t_{c1}}{h_{g2}} \quad (7.3-7)$$

Here,  $\lambda_{Be}$  : thermal conductivity of beryllium (87.0 W/m/K, at 300 °C, 85 % D.F.),

$\lambda_{c1}$  : thermal conductivity of stainless steel (18 W/m/K),

$\lambda_{Li_2O}$  : effective thermal conductivity of Li<sub>2</sub>O pebble packed layer (1.3 W/m/K, 60 % P.F.),

$Q_{Be}$  : nuclear heating rate in beryllium block (5.3 MW/m<sup>3</sup>),

$Q_{c1}$  : nuclear heating rate in stainless steel (10 MW/m<sup>3</sup>),

$Q_{Li_2O}$  : nuclear heating rate in Li<sub>2</sub>O pebble packed layer (44 MW/m<sup>3</sup>),

$t_{Be}$  : beryllium block thickness (34 mm),

$t_{c1}$  : clad thickness (1 mm),

$t_{Li_2O}$  : half thickness of Li<sub>2</sub>O pebble packed layer (4 mm),

$h_{g1}$  : heat conductance of gap 1,

$h_{g2}$  : heat conductance of gap 2.



The heat conductances of the gaps ( $h_{g1}$ ,  $h_{g2}$ ) are affected by heat conduction of filled gas, heat radiation and contact conductance. Since the beryllium blocks and clads are deformed due to temperature rise, the conductances might vary during the plasma operation. Figure 7.3.2 shows the calculated gap conductance taking only heat conduction with filled gas (helium of 0.1 MPa) into account. As shown in the figure, gap width of 0.02 and 2.0 mm give  $10^4$  and  $10^2$  W/m<sup>2</sup>/K, respectively. Though contribution of radiation and contact heat transfer have to be added to this conductances, the conductances are assumed to change in the range of  $10^2$  -  $10^4$  W/m<sup>2</sup>/K in this first step estimation.

The maximum and minimum breeder temperatures calculated as the function of the heat conductance are shown in Fig. 7.3.3. From the results, the heat conductance must be controlled in the range of 1000 W/m<sup>2</sup>/K to 3500 W/m<sup>2</sup>/K in order to keep the breeder temperature in the allowable range (400 to 1000°C). Since the breeder operating temperature should be kept in narrower range to accommodate to power variations and other uncertainties, the design window of heat conductance is more limited. From this point of view, the gap width must be properly controlled around 0.1 mm. On the other hand, heat radiation and contact heat conductance have large uncertainties since the beryllium block would be deformed during operation as shown in Table 7.3.1. These results indicate that it is difficult to control the breeder temperature properly with beryllium block layer. It is preferable to use more insensitive thermal resistance layer such as beryllium pebble layer and gas gap.

### 7.3.3 Thermal stress in beryllium block

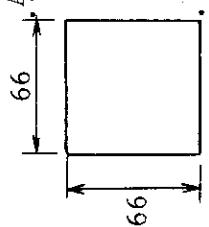
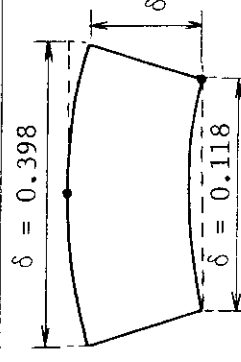
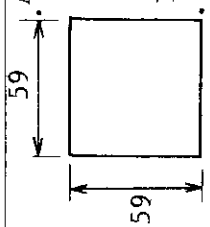
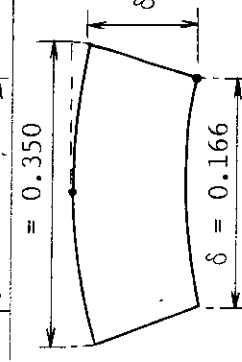
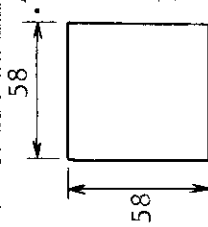
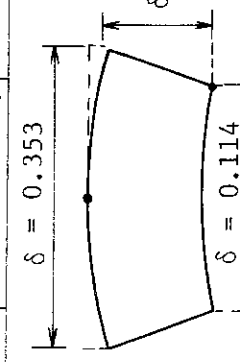
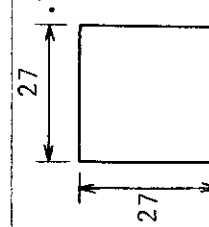
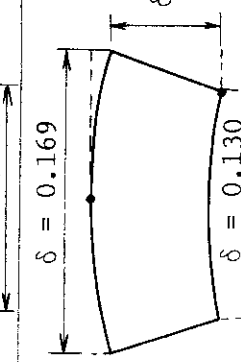
The thermal stress generated in the beryllium block has been evaluated with the following simple one-dimensional plate equation for rather severe constraint on bending.

$$\sigma = \frac{E \beta \Delta T_{Be}}{2 (1-\nu)} \quad (7.3-8)$$

here,  $E$  : Young's modulus (166 GPa, 300 °C, 85 % D.F.),  
 $\beta$  : volumetric expansion coefficient ( $43.8 \times 10^{-6} 1/K$ , 300 °C),  
 $\Delta T_{Be}$  : temperature difference across beryllium block,  
 $\nu$  : Poisson's ratio of beryllium (0.07).

Figure 7.3.4 shows the generated thermal stress as the function of temperature difference across the beryllium block. A thermal stress of 400 MPa will be generated for the temperature difference of 100 °C. Expected tensile strength of beryllium at 80 % D.F. is shown in Fig. 7.3.5. (The strength of sintered beryllium block depends on density factor, grain size and fabrication method. Detail mechanical properties of the beryllium block are not known yet). The beryllium block might be broken by the thermal stress during reactor operation since the temperature difference across the block should be up to 300 °C so as to satisfy the breeder temperature condition for in-situ tritium recovery. Though the reduction of thermal stress is expected to some extent because of the existence of surrounding contact gap, cracks might be initiated in the beryllium blocks resulting in the rise-up of the minimum breeder temperature. In the sense that smaller size of blocks is preferable in order to reduce the thermal stress, beryllium pebble packed layer for the breeder minimum temperature control is one of the candidates to keep the beryllium layer integrity.

Table 7.3.1 Deformation of Be block due to temperature difference across the block

Case	Dimesion/Temperature*	E (GPa)	$\nu$	$\beta$ (1/K)	Deformation (mm)
1	 66 A... 424.0°C B... 126.0°C	87.5 (65% D.F.)	0.07	$14.2 \times 10^{-6}$	 $\delta = 0.398$ $\delta = 0.300$
2	 59 A... 406.0°C B... 194.0°C	175.0 (85% D.F.)	0.07	$14.6 \times 10^{-6}$	 $\delta = 0.350$ $\delta = 0.297$
3	 58 A... 425.0°C B... 138.0°C	87.4 (65% D.F.)	0.07	$14.3 \times 10^{-6}$	 $\delta = 0.353$ $\delta = 0.267$
4	 27 A... 404.0°C B... 312.0°C	174.0 (85% D.F.)	0.07	$15.5 \times 10^{-6}$	 $\delta = 0.169$ $\delta = 0.155$

\* It was assumed that temperature profiles are uniform in the surfaces of A and B, linear decrease from A to B.

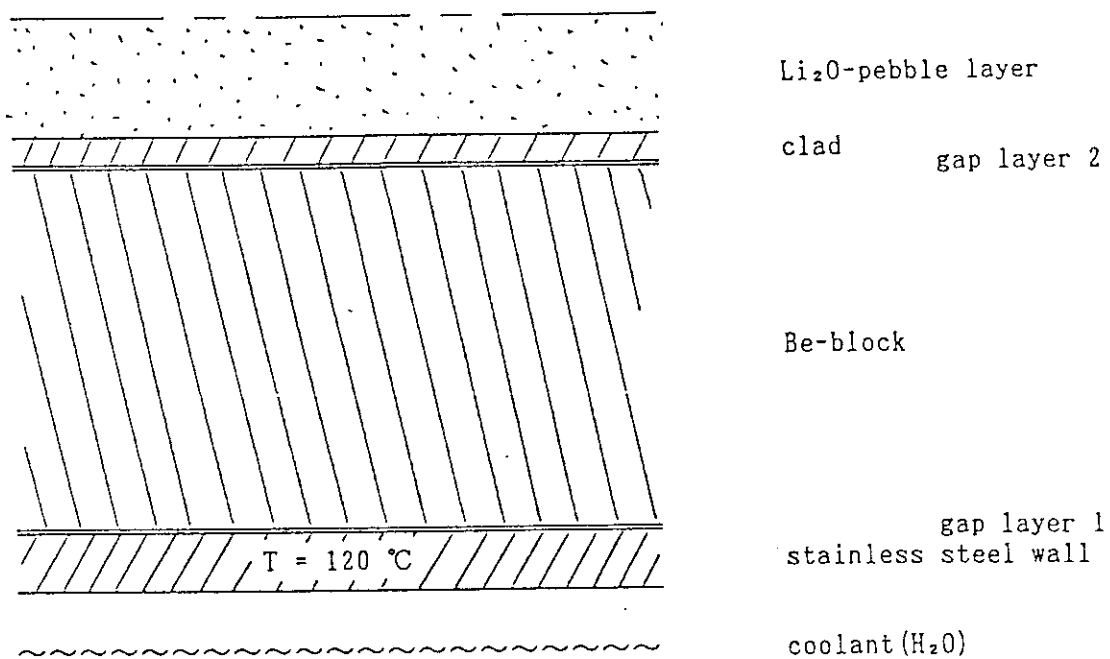


Fig. 7.3.1 One-dimensional analytical model of the pebble and block blanket

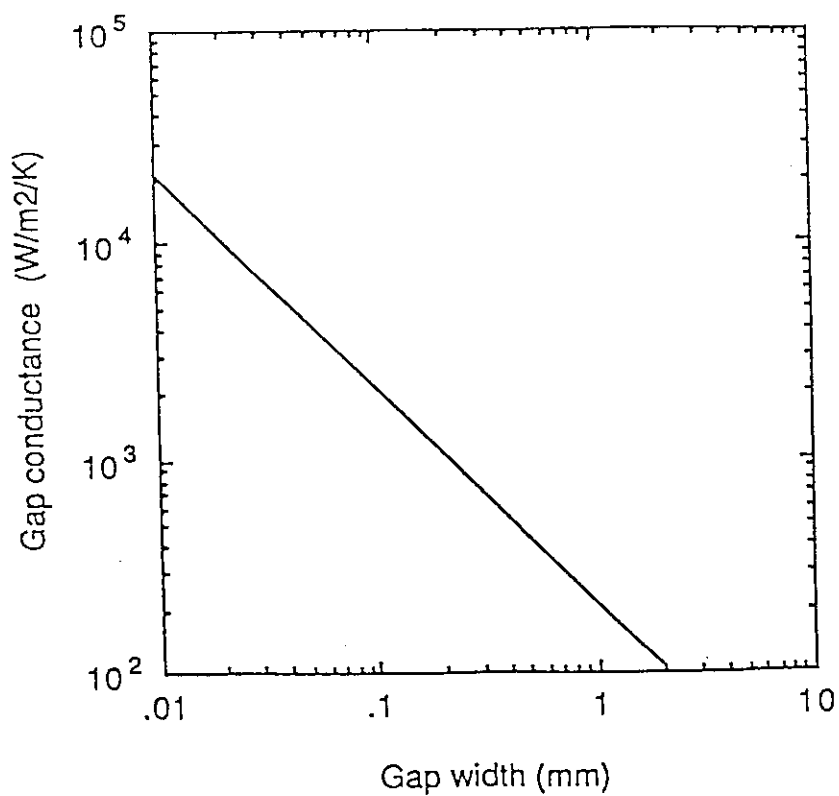


Fig. 7.3.2 Gap conductance due to heat conduction of He gas (0.1 MPa) as a function of gap width

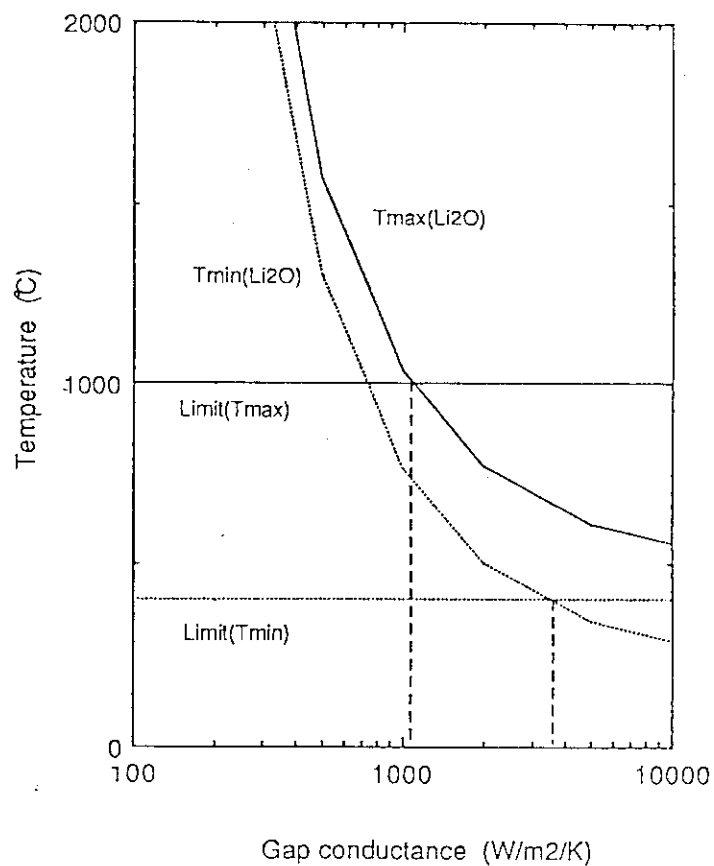


Fig. 7.3.3 Design window of gap conductance between Be block and SS clad to keep breeder temperature within allowable range

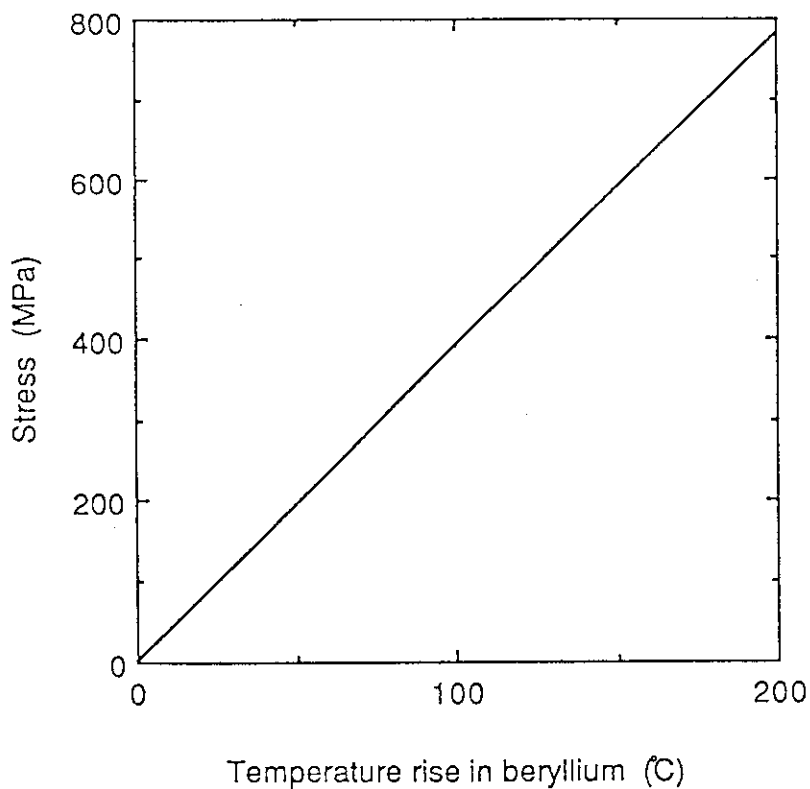


Fig. 7.3.4 Thermal stress generated in Be block as a function of temperature difference across the block

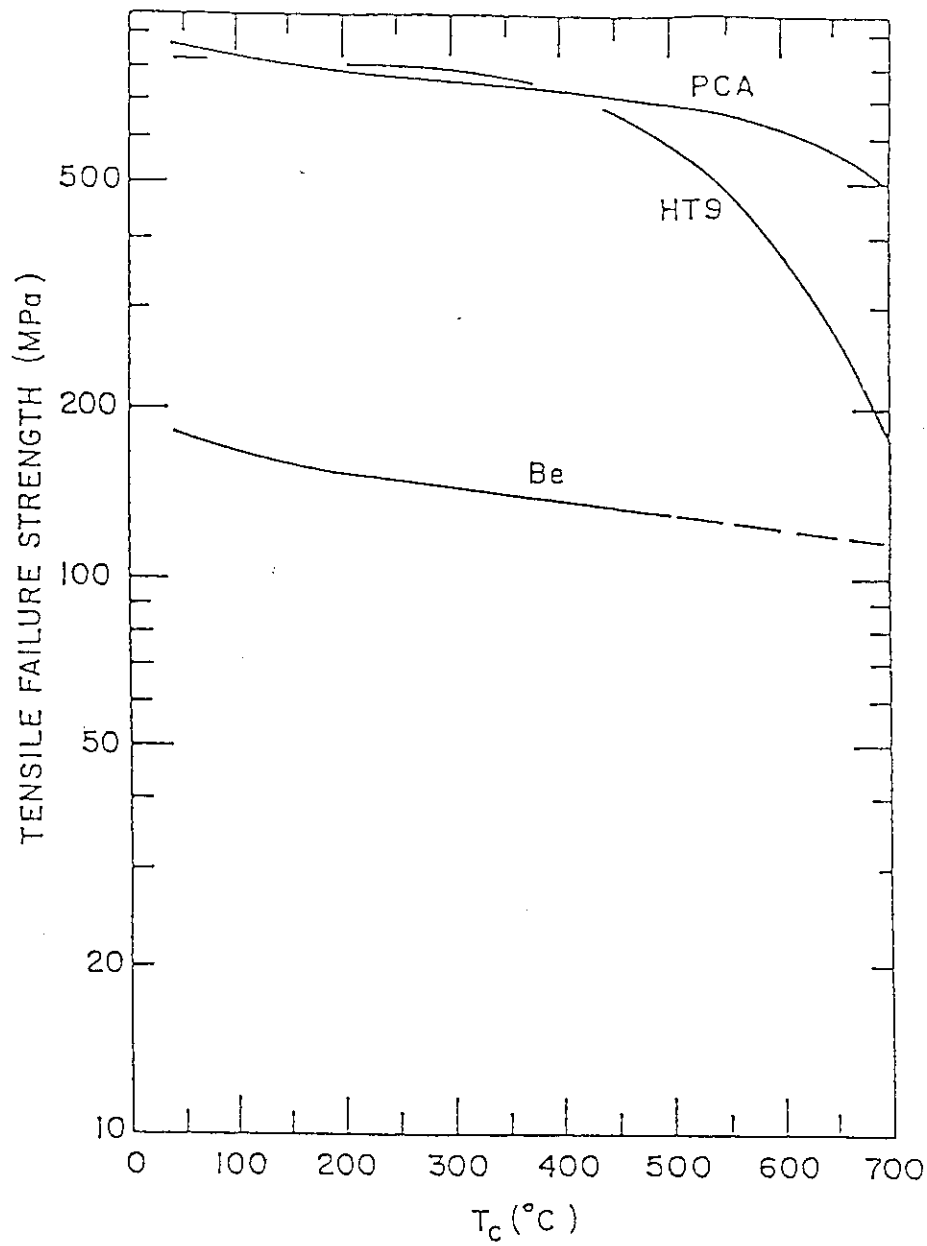


Fig. 7.3.5 Expected tensile failure strength of 80% dense sintered Be

#### 7.4 Conclusions

Preliminary thermal analyses show that temperatures of  $\text{Li}_2\text{O}$  in both type of blanket, the mixed pebble bed and the layered pebble bed blankets, can be maintained within the allowable operation range (400 - 1000 °C) for the reference neutron wall loading. In addition, it is expected that narrower  $\text{Li}_2\text{O}$  temperature range specified as a nominal range (450 - 700 °C), that permits power variations wider than -10 to +25 %, would be assured by an optimization of layer arrangements in the layered pebble bed blanket and cooling tube arrangement and helium gap widths in the mixed pebble bed blanket.

In the pebble and block blanket, the gap width between the clad of  $\text{Li}_2\text{O}$  pebble packed layer and the beryllium block must be kept around 0.1 mm to keep the breeder temperature within above nominal range. To keep the gap in such a small width is extremely difficult in terms of fabricability and deformation during a reactor operation. Thermal stress during operation has a possibility to generate thermal cracks in the beryllium block, which significantly affect the breeder temperature control.

## 8. Stress Analysis

Breeder, neutron multiplier and coolant tubes are contained in the vessel of the blanket. The front wall of the vessel also plays as the first wall. In Section 8.1, thermal stress due to surface heat flux on the first wall are analyzed taking into account of the whole blanket vessel, i.e. temperature difference between the first wall and the back wall. Stress due to inner pressure load are also calculated. For both analyses, two-dimensional elastic stress analyses have been performed with the finite element analysis code, ABAQUS, using a model of a blanket cross-section. Preliminary analyses of the stress due to electromagnetic force during a plasma disruption are described in Section 8.2.

### 8.1 Thermal Stress and Internal Pressure on the Blanket Box Structure

#### 8.1.1 Analytical model and conditions

The vessel of the breeding blanket has a box-like structure as shown in Fig. 8.1.1. Analytical model used in this study is shown in Fig. 8.1.2 taking a half of the vessel width. With this model, the following cases have been analyzed.

Case 1 : thermal load only

Case 2 : inner pressure load only

Case 3 : thermal load + inner pressure load

Case 4 : thermal load + inner pressure load with stiffening plate

Stiffening plates in the vessel are not taken into account in Cases 1-3 while a stiffening plate is included at vessel center in Case 4. For the thermal load, wall temperatures are assumed to be uniform at 200 °C in the first wall, 100 °C in the back wall, and linearly decreasing from 200 °C to 100 °C in the side wall as indicated in Fig. 8.1.3. As the inner pressure, 0.1 MPa of the purge gas pressure is taken into account. Boundary conditions for stress analyses are also shown in Fig. 8.1.3. Structural material of the vessel is type 316 stainless steel, of which mechanical properties used in the analyses are those at 150°C; Young's modulus is 186 GPa and Poisson's ratio 0.3.

#### 8.1.2 Analytical results

Stress distributions for four cases are shown in Figs 8.1.4 to 8.1.7, deformations of blanket vessel in Figs 8.1.8 to 8.1.11.



In Cases 1 to 3 (without the stiffening plate), stresses in the first wall due to thermal load are sufficiently small, which are about 8 MPa at both center and corner of the vessel. Maximum stress is about 20 MPa in the side wall near the back wall, which is insignificant. The inner pressure is dominant for stress and deformation of the vessel. At the center of the plasma side surface of the first wall, a tensile bending stress of about 120 MPa occurs due to the inner pressure. The maximum stress occurs at the corner of the blanket vessel, which is about 300 MPa and beyond the yield strength (260 MPa). The center of the first wall expands about 9 mm due to the inner pressure. Packing of the breeder and multiplier pebbles and temperature control of the breeder would be seriously affected by such a deformation.

The stress and the deformation due to the inner pressure can be reduced by one or combination of the following measures.

- Increase of the first wall thickness
- Installation of stiffening plates
- Decrease of the inner pressure of the blanket vessel (i.e., purge gas pressure)
- Larger curvature of the vessel corner, especially for reducing the stress at the corner (inner  $R=15$  mm and outer  $R=30$  mm in this study).

In this study, the effects of the stiffening plate and decrease of the inner pressure are investigated. By providing a stiffening plate at the vessel center, the stress at the corner is substantially reduced (from 300 MPa to 60 MPa) as seen from the results of Case 4. As for the effects of decreased inner pressure, stresses will be reduced in proportion to the inner pressure. Figure 8.1.12 indicates the expected relation between the inner pressure (purge gas pressure) and the maximum stress at the corner based on the results of Case 3 (without the stiffening plate). The maximum stress can be reduced below the yield stress by the reduction of the purge gas pressure to less than about 0.04 MPa.

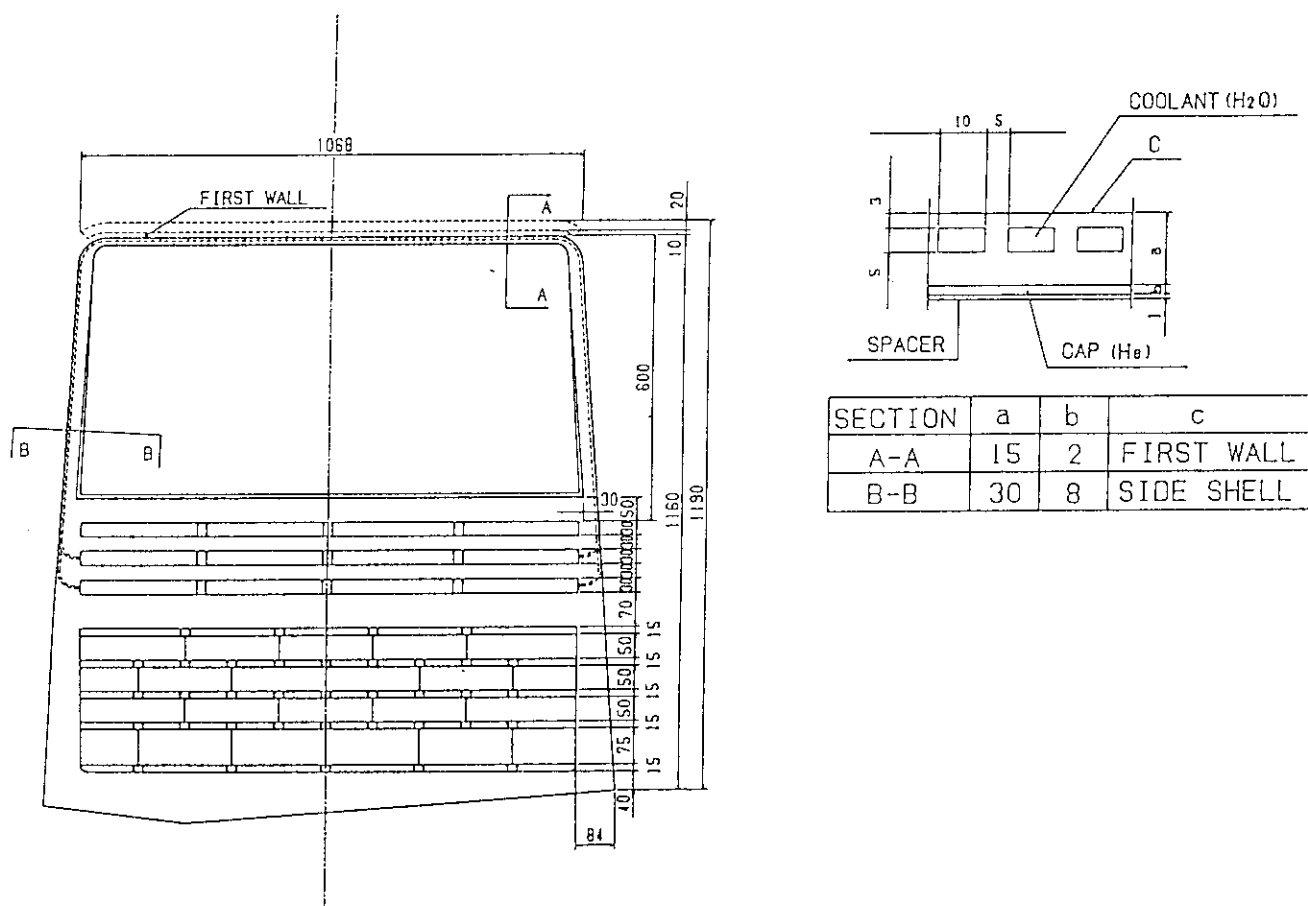


Fig. 8.1.1 Cross-section of blanket vessel (box structure) at outboard midplane

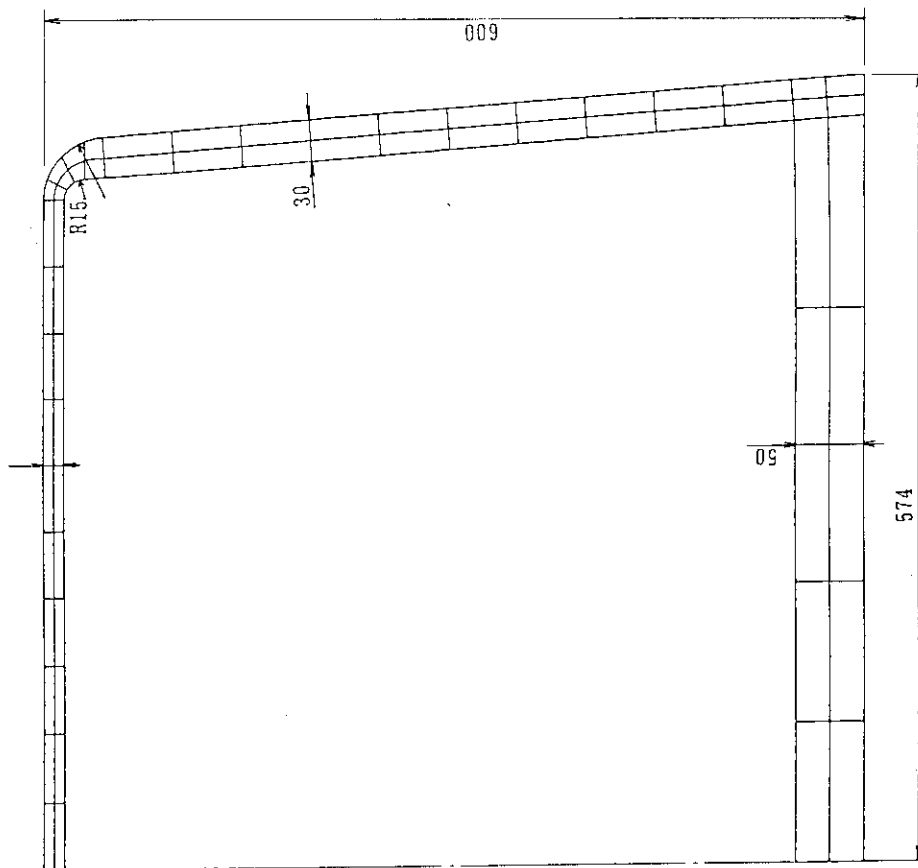


Fig. 8.1.2 Analytical model of blanket vessel

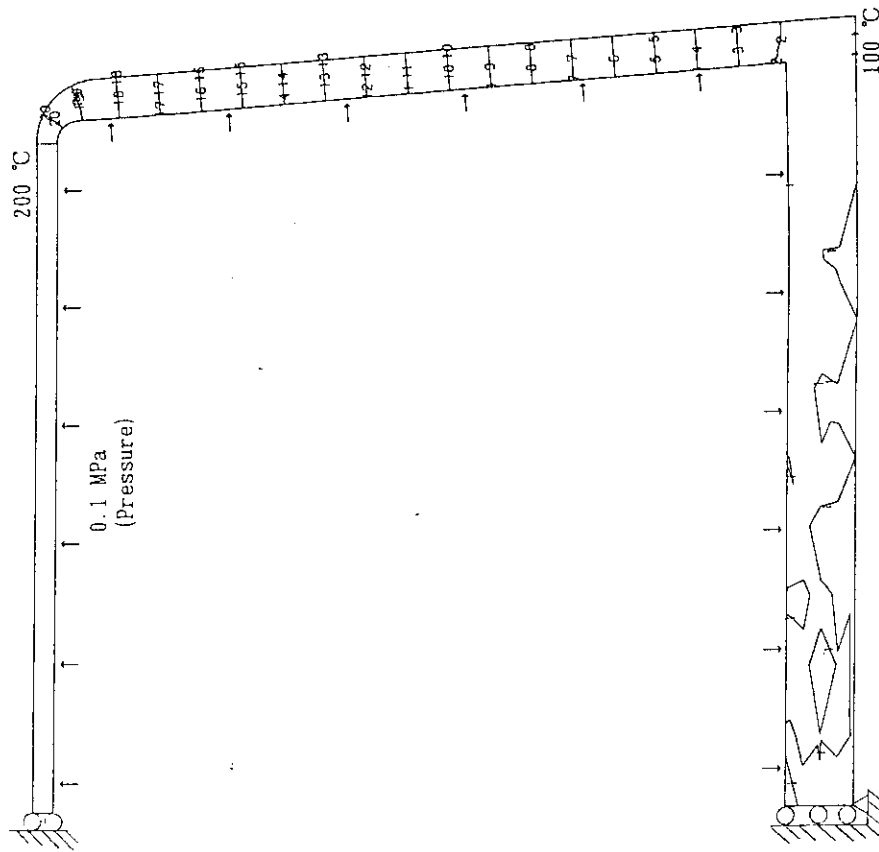


Fig. 8.1.3 Analytical conditions of blanket vessel

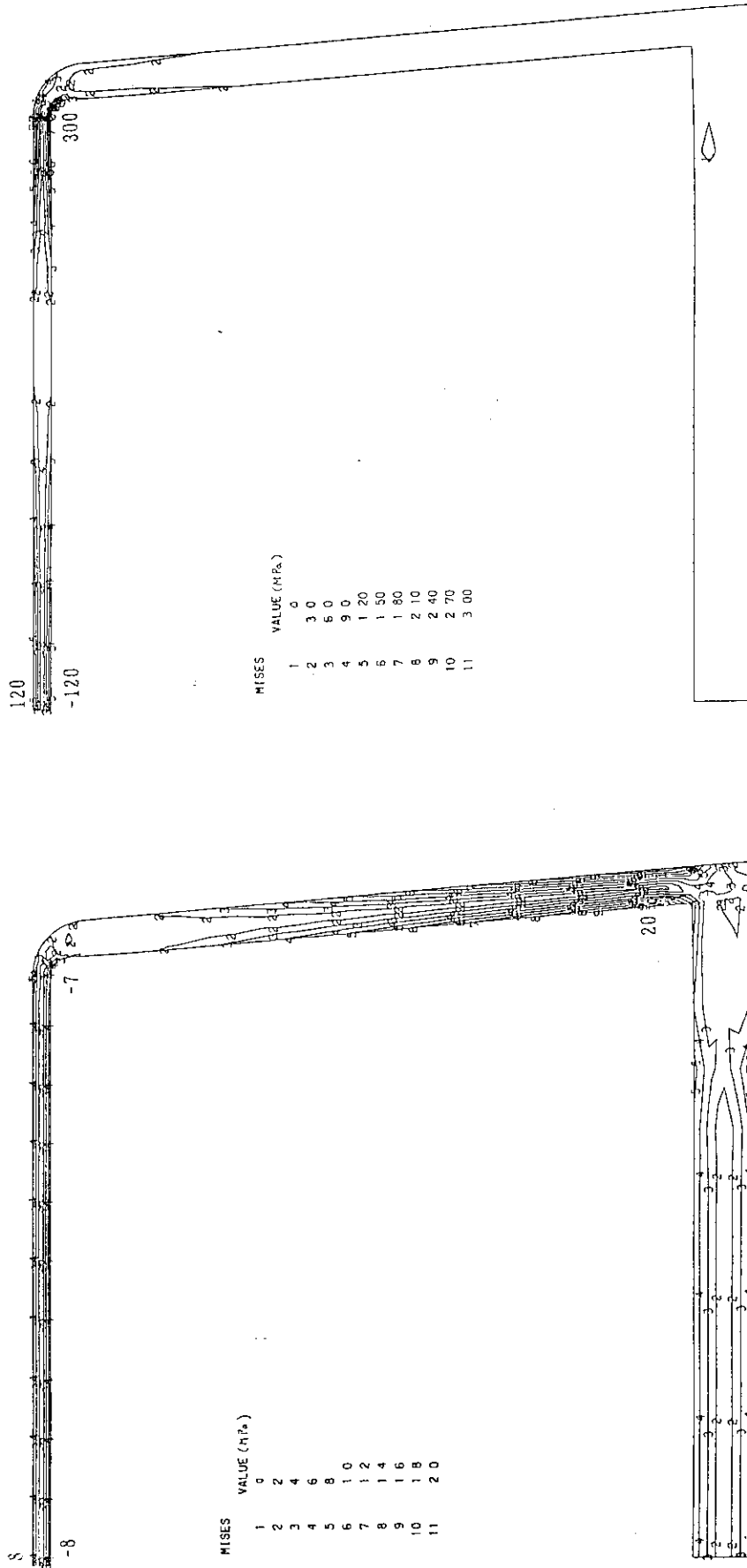


Fig. 8.1.5 Stress distribution due to inner pressure load (case 2)

Fig. 8.1.4 Stress distribution due to thermal load (case 1)

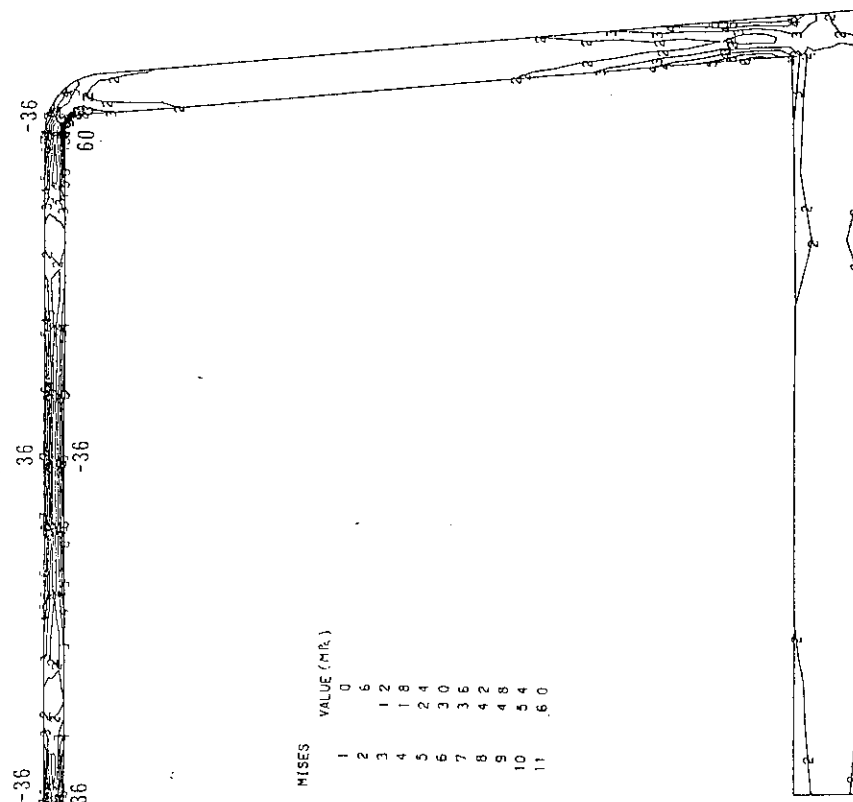


Fig. 8.1.1.6 Stress distribution due to thermal and inner pressure loads (case 3)

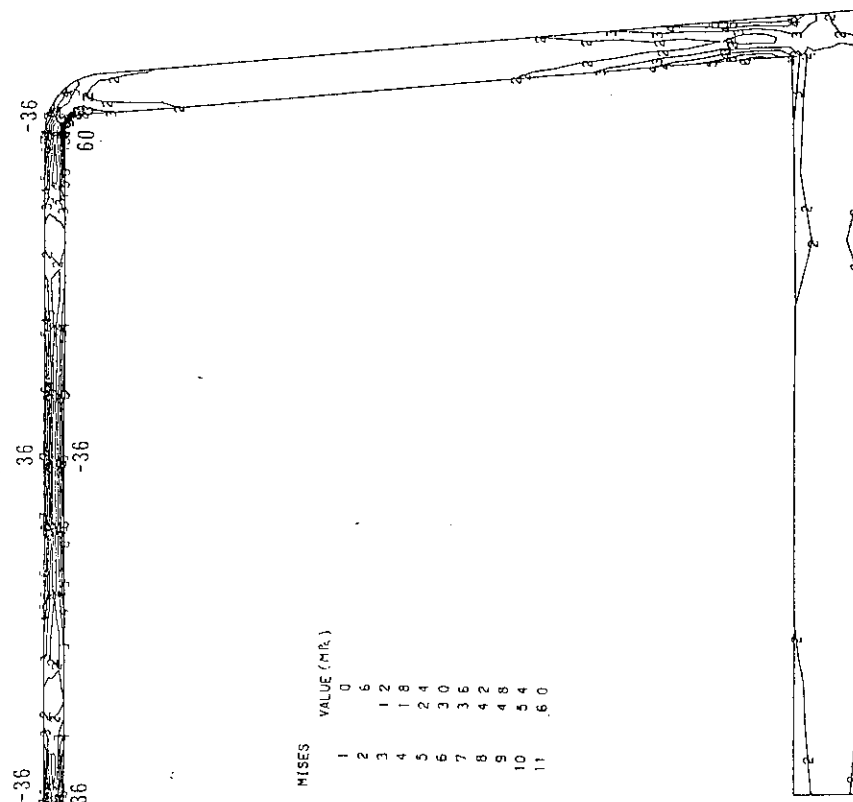


Fig. 8.1.1.7 Stress distribution due to thermal and inner pressure loads with inside stiffening plate (case 4)

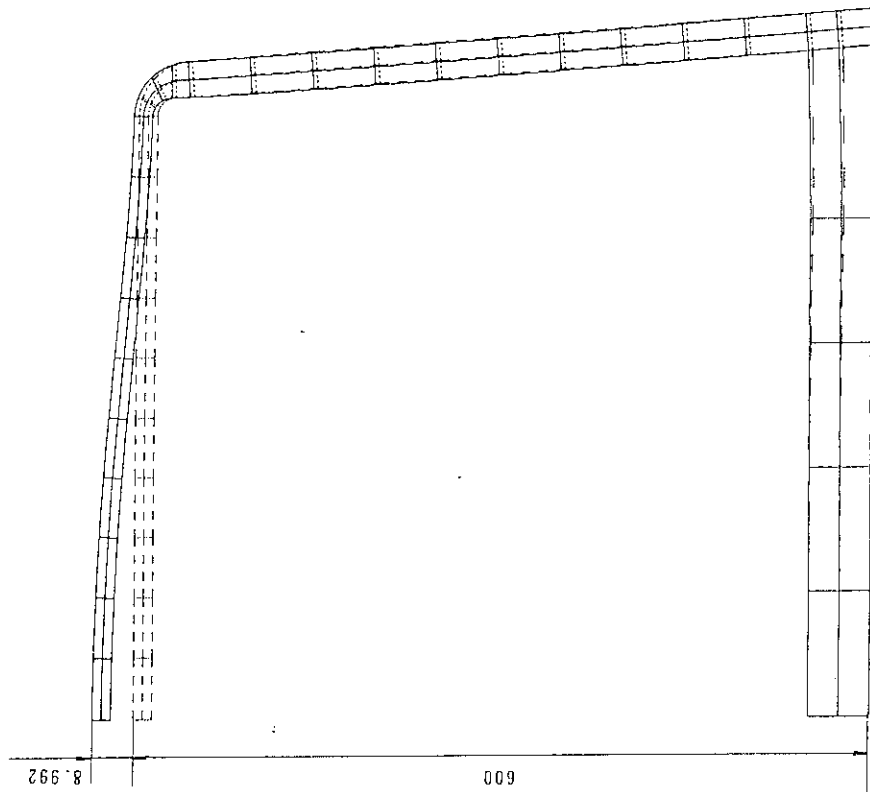


Fig. 8.1.1.9 Deformation due to inner pressure load (case 2)

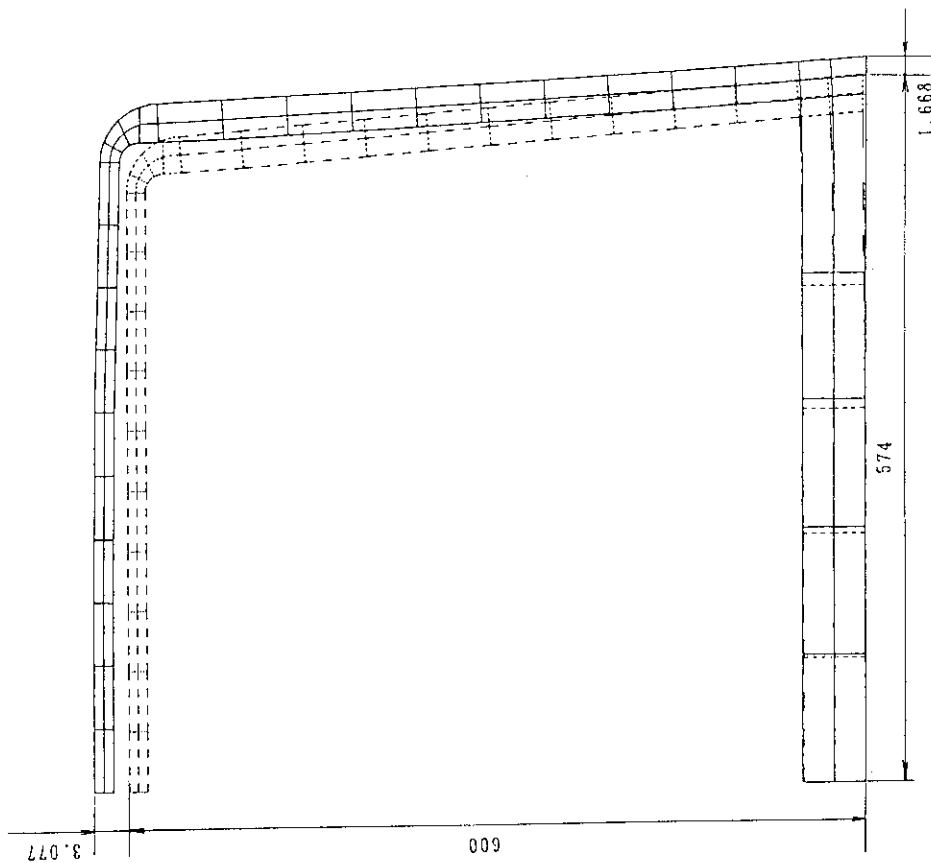


Fig. 8.1.1.8 Deformation due to thermal load (case 4)

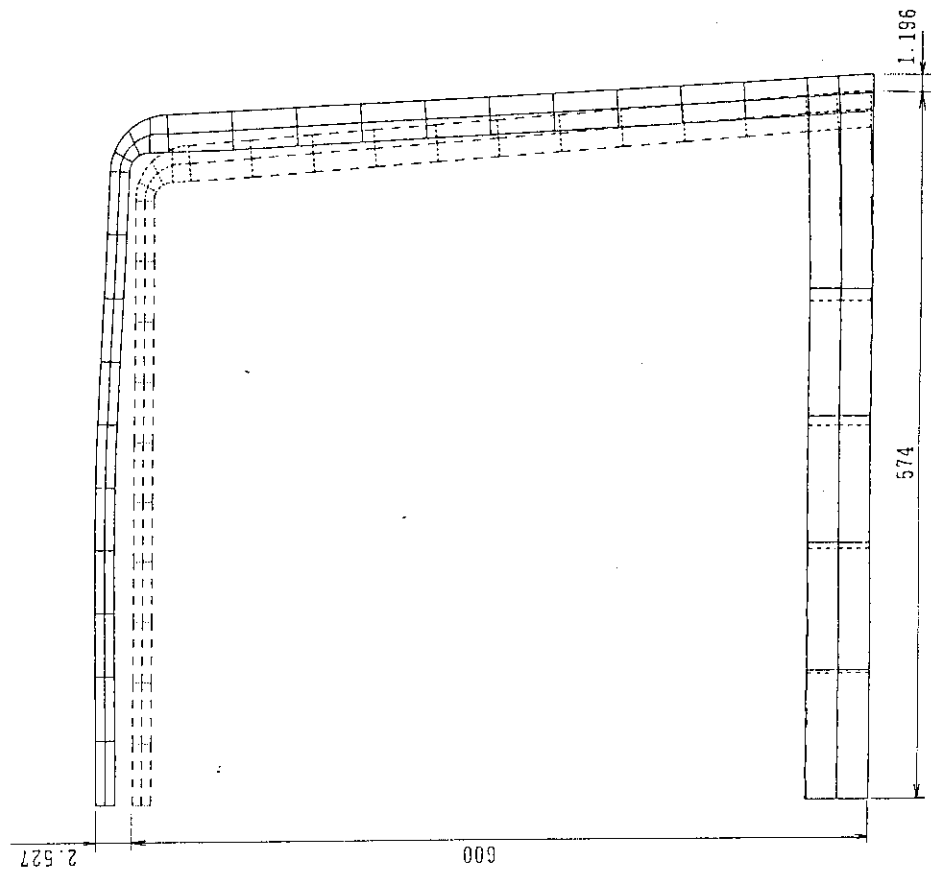


Fig. 8.1.11 Deformation due to thermal and inner pressure loads with inside stiffening plate (case 4)

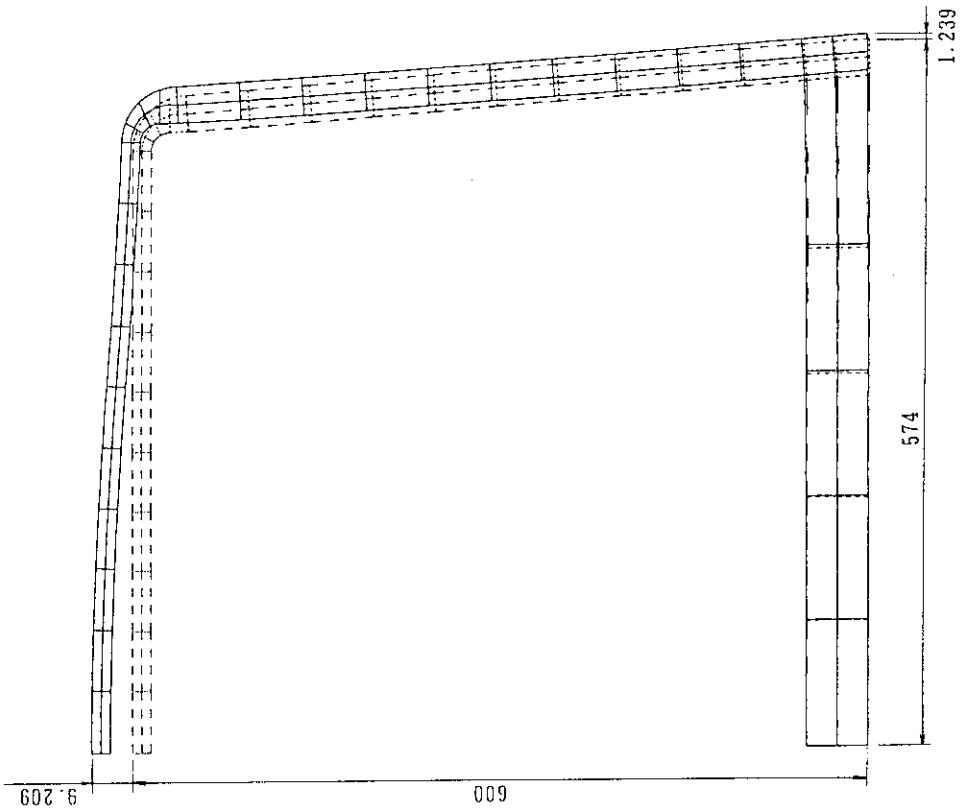


Fig. 8.1.10 Deformation due to thermal and inner pressure loads (case 3)

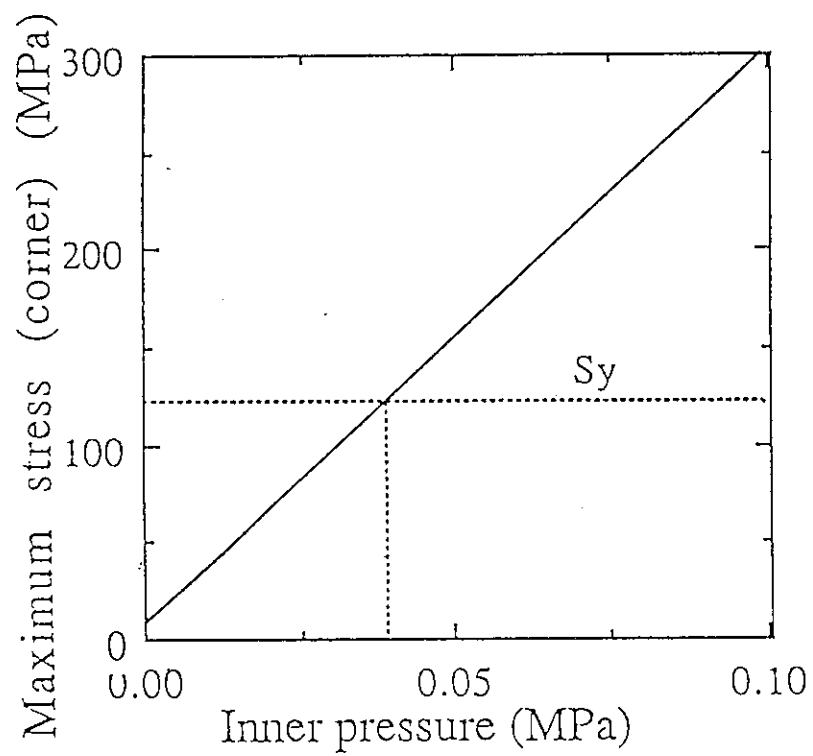


Fig. 8.1.12 Allowable inner pressure in case of no stiffening plate



## 8.2 Disruption Analysis

### 8.2.1 Electromagnetic forces on blankets

In transient electromagnetic (EM) analysis, the blanket/shield structure is modeled as a box structure integrated with the first wall and is analyzed all together at a time. As typical for EM loads during a plasma disruption, total EM loads on a quarter of an outboard (OB) module are 12 MN and 22 MN in radial and vertical directions, respectively, and those of an inboard (IB) module are 3 MN and 5 MN in radial and vertical directions, respectively.

### 8.2.2 Structural analysis of OB box structure

Simplified structural analysis of the OB module has been carried out to examine the effects of the support conditions and stiffening ribs on the stress and deformation of the OB box structure under disruption EM loads.

The OB box structure is modeled as a simple rectangular prism composed of shell elements, as shown in Fig. 8.2.1, with a 1 m square and a 10 m height. The effects of four kinds of support conditions which are

- rear panel full constraint,
- two lines (both side edges from top to bottom) of rear panel constraint,
- three lines (both side edges and center from top to bottom) of rear panel constraint,
- two lines (0 and 400 mm from rear panel from top to bottom) of side wall, and three kinds of stiffening ribs, i.e. lateral and two kinds of longitudinal ones, have been examined.

Distributed radial EM loads and uniform vertical EM loads, 10 MN and 10 MN in all, respectively, for a quarter of an OB box structure, are applied on the side walls. As EM loads on the first wall are much smaller than those of the side walls, they are neglected in this analysis.

Results obtained by three-dimensional FEM stress analysis are summarized in Fig. 8.2.2. Lateral and longitudinal stiffening ribs are effective against the radial and vertical EM loads, respectively. For three cases of the support conditions other than "side wall constraint", the effect of the

support conditions is negligibly small. On the other hand, "side wall constraint" can minimize the stress down to less than 60 MPa. Distributions of the stress and deformation are shown in Figs 8.2.3 and 8.2.4, respectively, for the case of structural model shown in Fig. 8.2.1 and "side wall constraint".

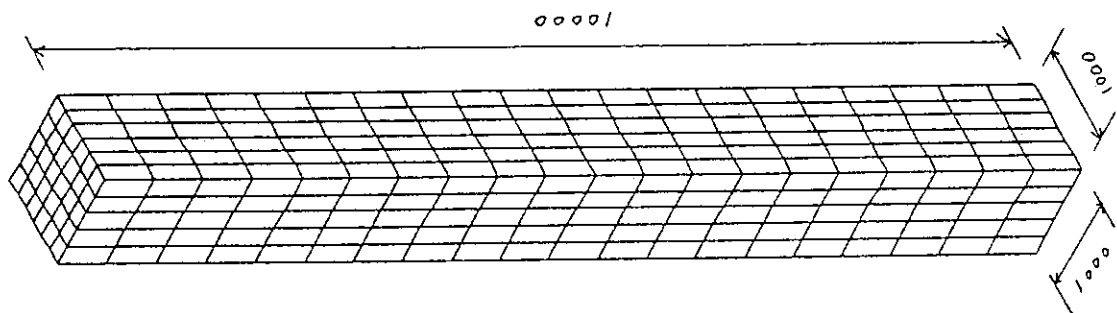


Fig. 8.2.1 Simplified model of outboard side module

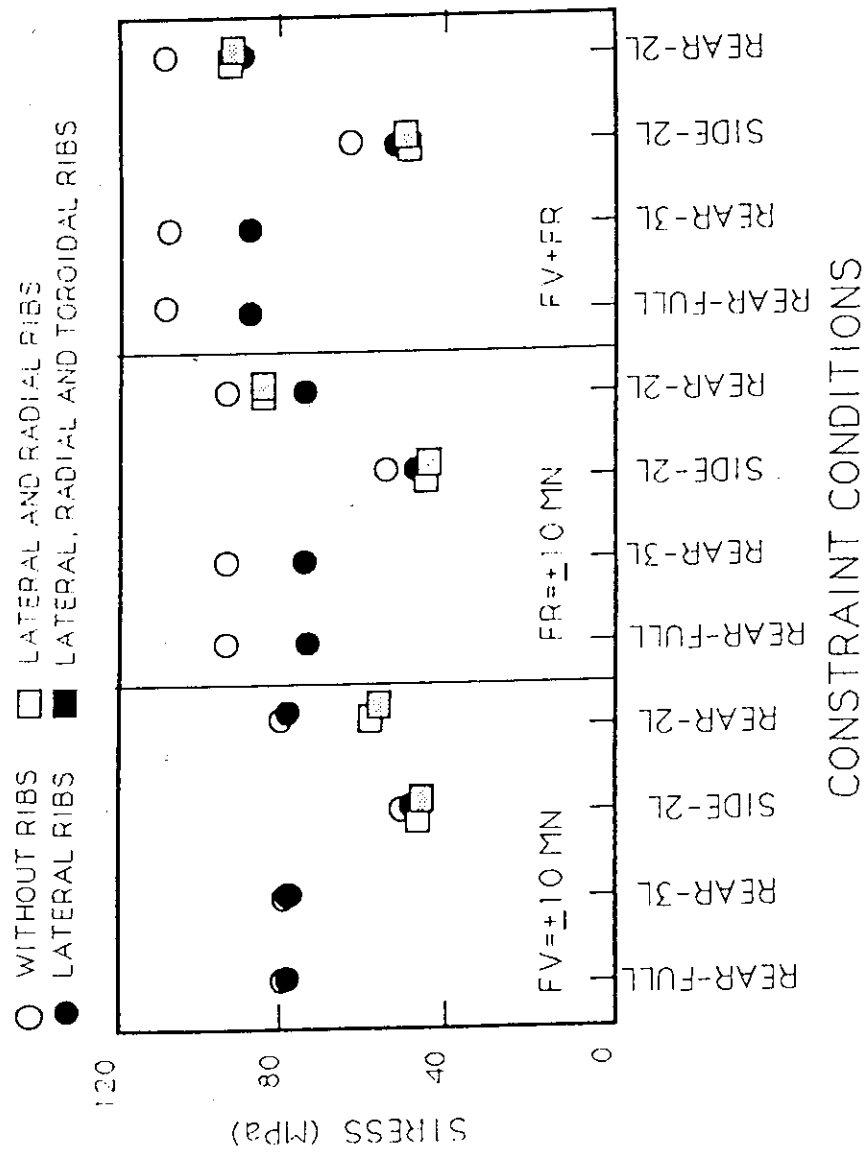


Fig. 8.2.2 Summary of structural analysis of outboard side module under disruption electromagnetic loads

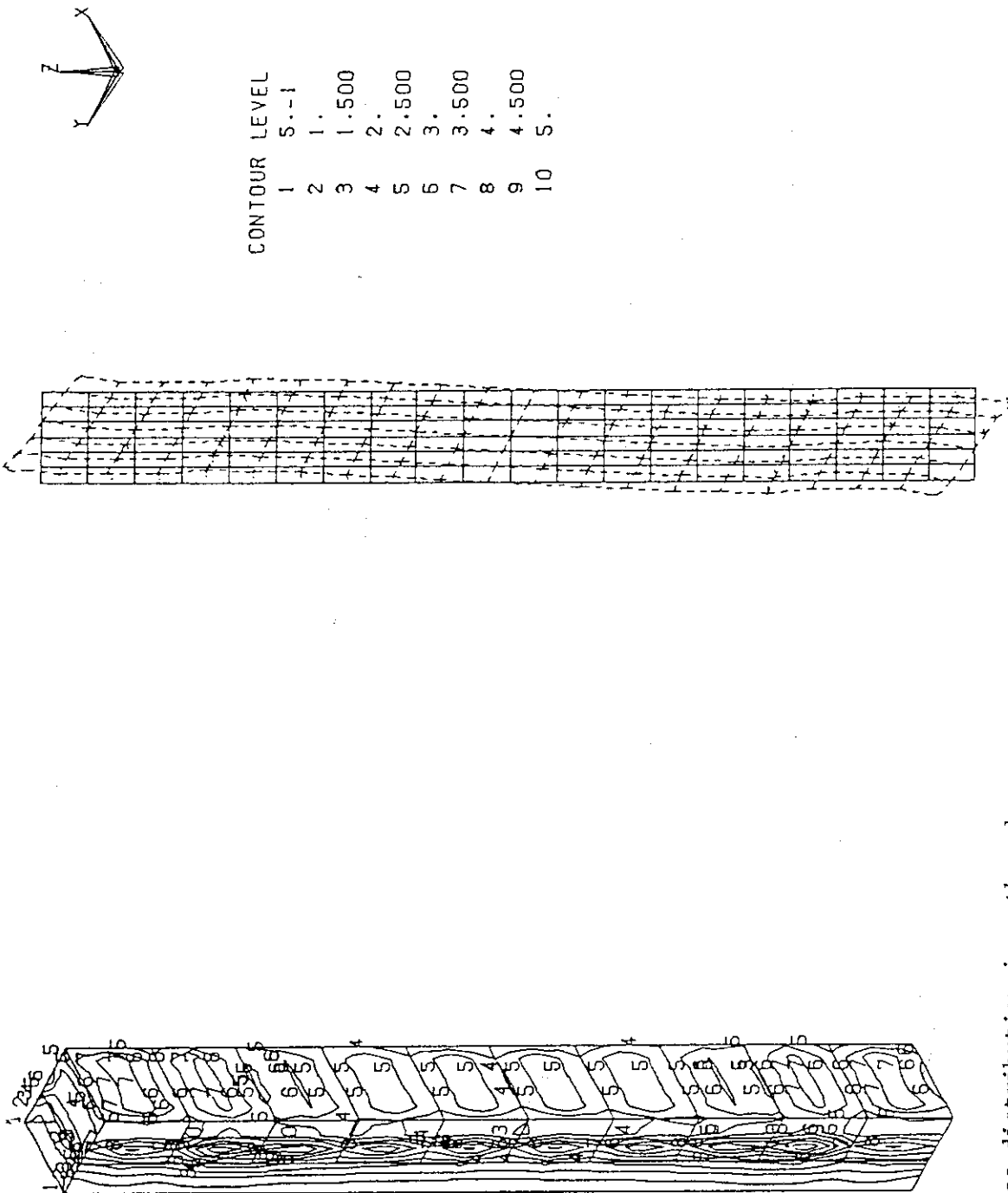


Fig. 8.2.3 Stress distribution in outboard side module due to disruption EM loads

Fig. 8.2.4 Deformation of outboard side module due to disruption EM loads

### 8.3 Conclusions

From the above stress analyses, the following conclusions can be obtained concerning to thermal and inner pressure (purge gas pressure) loads.

- The inner pressure mainly contributes to the stress and deformation of the blanket vessel.
- Without a stiffening plate, the maximum stress (300 MPa) at the corner of the blanket vessel exceeds the yield stress of type 316 stainless steel, and the maximum displacement is about 9 mm at the center of the first wall, which would seriously affect the packing of breeder and multiplier pebbles and temperature control of the breeder.
- Installation of a stiffening plate at the center of the blanket vessel substantially reduce the maximum stress to below the yield stress.
- Even without the stiffening plate, the maximum stress can be reduced below the yield stress by decreasing the inner pressure down to 0.04 MPa.

As for the EM loads, lateral and longitudinal stiffening ribs (plates) are effective against the radial and vertical EM loads, respectively. Among support conditions examined in this study, the "side wall constraint" is the most effective to support the blanket vessel and reduce the stresses due to disruption EM loads.

For further investigation, synergistic effects of thermal, inner pressure and EM loads on stresses and deformations should be taken into account. Based on this investigation, stiffening/support methods of blanket vessel should be developed.

## 9. Tritium Recovery/Inventory

Purge gas conditions for tritium recovery and tritium inventory in the blanket have been evaluated for the mixed pebble bed blanket (in Section 9.1) and the layered pebble bed blanket (in Section 9.2).

### 9.1 Mixed Pebble Bed Blanket

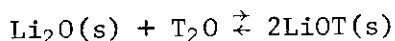
#### 9.1.1 Tritium recovery condition

Tritium recovery conditions are summarized in Table 9.1.1.

An operating temperature range of breeder zone is assumed to be from 400 °C to 600 °C in this evaluation. The minimum temperature limit has been determined at 400 °C to avoid excessive adsorption inventory of tritium. The minimum operating temperature of breeder zone is also considered so as to avoid precipitation of lithium hydroxide and excessive tritium inventory.

Swelling of beryllium may become a critical factor to determine the maximum operating temperature when beryllium pebbles are mixed with lithium oxide pebbles. Experimental results indicate that the swelling of beryllium becomes serious above 700 °C[1]. The maximum operating temperature of 600 °C has been considered also to avoid mass transfer of lithium oxide with a reasonable margin.

Thermal dissociation of tritiated lithium hydroxide (LiOT), shown below, is assumed to be a dominating mechanism in the course of tritium release from the breeder grain surface to purge gas stream.



Purge gas flow rate is determined to keep water partial pressure in blanket atmosphere (sweep gas stream) sufficiently less than water dissociation pressure in  $\text{Li}_2\text{O}-\text{H}_2\text{O}-\text{LiOH}$  system at 400 °C ( $\sim 10^{-3}$  atm)[2]. Purge gas flow rate is determined also to keep  $\text{T}_2\text{O}$  equivalent tritium pressure in purge gas stream less than  $10^{-4}$  atm including safety factor against data uncertainty and coolant water leakage into blanket atmosphere.

Protium gas ( $\text{H}_2$ ) is added into helium purge gas at an atomic mass flow rate of one hundred times as high as tritium production rate in the blanket.

based on in-reactor tritium recovery tests, which indicate that the addition of hydrogen isotopes is effective to enhance tritium release from the breeder and to reduce tritium inventory in the blanket. In-reactor tritium recovery tests also indicate that the chemical form of tritium released from  $\text{Li}_2\text{O}$  is 95 % of HT and 5 % of HTO when protium is added at sufficiently high concentration[3].

Pressure drop of helium purge gas through breeding zone is evaluated by using Ergun's equation[4] described below:

$$\Delta P = \frac{u_f^2 L}{D_p} \frac{(1-\epsilon)}{\epsilon^2} \left\{ 150 \frac{(1-\epsilon)\mu}{D_p u_f \rho_f} + 1.75 \right\}$$

where  $\Delta P$  : pressure drop (Pa)  
 $u_f$  : superficial velocity (m/s)  
 $D_p$  : pebble diameter (m)  
 $L$  : length of breeding zone (m)  
 $\epsilon$  : void fraction (-)  
 $\mu$  : viscosity (Pa·s)  
 $\rho_f$  : gas density ( $\text{kg/m}^3$ )

Pressure drop evaluated by this equation is 0.80 kPa (80 mmAq) for helium purge gas at 100 kPa and 673 K flowing with a total (for full torus) flow rate of  $240 \text{ Nm}^3/\text{h}$  through breeding zone packed with 1 mm diameter pebbles and void fraction of 0.4.

### 9.1.2 Tritium inventory

Steady state tritium inventory of the mixed pebble bed blanket is calculated taking pseudo three-dimensional temperature distribution into account. Tritium build-up mechanisms incorporated in the analytical model are bulk diffusion of tritium, surface decomposition of  $\text{LiOT}$ , adsorption of tritium oxide on  $\text{Li}_2\text{O}$ , and solution of elemental tritium in both of  $\text{Li}_2\text{O}$  and beryllium. The calculation formulae corresponding tritium build-up mechanisms are summarized in Table 9.1.2. The average tritium generation rate is used in place of the local generation rate in the calculation because it is presumed that the difference between them in the inventory estimation is small. Protium swamping is adopted in the design to reduce tritium inventory in the blanket. Tritium inventory in the case without the protium swamping is

also estimated for comparison.

Analytical conditions are summarized in Table 9.1.3. The temperature spectrum in the breeding zone is shown in Fig. 9.1.1 based on the result of two-dimensional thermal analysis and taking the poloidal variation into consideration.

The estimated tritium inventories in the mixed pebble bed blanket are shown in Table 9.1.4. Total tritium inventories are 470 g with protium swamping and 3800 g without protium swamping. As shown in these results, protium swamping is effective to reduce the tritium inventory in the blanket since adsorption inventory occupies the major portion of total inventory. High breeder temperature and low tritium oxide pressure are also effective to reduce tritium inventory in the blanket. For the mixed pebble bed blanket, however, increase of the breeder temperature would be unfavorable in terms of the breeder material compatibility with beryllium. Protium (or deuterium) addition mentioned above is effective to reduce tritium oxide partial pressure. Increase of purge gas flow rate can be also useful to reduce tritium oxide partial pressure. Since tritium inventory in the blanket is very sensitive to interaction of breeder material with water, accumulation of data base on the interaction behavior between breeder materials and water is required.



Table 9.1.1 Tritium recovery conditions for the mixed pebble bed blanket

Fusion power	1000 MW
Tritium Breeding Ratio	1.0
Tritium Production Rate	6.4 g/h
Nominal Temp. in Breeding Zone	400 - 600 °C
Pressure of Purge Gas	1 atm
Purge Gas Flow Rate	240 Nm <sup>3</sup> /h
Chemical Form of Released Tritium	HT/HTO = 95/5
Concentration of Protium Gas	100 vpm H <sub>2</sub>
Pressure Drop of Purge Gas	80 mmAq

Table 9.1.2 Calculation formulae for tritium inventory estimation

- Diffusive Inventory[5], $I_{df}$ (g/cm <sup>3</sup> )
$I_{df} = \frac{G r_g^2}{15 D}$
$G$ : local tritium generation rate (g/cm <sup>3</sup> -s)
$r_g$ : grain radius (cm)
$D$ : diffusion constant (cm <sup>2</sup> /s)
$D = 59.6 \exp(-36.9 [\text{kcal/mol}]/RT)$ [Okuno]
- Decomposition Inventory[5], $I_{dec}$ (g/cm <sup>3</sup> )
$I_{dec} = \frac{G}{k}$
$k$ : thermal decomposition rate constant (sec <sup>-1</sup> )
$k = 1.36 \times 10^6 \exp(-28.5 [\text{kcal/mol}]/RT)$ [Kudo]
- Adsorption Inventory of T <sub>2</sub> O on Li <sub>2</sub> O[5,6], $I_{ads}$ (mol/ton)
$I_{ads} = 0.563 \exp(13.8 [\text{kcal/mol}]/RT) P_{T_2O}^{0.64}$ [Yoshida]
$P_{T_2O}$ : partial pressure of T <sub>2</sub> O (atm)
- Solubility Inventory of T <sub>2</sub> in Li <sub>2</sub> O[5,7], $I_{sol}$ (mol/ton)
$I_{sol} = 13.8 \exp(-3.82 [\text{kcal/mol}]/RT) P_{T_2}^{0.5}$ [Katsuta]
$P_{T_2}$ : partial pressure of T <sub>2</sub> (atm)
- Solubility Inventory of T <sub>2</sub> in Be[5,8], $I_{sol}^{Be}$ (mol/ton)
$I = 7.9 \times 10^{-3} \exp(0.44 [\text{cal/mol}]/RT) P_{T_2}^{0.5}$ [Jones]

Table 9.1.3 Analytical conditions for tritium inventory estimation of the mixed pebble bed blanket

	with H <sub>2</sub> Swamping	without H <sub>2</sub> Swamping
Tritium Production Rate	1.53 × 10 <sup>2</sup> g/day (1000 MW, TBR=1.0)	
Purge Gas	He + 100 vpm	Pure He
Chemical Form of Tritium	HT/HTO = 95/5	T <sub>2</sub> /T <sub>2</sub> O = 10/90
Temperature of Breeder	400 - 840 °C (Fig. 9.1.1)	
Purge Gas Pressure	1 atm	
Purge Gas Flow Rate	240 Nm <sup>3</sup> /h	
Mass of Li <sub>2</sub> O	69.0 ton	
Mass of Beryllium	224 ton	
Grain size of Li <sub>2</sub> O	3 × 10 <sup>-5</sup> m	

Table 9.1.4 Tritium inventory in the mixed pebble bed blanket

	Unit : g	
	with H <sub>2</sub> Swamping	without H <sub>2</sub> Swamping
Diffusion	4.4 × 10 <sup>-1</sup>	
Decomposition	2.4 × 10 <sup>-1</sup>	
T <sub>2</sub> O Adsorption	4.6 × 10 <sup>2</sup>	3.8 × 10 <sup>3</sup>
T <sub>2</sub> Solubility in Li <sub>2</sub> O	4.0	1.9
T <sub>2</sub> Solubility in Be	3.3	1.5
Total	4.7 × 10 <sup>2</sup>	3.8 × 10 <sup>3</sup>

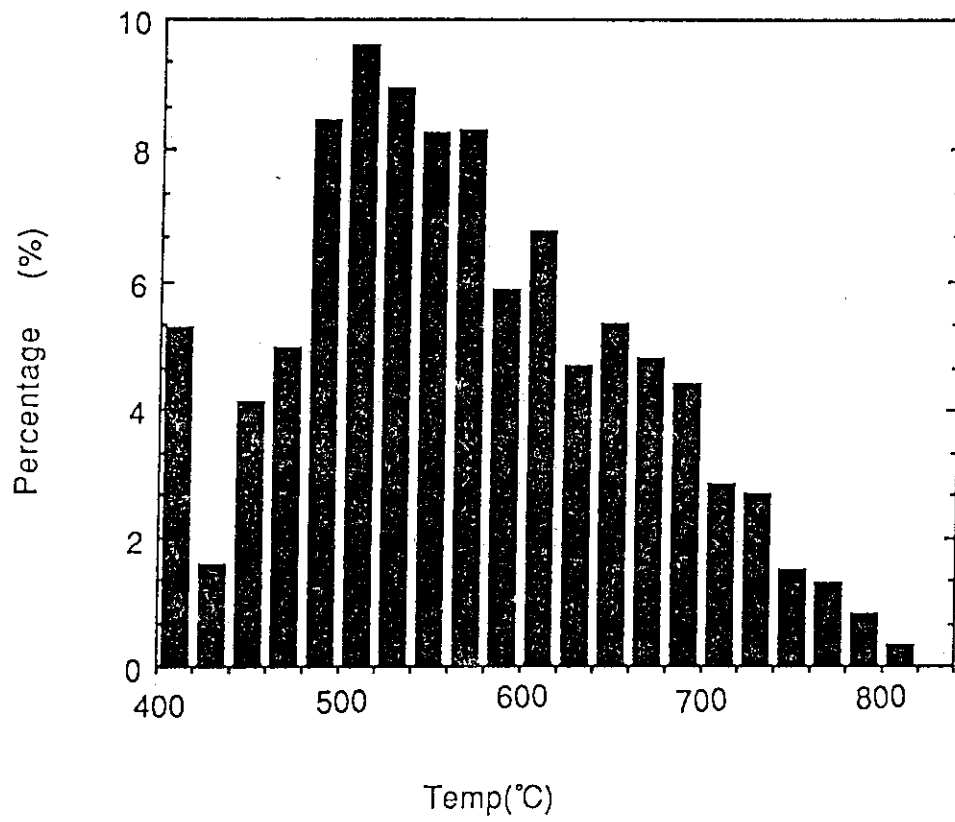


Fig. 9.1.1 Temperature spectrum in the mixed pebble bed blanket

## 9.2 Layered Pebble Bed Blanket

### 9.2.1 Tritium recovery condition

Tritium recovery conditions for the layered pebble bed blanket are summarized in Table 9.2.1. An operating temperature range of breeder zone is assumed to leave some margin for power variations. Tritium production rate in each  $\text{Li}_2\text{O}$  pebble bed layer is evaluated as shown in Table 9.2.2. The flow rate of purge gas is determined in the same way as the mixed pebble bed blanket (Section 9.1.1). Purge gas flows through each layered pebble bed in parallel. The parallel purge gas flow is divided and independently adjusted according to tritium production rate in each layer. The purge gas flow rate designed for each layer is also indicated in Table 9.2.2. Protium gas is added in the purge gas at an atomic mass flow rate of one hundred times as high as tritium production rate as described in Section 9.1.1. Chemical form of tritium released from  $\text{Li}_2\text{O}$  is 95 % of HT and 5 % of HTO when protium is added at sufficiently high concentration also as shown in Section 9.1.1.

With Ergun's equation[4] (shown in Section 9.1.1), Pressure drop of sweep gas through each  $\text{Li}_2\text{O}$  pebble bed layer is evaluated as indicated in Table 9.2.2. Among the pebble bed layers, pressure drop through the first layer (nearest to plasma) is 10 kPa which is the highest since the highest gas flow rate resulted from the highest tritium production rate is required in the first layer.

### 9.2.2 Tritium inventory

Steady state tritium inventory in the layered pebble bed blanket is calculated assuming quadratic temperature distribution in a slab geometry of the  $\text{Li}_2\text{O}$  pebble bed layer. The analytical model incorporates bulk diffusion of tritium, surface decomposition of  $\text{LiOT}$ , adsorption of HTO, and adsorption of elemental tritium except for the interaction of tritium with beryllium since beryllium pebbles are isolated from  $\text{Li}_2\text{O}$  pebbles by the stainless steel clad. Analytical conditions are summarized in Table 9.2.3. Calculation formulae used are the same as those in Table 9.1.2. Volume averaged tritium generation rate in each  $\text{Li}_2\text{O}$  layer is used in the calculation.

Tritium inventories evaluated for the layered pebble bed blanket are summarized in Table 9.2.4. Among tritium build-up mechanisms, adsorption of HTO dominates the tritium inventory in the layered pebble bed blanket as same as in the mixed pebble bed blanket. Tritium inventory due to adsorption of HTO is 87 g which corresponds to 94 % of total inventory. Bulk diffusion and surface decomposition have little impact on tritium inventory. Total tritium inventory in the layered pebble bed blanket is 93 g which is lower than that of the mixed pebble bed blanket. (Thermal control, i.e. cooling tube arrangement in the mixed pebble blanket and arrangement of layer thicknesses in the layered pebble bed blanket, is not optimized yet resulting in higher  $\text{Li}_2\text{O}$  operating temperature in the layered pebble bed blanket than in the mixed pebble bed blanket. This difference in operating temperatures between two blankets mainly contributes to the difference in tritium inventories. Therefore, tritium inventories should be reevaluated after the optimization of the thermal control in the blankets.)

Table 9.2.1 Tritium recovery conditions for the layered pebble bed blanket

Fusion Power	1000 MW
Tritium Breeding Ratio	1.0
Tritium Production Rate	6.4 g/h
Temperature in Breeding Zone	450 - 600 °C
Pressure of Purge Gas	1 atm
Purge Gas Flow Rate	250 Nm <sup>3</sup> /h
Chemical Form of Released Tritium	HT/HTO = 95/5
Concentration of Protium Gas	100 vpm H <sub>2</sub>
Pressure Drop of Purge Gas	0.1 atm

Table 9.2.2 Purge gas flow rate and pressure drop in the layered pebble bed blanket

Layer	Thickness mm	T Prod. Rate g/day	Area m <sup>2</sup>	He Flow Rate Nm <sup>3</sup> /h	Superficial Velocity cm/s	Press. Drop kPa
1	9	36.5	0.463	60	8.75	10.3
2	10	38.3	0.517	60	7.84	9.3
3	13	31.5	0.677	50	4.99	5.9
4	18	23.8	0.944	40	2.86	3.4
5	27	16.0	1.43	25	1.18	1.4
6	50	7.3	2.70	15	0.38	1.3
		153.4		250		

Gas : Helium  
 Temperature : 673 K  
 Pressure : 0.1 MPa  
 Pebble Diameter : 1 mm  
 Void Fraction : 0.4

Table 9.2.3 Analytical conditions for tritium inventory estimation  
of the layered pebble bed blanket

Parameter	Layer Number						Total
	1	2	3	4	5	6	
Li <sub>2</sub> O Mass (ton)	4.75	5.30	6.94	9.68	14.68	27.65	67.90
Volume (m <sup>3</sup> )							
Packing Zone	4.63	5.17	6.77	9.44	14.32	26.97	67.30
Pebble	2.78	3.10	4.06	5.66	8.59	16.18	40.38
Li <sub>2</sub> O	2.36	2.64	3.45	4.81	7.30	13.75	34.32
Thickness (mm)	9	10	13	18	27	50	
Grain Radius (μm)	15	15	15	15	15	15	
T Production Rate							
(g/day)	36.5	38.3	31.5	23.8	16.0	7.3	153.4
T <sub>max</sub> (K)	923	923	973	1023	1123	1123	
T <sub>min</sub> (K)	773	773	823	873	923	923	
He Gas Flow							
Rate (Nm <sup>3</sup> /h)	60	60	50	40	25	15	250
Pressure (MPa)	0.1	0.1	0.1	0.1	0.1	0.1	
Inlet H <sub>2</sub> (vpm)	1.0×10 <sup>2</sup>	1.0×10 <sup>2</sup>	1.0×10 <sup>2</sup>	1.0×10 <sup>2</sup>	1.0×10 <sup>2</sup>	1.0×10 <sup>2</sup>	
Inlet H <sub>2</sub> O (vpm)	1	1	1	1	1	1	

Table 9.2.4 Tritium inventory in the layered pebble bed blanket

Mechanism	Layer Number						Total
	1	2	3	4	5	6	
Diffusion	$4.0 \times 10^{-3}$	$4.2 \times 10^{-3}$	$9.4 \times 10^{-4}$	$1.6 \times 10^{-4}$	$3.1 \times 10^{-5}$	$1.4 \times 10^{-5}$	$9.4 \times 10^{-3}$
Decomposition	$6.8 \times 10^{-3}$	$7.2 \times 10^{-3}$	$2.2 \times 10^{-3}$	$5.1 \times 10^{-4}$	$1.3 \times 10^{-4}$	$5.8 \times 10^{-5}$	$1.7 \times 10^{-2}$
HTO Adsorption	$1.6 \times 10^1$	$1.8 \times 10^1$	$1.5 \times 10^1$	$1.1 \times 10^1$	$1.1 \times 10^1$	$1.7 \times 10^1$	$8.7 \times 10^1$
HT Absorption	$2.9 \times 10^{-1}$	$3.4 \times 10^{-1}$	$4.9 \times 10^{-1}$	$7.9 \times 10^{-1}$	1.4	2.4	5.7
Total	$1.6 \times 10^1$	$1.8 \times 10^1$	$1.5 \times 10^1$	$1.2 \times 10^1$	$1.3 \times 10^1$	$1.9 \times 10^1$	$9.3 \times 10^1$



### 9.3 Conclusions

Purge gas conditions and tritium inventories for the mixed pebble bed blanket and the layered pebble bed blanket have been evaluated. Flow rates of purge gas are determined to keep water partial pressure in blanket atmosphere sufficiently less than water dissociation pressure. Protium gas is added into helium purge gas at an atomic mass flow rate of one hundred times as high as tritium production rate in order to enhance tritium release from the breeder and reduce tritium inventories in the blankets. Pressure drops of purge gas through the mixed pebble bed and the layered pebble bed blankets are 0.8 kPa and 10 kPa, respectively, both of which are low enough to be accepted.

Tritium inventories in the mixed pebble bed blanket and layered pebble bed blanket corresponding to steady state are 470 g and 93 g, respectively, with the protium swamping. (Without protium swamping, the tritium inventory in the mixed pebble bed blanket increases up to 3800 g.) The dominant tritium build-up mechanism is adsorption of tritium oxide on  $\text{Li}_2\text{O}$ . Protium swamping is effective to reduce the amount of this adsorption. These tritium inventories should be reevaluated following the optimization of thermal control in both of blankets.

#### [Reference]

- [1] E.A. Gulbransen and K.F. Andrew, J. Electrochem. Soc. 97 (1950), 383
- [2] JANAF Thermochemical Tables 2nd ed. (1971)
- [3] H. Takeshita et al., JAERI-M 86-130 (1986) (in Japanese)
- [4] R.B. Bird et al., "Transport Phenomena", John Wiley & Sons, Inc.
- [5] T. Kobayashi et al., JAERI-M 87-219 (1988)
- [6] H. Yoshida et al., "JAERI-M 82-194 (1982) (in Japanese)
- [7] H. Katsuta et al., J. Nucl. Mater. 116 (1983), 244
- [8] P.M.S. Jones and G. Gibson, AWRE Report No. 0-2/67

## 10. Accommodation to Power Load Variation

Since ITER is an experimental reactor, some power variations from the rated power are foreseen. Even in the rated powers, there is a difference of about 25% between those of the Physics and the Technology Phases. Accommodation capability of the blankets to these power variations with respect to the temperature range of the breeder ( $\text{Li}_2\text{O}$ ) is discussed here.

The allowable temperature range for  $\text{Li}_2\text{O}$  has been determined to be 400-1000 °C (400 °C for enhancing tritium release from the breeder while 1000 °C for keeping the breeder material integrity). By choosing a nominal operating breeder temperature range which is narrower than the allowable range, operations other than the rated power can be permitted. Permissible power variations are indicated in Figs 10.1 and 10.2 as a function of breeder nominal temperatures. As seen from the figures, the permissible power variation can be adjusted by selecting the nominal operating temperatures of the breeder. For instance, a reduced power variation of -12.5 % will be permissible in case of the minimum nominal temperature of 450 °C. For increased power variations, 72 % and 46 % of increases will be permissible in case of the maximum nominal temperature of 600 °C and 700 °C, respectively. From the viewpoint of breeder temperature, a nominal temperature range of 500 - 700 °C or narrower would be desirable so as to permit the power variations of -22 % to +46 %.

As shown in Sections 7.1 and 7.2, power variations of 0 % to +20 % and -10% to +25 % are permissible for the present designs of the mixed pebble bed and the layered pebble bed blankets, respectively. Optimizations of the in-blanket configurations are required to obtain the desirable nominal operating temperatures and wider accommodation capability to power variations. In addition, further examinations for the nominal operating and allowable temperatures of beryllium multiplier and clad material (stainless steel) are also needed.

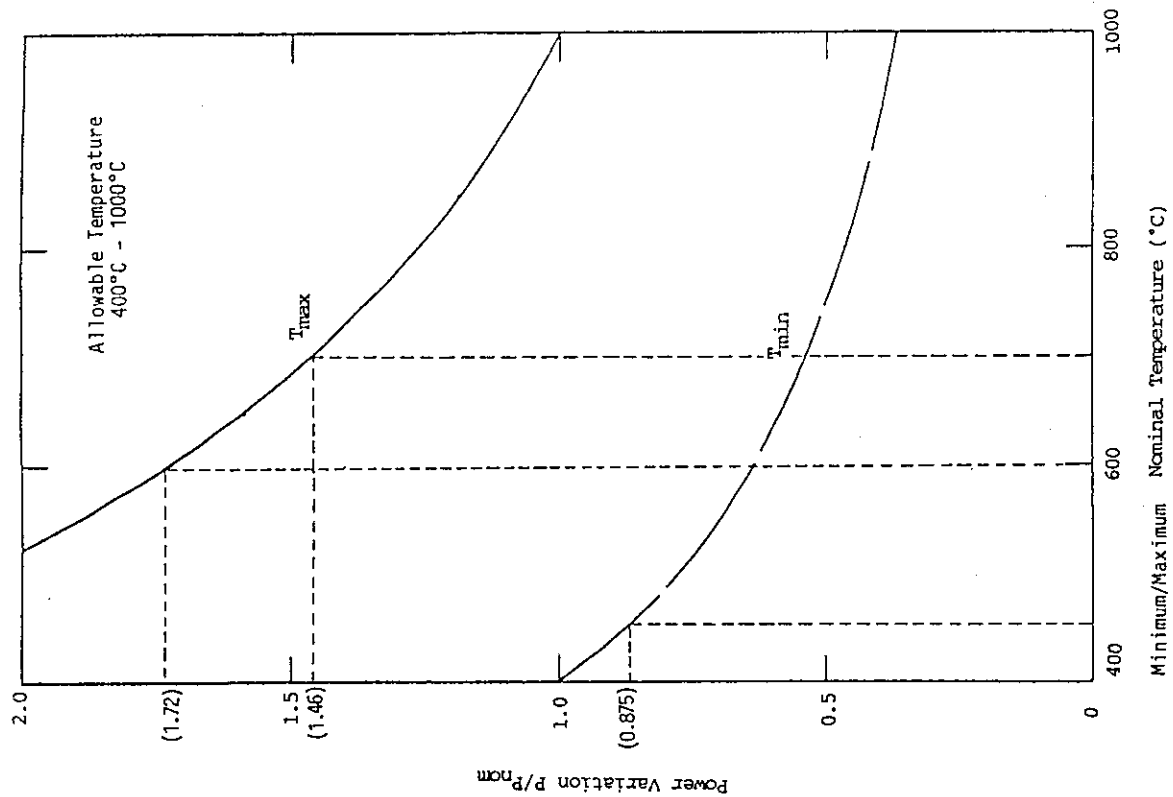


Fig. 10.1 Power variation window as a function of nominal operating temperature of  $\text{Li}_2\text{O}$

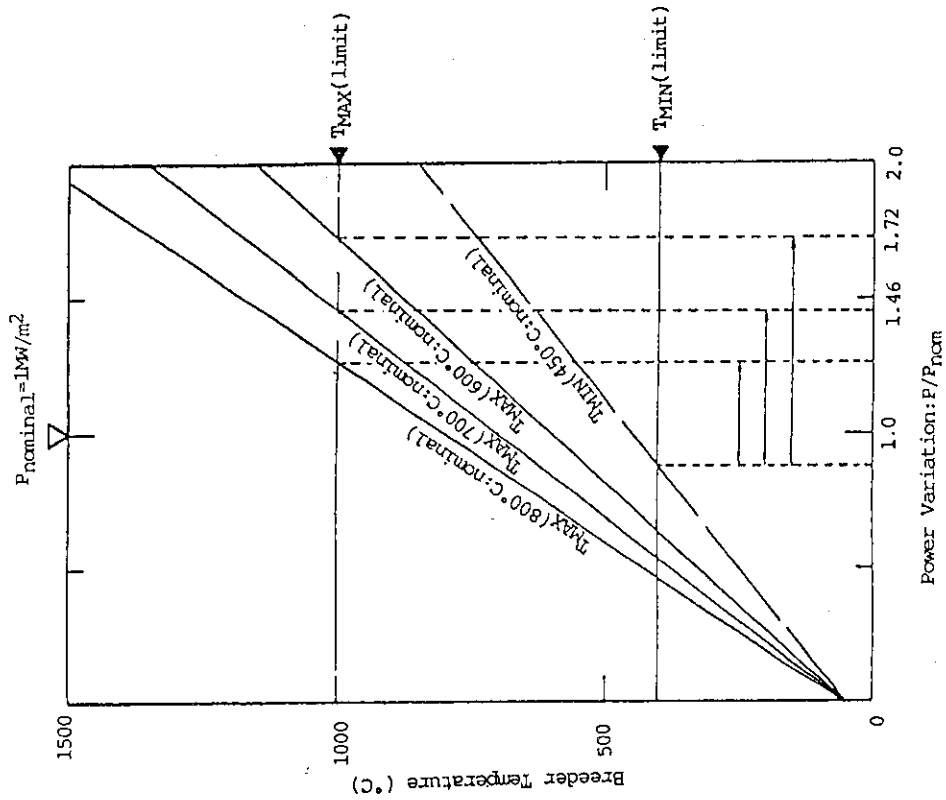


Fig. 10.2 Permissible power variations for the minimum nominal  $\text{Li}_2\text{O}$  temperature of  $450^\circ\text{C}$  and the maximum nominal  $\text{Li}_2\text{O}$  temperatures of  $600\text{--}800^\circ\text{C}$

## 11. Separate First Wall Design for Test Article Containment

A structural concept of a test article containment for engineering tests of the next generation devices is illustrated in Fig. 11.1. The container and the test port duct are hermetically sealed by lip seal welding at the support flange. The inside of the container is under atmospheric condition. Therefore, the plasma chamber is not contaminated even if some trouble, for example, coolant leakage would occur. Replacement and setting of the test module can be performed without breaking the vacuum boundary of the reactor.

The container has the same cooling mechanism as major part of the first wall. The wall of the container is a pile of ribbed panels which have rectangular coolant paths. The coolant is pressurized water which has the same conditions as those for the major first wall of the reactor, i.e. 1.5 MPa and 60/100 °C.

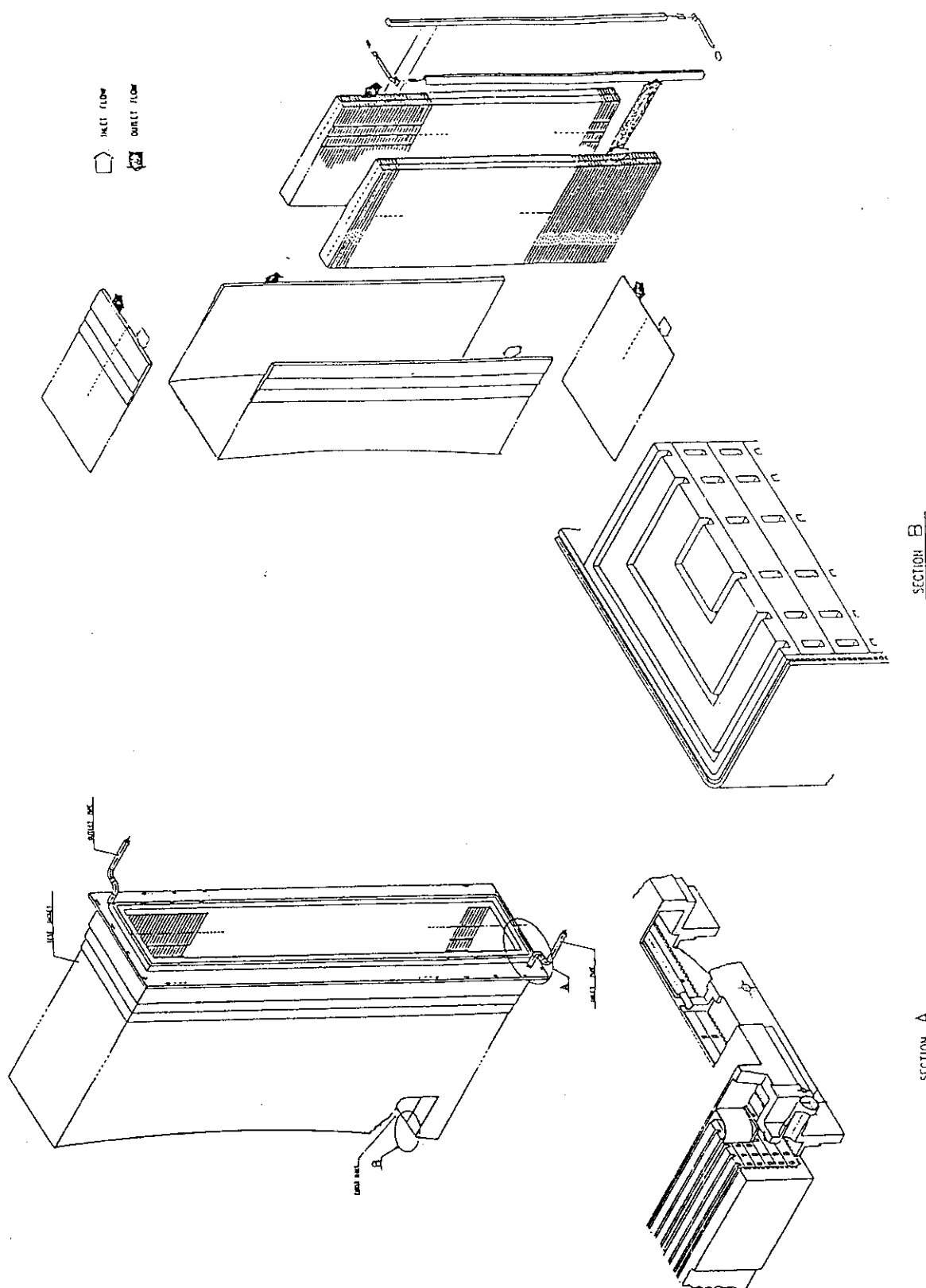


Fig. 11.1 Concept of test article containment

#### Acknowledgement

The authors would particularly like to thank CAD members in Fusion Experimental Reactor (FER) team of JAERI for their help to prepare many useful drawings. They would also like to thank members of the FER team for their helpful advices and comments concerning this work and those who have supported ITER Conceptual Design Activity.

## Appendix Material Properties of $\text{Li}_2\text{O}$ in Comparison with Other Ceramic Breeders and R&D Needs for $\text{Li}_2\text{O}$

### A.1 Role of Material Data Base and Comparison of Ceramic Breeder Properties

Roles of breeder materials are 1) production of tritium by nuclear reaction with neutrons, 2) transformation from nuclear energy to thermal energy, 3) shielding of neutrons. These depend on lithium ( $^6\text{Li}$ ) density which is determined by sort of ceramic breeder materials and enrichment of  $^6\text{Li}$ . However, the recoveries for tritium and thermal energy are also related to materials properties including tritium solubility/transport and thermal properties, physical and chemical stability, and mechanical properties etc.. Furthermore, such properties are influenced by the fusion blanket environments, especially irradiation conditions.

The materials database will play an important role in selection of the optimum ceramic breeder materials for ITER blanket, although the selection is a design decision based on many factors. The materials properties as basis for materials selection are 1) Li atom density, 2) activation, 3) thermal conductivity, 4) melting point/phase change, 5) thermal expansion, 6) mechanical strength, 7) creep/ductility, 8) chemical stability, 9) compatibility with water, 10) compatibility with structural materials, 11) compatibility with Be, 12) Li mass transfer, 13) tritium solubility, 14) tritium release (transport), 15) irradiation effects on physical properties, 16) irradiation swelling, 17) irradiation stability, 18) radiation effects on tritium transport and compatibility. In addition, large-scale production feasibility, which is not materials properties, should be checked, since a large amount of breeder materials will be used for the ITER blanket.

Table A.1 indicates a qualitative comparison of material properties of candidate ceramic breeders [1]. To help put Table A.1 into the proper perspective, the rationale behind the rankings is shown in the following. Lithium atom density is relatively straightforward.  $\text{Li}_2\text{O}$  has the highest lithium atom density and rates the highest ranking. The three ternary ceramics are all low relative to the oxide. The reason that their ranking is "fair" and not lower is that in all of the ITER designs proposed the

quantity of Be used is much greater than the quantity of breeder and  $^6\text{Li}$  enrichments as high as 95% are called for. Under these conditions, the Li density is not as significant a parameter as it would be in other reactor designs. The second category, Large-Scale Production Feasibility, is not, strictly speaking, a materials performance issue. However, significant quantities of ceramic breeder material have been fabricated in the context of the materials research program. Based on these experiences, all of the breeders were presumed to be ranked as "fair" in terms of large-scale production feasibility. The term "large scale" in the ITER context refers to 10-20 metric tons.

While activation of the breeder materials may not be a significant design issue relative to the large quantities of other activated materials in ITER, a relative ranking was made reflecting the higher activation potential of  $\text{Li}_2\text{ZrO}_3$ . Thermal conductivity is an important performance parameter. For unirradiated material at the same density,  $\text{Li}_2\text{O}$  has the highest thermal conductivity. More recent data on  $\text{LiAlO}_2$  suggest that its conductivity is fair and clearly better than earlier estimates indicated. The  $\text{Li}_2\text{ZrO}_3$  rating remains the same as in previous years. The major change is the lower rating for the  $\text{Li}_4\text{SiO}_4$  for which recent data on relatively phase-pure material indicate that its thermal conductivity is even lower than earlier estimates. The melting points of the four ceramics are all high relative to the anticipated operating temperatures. Some question was raised about a possible crystalline phase change temperature of 1100 °C for  $\text{Li}_2\text{ZrO}_3$ . However, experience with this ternary does not substantiate this.

The rankings for mechanical strength and creep/ductility have different meanings for breeder ceramics than for structural materials. The term "Mechanical Strength" refers more to the ability of the breeder materials to withstand differential thermal and swelling stresses and mechanical loads without cracking. In the case of "Creep/Ductility" high values for these are considered desirable. The evaluations are based primarily on the performance of these materials in in-reactor experiments such as FUBR-1A, as well as out-of-reactor separate effects tests.

Within the areas of tritium retention and transport,  $\text{LiAlO}_2$  was ranked as poor because of its slow release of tritium at low temperatures.



This ranking is based primarily on experiments in which several breeders were irradiated under similar conditions. A useful measure of tritium-transport performance in these experiments is tritium residency time. For example, the ITER blanket generates about 150 g of tritium per day. A residency time of one day for the breeder material corresponds to an anticipated inventory of 150 g. To have less than this inventory,  $\text{Li}_2\text{O}$  and  $\text{Li}_2\text{ZrO}_3$  would have to operate at temperatures above  $\sim 320^\circ\text{C}$ ,  $\text{Li}_4\text{SiO}_4$  above  $\sim 390^\circ\text{C}$ , and  $\text{LiAlO}_2$  above  $\sim 450^\circ\text{C}$ .

In the area of radiation effects,  $\text{LiAlO}_2$  and  $\text{Li}_2\text{ZrO}_3$  have demonstrated good in-reactor stability in terms of microstructure (e.g., negligible grain growth and densification), chemical stability, and low swelling. Problems associated with the other two ceramics are swelling (highest for  $\text{Li}_2\text{O}$ ) and transformations ( $\text{Li}_4\text{SiO}_4 \rightarrow \text{Li}_2\text{SiO}_3$ ). In terms of radiation effects on tritium transport and compatibility, the ranking of "Key Issue" for all of the breeder ceramics really refers to the fact that tritium release and compatibility have not been determined or demonstrated up to the end-of-life ITER burnups and neutron exposures (in dpa). The shorter-time data available do not suggest that these are problem areas for the ceramics. However, these items will continue to be listed as "Key Issues" until longer-time data become available to confirm the predictions based on short-time results.

## A.2 Critical Issues for $\text{Li}_2\text{O}$

As seen in the description of the previous section, critical issues for  $\text{Li}_2\text{O}$  are compatibility with Be, Li mass transfer and irradiation effects on tritium transport.

One of the proposed ITER blanket designs utilizes pebble-bed form of mixture of  $\text{Li}_2\text{O}$  and Be. The anticipated temperature range is  $400 - 700^\circ\text{C}$  ( $1000^\circ\text{C}$  at hot spots). The compatibility would be affected through irradiation-enhanced diffusion by neutron irradiation. At the present stage, there are limited data for the compatibility between  $\text{Li}_2\text{O}$  and Be both in non-irradiated condition and during irradiation. The compatibility between  $\text{Li}_2\text{O}$  and Be in the temperature range  $400 - 1000^\circ\text{C}$  during neutron irradiation is one of critical issue for  $\text{Li}_2\text{O}$ .

For  $\text{Li}_2\text{O}$ , Li mass transfer might be serious in the high temperature

region of the blanket. The calculation using the present database shows that if the only source of oxygen in the system comes from Li burnup, then mass transfer can be minimized by proper control of the purge flow system. However, these findings need to be substantiated on a component-scale level with prototypical temperature gradients. So, Li mass transfer still remains as a critical issue for  $\text{Li}_2\text{O}$ .

Transport phenomena such as tritium release and compatibility will be affected by neutron irradiation. The irradiation effect on the transport phenomena during irradiation may be different from that after irradiation. Also, the effects would depend on the fluence (burnup) and neutron spectra. The data of tritium release under neutron irradiation which were obtained so far suggest that there is no serious problem in irradiation effects on tritium release. However, such data were obtained at the low fluence (burnup) using neutron spectra softer than those in the ITER blanket environment. So, irradiation effects on transport phenomena, especially tritium release, still remain as one of critical issues. Confirmatory data at high fluence (burnup higher than 5 % and much more dpa) by using neutron irradiation with hard spectra similar to the neutron spectra in the ITER blanket environment are required.

### A.3 Status of Existing Data Base for $\text{Li}_2\text{O}$

Status of existing database for properties of  $\text{Li}_2\text{O}$  is summarized in Table A.2[1], together along that for the other candidates of ceramic breeder materials.

Baseline physical properties (density, melting temperature, vapor pressure, thermal expansion, specific heat) are judged to be reasonably complete.

The database for the mechanical properties (elastic modulus, Poisson's ratio, tensile strength, compressive strength, bending strength, creep properties) is more limited than for the other properties. The important variables in establishing correlations are porosity and grain size, temperature, and fast-neutron fluence/burnup. More data are needed for the compressive and bending strength of  $\text{Li}_2\text{O}$ . The mechanical properties are important in determining whether the ceramic breeder materials will crack under differential thermal and swelling strain and how much pressure they

can exert on cladding materials if contact is established. In evaluation for cracking, bending strength data are useful.

Considerable data of chemical stability/compatibility data (composition/purity, stability, vapor pressure/transport, compatibility with water, compatibility with stainless steel) exist for  $\text{Li}_2\text{O}$ .  $\text{Li}_2\text{O}$  has received the most attention in the area of vapor pressure ( $\text{LiOH/T}$ )/transport ( $\text{Li}$ ). In respect of compatibility with Be for  $\text{Li}_2\text{O}$ , baseline data and irradiation data are needed, since one of the proposed ITER blanket design utilizes pebble-beds of mixture of  $\text{Li}_2\text{O}$  and Be. There is important discrepancy among the data of compatibility with stainless steel for  $\text{Li}_2\text{O}$ . The more data are needed.

Tritium solubility and transport have been studied in detail for  $\text{Li}_2\text{O}$ , which is the only ceramic breeder material for which tritium diffusion data have been obtained using the single crystals. The solubility data for  $\text{Li}_2\text{O}/\text{H}_2\text{O}$  are quite good and consistent, but the solubility data for the  $\text{Li}_2\text{O}/\text{H}_2$  system are quite scattered. The desorption/decomposition data for moisture release from  $\text{LiOH}$  and  $\text{Li}_2\text{O}$  have a factor of 10 scatter. Adsorption, as well as solubility, needs to be determined more reliably for both the  $\text{Li}_2\text{O}/\text{H}_2$  and  $\text{Li}_2\text{O}/\text{H}_2\text{O}$  systems.

Radiation effects on the physical and mechanical properties, on swelling, on tritium trapping/transport and on He trapping/transport are, in general, poorly characterized in the anticipated range of ITER fast neutron fluence and burnup. Most of the data come from post-irradiation studies of FUBR-1A samples. While this was a good experiment, it should be pointed out that it was a closed-capsule experiment with questionable moisture control which may have had an influence on the results. In respect of irradiation effects on tritium transport in  $\text{Li}_2\text{O}$ , tritium diffusivity in single crystals has been determined as a function of thermal neutron fluence. However, it should be noted that the neutron spectra in the blanket region are much harder than thermal neutrons (i.e., from fast neutrons to 14 MeV neutrons), and that irradiation effects due to neutrons in the blanket region could be different from those due to thermal neutrons.

#### A.4 Key R&D Needs for $\text{Li}_2\text{O}$

The proposed ITER designs include those utilizing the pebble bed form of

ceramic breeder for  $\text{Li}_2\text{O}$ . The effective thermal conductivity of these beds depends on many parameters (size and density of pebbles, etc.). The effective thermal conductivity of the pebble-beds needs to be measured by adjusting the parameters for simulation of the proposed ITER blanket. In addition, similar data are needed for the  $\text{Li}_2\text{O}/\text{Be}$  mixed pebble-bed design. To generate such kinds of data, an active R&D program is on-going in Japan.

In respect of irradiation effects on the thermal conductivity of  $\text{Li}_2\text{O}$ , some data have been generated. The irradiation effects appear to be small, but there is a great deal of scatter in what amount to these "single data sets". Confirmatory data are needed.

For  $\text{Li}_2\text{O}$ , the scatter in solubility/adsorption/desorption data is too large to allow calculations to be made with confidence at this time. In particular, consistent data sets are needed for the  $\text{Li}_2\text{O}/\text{H}_2$  system under anticipated protium and moisture levels.

As described previously, the irradiation effect on tritium release is one of critical issues. In-situ tritium release studies have been carried out up to low burnup using thermal or mixed spectrum reactors. In addition, the tritium diffusivity in  $\text{Li}_2\text{O}$  single crystals has been investigated as a function of thermal neutron fluence. Confirmatory data need to be obtained at high fluence and high burnup using neutron irradiation with hard spectra simulating the ITER blanket environment.

The mechanical properties data are important in evaluating stress levels for cracking and pressure levels between ceramic breeder materials and cladding materials. The properties vary with materials parameters (porosity, grain size, etc.). More bending-strength data and fracture toughness data as a function of the materials parameters and temperature are needed. Furthermore, thermal tests with temperature gradients or changes anticipated for ITER blanket, which include cyclic pulsed tests, are desired.

For most of ITER blanket designs, operation temperatures for a significant fraction of the ceramic breeder materials are below  $700^\circ\text{C}$ , but the creep/ductility data for these temperatures are very limited. The data under in-reactor conditions below  $700^\circ\text{C}$  are needed to predict the mechanical

response of the breeder/cladding system.

The swelling of the ceramic breeder materials is important from two perspectives. Swelling is driving force for breeder/cladding contact and stresses on the cladding. Also, differential swelling within the ceramic breeder material can cause internal stresses which may crack the breeder. FUBR-1A experiment has provided the primary estimate of breeder swelling rates. However, as pointed out previously, FUBR-1A experiment data are not free from the influence due to questionable moisture control. More data of swelling by neutron irradiation with hard spectra simulating the ITER blanket environment in the temperature range 400 - 800 °C under well-controlled moisture conditions are needed.

The chemical stability and compatibility of the ceramic breeder materials are important in establishing upper temperature limits for the bulk of the breeder and for the breeder interfaces with other materials. Li mass transfer is one of critical issues for  $\text{Li}_2\text{O}$ . Component-scale tests for Li mass transfer of  $\text{Li}_2\text{O}$ , which can simulate the ITER blanket system in terms of temperature gradients, moisture levels and purge flow rate, are needed.

With regard to compatibility, compatibility between  $\text{Li}_2\text{O}$  and Be is a critical issue. The compatibility under both in- and out-of-reactor conditions in the temperature range anticipated for ITER blanket should be examined in detail. The reaction rate between  $\text{Li}_2\text{O}$  and stainless steel, while apparently faster than the other ceramic breeder materials, could be still reasonably slow at the temperatures anticipated for ITER blanket. However, there are some informations that the reaction rate depends on the purity of  $\text{Li}_2\text{O}$ . Additional data are desirable to resolve this point.

#### Reference

- [1] D. Smith, K. Noda, C. Wu et al., Report of specialist's Meeting on ITER Materials Data Base, Feb., 1990

Table A.1 Comparison of properties for various ceramic breeder materials

	Li <sub>2</sub> O	Li <sub>4</sub> SiO <sub>4</sub>	Li <sub>2</sub> ZrO <sub>3</sub>	LiAlO <sub>2</sub>
Li Atom Density	○	▲	▲	▲
Large Scale Production Feasibility	▲	▲	▲	▲
Activation	○	○	X	▲
Thermal Conductivity	○	X	X	▲
Melting Point/Phase Change	○	▲	○	○
Thermal Expansion	▲	▲	○	○
Mechanical Strength	▲	▲	○	○
Creep/Ductility	▲	X	X	X
Chemical Stability	▲	▲	○	○
Water Compatibility	X	▲	▲	○
Structural Compatibility	▲	▲	○	○
Be Compatibility	?	▲	○	○
Li Mass Transfer	?	○	○	○
Tritium Solubility	▲	▲	▲	▲
Tritium Release (Transport)	○	▲	○	X
Irradiation Effects on Physical Properties	○	○	○	○
Irradiation Swelling	X	▲	○	○
Irradiation Stability	▲	X	○	▲
Radiation Effects (T-Transport Compatibility)	?	?	?	?

○ Good	▲ Fair	X Poor	? Key Issue
--------	--------	--------	-------------

Table A.2 ITER materials data base assessment for ceramic breeder materials

## Ceramic Breeder Materials

## • Baseline physical properties

-	Density	■	■	■	■
-	Melting temperature	■	▲	●	■
-	Vapor pressure	▲	○	○	▲
-	Thermal expansion	■	▲	▲	■
-	Thermal conductivity	▲	●	▲	■
-	Specific heat	■	■	▲	■

## • Baseline mechanical properties

-	Elastic modulus	▲	▲	▲	■
-	Poisson's ratio	▲	▲	○	▲
-	Fracture strength				
-	Tensile				
-	Compressive	○	○	○	▲
-	Bending Strength	○	▲	▲	▲
-	Creep properties	▲	▲	○	▲

## • Chemical stability/compatibility

-	Composition/purity	■	■	■	■
-	Stability	■	■	■	■
-	Vapor pressure/transport	■	○	○	○
-	Compatibility				
-	Water	▲	▲	■	■
-	Beryllium		■	▲	■
-	SS	●	■	▲	■

## • Tritium solubility/transport

-	Tritium solubility	●			▲
-	Tritium diffusivity	■	○	○	●
-	Adsorption/desorption properties	●			▲

## • Radiation effects

-	Physical properties	○		○	○
-	Swelling	○	○	○	○
-	Creep				
-	Tritium trapping/transport	●	○	○	○
-	Helium trapping/transport	○	○	○	○
-	Fracture properties	○		○	○

■	— Adequate/good agreement
▲	— Limited/general agreement
●	— Limited/important discrepancies
○	— Single set of data
Blank	— Very limited/non-existent/high uncertainties